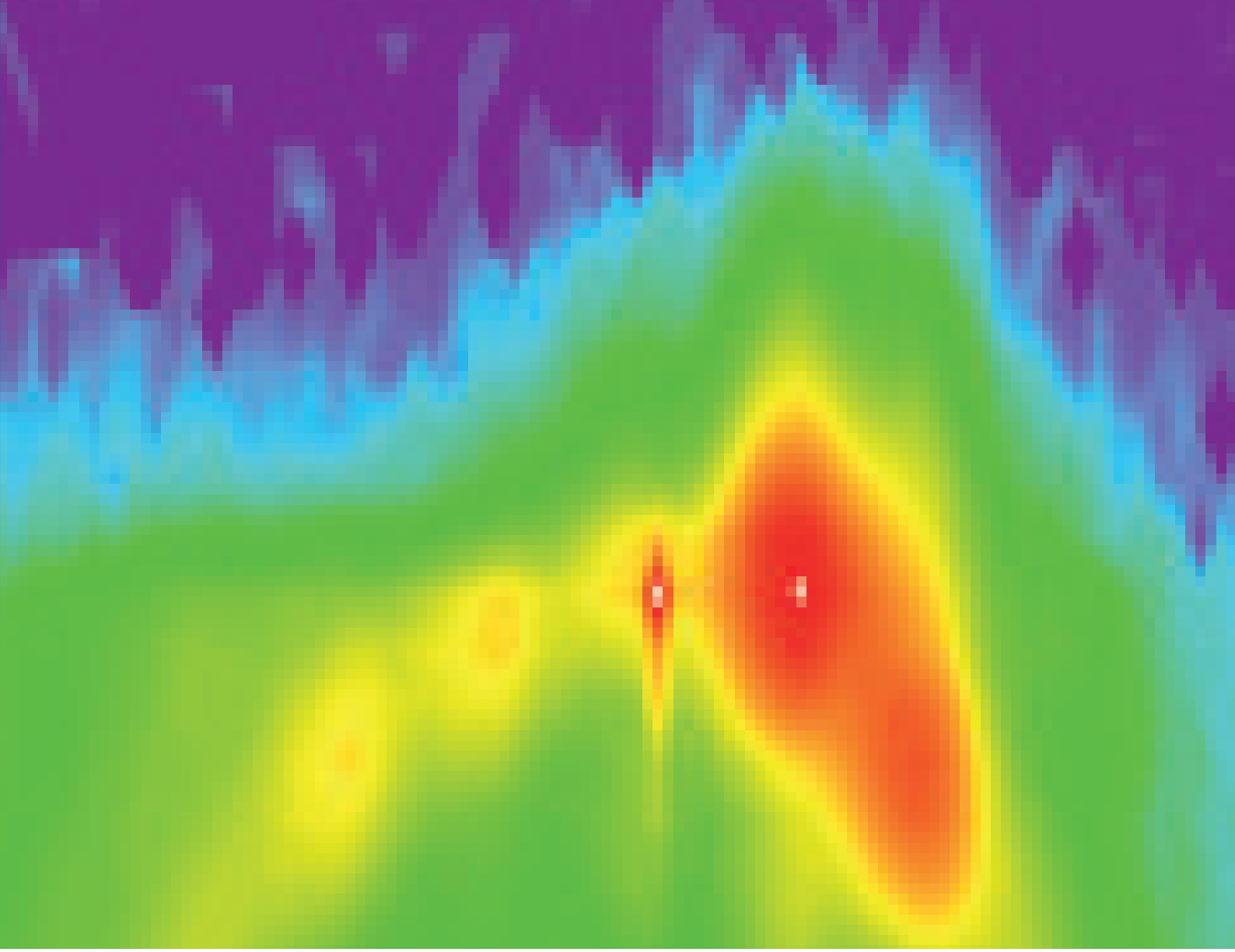

PHOTON SCIENCE 2011

Highlights and HASYLAB Annual Report

Accelerators | Photon Science | Particle Physics

Deutsches Elektronen-Synchrotron
A Research Centre of the Helmholtz Association

EMBL

PIER

Helmholtz-Zentrum Geesthacht
Centre for Materials and Coastal Research

MAX-PLANCK-GESELLSCHAFT

Universität Hamburg
DER FORSCHUNG | DER LEHRE | DER BILDUNG

European XFEL

Cover

Bragg reflection of a $PbTiO_3$ film: scan around the (200) in-plane reflection as a function of the incidence angle (grazing incidence geometry). The presence of strain gradients, coupled to gradients of both the lattice distortions and the twinned angles, can be observed. More information about this measurement can be found in the contribution “Enhanced flexoelectricity in twinned thin films” on page 34.

PHOTON SCIENCE 2011.

Highlights and
HASYLAB Annual Report

User Contributions to the Annual Report.

DESY Photon Science

A deeper insight into the photon science activities at DESY is provided by the several hundred annual user experiment and development reports. Formerly published in the “HASYLAB Jahresbericht”, they are now available online:

http://photon-science.desy.de/annual_report/

A search function and an authors’ index are also provided.

The users’ reports present all activities/experiments performed by user groups and in-house research at the DESY light sources DORIS III, PETRA III and FLASH and are published online every year in May.
Furthermore, a list of publications concerning work done at DESY is accessible online:

http://photon-science.de/publications
http://pubdb.desy.de (search function in the left frame)

DESY tries to keep the list as complete and as updated as possible, but relies on the cooperation of all users to achieve this goal.

Contents.

The year 2011 at DESY.

Chairman's foreword

A highlighting activity of and for DESY in 2011 has been the so called Helmholtz Portfolio process in which the Helmholtz centres have been striving to identify new topics of key relevance for our society requiring in future a more focused attention at the Helmholtz centres. With the strong guidance of DESY three urgent research and development (R&D) areas have been identified and successfully implemented: First, accelerator R&D to bundle the accelerator competences of the Helmholtz centres by integrating the accelerator activities carried out at universities; secondly, detector technology and detector systems which strive for a new and enhanced collaboration across disciplines to develop better detection systems; and finally, the large scale data management and analysis project which is dealing with the rapidly increasing demand in handling large data sets which are harvested at ever shorter time scales.

The successful implementation of these portfolio topics will be transformed into new programs in the upcoming funding period. Clearly, all these technologies are also of key relevance for DESY and for our photon science program, in particular at the X-ray laser facilities which have the highest demand for the most advanced technologies in all these areas.

The construction of the European XFEL has made enormous progress. The 2 km long accelerator tunnel has been successfully completed in August. Now all necessary preparations are currently made to start the installation of the superconducting accelerator modules in February next year. Thanks to a unique financial effort of the Russian-German collaboration, the XFEL is also back in laminar financial waters allowing the realization of a 17.5 GeV accelerator design.

Our CFEL scientists produce almost monthly headlines on novel scientific achievements using the X-ray laser facility at SLAC and DESY's FLASH. Henry Chapman's experiments on nanocrystals demonstrate very impressively the breathtaking scientific opportunities of theses novel light sources showing the first glimpses of impact into biology and nanomaterials design.

It is also gratifying to see how the perfect operation of our X-ray facilities DORIS III, PETRA III and FLASH are pushing DESY at the international forefront of photon science. The scientific

Recovering of the TULA cutterhead on the construction site DESY-Bahrenfeld after tunnel completion in August 2011 (Photo: European XFEL).

output of DORIS III is most impressive and sheds a brilliant light onto our user community. It is clear that DESY will undertake every effort to further attract – after the shutdown of DORIS III end of next year – its users to Hamburg.
I am convinced that the new facilities PETRA III and FLASH with their extraordinary qualities and instrumentations will exert enough attractive forces to achieve this goal. In fact, both facilities are already producing outstanding scientific results.

The users' run onto FLASH and PETRA III is overwhelming and is urging us to extend our experimental capabilities. FLASH II and the PETRA III extensions are already under construction and will soon offer additional and novel possibilities for research with super-brilliant X-ray light. A premier user of PETRA III and FLASH will be the new Centre for Structural Systems Biology (CSSB) which aims for a better understanding of infection

Signing of cooperation agreement between DESY and Kiel University (11 November 2011), from left to right: Edgar Weckert, Helmut Dosch, Christian Scherf (all DESY), Frank Eisoldt (Chancellor Kiel Univ.), Gerhard Fouquet (President Kiel Univ.) and Lutz Kipp (Dean MIN-Faculty Kiel Univ.).

processes on a molecular level. DESY's brilliant light has also attracted new international partners from India, Sweden and Russia who will use DESY's facilities within a strategic collaboration that includes the construction of three dedicated experimental stations at the PETRA III extensions. This is also good news for our user community as these advanced facilities will be open to a substantial fraction for public access.

In November, DESY has signed a collaboration agreement with the University of Kiel. The Kiel outstation at DESY will carry the name of a DESY pioneer, Ruprecht Haensel, who was one of the first world-wide to explore the properties and potential applications of synchrotron light in the early 1960ies.

Finally, a peculiar event that DESY hosted in May this year was the international Symposium "Solar Energy for Science" under the auspices of UNESCO and chaired by Klaus Töpfer, Head of an Energy Advisory Committee to the German Government. International key authorities from science, including Nobel Laureates Carlo Rubbia and Walter Kohn, have met to discuss with policy makers from Europe and Middle East/North Africa (MENA) a novel energy/science partnership between Europe and MENA by stimulating further scientific cooperation for a sustainable development around the Mediterranean basin. DESY – as a research laboratory at international level – was an ideal host and moderator for this event that strived to build bridges between Europe and MENA.

I warmly thank the many committed collaborators at DESY for their impressive work during this year.

Helmut Dosch
Chairman of the DESY Board of Directors

Photon Science at DESY.

Introduction

The most dominant activities apparent around the DESY photon science installations in 2011 were the many civil constructions. These have been taking place at almost every corner of the DESY site. This situation will continue for at least another two years. Importantly for our science perspectives was the start of the construction work for the new FLASH II tunnel in September. Meanwhile the façade of the new CFEL building was finished. However, installation work is still on going inside and the move-in date of the CFEL groups is scheduled for May 2012. Additional laser laboratory buildings for the CFEL and the new laser development and support groups are under construction as well as the refurbishment of DESY's entire underground technical infrastructure. Preparations for the construction of the new DESY photon science building including the NanoLab, the PETRA III extension experimental halls and the new CSSB building are underway.

The operation of DORIS III has been quite smooth over most of 2011, as if this elderly machine is showing us it does not like the scheduled final shutdown for synchrotron radiation experiments at the end of October 2012. Also our users still appreciate the experimental facilities at DORIS III and we counted a record number of proposals submitted in the last proposal round. Experiments at DORIS III have again provided excellent results – some of these highlights are presented in this report. We would like to invite all of you to attend a scientific symposium to be organized in the first half of 2013 to celebrate the most important scientific achievements made at DORIS III during its runtime as a synchrotron radiation source.

Experimental techniques that so far have only been available at DORIS III will be continued in the PETRA III extension, with the addition of 12 parallel useable experimental stations to the portfolio of techniques at PETRA III. They will be built in two new experimental halls in the north and east of the PETRA III storage ring close to the present experimental hall. Detailed planning of the experimental stations is still on-going with strong involvement of our user community, who actively participated in a series of dedicated workshops. Construction work for the PETRA III extension is scheduled to start in March 2013. Nearly all PETRA III instruments have been completed, and all the DESY operated beamlines at PETRA III were offered in the latest call for proposals. We expect that in 2012 all PETRA III beamlines will have taken up normal user operations. As one can see from the first highlight presented in this report, experiments at PETRA III are starting to result in exciting achievements. Due to the small emittance and beam sizes, focal spots around 80 nm are obtained routinely at some of the experimental stations; the minimum achieved were in the 10 to 25 nm regime. This will open up totally new areas for spatially resolved analytical techniques at very high resolution.

The operation of the free-electron laser FLASH in the year 2011 after the upgrade in 2009/2010 was almost as reliable as expected and similar to that of a storage ring facility. Down times were significantly reduced as compared to the time before the upgrade. Future activities will concentrate on the establishment of optimized operation conditions for extremely short pulses possible at or below 50 fs duration. A total of 29 user experiments taking place over 5000 operation hours were carried out during the last SASE run ending in September 2011. For the next run starting in January 2012, 77 proposals were submitted out of which about 20 will be able to receive beamtime. Despite the on-going construction work for FLASH II, we plan to provide roughly 3000 hours of beamtime per year as in the past years. This might be somewhat optimistic, since we currently do not have a reliable estimate of the influence that the construction work will have on FEL operations. We will do our best to provide excellent conditions for experiments but we also rely upon our users' understanding that conditions might not be ideal during that period.

The civil construction work for FLASH II began in September 2011, requiring the temporary shutdown of FLASH operations. In the first phase a new radiation protection building will be constructed close to the position of the present FLASH tunnel, where the beams for the two FEL undulators will be split. During the 2011/2012 winter shutdown of PETRA III the buildings at the crossing point of FLASH II and PETRA III will be established. In 2012 the FLASH II tunnel housing the FEL undulator and the new experimental hall to the east of the present FLASH hall will be built. The medium term goal is to also upgrade the present FLASH undulators to tuneable gap devices. We expect commissioning of FLASH II to start in 2013.

Brazil's Minister of Science and Technology Aloízio Mercadante (left) together with Edgar Weckert during his visit at DESY in April 2011.

With strong support by the German and Russian governments the financial gap caused by the financial dropout of some European countries for the European XFEL could be closed. The other contributing countries also indicated that they will increase their support. Being the German shareholder of the European XFEL GmbH, DESY particularly appreciates this positive development. So far the construction and preparation work for the European XFEL is perfectly on schedule. As a major milestone the boring of the main linac tunnel was finished in August 2011. The two electron beam tunnels and three out of five photon beam tunnels are also finished, allowing installation work to start. The shell of the six-story deep underground injector building is completed as well as the modulator hall and the access shafts. The concrete work for the underground experimental hall has started as well as design work for the laboratory and office buildings on the Schenefeld site. Almost all major components for the superconducting linear accelerator have been ordered. If everything continues to run smoothly, commissioning of the accelerator will start end of 2015 and possibly first user experiments will be carried out at the European XFEL in 2016.

The Center for Free-Electron Laser Science (CFEL) in Hamburg – a collaboration of the Max-Planck-Society, University of Hamburg and DESY to promote science at FELs – now numbers more than 140 people. Due to further delays of the construction of the new CFEL building, the move-in is now scheduled for May 2012. All people involved are desperately waiting for the new laboratories and offices. Scientists from CFEL have been extremely successful with their experiments at FLASH and LCLS at SLAC in Stanford. Highlights of their research can be found in this report.

The planning for a new Photon Science building at DESY has been further advanced. This building will be established in close proximity to the FLASH and PETRA III experimental halls. It is built in collaboration with the Helmholtz-Zentrum Geesthacht and will also house the DESY NanoLab with instrumentation to prepare, handle and characterize samples for experiments at PETRA III and FLASH. With this laboratory we intend to further strengthen our in-house research in that field but also to support users needing these techniques for their experiments at our photon facilities. According to the present plans the construction of the Photon Science building can start beginning of 2013. Another important building on our site will house the Centre for Structural Systems Biology (CSSB). CSSB is a collaboration of almost all renowned institutions dealing with infection research in the northern part of Germany. The main research direction of this institute will target the molecular mechanisms from the very first steps of infection using the different techniques available at the DESY photon sources. The federal government together with the local ministers of science and education (Hamburg and Niedersachsen), made available about 50 M€ in total for civil construction and first instrumentation. The new building will be constructed close to the EMBL laboratories and the PETRA III experimental hall. It will provide offices and laboratory space for about 180 people. The expected date for the start of construction is in 2013 as well.

During 2011 many interesting scientific results have been achieved by our users and by in-house staff in measurements conducted not only at our own sources but also at other facilities. This report provides a glimpse of these activities. We hope that you will enjoy reading the different science highlights as well as about technical and instrumental developments. Without dedicated and very motivated people all the activities taking place at present in photon science at DESY would not be possible. This applies to our DESY staff members, and also to our collaborators and users. Let me take this opportunity to thank all for their effort and continuous support.

Finally, let me wish all of you a personally and scientifically most successful year 2012,

Edgar Weckert
Director Photon Science

News and Events.

News and Events.

A busy year 2011

January

7 January:
Signing of the agreement for the construction of the Centre for Structural Systems Biology

On 7 January the Federal Minister of Education and Research Annette Schavan, Hamburg State Minister Herlind Gundelach, and Lower Saxony Minister of Science and Culture Johanna Wanka signed the federal and state-government agreement for the construction of the "Centre for Structural Systems Biology (CSSB)". In the future, infection researchers and physicists in Northern Germany will collaborate in the hunt for pathogens: the interdisciplinary centre with several universities and research facilities from Hamburg, Lower Saxony and Schleswig-Holstein as partners will pursue the goal to identify attacks by pathogens at atomic resolution. The new CSSB research centre will foster interdisciplinary projects, thus easing the use of the ultra-modern radiation sources on the DESY campus. The CSSB is funded with 50 million Euros. The call for tender for detailed planning is in preparation.

Federal Minister Annette Schavan (centre), Hamburg State Minister Herlind Gundelach (right), and Lower Saxony Minister Johanna Wanka (left) signed the federal and state-government agreement for the construction of CSSB.

26-28 January:
Joint European XFEL and HASYLAB Users' Meeting

For the second time the European XFEL Users' Meeting and the Annual Users' Meeting of HASYLAB were organized in a joint 3-day program with sessions devoted to the European XFEL in its project and building phase, scientific applications at the Free-Electron Laser FLASH, and the photon science activities at DORIS III and PETRA III.
The large number of participants reflected the success of the meeting. DESY could welcome more than 400 guests from 25 countries. They enjoyed the opportunity to learn at a single meeting about progress in the areas of soft and hard X-ray free-electron laser (FEL) and of synchrotron radiation experiments. The meeting started with a full day of lectures on the status of the European XFEL project, including user activities and envisaged scientific applications.
On the second day, two sessions presented the status of the FLASH facility with the FLASH II extension, and scientific experiments carried out using soft X-ray FEL radiation. In parallel a satellite meeting on status and perspectives of small angle X-ray scattering at DESY took place with more than 80 participants.

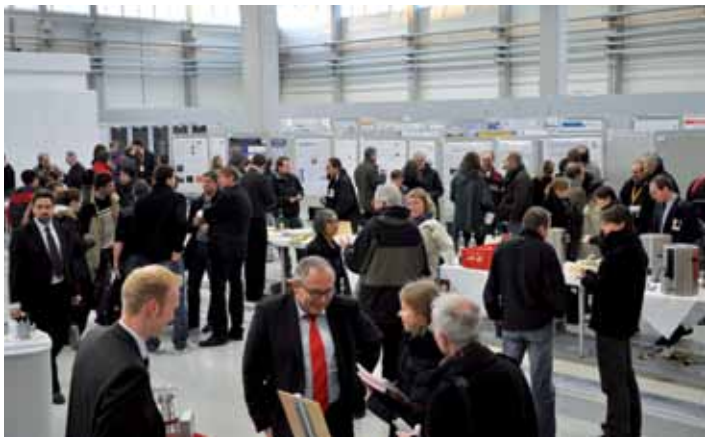

The concluding poster session of the joint European XFEL and HASYLAB users' meeting took place in the DESY AMTF hall.

The third day gathered 350 attendees to hear about present and future activities of Photon Science at DESY as well as selected scientific highlights obtained at the DESY photon sources in 2010. The concluding poster session brought together 200 user contributions and an industrial exhibition with 41 vendors.

February

27 January:
Old Masterpieces in new light

The HASYLAB Users' Meeting opened to the public with lectures on research at DORIS III and PETRA III on cultural heritage topics. International experts on art conservation presented modern methods to unravel techniques and materials applied by artists. Examples presented the visualisation of "lost paintings" underneath paintings on reused canvases, hidden handwritings as well as texture analysis of medieval jewellery. In addition, case studies were presented on conservational aspects of cultural heritage objects and exciting perspectives were outlined.

The lectures about research on cultural heritage using synchrotron radiation in the DESY auditorium were well-attended.

The lecturers together with a typical subject of investigation.

21 February:
Workshop on XUV photoionization phenomena of dilute species

This "Joint Kick-off" workshop gathered 39 participants to initialize the working periods of two projects funded by the German BMBF (Bundesministerium für Bildung und Forschung) within the framework of the German-Russian Cooperation "Development and Use of Accelerator-Based Photon Sources". The workshop featured oral and poster contributions ranging from X-ray photon diagnostics to the details of molecular photoionization including fundamental physics and was even touching philosophical aspects. The two bilateral cooperation projects ("A photoionization database for FEL photon diagnostics" led by Kai Tiedtke and "Correlation and Polarization Phenomena" led by Jens Viefhaus) will collaborate on joint theoretical and experimental efforts and include also collaborators from other European countries besides Russia.

Attendees of the workshop on XUV photoionization phenomena of dilute species.

March

25 February:
Memorandum of Understanding for a Swedish Materials Science Beamline at PETRA III

On 25 February Sweden became a partner of PETRA III. Leif Eriksson from the Swedish Research Council and the DESY Directors Helmut Dosch and Edgar Weckert signed a memorandum of understanding about the „Swedish Materials Science Beamline“, a beamline for materials and nano science experiments at high photon energy (E > 50 keV), which will be realised with substantial funding from the Swedish Research Council. Whereas DESY contributes its expertise in the construction of the beamline, representatives of the scientific communities of both countries share the responsibility for the scientific case. With this beamline and its specific research focus one can look forward to strengthening the use of synchrotron radiation by industrial users at the photon sources at DESY.

Signing of the memorandum of understanding for a Swedish materials science beamline at PETRA III. From left to right: Ulf Karlsson, State Secretary Peter Honeth, Leif Eriksson (sitting), State Secretary Georg Schütte, Helmut Dosch (sitting), and Edgar Weckert.

17 March:
First European XFEL accelerator module delivered

The first European XFEL accelerator module assembled at Saclay (France) has been delivered at the Accelerator Module Test Facility (AMTF) hall. The module is 12 metres long and weighs 7.5 tons. In the AMTF hall every single accelerator module and cavity of the upcoming serial production will be tested under operating conditions before being installed into the European XFEL tunnel.

The first accelerator module for the European XFEL is unloaded with the AMTF hall crane.

30 March:
X. Research Course on X-Ray Science: Ultrafast X-Ray Science with X-Ray Free-Electron Lasers

The aim of the periodic DESY research courses is to provide basic knowledge about new directions of X-ray research to Diploma (Master) and PhD students and to young research fellows. The 10th course of this series was dedicated to the topic of ultrafast X-ray science. Twelve international speakers presented the latest experimental developments and scientific applications of ultrafast X-ray science at free-electron laser sources. The young researchers had the opportunity to obtain first-hand information about new results and achievements from LCLS and FLASH and to discuss with the leading experts in the field. Overall 100 participants from all over Europe assembled during the 3 day course in the FLASH seminar hall. The course was accompanied by a poster session and tours of FLASH and PETRA III.

6 April and 5 May:
Cooperation agreement with Brazil

A visit of Brazil's Minister of Science and Technology Aloízio Mercadante on 6 April to DESY and the European XFEL GmbH concluded the "German-Brazilian Year of Science, Technology and Innovation". He was accompanied by the director of the Brazilian Synchrotron Light Laboratory (LNLS, Campinas-SP), José Roque da Silva. Brazil is Germany's most important scientific partner in South America: it operates the only synchrotron radiation source on that continent and plans the construction of a 3rd generation synchrotron radiation source. Moreover, the country is interested in the development of accelerator-based free-electron lasers.

On the occasion of his visit to DESY and European XFEL Brazil's Minister of Science and Technology, Aloízio Mercadante receives a present from Helmut Dosch and Massimo Altarelli: the model of a superconducting accelerator cavity.

The three directors of DESY, the European XFEL GmbH and the Brazilian synchrotron laboratory LNLS signed an agreement on future cooperation. This event took place on 5 May in Brasilia in the presence of Germany's Federal President Christian Wulff and Brazil's President Dilma Rousseff. President Roussef pointed out Brazil's plans to create 75 000 international scholarships in the coming years for university students, 10 000 of them will be going to Germany. Thus, DESY is looking forward to one of the first consequences of this trilateral agreement: the admission of Brazilian students and junior scientists to DESY and the European XFEL GmbH.

After signing the cooperation agreement with Brazil in the President's Palace in Brasilia. From left to right: José Roque da Silva, Christian Wulff, Dilma Rousseff, Helmut Dosch, and Massimo Altarelli (Photo: DWIH São Paulo).

5 May:
Workshop on Dynamic X-ray Diffraction & Spectroscopy Experiments at Extreme Conditions: Implementing time resolved experiments at 3rd and 4th generation light sources

Dynamic diffraction and spectroscopy experiments at extreme high temperatures and pressures have been capturing the interest of the high pressure community during the last few years. The Extreme Conditions Beamline (ECB) P02 at PETRA III will have a strong research focus on dynamic diffraction experiments at extremes. A similar research focus is being pursued for the High Energy Density (HED) instrument at the European XFEL. Therefore, DESY and European XFEL co-organized a workshop to discuss the scientific case addressed with time resolved diffraction and spectroscopy experiments and the corresponding technical requirements at 3rd and 4th generation light sources. Future plans for time resolved techniques were presented as well as dynamic experiments using a laser heated diamond anvil cell (DAC), gun and laser shock. Two major research areas solidified: Time-resolved experiments and experiments at not yet accessible regimes of pressure, temperature, and electromagnetic-field strength.

Participants of the workshop on experiments under extreme conditions.

16 May:
Workshop of the Helmholtz High Data Rate Initiative

The High Data Rate Initiative (HDRI) is a project of the six centres of the Helmholtz Association dedicated to research with photons, neutrons, and ions, i.e. DESY, KIT (Karlsruhe), FZJ (Jülich), HZB (Berlin), HZG (Geesthacht), and GSI (Darmstadt). The project addresses the challenges related to the increasing data volumes and data rates of present and future experiments in these research fields. It comprises three work packages: Data Management (WP1), Real Time Data Processing (WP2), and Data Analysis, Modelling and Simulation (WP3). Fields covered were a common standard data format based on NeXus/HDF5, the status of the development of detector front end electronics based on field programmable gate arrays (FPGA) and the first Graphics Processing Unit (GPU) based demonstrator for fast data evaluation, which at present serves as a prototype for reconstruction of tomographic data.

23 May:
Starting shot for the "Ioffe-Röntgen Institute"

DESY and the Kurchatov Institute started the German-Russian Year of Science with the creation of a common institution. On 23 May in Moscow, DESY directors Helmut Dosch and Edgar Weckert and the director of the Kurchatov Institute Mihail Kovalchuk signed a letter of intent for the foundation of the Ioffe-Röntgen Institute (IRI). The signing took place in the presence of German Federal Minister of Research Annette Schavan and her Russian colleague Andrei Fursenko. Both ministers had previously inaugurated the German-Russian Year of Education, Science and Innovation at a festive event that took place in the auditorium of the Lomonossov University. The new Ioffe-Röntgen Institute will be the "umbrella institution" for all bilateral projects and initiatives within the scope of large research facilities. The names of the institute go back to the discoverer of X-ray radiation Wilhelm Conrad Röntgen and the Russian physicist Abram Fjodorowitsch Ioffe who was a PhD student of Röntgen and who is considered to be the father of Russian semiconductor physics.

Helmut Dosch and the director of the Kurchatov Institute, Mihail Kovalchuk in Moscow.

31 May:
Cooperation agreement signed in Delhi with the Saha Institute of Nuclear Physics

In India's capital Delhi Chancellor Angela Merkel accompanied by a delegation including the DESY directors Helmut Dosch and Christian Scherf signed an agreement for co-operation between DESY and the Saha Institute of Nuclear Physics (SINP, Kolkata) represented by its director Milan Sanyal. The intention of the partners is to extend future co-operation between both countries in the field of large-scale research infrastructures. The current agreement with SINP now provides the legal framework for a variety of individual projects and initiatives. The first concrete activity is already arranged to a great extent: within the framework of a collaboration to use the high-energy synchrotron radiation, SINP will contribute 14 million Euros for the construction and operation of a beamline in one of the PETRA III extensions.

Signing Ceremony for the German Indian cooperation agreement. From left: DESY Director Helmut Dosch, German Chancellor Angela Merkel, Indian Prime Minister Manmohan Singh and SINP Director Milan Sanyal.

June

20 June:
Ultrafast X-ray Summer School 2011

The Center for Free-Electron Laser Science (CFEL) hosted the Ultrafast X-ray Summer School 2011 (UXSS 2011). The school was jointly organized by CFEL and the PULSE institute at SLAC National Accelerator Laboratory, whereas financial support was provided by the VolkswagenStiftung. The summer school program was highly interdisciplinary, with topics ranging from accelerator physics to molecular biology, and gave doctoral students and postdoctoral researchers the opportunity to familiarize themselves with the latest developments in ultrafast X-ray science. Each lecturer gave a 60-minutes didactic introductory talk to provide a broad overview of a certain research area, followed by a 30-minutes discussion. After that, a 30-minutes talk on the lecturer's own work allowed a deeper insight into state of the art research themes. The feedback given by the school participants clearly showed that the format was very well received.

July

1 July:
DESY participates in two new Virtual Institutes of the HGF

With beginning of July the Helmholtz Association started the funding of new Virtual Institutes. They are intended to promote the cooperation of university and non-university scientists in common projects. DESY is partner in two of them. In the Virtual Institute "In-Situ Nano-Imaging of Biological and Chemical Processes", launched under the aegis of DESY, the expertise of X-ray microscopy, biology, and chemistry is brought together to develop in-situ imaging methods of biological and chemical processes. The methods involve X-ray microscopy at PETRA III and FLASH and in the future also at the European XFEL. This Virtual Institute will be funded for a period of five years with a total of 2.5 million Euros. Besides DESY, participating institutions are Karlsruhe Institute of Technology, KIT and the universities of Dresden, Göttingen and Heidelberg. Moreover, DESY takes part in the Virtual Institute "Dynamic Pathways in Multidimensional Landscapes", funded by the Helmholtz Association for a period of four years with a total of 2 million Euros. This institute is coordinated by HZB (Berlin) and has several national and international partners, including SLAC (United States). Using the accelerator-based X-ray sources of both participating Helmholtz centres, it will analyse the behaviour of complex materials in dependence of energy, space and time.

19 July:
Start of DESY Summer Student Program 2011

The DESY summer student program started on 19 July. The part of the program related to research with synchrotron radiation was attended by 28 undergraduate students from Italy, Belgium, Colombia, Hungary, Poland, Russia, Slovakia, Spain, Thailand, and Germany. The students were selected from 74 applicants, graduating in various fields of natural sciences. They were distributed among the different photon science research groups at DESY, CFEL, EMBL, and European XFEL, where they participated in the everyday work and were assigned a small project of their own to work on. This was accompanied by a series of common lectures about DESY activities in general, including

The students of the photon science related part of the DESY summerstudent program 2011.

accelerator and particle physics and a series of lectures on research with synchrotron radiation introducing the different experimental techniques in greater detail. The lecture series was followed by an exercise week, in which the students had the possibility to perform experiments in small groups at various experimental stations at DORIS III. The stay of all DESY summer students ended on 8 September with a final student session during which selected participants gave brief presentations of their projects during the stay. The program was again very well received by the students who also appreciated the pleasant atmosphere at DESY. Many participants consider coming back to DESY as a PhD student or postdoc.

27 July:
Boring of European XFEL accelerator tunnel completed

The tunnel boring machine TULA (TUnnel for LAser) arrived at the injector building on the DESY-Bahrenfeld site with a “landing precision” of one millimetre. Drilling this 2.1-kilometre-long tunnel for the accelerator part of the European XFEL has been completed after only 13 months, in time and without accidents. The remaining tunnels for the different undulator segments should be completed at the end of 2011.

On 29 July 2011, two days after TULA’s arrival at the DESY site, the tunnel builders opened the travel-out panel so that the cutterhead showed again after seven months of underground work.

August

29 August:
Workshop on the Swedish beamline at PETRA III

The 2nd workshop on the Swedish Materials Science (SMS) beamline at PETRA III was held at DESY to further discuss the possibilities for scientific applications and techniques at the new beamline and to foster the interaction of interested scientists from Sweden with colleagues at DESY. It was organized by the Swedish Research Council which is funding the construction of the beamline and, later on, will give a substantial contribution to its operation.
Edgar Weckert presented an overview of the scientific program at PETRA III stressing the new opportunities enabled by the extremely high-brilliance in the hard X-ray regime in the main working range 50 - 150 keV of the beamline. Ulf Karlsson (Royal Institute of Technology, Stockholm), one of the architects of the Röntgen-Ångstrom Cluster (RAC), spoke on the guiding idea of the RAC and of the participation of the Swedish scientific community in the SMS beamline, emphasizing the complementarity of the high-energy SMS beamline to the lower energy MAX-IV beamlines. Wolfgang Drube introduced the PETRA III extension project which will provide ten additional beamlines in two new experimental halls (East and North). The SMS beamline will be located in hall East making use of a long straight section of the storage ring. In the following, scientists from DESY, MAX-IV and from several Swedish universities presented their current activities in the field of materials science and gave an outline of future perspectives.

September

14 September:
HAXPES 2011, 4th International Workshop on Hard X-ray Photoelectron Spectroscopy

DESY was hosting the International Workshop on Hard X-ray Photoelectron Spectroscopy, "HAXPES 2011", the 4th in a series of workshops which started at ESRF in 2003, followed by SPring-8 in 2006 and NSLS in 2009. The HAXPES technique is rapidly developing at synchrotron facilities worldwide since it adds true bulk sensitivity to the well-known strengths of photoelectron spectroscopy, making it a powerful tool for electronic structure studies of complex materials, buried nano-structures and multi-layered systems relevant for device applications. The three-day workshop brought together experts in the field, presented an overview of recent activities and achievements and provided a platform for the discussion of emerging new applications and future trends. It was very well attended by 140 participants; 57 % came from abroad demonstrating the strong international interest in this field. The largest foreign group was from Japan reflecting the numerous HAXPES activities at SPring-8.

The participants of the HAXPES 2011 workshop.

20 September:
Construction start for FLASH II

In recent years, the free-electron laser FLASH has been generating X-ray laser light for an ever increasing community of users. Now construction started for the next expansion stage FLASH II, with the aim to serve more users and at the same time apply the most recent developments of FEL technology. The extension of FLASH is one of the strategic investments of the Helmholtz Association, which provides nearly 30 million euros for the FLASH II project. Commissioning of the free-electron laser is planned for 2013. In a new experimental hall next to the existing FLASH hall, five measuring stations will gradually be available for the use of the highly demanded FEL light for research. For this purpose, the existing superconducting linear accelerator is extended with a second tunnel section including a second line of undulators. These special magnets generate X-ray light by forcing up to 8000 electron bunches per second on a slalom run through the accelerator, thus emitting radiation. The laser light is then distributed to individually equipped beamlines, with the possibility to use wavelengths down to 4 nanometres.

First digging at the FLASH accelerator tunnel marks the construction start for FLASH II.

Sketch of FLASH II (left) and FLASH (right).

22 September:
Workshop on Temporally and Spatially Resolved Dynamical Phenomena

This workshop took place at the DESY campus on 22 and 23 September, jointly organized and supported by DESY and European XFEL. It consisted of 12 invited presentations from world-class experts in the dynamics of complex systems, and a total of about 35 participants, experts in X-ray and ultrafast science. The aim of the workshop was to identify those scientific key challenges that, if solved, would have a big impact in their fields, and which could represent a next generation of ground breaking applications for XFELs. Various topics ranging from protein dynamics to solvated molecules, phase transitions and material science were covered. The workshop allowed much time for discussion, and several proposals for possible experiments and future research directions emerged from the event.

27 September:
X-ray micro-fluorescence spectroscopy at the PETRA III extension: 2nd user workshop

The PETRA III extension project will provide new experimental infrastructure, partially to compensate for the shutdown of DORIS III end of 2012. Among these, DESY is planning to build a micro-fluorescence spectroscopy beamline (P63) which will be designed to cover and extend the range of applications currently in the focus of the DORIS III beamline L, namely X-ray microanalysis using different methods like fluorescence and absorption. The workshop was held with the aim to finalize the conceptual design by presenting the current layout of the beamline optics and discussing the user requirements for the experimental area. The workshop was attended by about 25 participants including four invited speakers. Besides the present status of the project, the possible source and the optical layout of the beamline, similar facilities at the Diamond and Soleil light sources were presented and discussed with the user community. Further important themes addressed by the workshop were new technical developments, especially in the field of fluorescence detectors. The presentation of the planned experimental layout and a lively discussion about the user demands concerning the experimental area concluded the workshop.

29 September:
EXAFS-Beamlines at the PETRA III Extension: 2nd user workshop

The 2nd user workshop on the planned two EXAFS beamlines at the PETRA III extension (beamlines P64 and P65) took place on 29 and 30 September. About 20 participants from Germany and from abroad discussed the layout especially that of the insertion device and the high heat load monochromator for P64, as well as instrumentation and scientific applications. An overview of the beamline status given by Wolfgang Caliebe and Edmund Welter was followed by status reports of two related projects supported in the frame of the BMBF collaborative research (“Verbundforschung”). Talks about the bio-XAFS project, the PETRA III beamline P06 and the XAFS beamlines at both the Diamond Light Source and the Australian Synchrotron gave important input to the discussions.

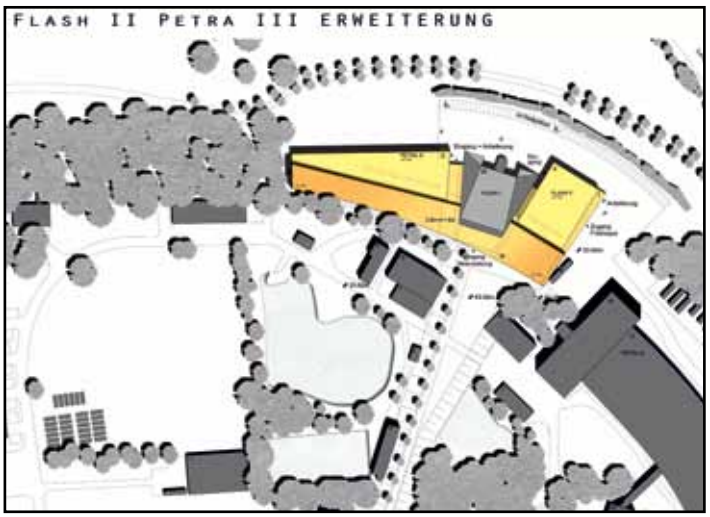

The architects’ conception of the building complex PETRA III extension and FLASH II. (Courtesy Architekturbüro Renner Hainke Wirth)

October

10 October:
GISAXS 2011

After previous GISAXS workshops held at DESY in 2005 and 2007 the third workshop on grazing incidence small angle X-ray scattering took place from 10 to 12 October. The event was mainly addressed to young scientist using or planning to use GISAXS. The workshop was attended by 90 participants and offered a series of lectures on different aspects of the method. The talks, grouped in the sessions “Theory”, “From 2D to 3D”, “Advanced Materials”, “Soft X-rays”, “Soft Films”, “Deposition Methods”, and “Instrumentation”, introduced on one hand the fundamental basics and on the other illustrated actual research in this field. The 15 lecturers came from European countries, the United States, and Japan. In a poster session with 28 contributions the participants could present and discuss their own research work. Practical courses in smaller groups at the DESY SAXS experimental stations BW4 and P03 and training in data analysis and data modelling were also on the agenda. The reaction of the participants after the workshop was again very positive and encourages the organizers to offer further GISAXS workshops in the future.

The participants of the GISAXS 2011 workshop.

12 October:
Workshop on New Science Opportunities at FLASH

The construction of FLASH II, which will double the beamtime capacity of FLASH, has started in September 2011. This was the motivation to discuss new science opportunities at FLASH with its user community. On the first day of the three day workshop the expected parameters of FLASH II and first concepts for the beamlines, photon diagnostics, and pump-probe facilities were introduced to over 150 participants. A set of 10 facility talks was rounded off with news about FLASH and the long term perspective for the entire FLASH facility. The second and third day were devoted to new scientific achievements at FLASH and novel ideas for FLASH instrumentation and experimental setups, which were presented by the user community in 20 contributed talks and a poster session with over 40 contributions. A special focus was given to proposals for long-term experimental end stations of user collaborations. The experiment proposals span a large range of source parameters. A wavelength range from 80 nm to below 2 nm to cover the transition metal L edges, as well as a variety of pulse lengths and bunch train repetition schemes pose new challenges for the beamline and diagnostics design.

The attendees of the workshop on new science opportunities at FLASH looking upward to a bright future.

13 October:
Small Angle X-ray Scattering at the PETRA III Extension: 2nd user workshop

The second user workshop on the small angle X-ray scattering beamline P62 planned at the PETRA III extension took place on 13 and 14 October. Many of the discussion results of the first workshop held in June 2010 found their way into the conceptual design which was now presented by Rainer Gehrke to the 25 participants as a basis for further discussion. The experiment setup will feature a SAXS camera with up to 20 m sample-to-detector distance and a large variety of experimental options including measurements in transmission or grazing incidence geometry with different positions of sample and detectors as well as the

use of anomalous scattering. Along with a couple of presentations by users about their scientific plans, the technical demands on sample environments and possible joint user contributions to the experimental infrastructure were discussed and possible co-operations among the users were identified. It turned out that in this context in situ rheometry is one of the most prominent fields for joint effort of various user groups.

29 October:
DESY Open Day and Hamburg Science Night

Practical experiments during the DESY open day likewise attracted the attention of young visitors and experienced scientists (Photo: Daniel Drexelius).

It was a Science Festival at DESY: until midnight, thousands of curious people flocked to the DESY campus. The DESY Open Day and Hamburg Science Night census counted a total of 13 621 visitors at the DESY admission points. More than 20 000 people participated in the 4th Hamburg Science Night. DESY was one of 45 science facilities opening their doors to the public. Thus, two out of three participants of the 4th Hamburg Science Night also visited DESY. One of them was the Hamburg Science Senator, Dr. Dorothee Stapelfeldt. Visitors could gain insight into work at DESY at more than 60 attractions. They were fascinated by numerous highlights including the tunnel of Germany's largest accelerator HERA, the X-ray laser FLASH or the huge experimental hall of PETRA III. The first visitors already came before the official opening at noon and the last ones a quarter to midnight. Not only top-level research interested many people, but also activities of the DESY workshops and the school lab were very popular among both young and old. There were many possibilities for hands-on experiences like getting your own Bobby Car driving distance precisely measured with a laser or making a vacuum experiment with a chocolate marshmallow in a preserving jar. About 850 helpers explained DESY to guests, distributed 21600 gum bear bags, 4400 balloons and 3000 apples with a DESY logo on it. More than 1000 young scientists took a rally through the FLASH X-ray laser hall to win a Pixibook special edition about DESY.

November

3 November:
PhD Thesis Prize for Martin Beye

This year's PhD thesis prize of the Association of the Friends and Sponsors of DESY is shared by Martin Beye and Roman Kogler, both from the University of Hamburg. The very intensive and ultra-short X-ray pulses of FLASH allow taking snapshots of the movement of electrons and atoms with highest time resolution. For his PhD thesis on this subject Martin Beye worked in the group of Professor Wurth at a series of internationally much-noticed experiments and gained completely new insights into the dynamics of matter. Among other things he experimentally observed a new liquid phase of silicon for the first time. This has a far reaching significance to understanding the properties of liquids, e.g. the well-known density anomaly of water at 4 centigrade. Martin Beye, born 1981 in Salzgitter, began to study physics in 2002 at the University of Hamburg. In 2007 he obtained his diploma degree with distinction. He graduated at the free-electron laser FLASH within the frame of a DESY scholarship. The thesis of Roman Kogler was elaborated in the H1 Collaboration at HERA. The PhD thesis award of the Association of the Friends and Sponsors of DESY includes 3000 euros prize money. Every year, the association presents this prize for one or two outstanding PhD theses.

Friedrich-Wilhelm Büßer, chairman of the "Association of the Friends and Sponsors of DESY" and Helmut Dosch together with the winners of the PHD thesis award 2011 Martin Beye (left) and Roman Kogler (right).

December

11 November:
DESY and University of Kiel sign co-operation Agreement

The Christian-Albrechts-University (CAU) of Kiel and DESY intensify their long lasting co-operation which started already back in the 1970th. The president of CAU, Gerhard Fouquet, the dean of the faculty of mathematics and natural science, Lutz Kipp and the DESY directors Helmut Dosch and Edgar Weckert signed an agreement for an even closer collaboration. Research groups in Kiel with the exploratory focus on nano science will actively participate in further development and operation of the synchrotron radiation facilities at DESY. This includes the creation of two new research groups led by professors commonly appointed by CAU and DESY.

Signing of the cooperation agreement between DESY and Kiel University. From left: Edgar Weckert, Christian Scherf, Helmut Dosch, Lutz Kipp (Dean of the faculty of mathematics and natural science), Frank Eisoldt (Chancellor of CAU), and Gerhard Fouquet (President of CAU).

1 December:
Innovation Award on Synchrotron Radiation for DESY Scientists

The 2011 Innovation Award on Synchrotron Radiation of the Association of Friends of Helmholtz-Centre Berlin was bestowed to Sergey V. Bobashev (Loffe Physico-Technical Institute, St. Petersburg), Ulf Jastrow (DESY Hamburg), Udo Kroth (PTB Berlin), Mathias Richter (PTB Berlin), Andrey A. Sorokin (DESY Hamburg), and Kai Tiedtke (DESY, Hamburg) for their decisive role and excellent contributions in the development and implementation of gas monitor detectors for FEL radiation applications. Since 2001, this prize is announced Europe wide for outstanding technical achievements or experimental methods that promise to extend the frontiers of research with synchrotron radiation.

The prize winners of the 2011 Innovation Award on Synchrotron Radiation of the Association of Friends of Helmholtz-Centre Berlin. From the left: Udo Kroth, Mathias Richter, Andrey Sorokin, Kai Tiedtke, Ulf Jastrow, Sergey Bobashev.

7 December:
Advanced Grant of the European Research Council for Stephan Förster

For his investigations on nanoparticle growth at DESY's X-ray source PETRA III, Professor Stephan Förster from Bayreuth University is honoured with the highest science award of the European Research Council (ERC). The so-called ERC Advanced Grant is endowed with 2.4 million euros and is presented for particularly promising research projects.
Förster investigates how atoms accumulate to small clusters in liquids and how these nanoparticles grow. These findings are not only important for basic research but also valuable for the development of new materials and for energy, information and medical technologies. For his experiments, the Bayreuth scientist uses the microfocus beamline P03 (MiNaXS) at PETRA III.

Research Highlights.

X-ray optical transparency induced by nuclear excitation.

Vanishing X-ray absorption via quantum interference in a cavity

Electromagnetically induced transparency (EIT) is a basic phenomenon in quantum optics through which an opaque medium becomes transparent near an atomic resonance by the coupling of two laser fields to the same excited state [1]. Utilizing EIT, one can employ light to control the optical properties of matter, enabling numerous applications like nonlinear optics at the few-photon level [2], light speed reduction to a few m/s [3], lasing without inversion [4] and others. Using high-brilliance synchrotron radiation at PETRA III, we demonstrate EIT in the regime of hard X-rays by exploiting the collective emission from ensembles of ^{57}Fe Mössbauer nuclei embedded in a planar cavity. This opens new routes to exploit EIT and its applications at X-ray energies, effectively establishing the field of nuclear quantum optics.

The phenomenon of EIT arises when two laser fields compete for the excitation of the same atomic level from both the ground state and another (metastable) state. If one of the fields is very strong, it prevents the absorption of the other due to quantum interference effects – the material appears to be transparent for this wavelength. EIT is well established in optical sciences [1] and currently receives renewed interest because it holds promises, e.g., for quantum information processing at the level of single quanta of light and matter [5].

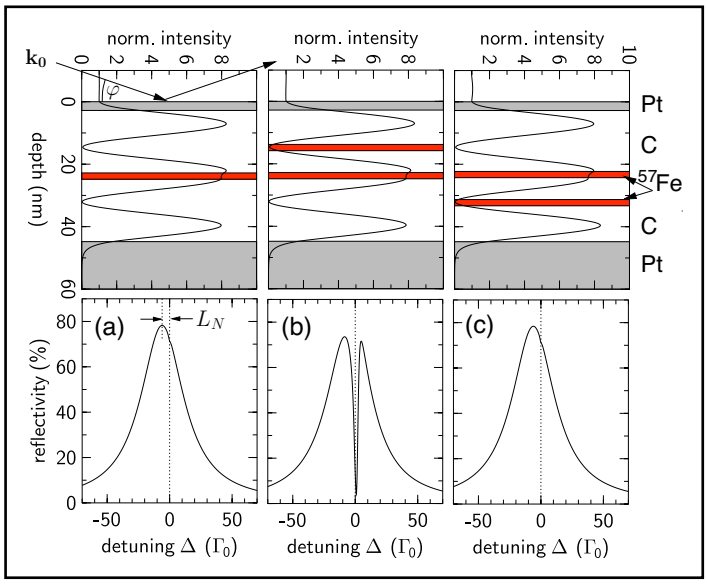

Figure 1

Nuclear resonant reflectivity spectra (bottom) of a planar Pt/C/Pt X-ray cavity containing thin layers of ^{57}Fe nuclei (red) in different locations relative to the standing wave within the third-order mode of the cavity (top). The spectrum in (b) exhibits a strong dip at the exact resonance energy (detuning $\Delta = 0$) which is the signature of electromagnetically induced transparency (EIT).

Here we extend the concept of EIT into the X-ray regime by employing the Mössbauer isotope ^{57}Fe which is a nuclear two-level system with a transition energy of 14.4 keV and a natural linewidth of $\Gamma_0 = 4.7$ neV. At first sight it seems to be unclear how to achieve nuclear EIT because nuclear three-level systems with a metastable level are not available to establish conventional EIT schemes.

The key to the realization of nuclear EIT is cooperative emission from ensembles of Mössbauer nuclei that are properly placed in a planar cavity. The resonant interaction of a large number of identical atoms with a common radiation field leads to a profound modification of the temporal, directional and spectral characteristics of the collective (= cooperative) emission compared to that of a single atom. Due to its high resonant cross section the 14.4 keV transition of ^{57}Fe is a well-suited two-level system for such studies. We already used this isotope to explore superradiant emission and the collective Lamb shift for a single ensemble of atoms located in an antinode of the field within a planar cavity [6]. Fig. 1a shows the calculated energy spectrum of the reflectivity of such a cavity that is excited in its third-order mode at a grazing angle of $\varphi = 3.5$ mrad.

A qualitatively new situation is encountered when two resonant ^{57}Fe layers instead of one are placed in a cavity. A pronounced dip in the spectral response appears when one of the ^{57}Fe layers is placed in a node, the other one in an antinode of the standing wave in the cavity, see Fig. 1b. This dip is the spectral fingerprint of EIT. It depends sensitively on the distance and the location of the two resonant layers within the cavity. For example, the EIT effect completely vanishes if the two layers occupy the sequence antinode-node instead of node-antinode if seen from the top surface of the cavity, see Fig. 1c.

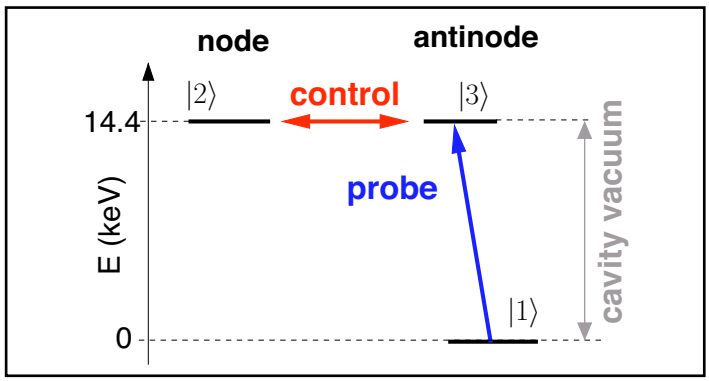

Figure 2

Effective three-level scheme of the nuclei in the cavity, resulting from the placement of two nuclear ensembles in a node and an antinode of the cavity field. The cavity vacuum field couples the two upper states and induces a strong control field from which the transparency for the probe field originates.

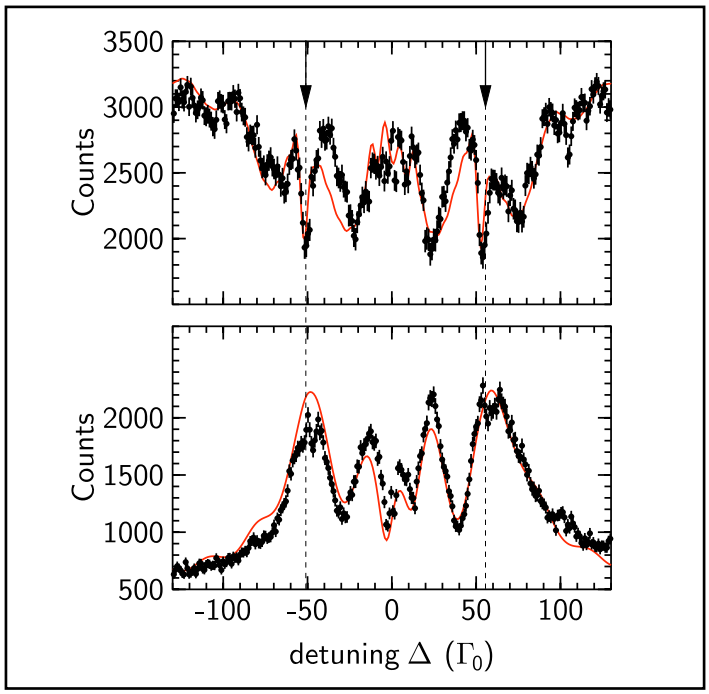

Figure 3

Measured energy spectra of the reflectivity of sample A (top) and sample B (bottom). The EIT effect manifests as pronounced dips at the position of the arrows. Due to the particular method of data acquisition the off-resonance baseline in both datasets is located at different levels. Both spectra are well described by the theoretical simulation (red solid lines).

Cooperative emission plays a crucial role for EIT in this system. While the layer in the antinode exhibits a very fast superradiant decay, the layer located in the node remains subradiant with a slow decay, thus representing the metastable state in the three-level scheme of EIT. Effectively, the cavity causes the nuclei to behave as three-level systems, see Fig. 2. Eventually, the radiation field in the cavity mixes the two upper levels and the resulting quantum interference leads to a pronounced transparency at the exact resonance energy of the nuclei where the system would be completely opaque otherwise. The formal description of the spectral response is fully equivalent to that of conventional EIT so that in case of nuclear EIT the same quantum optical phenomenology can be expected.

For an experimental verification of the EIT effect we have prepared two planar X-ray cavities consisting of a (3 nm Pt)/(38 nm C)/(10 nm Pt) layer structure with two 3 nm thick ^{57}Fe layers embedded in the C guiding layer, located in a node and an antinode of the third-order cavity mode as sketched in Fig. 1b (sample A) and Fig. 1c (sample B). The internal magnetic hyperfine field causes a splitting of the nuclear resonance into four well-separated lines. The experiments were performed at the Dynamics Beamline P01 of PETRA III in the 40-bunch mode of operation. To determine the energy spectrum of the cavity reflectivity from the time-resolved data we have employed a resonant energy analyzer foil mounted on a Doppler drive to vary the energy detuning Δ around the resonance [7]. The results are shown in Fig. 3. Sample A shows striking evidence for EIT as predicted. Its spectral response exhibits transparency dips (indicated by the arrows) that are particularly pronounced at the outer (and strongest) resonance lines of the hyperfine-split spectrum at detunings of $\Delta = \pm 51\ \Gamma_0$. As expected, in sample B the EIT effect vanishes due to the reversal of the layer sequence in node and antinode of the cavity field.

Our experiment paves the way towards coherent control of nuclear levels with X-rays. It opens the door to explore quantum optical concepts and nonlinear optics at X-ray energies, which is particularly appealing in view of the upcoming X-ray laser sources.

Contact: Ralf Röhlsberger, ralf.roehlsberger@desy.de

Authors

Ralf Röhlsberger, Hans-Christian Wille, Kai Schlage, Balaram Sahoo
DESY, Notkestraße 85, 22607 Hamburg, Germany

Original publication

"Electromagnetically Induced Transparency via Resonant Nuclei in a Cavity", Nature (in press, 2011).

References

1. **M. Fleischhauer, A. Imamoğlu, J. P. Marangos, "Electromagnetically induced transparency : Optics in coherent media", Rev. Mod. Phys. 77, 633 - 672 (2005).**
2. **H. Schmidt and A. Imamoğlu, "Giant Kerr nonlinearity obtained by electromagnetically induced transparency", Opt. Lett. 21, 1936 – 1938 (1996).**
3. **L. V. Hau, S. E. Harris, Z. Dutton, and C. H. Behroozi, "Light speed reduction to 17 metres per second in an ultracold atomic gas", Nature 397, 594 - 598 (1999).**
4. **M. O. Scully and M. Fleischhauer, "Lasers without inversion", Science 263, 337-338 (1994).**
5. **M. Mücke, E. Figueroa, J. Bochmann, C. Hahn, K. Murr, S. Ritter, C. J. Villas-Boas and G. Rempe, "Electromagnetically induced transparency with single atoms in a cavity", Nature 465, 755 (2010).**
6. **R. Röhlsberger, K. Schlage, B. Sahoo, S. Couet and R. Rüffer, "Collective Lamb shift in single photon superradiance", Science 328, 1248-1251 (2010).**
7. **R. Callens, R. Coussement, T. Kawakami, J. Ladriére, S. Nasu, T. Ono, I. Serdons, K. Vyvey, T. Yamada, Y. Yoda, and J. Odeurs, "Principles of stroboscopic detection of nuclear forward scattered synchrotron radiation", Phys. Rev. B 67, 104423 (2003).**

Timing a FLASH.

Synchronising FEL pulses via single-cycle THz edge radiation

Many fundamental processes in nature, like chemical reactions or phase transitions occur on the few femtosecond time and few nanometres to few angstroms length scale. On a way to their understanding, great potential lies in investigations of their dynamics using the bright, coherent X-ray pulses from free-electron lasers (FELs) which have a duration and wavelength commensurate with that of these processes. We developed a method to measure the arrival time of the X-ray pulses at FLASH with respect to the optical pump-probe laser in the experimental hall on a few femtosecond timescale, making use of the THz beamline [1]. This technique is easily transferable to other advanced light sources operating with ultrashort electron bunches and therefore of high general interest.

Some of the most important processes in the atomic and molecular, material or life sciences occur on extremely short time and length scales – as a rule within quadrillionths of a second (femtoseconds) and lengths of billionths of a metre (nanometres). As it is well-known from photography, the faster a process occurs, the shorter the exposure must be to resolve it. Another rule in physics states that the wavelength of the photons used to take the image should be equal to or shorter than the size of the imaged structures, so ideally ultrashort X-ray pulses would be employed in studies of such phenomena.

Recent developments of 4th generation X-ray sources, such as FLASH in Hamburg, allow shedding light on these processes with the required (near) atomic resolution. Although their ultrashort pulse durations also approach the crucial few femtosecond timescale, the intrinsic time jitter that plagues X-ray FELs limits the achievable timing accuracy to several tens or even few hundreds of femtoseconds. This jitter at the accelerator-based sources is to a large extent a consequence of the unavoidable energy fluctuations between individual electron bunches, which lead to path-length differences in energy-dispersive elements such as bunch compressors or

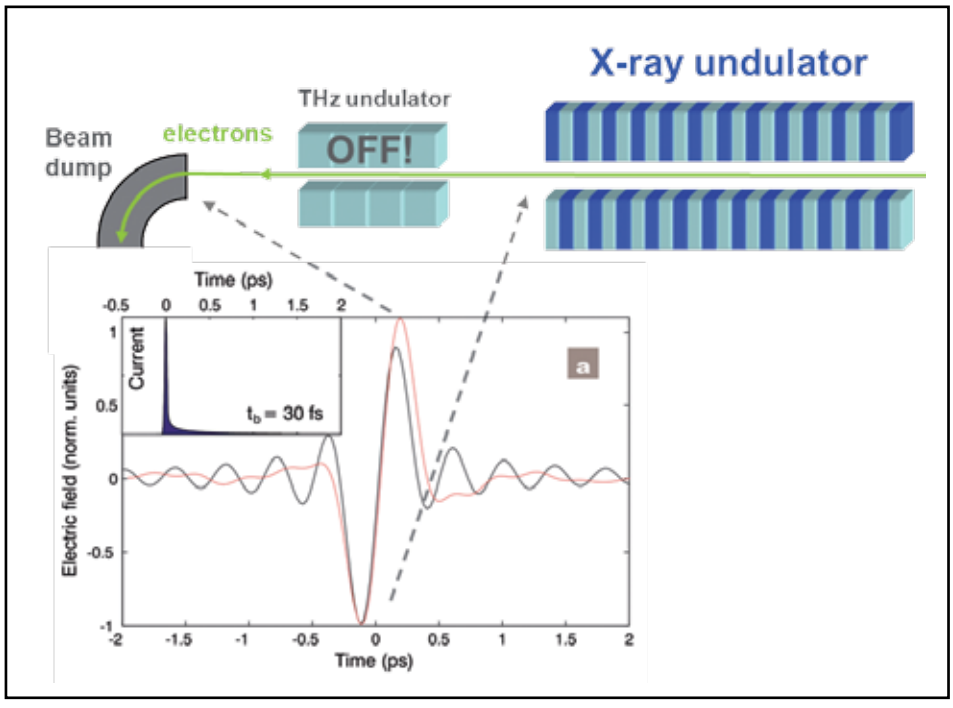

Figure 1

Schematic illustration of edge radiation at FLASH. The electron bunch generates a single cycle pulse at the magnetic edges of the X-ray undulator exit and the beam dump magnet entrance. The red curve represents the electrical field measured in the experiment, the black curve is an analytical calculation. The inset shows the electron bunch form factor assumed for the calculation.

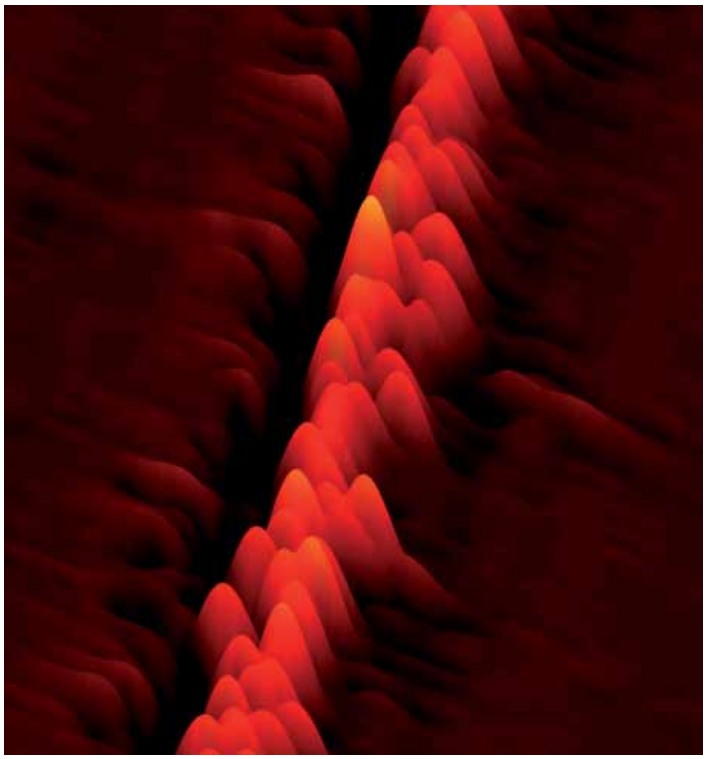

Figure 2

3D-visualisation of a sequence (bottom to top) of single-shot measurements (left to right) of the THz electric field distribution (similar to data presented in Figure 1, same time (x-) scale). In the "camera view" the time axis is tilted for better visibility of the peaks. The actual displacement of the electric field peaks is a direct measure for the timing jitter between X-ray (FEL) pulse and optical pump-probe laser pulse.

dipole magnets in the accelerator. As a result, the arrival time of the electron bunches at the X-ray undulator varies from shot to shot, leading to a timing jitter between the X-ray FEL pulse and the accelerator master oscillator. This jitter translates into jitter between the FEL and any external pulsed laser source that is synchronised to it.

For a well-optimised FEL operation and even with the most advanced feedback systems available to date [2], the theoretical lower limit for this intrinsic timing jitter is believed to be several tens of femtoseconds. Hence the synchronisation between pump and probe pulse will still be an order of magnitude less accurate than the actual pulse duration. One possibility for overcoming this problem is to accurately monitor the intrinsic jitter between the X-rays and the external sources and sort the experimental data afterwards. Many pioneering developments have been made in this area at FLASH over the past years. Nevertheless all techniques developed up to now did not allow reaching the important sub-10-femtosecond precision [3, 4].

We present a timing scheme for monitoring the arrival time jitter with a temporal resolution as good as a few femtoseconds. In contrast to earlier attempts, which aimed at monitoring the arrival time of the electron bunches or used X-ray/optical cross-correlation techniques, we make use of a cross-correlation between coherent terahertz (THz) radiation and the external optical laser system. The THz radiation used here does not originate from the electromagnetic THz undulator, which was intentionally switched off. It is generated parasitically at the magnetic exit edge of the X-ray undulator (see Fig. 1) with the consequence that – as for the THz undulator – the THz pulses are naturally synchronised to the X-ray pulses [5]. The THz beamline at FLASH [1] transports this edge radiation to the FLASH experimental hall into the photon diagnostics station. Here we measured the cross-correlation between the electric field of the THz pulse and a pulse from–– the near-infrared optical laser for pump-probe experiments, using a variation of the electro-optic sampling technique. The THz electric field induces an electro-optical effect in a nonlinear (birefringent) crystal, what in turn imposes a time-dependent polarisation modulation onto the co-propagating optical probe pulse. Figure 2 shows a 3D representation of consecutive single-shot measurements of the electric field of the THz edge radiation collected over several seconds. Evaluating the position of the electric field peak for each shot, we can retrieve the relative timing jitter of the terahertz pulses and therefore that of the X-ray FEL pulses, with respect to the external laser.

The technique has no effect on the X-ray pulse and it is independent of the X-ray photon energy. The pilot experiments, developed and performed in a cooperative effort with colleagues from the European XFEL and Helmholtz-Zentrum Dresden-Rossendorf (HZDR), have shown that the technique could serve as a routine timing tool at FLASH but also at other X-ray FEL sources around the world. This would open up the possibility to fully exploit the few femtosecond timescale at these large-scale facilities for the first time.

Contact: Nikola Stojanovic, nikola.stojanovic@desy.de

Authors

F. Tavella[1, 2], N. Stojanovic[1], G. Geloni[3] and M. Gensch[4]

1. Deutsches Elektronen-Synchrotron DESY, HASYLAB, Notkestrasse 85, 22607 Hamburg, Germany
2. Helmholtz-Institut Jena, Helmholtzweg 4, 07743 Jena, Germany
3. European XFEL GmbH, Albert-Einstein-Ring 19, 22603 Hamburg, Germany
4. Helmholtz-Zentrum Dresden-Rossendorf, Bautzner Landstr. 400, 01328 Dresden, Germany

Original publication

"Few-femtosecond timing at fourth-generation X-ray light sources", Nature Photonics 5, 162–165 (2011), DOI:10.1038/nphoton.2010.311

References

1. **M. Gensch et al., "New infrared undulator beamline at FLASH", Infrared Phys. Technol. 51, 423-425 (2008).**
2. **F. Loehl et al., "Electron Bunch Timing with Femtosecond Precision in a Superconducting Free-Electron Laser", Phys. Rev. Lett. 104, 144801 (2010).**
3. **A. Azima et al., "Time-resolved pump–probe experiments beyond the jitter limitations at FLASH", Appl. Phys. Lett. 94, 144102 (2009).**
4. **T. Maltezopoulos et al.,"Single-shot timing measurement of extreme-ultraviolet free-electron laser pulses", New J. Phys. 10, 033026 (2008).**
5. **U. Frühling et al., "Single-shot Terahertz-field-driven streak camera", Nature Photon. 3, 523-528 (2009).**

Imaging non-repetitive ultrafast dynamics on the nanoscale.

Catch the moment – and the next one

The evolution of triggerable, deterministic processes in the microscopic world can be followed in real space via single-shot imaging in pump-probe experiments [1]. In contrast, stochastic processes such as fluctuations in thermal equilibrium or non-predictable failure processes cannot be accessed in this fashion. Here, a sequence of independent images is required to capture the untriggered evolution in real space. We introduce a holographic approach that allows recording of sequential images of a nanoscale object with femtosecond temporal resolution. In this proof-of-principle experiment, we demonstrate that holographic encoding of the consecutive states of the system allows overcoming the fundamental readout limitations of pixelated detectors required for image formation. Two consecutive snapshots of an object, separated by 50 femtoseconds only, were recorded in a single hologram exposure and disentangled afterwards. The approach opens a new route to follow the spatial evolution of nano-objects on femtosecond timescales and is an important step towards the ultimate goal of recording a "molecular X-ray movie".

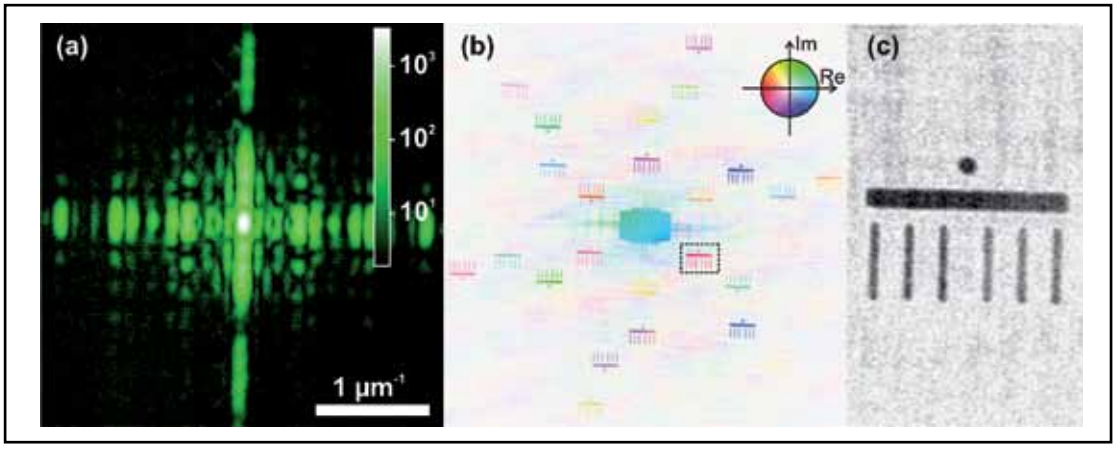

Figure 1

(a) Centre of a single-shot X-ray hologram on logarithmic scale. (b) In the reconstruction the magnitude is encoded by saturation and the phase by hue. Twelve independent twin-image pairs, each of them featuring point symmetry to the reconstruction centre, are generated by the twelve reference holes. (c) Enlarged magnitude of the marked image.

The short and bright pulses of (soft) X-ray free-electron lasers (XFELs) allow capturing images of nano-objects using a single X-ray pulse of femtosecond duration [1, 2]. To this end, a coherent diffraction pattern of the object to be investigated is recorded on a 2D pixelated detector. From such data an image can be reconstructed either via iterative phase retrieval [1-3] or via direct Fourier inversion if the phase has been holographically encoded in the experiment via interference with a reference wave [4, 5]. While XFELs are bright enough to generate an image of a nanoscale object in a single exposure, shooting a real "movie" of sub-picosecond dynamics requires the consecutive acquisition of such images spaced only femtoseconds apart.

We demonstrate an approach capable of recording an ultrafast image sequence in a single 2D detector exposure utilising holographic encoding of the temporal sequence in a spatially multiplexed hologram [6, 7]. The lithographically fabricated test sample consists of the object to be imaged – in our case a simplified replica of the Brandenburg Gate – in the centre, surrounded by several circular apertures which generate reference waves for Fourier transform holography (FTH) when illuminated coherently together with the object. This object-reference mask was produced in a free-standing 5-µm-thick NiFe foil. In our experiment, we used unfocused FLASH pulses with a wavelength of $\lambda = 23.5$ nm. The beam was 5 mm in diameter with an average pulse energy of 14 µJ, corresponding to 1.7×10^{12} photons per pulse. Under these conditions, our (relatively large, 72 µm x 50 µm) test object could be imaged with a single pulse of about 30 fs duration, as illustrated in Fig.1. It is important to realise that images of the object will appear in the reconstruction of the hologram at the positions defined by the vector $\vec{R}_n$ connecting the object and a specific reference hole, as well as at $-\vec{R}_n$ (for comparison, the real-space sample map is depicted in Figure 2a). As a result, a single shot generates multiple images of the object, which are encoded simultaneously in a single hologram.

The images are completely independent of each other, except for the conjugated image pairs at $\pm\vec{R}_n$ generated by the same reference hole.

For ultrafast two-shot consecutive imaging, two subsequent femtosecond pulses are generated from a single FLASH pulse using a wavefront-dividing split-and-delay setup [8]. In our experiment, two pulses spaced 50 fs apart are incident on the sample, with an included angle of 0.06° only, i.e. with a very small parallax under which the sample is imaged. The time sequence of the pulses and the shape of the object at these times are encoded in the hologram by ensuring that some references are exclusively illuminated by the first split pulse, while others are illuminated by the delayed pulse only, as illustrated in Fig. 2a. In this way, we encode the temporal sequence spatially into a single hologram (Fig. 2b). Now, images of the object appearing at different points in the reconstruction show the object at the particular time at which the corresponding image-forming reference was illuminated. The approach thus allows to record two frames of a movie in the femtosecond regime – this is the pivotal result of the experiment. Note that indeed complete and independent images of the object at different times are encoded, in contrast to a complementary approach where only the difference between initial and final state is detected [9].

While this particular "movie" is especially boring – as the micrometre-scale Brandenburg gate replica has no chance of showing any dynamics during 50 fs – it illustrates how an initial and a final state of an ultrafast nanoscale process can be imaged in principle. Of course, the (diffraction-limited) resolution achieved in this pilot experiment with an unfocused beam at 23.5 nm wavelength is insufficient to reach sub-100-nm resolution and thus the realm where dynamics on a femtosecond scale matters. Using shorter X-ray wavelengths on the order of $\lambda = 1$ nm and significantly increased photon density via a focused X-ray beam, a spatial resolution of 30 nm, as typical today in X-ray holographic imaging at storage ring synchrotron radiation sources [10,11], can be achieved in a straight forward manner. A further dramatic increase in resolving power can be expected when switching to hard X-rays on the order of 0.1 nm wavelength and, e.g., optically inverted [12] or otherwise adapted schemes to generate reference waves. The temporal resolution is limited by the duration of individual XFEL pulses and by the ability to separate them in a split-and-delay unit. With the latter featuring sub-fs delays [8] and XFEL pulses pushing towards the attosecond regime as well [13], our approach will be useful for even faster imaging in the future. Finally, we point out that, while Hollywood-length movies are out of the question, more than two frames are of course possible and in practice only limited by the efficiency and steering accuracy for splitting the incident pulses in conjunction with the total number of incident photons per pulse.

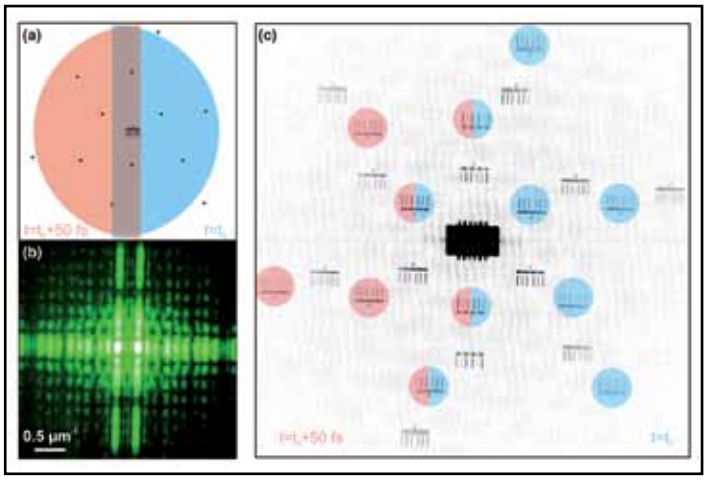

Figure 2

(a) Real-space sample map featuring twelve reference holes. The illumination by the split FLASH pulses is indicated by the two half-circles in blue and red. (b) Centre of the superimposed hologram created by the split pulses. (c) In the reconstruction the independent images correspond to the two recording times (colour coded overlay in red and blue).

Contact: Christian M. Günther, christian.guenther@tu-berlin.de
Stefan Eisebitt, eisebitt@physik.tu-berlin.de

Authors

Christian M. Günther[1,2], Bastian Pfau[1,2], Rolf Mitzner[2,3], Björn Siemer[3], Sebastian Roling[3], Helmut Zacharias[3], Oliver Kutz[2], Ivo Rudolph[2], Daniel Schondelmaier[2], Rolf Treusch[4], Stefan Eisebitt[1,2]

1. Institut für Optik und Atomare Physik, TU Berlin, Straße des 17. Juni 135, 10623 Berlin, Germany
2. Helmholtz-Zentrum Berlin, Hahn-Meitner-Platz 1, 14109 Berlin, Germany
3. Physikalisches Institut, Westfälische Wilhelms-Universität Münster, Wilhelm-Klemm-Straße 10, 48149 Münster, Germany
4. HASYLAB at DESY, Notkestraße 85, 22607 Hamburg, Germany

Original publication

"Sequential femtosecond X-ray imaging", Nature Photonics 5, 99–102 (2011).

References

1. **A. Barty et al., "Ultrafast single-shot diffraction imaging of nanoscale dynamics", Nature Photon. 2, 415-419 (2008).**
2. **H. N. Chapman et al., "Femtosecond diffractive imaging with a soft-X-ray free-electron laser", Nature Phys. 2, 839-843 (2006).**
3. **J. Miao et al., "Extending the methodology of X-ray crystallography to allow imaging of micrometre-sized non-crystalline specimens", Nature 400, 342-344 (1999).**
4. **I. McNulty et al., "High-Resolution Imaging by Fourier Transform X-ray Holography", Science 256, 1009-1012 (1992).**
5. **S. Eisebitt et al., "Lensless imaging of magnetic nanostructures by X-ray spectro-holography", Nature 432, 885-888 (2004).**
6. **B. Pfau et al., "Femtosecond pulse x-ray imaging with a large field of view", New J. Phys. 12, 095006 (2010).**
7. **W. F. Schlotter et al., "Multiple reference Fourier transform holography with soft x rays", Appl. Phys. Lett. 89, 163112 (2006).**
8. **R. Mitzner et al., "Spatio-temporal coherence of free electron laser pulses in the soft x-ray regime", Optics Express 16, 19909-19919 (2008).**
9. **H. N. Chapman et al., "Femtosecond time-delay x-ray holography", Nature 448, 676-679 (2007).**
10. **B. Pfau et al., "Origin of magnetic switching field distribution in bit patterned media based on pre-patterned substrates", Appl. Phys. Lett. 99, 062502 (2011).**
11. **D. Zhu et al., "High-Resolution X-Ray Lensless Imaging by Differential Holographic Encoding", Phys. Rev. Lett.105, 043901 (2010).**
12. **L.-M. Stadler et al., "Hard X Ray Holographic Diffraction Imaging", Phys. Rev. Lett. 100, 245503 (2008).**
13. **P. Emma et al., "Femtosecond and Subfemtosecond X-Ray Pulses from a Self-Amplified Spontaneous-Emission--Based Free-Electron Laser", Phys. Rev. Lett. 92, 074801 (2004).**

Clocking molecular dynamics with a femtosecond XUV stopwatch.

Isomerisation in acetylene cations

The ultrafast dynamics of geometrical rearrangements in photo-excited acetylene molecules $(HCCH)^+$ leading to the formation of vinylidene cations $(CCH_2)^+$ has been traced in an XUV-pump/XUV-probe experiment with FEL pulses at FLASH. Recording the yield of characteristic $C^+ + CH_2^+$ fragment-pairs that emerge from the dissociation of the product molecule (CCH_2) as a function of the pump-probe time delay allowed us to directly access the mean isomerisation time of (52 ± 15) fs, thus measuring the time it takes for one of the hydrogen atoms to migrate from one side of the molecule to the other. This first temporally resolved observation of isomerisation on a femtosecond time-scale may pave the way to visualise, control and possibly even manipulate molecular reactions in real time, with attractive perspectives and potential applications to bio-chemical reactions.

Being at the heart of photo-chemistry and biology, light-induced isomerisation drives many fundamentally important bio-chemical reactions, e.g. in photosynthesis, in eye vision, and even in immunity and viral infection (HIV isomerisation) [1]. In all of these reactions it is the migration of individual atoms within a molecule that results in a change of the geometrical structure and thus leads to a product with sometimes drastically different properties and functionalities. For example, while one isomer of the essential oil carvon is responsible for the aroma of mint, the other one smells like caraway. During the course of isomerisation often a sequence of transient species is involved, which, as intermediate states with various geometrical structures, control the details of the reactant-to-product process. In general, the system evolves along multi-dimensional electronic potential energy surfaces, it may pass through conical intersections, and typically several vibrational modes are involved whose energies are redistributed to achieve a stable product state [2]. Even small molecules comprising only a few atoms may undergo isomerisation. With typical rearrangement times from ten to few hundreds of femtoseconds they serve as prototype systems to advance our understanding of larger molecules that are more relevant for applications. The acetylene cation, for example, has been studied extensively in particularly for the low-lying excited $A^2\Sigma_g^+$-state, which is known to decay unexpectedly fast via non-radiative mechanisms.

In our experiment at FLASH we used a Reaction Microscope (REMI) [3] equipped with an on-axis back-reflection split-mirror setup [4] for focusing and FEL pulse-pair creation as schematically depicted in Fig. 1. The REMI enables the coincident and momentum-resolved detection of ionic fragments

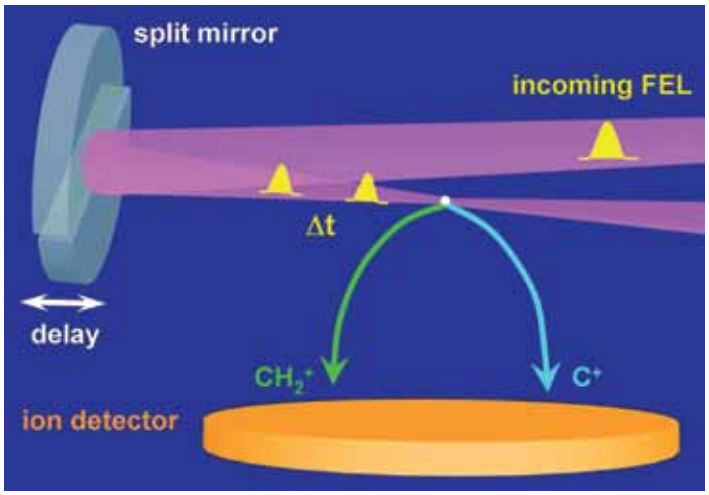

Figure 1

Schematic drawing of the experimental setup with split-mirror stage and ion detection part of the Reaction Microscope.

that emerge from the dissociation or Coulomb-explosion of single acetylene molecules which are provided by means of a localised and intrinsically cold molecular beam. The split-mirror consists of a spherical multi-layer mirror (1 inch Mo/Si mirror, 50 cm focal length, 20 µm focus diameter) that is cut into two identical “half-mirrors”. While one of them is mounted at a fixed position, the other one is movable along the FEL beam axis by means of a high precision piezo-stage. This results in an adjustable time delay between the two reflected parts of the incoming pulse. FLASH-pulses with an average pulse duration of ~40 fs (coherence length less than 10 fs [5]), peak intensities of $I \cong 1 \cdot 10^{13}$ W/cm^2, and a photon energy of 38 eV (32.6 nm) were employed for the measurements.

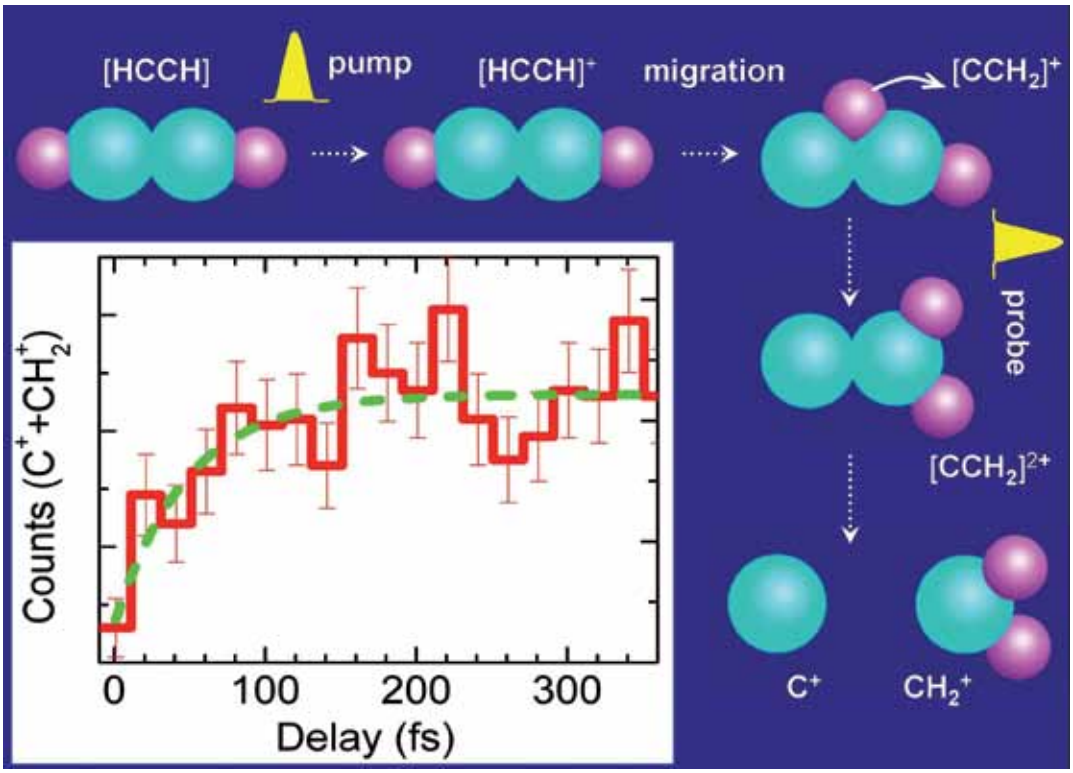

Figure 2

Sketch of the isomerisation pathway in acetylene cations induced by a first XUV-pulse and probed with a second time-delayed XUV-pulse from FLASH. Inset: delay-time dependent yield of coincident $C^+ + CH_2^+$ fragments (red histogram) together with fit (green dashed line).

As illustrated in Fig. 2, the absorption of one photon from the pump-pulse leads to the formation of an acetylene cation $(HCCH)^+$ in the low-lying excited $A^2\Sigma_g^+$ state. This serves as a trigger for the migration of a hydrogen atom from one end (breaking of CH bond) to the other end of the CC core (making of CH bonds), since there are almost no potential barriers for isomerisation into the $(CCH_2)^+$ vinylidene configuration. During its course of isomerisation the molecular cation is ionised further by absorption of an additional photon, now from the probe-pulse, and then, depending on the delay-time, it dissociates into the $C^+ + CH_2^+$ channel, which is considered to be a unique signature for the H-transfer. Hence, the probe-pulse "clocks" the hydrogen migration in real time at various positions along the isomerisation reaction-coordinate like "a femtosecond XUV stopwatch" by measuring the fragment-pairs that are characteristic for the vinylidene product state. A mean isomerisation time of (52 ± 15) fs was extracted by fitting an exponential function (green dashed line in Fig. 2). Confirmed by recent calculations [6], our findings provide first evidence that isomerisation is responsible for the ultrafast non-radiative $A^2\Sigma_g^+$ relaxation dynamics ending a long lasting controversial debate. Due to the perturbative nature of the XUV pump-probe scheme, essentially not imposing any field-induced modifications of the potential surfaces, a wealth of chemical reactions as well as molecular dynamics can be explored on the few-femtosecond time scale under unprecedented clean conditions in the future.

Contact: Robert Moshammer, Robert.Moshammer@mpi-hd.mpg.de

Authors

Yuhai Jiang[1], Artem Rudenko[2], Oliver Herrwerth[3], Lutz Foucar[2], Moritz Kurka[1], Kai-Uwe Kühnel[1], Matthias Lezius[3], Matthias Kling[3], Jan van Tilborg[4], Ali Belkacem[4], Kiyoshi Ueda[5], Stefan Düsterer[6], Rolf Treusch[6], Claus Dieter Schröter[1], Robert Moshammer[1] and Joachim Ullrich[1,2]

1. Max-Planck-Institut für Kernphysik, Saupfercheckweg 1, 69117 Heidelberg, Germany
2. Max-Planck Advanced Study Group at CFEL at DESY, Notkestraße 85, 22607 Hamburg, Germany
3. Max-Planck-Institut für Quantenoptik, Hans-Kopfermann-Str. 1, 85748 Garching, Germany
4. Lawrence Berkeley National Laboratory, 1 Cyclotron Road, Berkeley, CA 94720, USA
5. Institute of Multidisciplinary Research for Advanced Materials, 2-1-1 Katahira, Aoba-ku, Tohoku University, 980-8577 Sendai, Japan
6. HASYLAB at DESY, Notkestraße 85, 22607 Hamburg, Germany

Original publication

"Ultrafast extreme ultraviolet induced isomerization of acetylene cations", Phys. Rev. Lett. 105, 263002 (2010).

References

1. **D. Polli et al., "Conical intersection dynamics of the primary photoisomerization event in vision", Nature 467, 440–443 (2010).**
2. **A. H. Zewail, "Femtochemistry: Atomic-Scale Dynamics of the Chemical Bond", J. Phys. Chem. A 104, 5660–5694 (2000).**
3. **J. Ullrich et al., "Recoil-ion and electron momentum spectroscopy: reaction microscopes", Rep. Prog. Phys. 66, 1463–1545 (2003).**
4. **Y. H. Jiang et al., "Temporal coherence effects in multiple ionization of N_2 via XUV pump-probe autocorrelation", Phys. Rev. A 82, 041403(R) (2010).**
5. **Y. H. Jiang et al., "Investigating two-photon double ionization of D_2 by XUV-pump/XUV-probe experiments at FLASH", Phys. Rev. A 81, 051402(R) (2010).**
6. **M. E. Madjet, O. Vendrell, and R. Santra, "Ultrafast Dynamics of Photoionized Acetylene", accepted for publication in PRL (2011).**

Bright XUV laser source with dual-gas high harmonic generation.

Enhancement and control for a seeded future at FLASH II

High harmonic generation (HHG) is a central driver of the rapidly growing field of ultrafast science. Attosecond science would not be possible without the ability to convert femtosecond laser pulses into coherent harmonics in the extreme ultraviolet (XUV). While low-flux attosecond sources have been a true success story, further scientific goals are constrained by the lack of a generally applicable technique to achieve full phase control in HHG allowing for a substantially higher photon flux in the XUV regime. Accurate phase control for more than two HHG sources could now be demonstrated with a novel dual-gas HHG scheme, allowing near-ideal control of quasi-phase matching.

Coherent XUV pulses of femtosecond to attosecond duration generated by HHG are central to applications in ultrafast science [1-3] and the external seeding of free-electron lasers (FELs) [4]. In terms of enhancing the brightness of such pulses, achieving absolute and independent phase control between multiple harmonic generation zones represents a major advance for HHG sources. It will allow the coherent superposition of multiple sources created by the same laser – an approach commonly known as quasi-phase matching (QPM) [5]. For scenarios that aim to exploit the high peak power [6] or high average power of current-day lasers [7], free-propagating laser geometries are the only solution to avoid damages at capillary systems for example. In order to meet the requirements for fully controlled coherent buildup, we have developed a novel dual-gas QPM concept based on alternating a HHG generating medium with passive matching hydrogen zones (see Fig. 1). QPM is typically implemented by allowing the signal to build up over one coherence length $L_c = \pi/\Delta k$ (the HHG half-period) and subsequently suppressing HHG for another coherence length (the matching half-period) until the driving field and harmonic field are in phase again (here $\Delta k = k_q - qk_f$ is the k-vector mismatch between the q^{th} harmonic and the fundamental). In the dual-gas QPM scheme it needs to be ensured that hydrogen is fully ionised at the raising slope of the driver pulse what can be achieved with laser intensities above $3 \cdot 10^{14}$ W/cm^2. Completely ionised hydrogen does not contribute to the HHG process. Due to the plasma dispersion effect it only adds a phase to the electric field of the passing harmonic photons. Thus, full control of the phase between successive harmonic sources can be achieved simply by tuning the pressure of the hydrogen jets. Since the intensity of radiation emitted by N atoms coherently increases as N^2, the coherent superposition of N_{QPM} identical HHG sources will increase the intensity of the q^{th} harmonic as $I_q \sim (N_{QPM})^2$ under ideal conditions.

In order to show the effect of hydrogen as phase tuning for more than two successive sources, an experiment was performed at CFEL at DESY. The idea was to demonstrate the QPM effect by comparing a single argon jet of 700 µm length with a QPM setup using the same length of argon interspaced with 100 µm hydrogen jets. In a first step, the reference single jet was used to determine the dependence of the harmonic yield on the generating argon density. For each argon pressure a spectrum was recorded. In a second step the target was extended by five hydrogen jets separating the

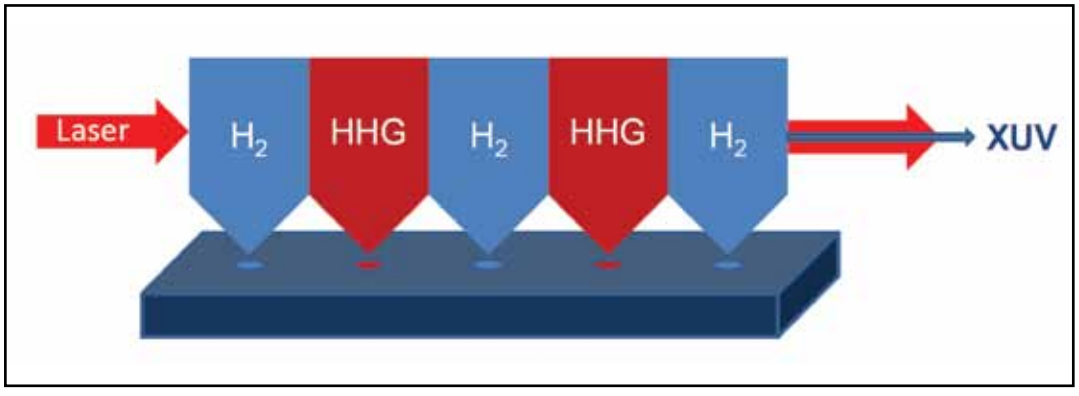

Figure 1

The dual-gas HHG principle. The driver jets are interspaced with hydrogen as matching zone in which the harmonic phase can be tuned such that constructive interference between successive jets can be observed. This leads to significant enhancements of XUV output. The two enclosing hydrogen jets just confine the geometry of the jet array.

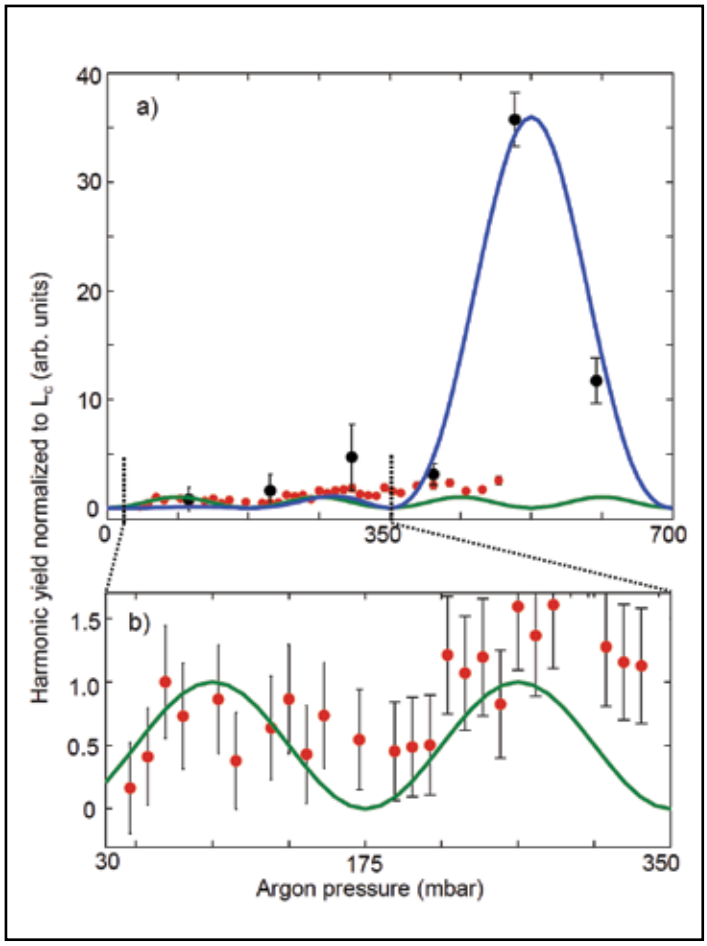

Figure 2

a) Comparison of the harmonic yield vs. argon pressure for the 27th harmonic using a 700 µm merged argon jet (red dots) and a dual-gas multijet with 5 hydrogen intersections while maintaining the total length of the argon nozzles (black dots). For comparison, the theoretical curves were included for N_{QPM} = 1 (green line) and for N_{QPM} = 6 (blue line). b) Enlarged plot of the phase oscillations measured with the merged argon jet corresponding to N_{QPM} = 1. All uncertainties stem from shot-to-shot fluctuations during the measurement and from background subtraction.

argon zones, whereas the total generation length was kept constant. For two sets of data the harmonic yield was plotted vs. argon backing pressure in Fig. 2 for the 27th harmonic of the 800 nm driver laser amplifier. At first, the merged argon jet of 700 µm length showed the characteristic phase oscillations with increasing argon pressure. The theoretically expected oscillations are also depicted in Fig. 2 (the corresponding theory has been discussed by Seres et al. [8]).
The QPM effect can be demonstrated with the dataset based on six sources separated with hydrogen. The hydrogen pressure was chosen to maximise the output at an argon backing pressure of p = 6 · 87.5 = 525 mbar, where 87.5 mbar corresponds to the density where the harmonic signal of argon showed the first maximum. With the hydrogen jets at constant pressure the argon pressure scan was repeated (Fig. 2). This is the first demonstration of an enhancement factor of 36 for a multijet array consisting of six sources. The measured data fit well to the theoretical expectation. This result confirms the QPM scalability with dual-gas QPM and led to a conversion efficiency of up to $1 \cdot 10^{-5}$ in that wavelength regime. This is already competitive with highest conversion efficiencies measured for an 800 nm driver laser system [9,10]. In principle, our scheme will extend to almost any medium as long as the ionisation potential of the HHG medium exceeds that of hydrogen. The number of nozzles is not limited. Due to the high potential of this source, the dual-gas QPM target will be used as XUV seeding source for FLASH II at DESY. In order to meet all requirements for seeding, further improvements are currently under development.

Contact: Arik Willner, arik.willner@desy.de

Authors

A. Willner[1,2], F. Tavella[2], M. Yeung[3], T. Dzelzainis[3], C. Kamperidis[4], M. Bakarezos[4], D. Adams[3], M. Schulz[1,5], R. Riedel[2,5], M. C. Hoffmann[6], W. Hu[6], J. Rossbach[5], M. Drescher[5], N. A. Papadogiannis[4], M. Tatarakis[4], B. Dromey[3], M. Zepf[3]

1. Deutsches Elektronen Synchrotron, Notkestrasse 85, 22607 Hamburg, Germany
2. Helmholtz-Institut Jena, Max-Wien-Platz 1, 07743 Jena, Germany
3. Queens University, University Road, Belfast BT7 1NN, United Kingdom
4. Centre for Plasma Physics and Lasers, TEI of Crete, Evangelou Daskalaki Street 1, 74100 Rethymno and Romanou Street 3, 73133 Chania, Crete, Greece
5. University of Hamburg, Luruper Chaussee 149, 22603 Hamburg, Germany
6. Max Planck Research Department for Structural Dynamics, University of Hamburg, CFEL, Notkestrasse 85, 22607 Hamburg, Germany

Original publication

"Coherent Control of High Harmonic Generation via Dual-Gas Multijet Arrays", Phys. Rev Lett. 107, 175002 (2011).

References

1. **R. L. Sandberg et al., "Lensless diffractive imaging using tabletop coherent high-harmonic soft-x-ray beams", Phys. Rev. Lett. 99, 098103 (2007).**
2. **E. Gagnon et al., "Soft x-ray-driven femtosecond molecular dynamics", Science 317, 1374-1378 (2007).**
3. **T. Haarlammert, H. Zacharias, "Application of high harmonic radiation in surface science", Current Opinion in Solid State and Materials Science 13, 13-27 (2009).**
4. **G. Lambert et al., "Injection of harmonics generated in gas in a free-electron laser providing intense and coherent extreme-ultraviolet light", Nature Physics 4, 296-300 (2008).**
5. **A. Paul et al., "Quasi-phase-matched generation of coherent extreme ultraviolet light", Nature 42, 51-54 (2003).**
6. **C.J. Hooker et al., "The Astra Gemini project - A dual-beam petawatt Ti:Sapphire laser system", Journal De Physique IV 133, 673-677 (2006).**
7. **J. Rotthardt et al., "High average and peak power few-cycle laser pulses delivered by fiber pumped OPCPA system", Opt. Express 18, 12719-12726 (2010).**
8. **J. Seres et al., "Coherent superposition of laser-driven soft-X-ray harmonics from successive sources", Nature Physics 3, 878-883 (2007).**
9. **E. Constant et al., "Optimizing High Harmonic Generation in Absorbing Gases: Model and Experiment", Phys. Rev. Lett. 82, 1668-1671 (1999).**
10. **J. F. Hergott et al., "Extreme-ultraviolet high-order harmonic pulses in the microjoule range", Phys. Rev. A 66, 021801(R) (2002).**

Enhanced flexoelectricity in twinned thin films.

Power from strain gradients

Decreasing the size of piezoelectric materials while still keeping large enough responses is one of the main challenges in the field of ferroelectrics. This would allow a multitude of new applications as e.g. nano-generators for energy harvesting. It is, thus, of importance to investigate new mechanisms that can potentially increase the piezoelectric response in nanoscaled materials. Diffraction of synchrotron radiation, combined with high-resolution transmission electron microscopy, has revealed that one of these mechanisms is the so-called flexoelectric effect, which can be engineered in periodically twinned ferroelectric thin films.

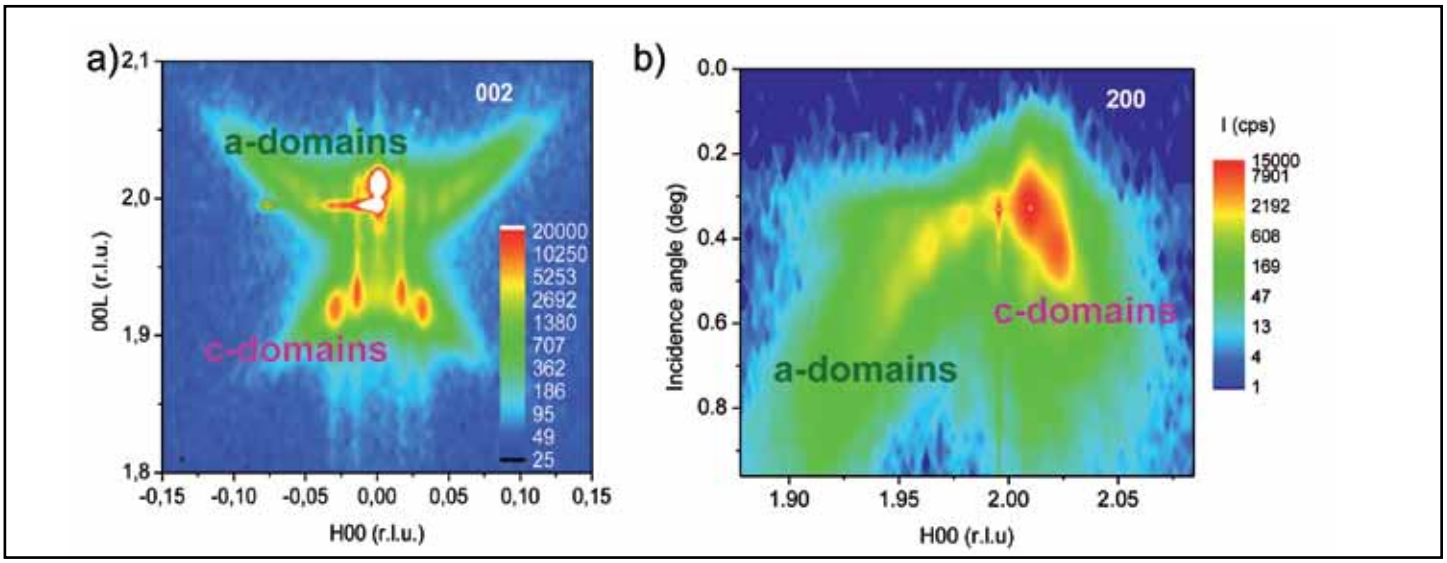

Figure 1

a) Reciprocal space map around the (002) Bragg reflection of a $PbTiO_3$ film with engineered twinned domains. b) (H00)-line scan around the (200) in-plane reflection of the same film as a function of the incidence angle (grazing incidence geometry). The presence of strain gradients, coupled to gradients of both the lattice distortions and the twinned angles, γ (see also Fig. 2) can be observed in these maps. The periodicity of the twinned domains along the in-plane direction is also clearly visible.

Piezoelectric materials can transform mechanical energy into electrical energy and vice versa. Because of that they are used in a multitude of everyday applications from ultrasound generators in medical applications (echography devices, blood sensors, lithotripters…) to vibration dampers (in cars, skis, helicopter blades…) and many others. Despite their widespread use, one of the main challenges in the field is further decreasing the size of piezoelectric materials while maintaining the material's responses above detectable levels. Miniaturization of piezoelectrics would allow dozens of new applications, in particular in the areas of nano-generation and energy harvesting. It is then relevant to look into new mechanisms that can potentially increase the piezoelectric response at the nanoscale.

It is well known that lattice strain couples to electrical polarization via the piezoelectric effect. What is not so widely recognized is that strain gradients can also give rise to electrical polarization by means of the so-called flexoelectric effect [1,2]. This effect is present in all dielectrics but it is typically too small to be taken into consideration. It has been recently pointed out that this ceases to be true at the nanoscale, where strain gradients can be so large that even small flexoelectric effects can give rise to large electrical polarizations [3,4]. Using thin film diffraction, both in reflection and grazing incidence geometries, on epitaxial, ferroelectric thin films with adequately chosen film-substrate combinations and film thicknesses, nano-twinned films can be grown with a well-defined periodicity of the order of the film thickness, ranging between 15 and 100 nm (see Fig.1) [5,6].

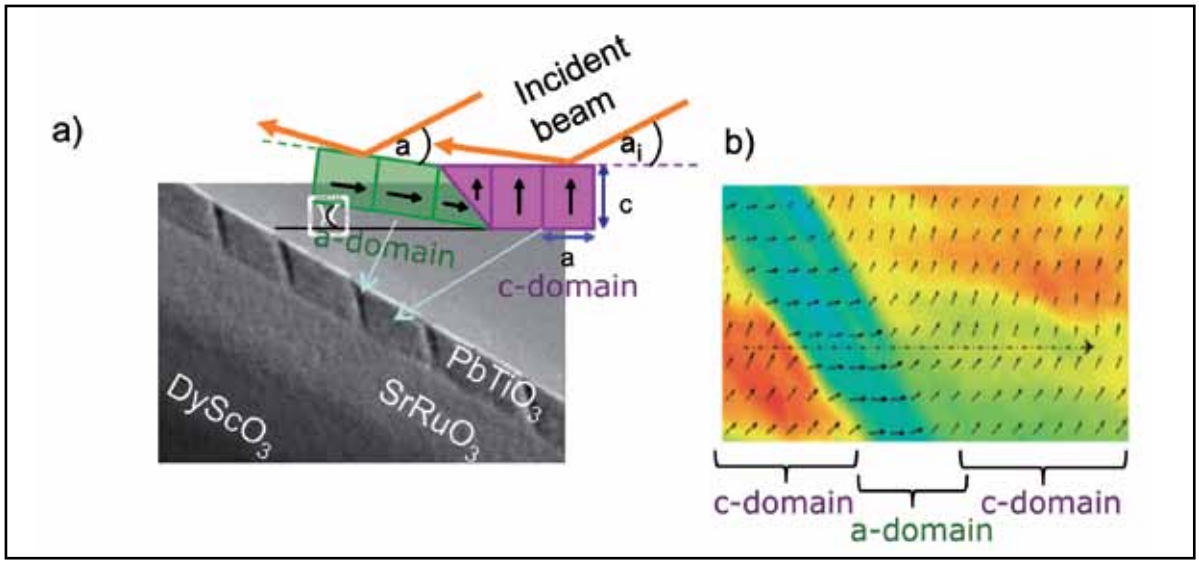

Figure 2

a) Cross-section TEM image of a twinned film. In the inset one a-domain and one c-domain are sketched indicating the twin angle, γ, which makes the nominal (a_i) and real (a) incident angles different (γ is highly exaggerated in the sketch). The black arrows in the inset of a) indicate the direction of the intrinsic ferroelectric polarization in the a- and c-domains. b) From a TEM image we obtained the strain gradients (different colour means different strain) and the direction of the polar axis at the unit cell level (small black arrows), clearly showing that the polarization is largely rotated away from the surface normal in the c-domains in agreement with the expectations of the flexoelectric effect.

Our recent experiments at beamline W1 at DORIS have revealed that strain gradients are present in these films, not only in the vertical direction, as one would expect from the different elastic boundary conditions at the top and bottom interfaces, but also in the horizontal direction in between domain walls (see Fig. 2). On thin films with a c-domain width of w = 40 nm, the measured out-of-plane strain difference between the acute and obtuse corners of the c-domain is as large as $\Delta\varepsilon_{33} \sim 0.03$. This would give rise to an average horizontal flexoelectricity across the domain of $P_{x(flexo)} = f_{13}(\Delta\varepsilon_{33}/w) \sim 15\ \mu Ccm^{-2}$, with $f_{13} = 200\ nCm^{-1}$ being the relevant component of the flexoelectric tensor. This flexopolarization, which is induced horizontally in the c-domains is the largest ever reported and it is of the same order of magnitude of the intrinsic, vertically oriented, ferroelectric polarization of the same domains. Therefore, the combination of ferro- and flexo-polar vectors is able to rotate the overall polarization in the c-domains (see Fig. 2b). Since the rotation of the polarization is associated to a lowering of symmetry, softening of the lattice and the increase of the piezoelectric response [7-9], this mechanism points to a novel way to increase the piezoelectric response in very thin films by purely physical means.

Contact: Gustau Catalan, gustau.catalan@cin2.es
Beatriz Noheda, b.noheda@rug.nl

Authors

G. Catalan[1,2], A. Lubk[3], A. H. G. Vlooswijk[1], E. Snoeck[3,4], C. Magen[4,5], A. Janssens[6], G. Rispens[1], G. Rijnders[6], D. H. A. Blank[6], and B. Noheda[1]

1. Zernike Institute for Advanced Materials, University of Groningen, 9747 AG Groningen, The Netherlands
2. ICREA and CIN2, Campus Universitat Autonoma de Barcelona, Bellaterra 08193, Barcelona, Spain
3. CEMES-CNRS, 29, rue Jeanne-Marvig, 31055 Toulouse, France
4. Transpyrenean Associated Laboratory for Electron Microscopy, CEMES–INA, CNRS–University of Zaragoza, France/Spain
5. Laboratorio de Microscopías Avanzadas (LMA), Instituto de Nanociencia de Aragón (INA)–ARAID, and Departamento de Física de la Materia Condensada, Universidad de Zaragoza, 50018 Zaragoza,Spain
6. MESA+ Institute for Nanotechnology, University of Twente, 7500 AE Enschede, The Netherlands

Original publication

Flexoelectric rotation of polarization in ferroelectric thin films, Nature Materials 10(12), 963 (2011)

References

1. **L. E. Cross, "Flexoelectric effects: Charge separation in insulating solids subjected to elastic strain gradients", J. Mater. Sci. 41, 53 (2006).**
2. **A. K. Tagantsev, L. E. Cross, and J. Fousek, "Domains in Ferroelectric Crystals and Thin Films", Springer, 637 (2010).**
3. **W. Zhu, J. Y. Fu, N. Li, and L. Cross, "Piezoelectric composite based on the enhanced flexoelectric effects", Appl. Phys. Lett. 89, 192904 (2006).**
4. **D. Lee et al., "Giant flexoelectric effect in ferroelectric epitaxial thin films", Phys. Rev. Lett. 107, 057602 (2011).**
5. **U. Gebhardt et al., "Formation and thickness evolution of periodic twin domains in manganite films grown on $SrTiO_3$(001) substrates", Phys. Rev. Lett. 98(9), 096101(2007).**
6. **A. H. G. Vlooswijk et al. "Smallest 90 domains in epitaxial ferroelectric films", Appl. Phys. Lett 91, 112901 (2007).**
7. **L. Bellaiche, A. Garcia, and D. Vanderbilt, "Finite-temperature properties of $Pb(Zr_{1-x}Ti_x)O_3$ alloys from first principles", Phys. Rev. Lett. 84, 5427-5430 (2000).**
8. **H. Fu and R. E. Cohen, "Polarization rotation mechanism for ultrahigh electromechanical response in single-crystal piezoelectrics", Nature 403,70 281283 (2000).**
9. **B. Noheda, and D. E. Cox, "Bridging phases at the morphotropic boundaries of lead oxide solid solutions", Phase Transitions. 79, 5-20 (2006).**

3D elemental speciation of inclusions in natural diamonds.

News from the deep Earth

The three-dimensional speciation of Fe containing inclusions in a cloud of micrometer-sized inclusions within an "ultra-deep" natural diamond from the Juina region in Brazil is determined by confocal µXANES. The inclusions encapsulated in this diamond originate from a depth below 670 km, the so-called deep Earth, and provide information on the physical and chemical conditions of the Earth's lower mantle. The confocal µXANES methodology allowed to determine the fraction of ferropericlase ((Fe,Mg)O) and hematite (Fe_2O_3) for the Fe containing inclusions within a part of the inclusion stream in this diamond.

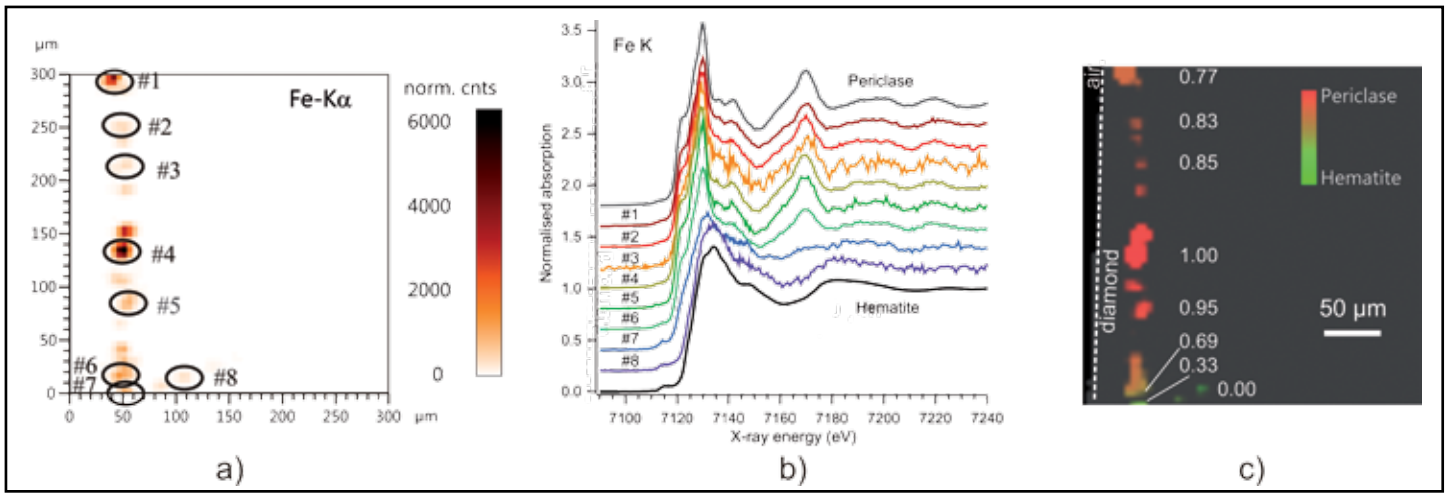

Figure 1

(a) Fe Kα elemental map in the left confocal map; (b) Confocal Fe K µXANES spectra measured on the Fe containing inclusion indicated in (a); (c) Fitted fractions of ferropericlase (red) and hematite (green) in the observed Fe containing inclusions.

The majority of the natural diamonds are formed in the Earth's lithospheric upper mantle (< 200 km depth). During the growth of the diamond, fluids, minerals and rock fragments can be trapped inside it. These inclusions are then shielded from the environment during the diamond's journey towards the Earth surface preserving their original capture composition. Only a few sources, e.g. Juina in Brazil and Kankan in Guinea, provide so called "ultra-deep" rare diamonds which are formed in the transition zone and the lower mantle regions of the deep Earth at depths of several hundreds of km. These unique diamonds and their inclusions are the only direct source of information available on the physical and chemical conditions in the deep Earth down to at least the upper part of the lower mantle [1-4].

3D elemental imaging of trace elements within low absorbing matrices can be achieved with confocal µ X-ray fluorescence (µXRF) [5]. The confocal detection mode confines the view of the detector on the interaction path of the excitation beam with the sample to a small microscopic sub-volume. Confocal µXANES in fluorescence detection mode represents a natural extension of the corresponding µXRF technique, expanding the obtained spatially resolved elemental information to the speciation level.

The scanning XRF microprobe installed at Beamline L of DORIS III was used for the confocal µXRF and µXANES measurements presented here. Glass polycapillary half-lenses were used to focus the incoming monochromatic beam and to realise the confocal detection mode. The detection volume was determined to be 21×26×17 μm^3 (FWHM).

The examined diamond (RS69) was collected from an alluvial deposit in the Juina area [3-4]. This diamond contains a stream of microscopic inclusions of 1-10 µm in size. In order to access the inclusions within the diamond by the confocal set-up and to reduce matrix absorption, a window was

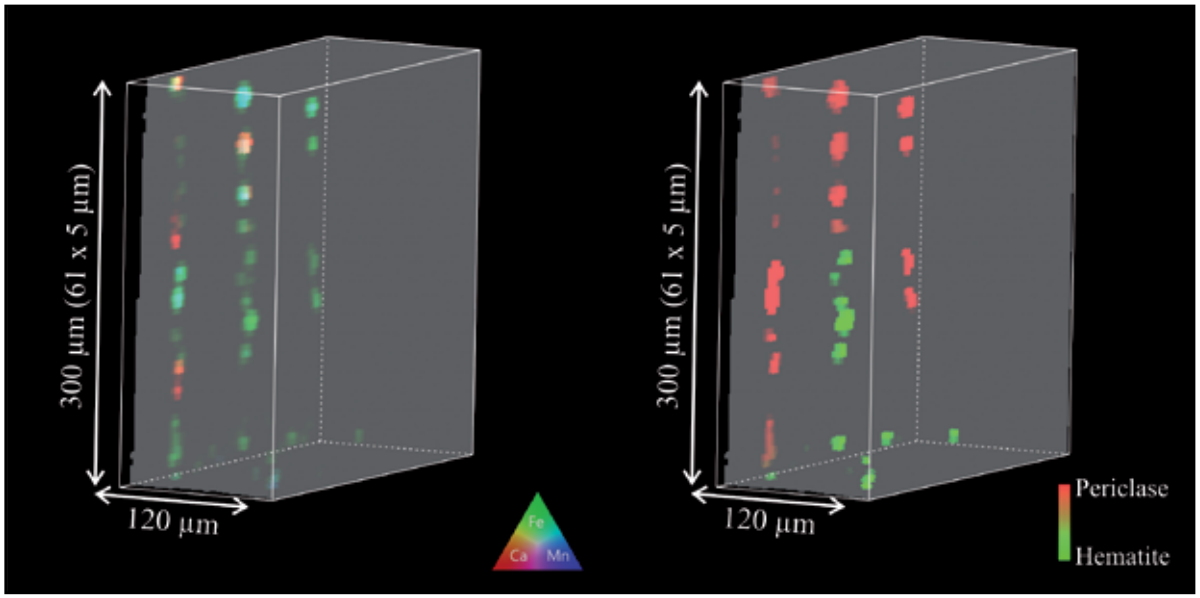

Figure 2

left: Combined 3D RGB image showing the elemental distributions of Ca (red), Fe (green) and Mn (blue) for a 300 µm long part of the inclusion stream within diamond RS69; right: interpolated 3D composition image showing the fraction of ferropericlase (red) and hematite (green) for the Fe containing inclusions. The diamond matrix is shown in dark grey.

polished in the diamond close to the inclusion stream at a distance below 100 µm.
Elemental maps from three vertical confocal µXRF planes, separated by a 50 µm distance, were collected. As a representative example, the normalised Fe Kα intensity map for one of the confocal planes recorded is given in Fig. 1a. Confocal Fe K XANES spectra were collected on a selection of the observed Fe-rich inclusions over the three vertical maps. The Fe K XANES spectra for the eight measurement locations indicated on the Fe Kα intensity map (Fig. 1a) are given in Fig. 1b together with hematite (Fe_2O_3) and ferropericlase ((Fe,Mg)O) reference spectra. The spectra obtained on the inclusions can be regarded as linear combinations of the hematite and ferropericlase spectra, with the inclusions in the upper part having a large ferropericlase fraction and the lower inclusions being hematite. The corresponding ferropericlase and hematite fit fractions for the Fe containing inclusions within the confocal plane shown are given in Fig. 1c.

Combining the data from all three confocal maps allows the visualization of the Fe, Mn and Ca distribution in a 300 µm long section of the inclusion cloud within the diamond in 3D (Fig. 2, left). Confocal µXANES further showed that Mn, which is about 100 times less abundant than Fe, occupies Fe sites within the mineral crystal structure.

As illustrated, the confocal µXANES technique provides complementary structural information on the Fe containing inclusions in a non-destructive 3D fashion (Fig. 2, right). With respect to the inclusions investigated, pristine inclusions were identified and their phases characterised. These results enable for the first time the study of natural mantle phases originating from the deep mantle and open new perspectives for mantle geochemistry studies.

Contact: Laszlo Vincze, laszlo.vincze@ugent.be
Frank E. Brenker, f.brenker@em.uni-frankfurt.de

Authors

Geert Silversmit[1], Bart Vekemans[1], Karen Appel[2], Sylvia Schmitz[3], Tom Schoonjans[1], Frank E Brenker[3], Felix Kaminsky[4], Laszlo Vincze[1]

1. X-ray Microspectroscopy and Imaging Research Group (XMI), Department of Analytical Chemistry, Ghent University, Krijgslaan 281 S12, B-9000 Gent, Belgium
2. HASYLAB at DESY, Notkestr. 85, 22607 Hamburg, Germany
3. Geoscience Institute - Mineralogy, Goethe University, Altenhoeferallee 1, 60438 Frankfurt am Main, Germany
4. KM Diamond Exploration Ltd., 2446 Shadbolt Lane, West Vancouver, BC, Canada, V7S 3J1

Original publication

"Three-Dimensional Fe Speciation of an Inclusion Cloud within an Ultradeep Diamond by Confocal µ-X-ray Absorption Near Edge Structure: Evidence for Late Stage Overprint", Analytical Chemistry 83, 6294–6299 (2011).

References

1. **T. Stachel , G. P. Brey, and J. W. Harris, "Kankan diamonds (Guinea) I: from the lithosphere down to the transition zone", Contrib. Mineral. Petrol. 140, 1-15 (2000).**
2. **T. Stachel, J. W. Harris, G. P. Brey, and W. Joswig, "Kankan diamonds (Guinea) II: lower mantle inclusion parageneses", Contrib. Mineral. Petrol. 140, 16-27 (2000).**
3. **F. Kaminsky, O. D. Zakharchenko, R. Davies, W. L. Griffin, G. K. Khachatryan-Blinova, A. A. Shiryaev, "Superdeep diamonds from the Juina area, Mato Grosso State, Brazil", Contrib. Mineral. Petrol. 140, 734–753 (2001).**
4. **P. Hayman, M. Kopylova, F. Kaminsky, "Lower mantle diamonds from Rio Soriso (Juina area, Mato Grosso, Brazil)", Contrib. Mineral. Petrol. 149, 430–445 (2005).**
5. **L. Vincze, B. Vekemans, F. E. Brenker, G. Falkenberg, K. Rickers, A. Somogyi, M. Kersten, F. Adams, "Three-dimensional trace element analysis by confocal X-ray microfluorescence imaging", Analytical Chemistry 76, 6786-679 (2004).**

Non-linear behaviour of liquid crystals under shear.

New insights from a new setup at DORIS III

New stable states of octylcyanobiphenyl liquid crystal could be induced by non-linear shear conditions and observed by a newly developed Rheology- and X-ray scattering setup using synchrotron radiation. Non-linear oscillatory shear created a distorted 6th order orientational structure. Even when the oscillatory shear is switched off, the induced structure remains stable and can be removed – only by heating the system – into the isotropic state. We assume the structure to be stabilized by defects which pin the new six-fold phase.

Liquid crystals belong to the wide class of complex fluids, which are easily deformable by external stresses [1]. In the present work we studied the influence of steady and oscillatory shear on the time evolution of the microstructure of 4-cyano-4'-octylbiphenyl (8CB) in the lamellar smectic A phase, which is a layered orientational ordered structure. Applying a shear field to liquid crystalline phases is one of the most successful methods employed to deform and orient anisotropic phases. When a shear field is applied, the system is transferred from the equilibrium into a non-equilibrium state. The transfer causes orientational order that arises from the complex interplay between structure and flow [2-4]. Only little is known about the nature of the non-equilibrium state and its consequences that are reflected in the viscoelastic and anisotropic properties of a material.

Any X-ray scattering process is based on the interaction between the incoming electromagnetic wave and electron density variations in the sample. When shear is applied in between the two plates of the rheometer geometry to the 8CB sample, the molecules have a tendency to form a periodic architecture that aligns perpendicular to the plates accordingly to the shear flow. This periodic architecture consists of a translational mass density modulation that generates the characteristic lamellar structure. The molecular long axis is perpendicular to the lamellae plane in this case and parallel to the so-called director n (Fig. 1). Local molecular orientation in liquid crystals, exhibiting singular behaviour along lines, points or walls, is far from perfect and is characterized by a wide variety of defects, leading e.g. to order parameter discontinuities and dislocations [5]. In order to obtain simultaneously information about the viscoelastic properties and the structural organisation on the nanoscale of 8CB

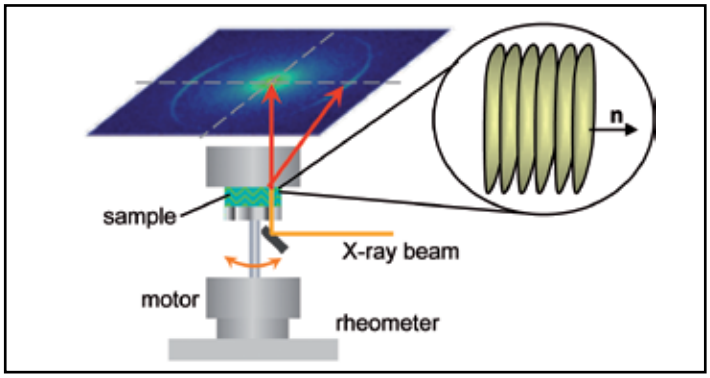

Figure 1

Plate/plate geometry with X-ray beam passing vertically through the setup. The expected orientation of the smectic lamellae defined by the director n can be ideally observed with the above presented setup. Text and figures are reprinted with permission from Langmuir. Copyright 2011 American Chemical Society.

or of any other molecular organization ordered similarly in a shear field, we have designed and commissioned a new set-up allowing a synchrotron X-ray beam passing vertically through the plates. The oriented sample produces a characteristic X-ray scattering pattern with two reflections separated by 180° in this case (Fig. 1).

We compared the effect of steady and oscillatory shear on the time evolution of the microstructure of 4-cyano-4'-octylbiphenyl in the lamellar smectic A phase. During both series of experiments, the system did not return to its initial state after stopping the experiment. Furthermore, the system did not relax from the shear induced non-equilibrium state to the equilibrium state. Shear of both kinds – steady and oscillatory – induced a reduction of misalignment and defects and

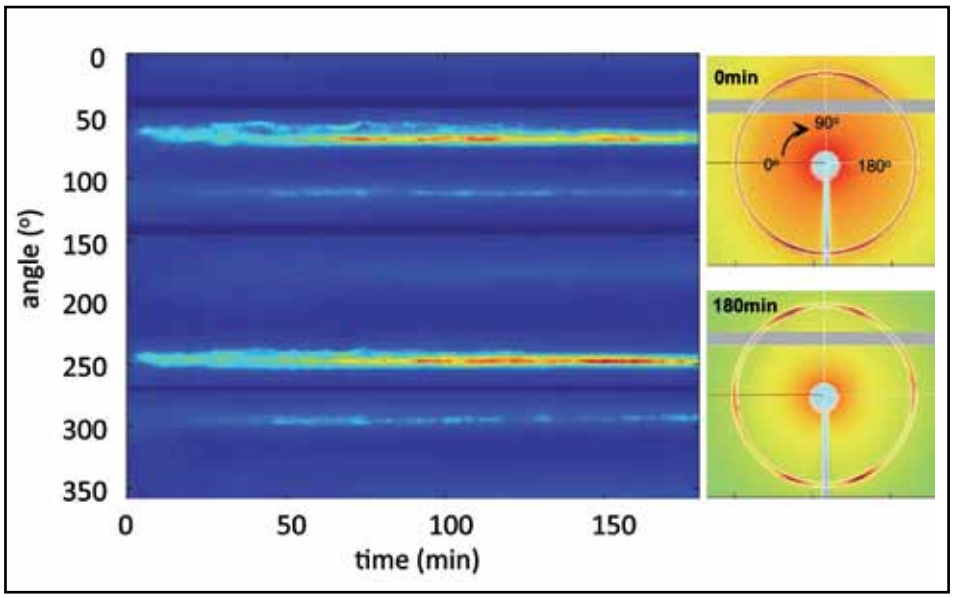

Figure 2

The appearance of 6 reflections was observed during LAOS experiments. The experimental conditions were strain = 1 and frequency = 1 Hz. The sample was preoriented from quenching from the isotropic to the smectic phase (0 min). After 180 min, six reflections could be observed. The stripes on the images are due to the gaps between the modules of the Pilatus 300K detector.

initiated growth of the smectic grains. Growth of these grains continued for hours after the shear was stopped. Our experiments showed that in the 8CB system shear history could not be removed by additional shear or long relaxation periods in the smectic phase. During LAOS (large amplitude oscillatory shear) experiments the shear history seemed to play an important role for the structural evolution of the system. The X-ray pattern obtained during the LAOS experiments showed for the non-linear regime 3 pairs of clearly separated reflections (Fig. 2). During all experiments peak intensities increased and the circular width of the reflections decreased. We conclude that defects were driven out and smectic layers were aligned. Additionally our new setup geometry allowed for the observation of a complete restructuration process leading to the characteristic X-ray pattern with three pairs of reflections.

With these findings a whole range of questions arises both from the experimental and the theoretical side. Our new observations and first very qualitative analyses will help gaining new and deeper insight into the complex rheological behaviour of smectic systems under LAOS conditions, although exact or even approximate theoretical results are currently not available. The new setup will enable to determine structural as well as dynamic features of fluid materials in non-equilibrium states ranging from complex fluids to cosmetics, food and mineral or metal melts under a huge variety of experimental conditions such as temperature, magnetic and electric fields and other external forces.

The rheology and SAXS setup was designed, built and commissioned as a pilot installation at beamline BW1 at DORIS III. Since June 2011, a new preliminary setup is available for users at beamline P10 at PETRA III.

Contact: Bernd Struth, bernd.struth@desy.de

Authors

Bernd Struth[1], Kyu Hyun[1], Efim Kats[2], Thomas Meins[3], Michael Walther[1], Manfred Wilhelm[3], Gerhard Grübel[1]

1. DESY, Notkestr. 85, 22607 Hamburg, Germany
2. ILL, BP 156, 6, rue Jules Horowitz, 38042 Grenoble Cedex 9, France
3. KIT, Institut für Technische und Polymerchemie, Abt. Polymerchemie, Engesserstr. 18, 76128 Karlsruhe, Germany

Original publication

"Observation of New States of Liquid Crystal 8CB under Nonlinear Shear Conditions as Observed via a Novel and Unique Rheology/Small-Angle X-ray Scattering Combination" LANGMUIR 27, 6, 2880-2887 (2011).

References

1. **R. G. Larson, "The Structure and Rheology of Complex Fluids", Oxford Univ Press, New York, (1999).**
2. **E. Loizou, L. Porcar, P. Schexnailder, G. Schmidt, and P. Batler, "Shear Induced Nanometer and Micrometer Structural Responses in Nanocomposite Hydrogels", Macromolecules 43, 1041–1049 (2010).**
3. **E. Brown, N. A. Forman, C. S. Orellana, H. Zhang, B. W. Maynor, D. E. Betts, J. M. DeSimone, and H. M. Jaeger, "Generality of shear thickening in dense suspensions", Nature Materials 9, 220–224 (2010).**
4. **S. Manneville, "Recent experimental probes of shear banding", Rheol. Acta, 47, 301–318 (2008).**
5. **N. A. Clark and T. P. Rieker, "Smectic-C ''chevron,'' a planar liquid-crystal defect: Implications for the surface-stabilized ferroelectric liquid-crystal geometry", Physical Review A, 37, 1053–1056 (1988).**

Switchable block copolymer membrane.

A chemical gate

Membranes with pH-responsive monodisperse nanochannels were prepared by the supramolecular assembly of block copolymer micelles in solution and metal-polymer complexation. Very high pore densities (> $2x10^{14}$ pores per m^2) were reproduced in m^2 scale. The membrane morphology and the capability of the pores to act as chemical gates by opening and closing when changing pH could be demonstrated by cryo field emission scanning electron microscopy, small-angle X-ray scattering (SAXS) and ultra/nanofiltration experiments.

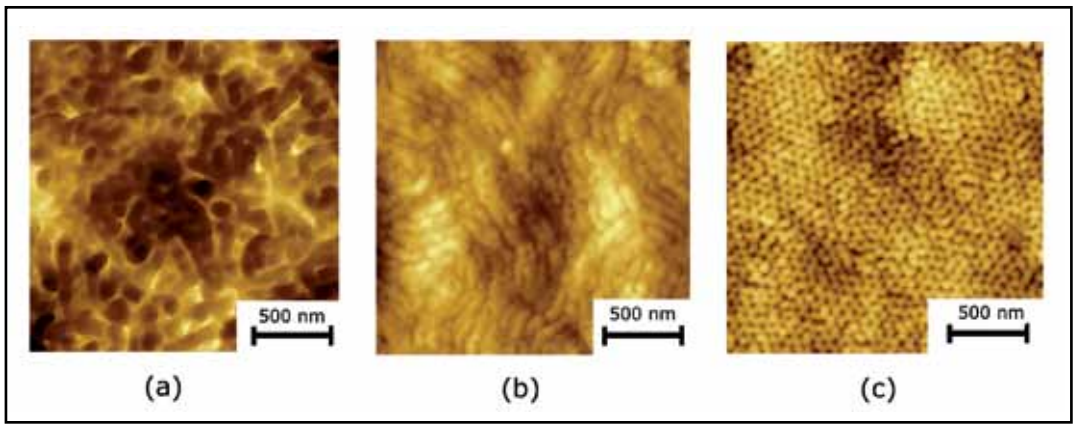

Figure 1

Atomic force microscopy surface images of PS-b-P4VP block copolymer membranes prepared in tetrahydrofurane/dimethylformamide (a) without and with addition of (b) Fe^{2+} and (c) Cu^{2+} ions.

New challenges for water purification require membranes with high selectivity (sharp pore size distribution) and flux (high porosity). Response to pH, and closing and opening pores are now needed for analytical sensors and biomedical devices for example to achieve controlled drug delivery. We recently demonstrated the manufacture of pH-responsive nanoporous films by combining the self-assembly of block copolymer micelles and conventional methods of membrane production by phase inversion [1-3]. An extremely regular morphology could be reproduced in m^2 scale, as needed for technical applications. The morphology was controlled by changing the solvent mixture composition [3] and by complexation with different metals [1,2]. The mechanism of pore formation could be understood with help of transmission electron microscopy tomography, cryo electron microscopy and small-angle X-ray scattering (beamline B1 at DORIS III).

We cast solutions of the block copolymer polystyrene-b-poly (4-vinylpyridine) (PS-b-P4VP) on a flat substrate. The solvent mixture strongly interacts with the hydrophilic P4VP block, leading to the formation of micelles with PS core. After partial evaporation of the most volatile solvent mixture component, the top layer becomes more concentrated in micelles, which have the chance to self-organize. The system is then immersed in water and the final morphology is consolidated by a fast water-solvent exchange. An asymmetric nanoporous film with very ordered top layer (approx. 400 nm thick) and a more random structure of increasing pore sizes below was obtained. A key point was the addition of metal ions to the casting solution. Pyridine is known to coordinate with different metal ions through both σ-bonding and π-bonding. Membranes prepared with copper ions were the most ordered, followed by nickel and cobalt. Films prepared with iron acetate have elongated or lamellar domains and do not have the characteristic pore morphology seen with other metal complexes, as confirmed by atomic force microscopy (Fig. 1). This observation follows the stability constant strength of pyridine-metal complexes. Stronger complexes stabilize the copolymer micelles and the link between them, leading to ordered supramolecular structures.

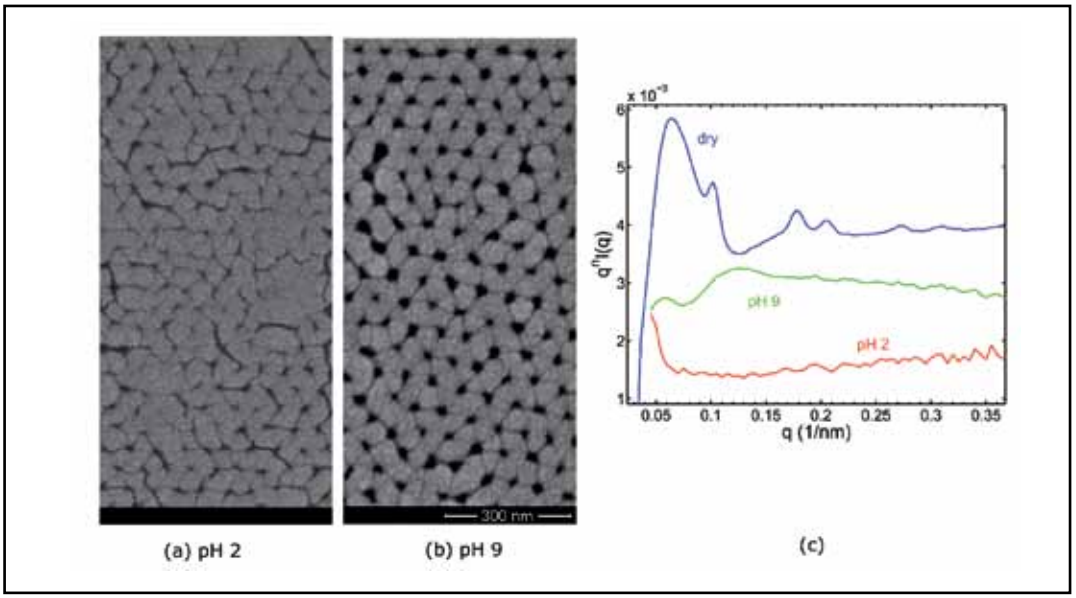

Figure 2

Cryo field emission scanning electron microscopy of membranes immersed in solutions with pH 2 (a) and 9 (b); and SAXS (c) of a dry membrane (in vacuum) and in aqueous solutions with pH 9 and pH 2; intensities have been weighted with q^n (n= 2, 3.2 and 4 for pH 2, pH 9 and dry sample, respectively).

Even more attractive was the fact that the pores in the membrane can be used as chemical gates without any further modification. We imaged the corresponding pore size change in different pH values by using cryo field emission electron microscopy, environmental microscopy and SAXS. We also measured water flux and selectivity to solutions containing different molecular weights of polyethylene glycol. Pyridine is the block preferentially exposed in the pore walls. At low pH pyridine is protonated and a coulombic repulsion leads to the stretching of the polymer segments, closing the pore. Furthermore, this process is reversible. By increasing the pH an abrupt recovery of the original pore size is observed. The very high water flux at high pH is an order of magnitude larger than those measured for commercial track etched membranes [4] with similar pore size, demonstrating the exceptional porosity.

Figure 2 shows the pore changes with pH imaged by cryo field emission scanning electron microscopy and the SAXS analysis of the dry membrane and that of membranes immersed in different pH solutions. The two-dimensional (2D) hexagonal morphology could be confirmed by SAXS analysis of dry membranes. The distance between pore centres was estimated as 70.3 ± 0.4 nm. When immersed in solutions of pH 9 and 2, instead of sharp peaks characteristic of hexagonal ordering in the dry membrane, only one broad peak can be observed. At high pH, the peak width was found to be about 6-fold larger than that of the dry membrane, indicating significant structure distortion in the wetted membrane. The position of the first reflection was shifted, giving a characteristic length scale of 64 ± 2 nm for the membrane in high pH, slightly lower than for the dry state. When the membrane was immersed in a solution of low pH, the scattering intensity decreased substantially and a broad hump could only be recognized above q = 1 nm^{-1}, corresponding to much smaller structures, probably remaining water channels with width of 1 – 3 nm.

Contact: Suzana Nunes, suzana.nunes@kaust.edu.sa
Klaus-Viktor Peinemann, klausviktor.peinemann@kaust.edu.sa

Authors

Suzana P. Nunes[1,4], Ali Reza Behzad[2], Bobby Hooghan[3], Rachid Sougrat[1], Madhavan Karunakaran[4], Neelakanda Pradeep[4], Ulla Vainio[5], Klaus-Viktor Peinemann[4]

1. Water Desalination and Reuse Center at King Abdullah University of Science and Technology (KAUST), 23955-6900 Thuwal, Saudi Arabia (current address)
2. Imaging and Characterization Lab at King Abdullah University of Science and Technology (KAUST), 23955-6900 Thuwal, Saudi Arabia
3. FEI at King Abdullah University of Science and Technology (KAUST), 23955-6900 Thuwal, Saudi Arabia
4. Advanced Membranes and Porous Materials Center at King Abdullah University of Science and Technology (KAUST), 23955-6900 Thuwal, Saudi Arabia
5. HASYLAB at Deutsches Elektronen-Synchrotron (DESY), 22607 Hamburg, Germany

Original publication

"Switchable pH-Responsive Polymeric Membranes Prepared via Block Copolymer Micelle Assembly", ACS Nano 5, 3516-3522 (2011).

References

1. **S. P. Nunes, A. R. Behzad, B. Hooghan, R. Sougrat, M. Karunakaran, N. Pradeep, U. Vainio, and K.-V. Peinemann, "Switchable pH-Responsive Polymeric Membranes Prepared via Block Copolymer Micelle Assembly", ACS Nano 5, 3516 –3522 (2011).**
2. **S. P. Nunes, R. Sougrat, B. Hooghan, D. H. Anjum, A. R. Behzad, L. Zhao, N. Pradeep, I. Pinnau, U. Vainio, and K.-V. Peinemann, "Ultraporous Films with Uniform Nanochannels by Block Copolymer Micelles Assembly", Macromolecules 43, 8079–8085 (2010).**
3. **S. P. Nunes, M. Karunakaran, N. Pradeep, A. R. Behzad, B. Hooghan, R. Sougrat, H. He, and K.-V. Peinemann, "From Micelle Supramolecular Assemblies in Selective Solvents to Isoporous Membranes", Langmuir, DOI: 10.1021/la201439p (2011).**
4. **E. N. Savariar, K. Krishnamoorthy, S. Thayumanavan, "Molecular Discrimination inside Polymer Nanotubes", Nature Nanotechnology 3, 112 –117 (2008).**

New family of layered titanium dioxide nanomaterials.

Nanohybrid hydrazinium titanate and its derivatives

Layered hydrazinium titanate (LHT-9) is a new nanohybrid material combining the redox functionality of hydrazine, the ion exchange properties of the layered TiO_2 host matrix, the large surface area of quasi-2D crystallites, the surface Brønsted acidity, and the occurrence of surface titanyl groups. Due to its high uptake capacity towards 50 elements of the Periodic System and its complex thermal behaviour, LHT-9 can be used as a versatile chemical toolkit for the design of TiO_2 nanomaterials such as a new layered modification of titanium dioxide, TiO_2(L). EXAFS studies of the coordination environment of Ti in LHT-9 and its derivatives indicate the coexistence of octahedral Ti sites along with surface titanyl (Ti = O) bonds which are likely responsible for the high surface activity of new compounds.

Nanocrystalline layered titanates constitute a family of compounds that attracts considerable interest due to its catalytic and ion-exchange properties and its potential to serve as precursors for synthesis of novel TiO_2 nanomaterials. The peculiar structural feature of layered titanates is their capability to accommodate guest cations and molecules between the stable titanium dioxide sheets thus providing a straightforward route towards the construction of nanohybrid TiO_2-based compounds [1].

A striking example of such nanohybrid material is layered hydrazinium titanate $(N_2H_5)_{1/2}Ti_{1.87}O_4$ (LHT-9), a compound that is structurally related to lepidocrocite-type titanates [2]. This material inherits the rich chemical functionality of the toxic and unstable hydrazine (N_2H_4) and can be used as solid stable source of the latter in those applications where the usage of liquid hydrazine is restricted for safety reasons. LHT-9 is a versatile adsorbent possessing high uptake capacity of ~50 elements of the Periodic System (Fig. 1). Its polyfunctional adsorption behavior results from the superposition of several factors: The strong reductive properties inherited from parent hydrazine, the ion exchange activity of the layered titanate structure, and the large surface area of quasi-2D nanoleaves. LHT-9 is likely the sole known adsorbent simultaneously possessing reductive and ion exchange properties. Besides that, the surface structure of the titanate

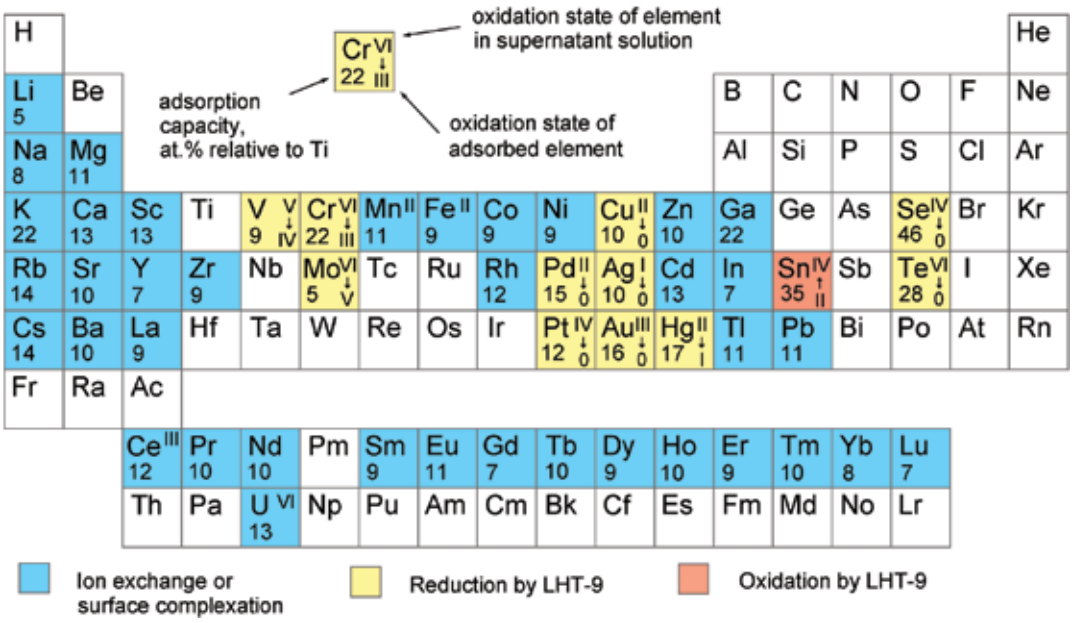

Figure 1

The Periodic Table with the elements that can react with nanocrystalline layered hydrazinium titanate (LHT-9) in aqueous solutions. Depending on the properties of each element, different adsorption mechanisms are expected. (Reprinted with permission from Journal of the American Chemical Society. Copyright 2011 American Chemical Society.)

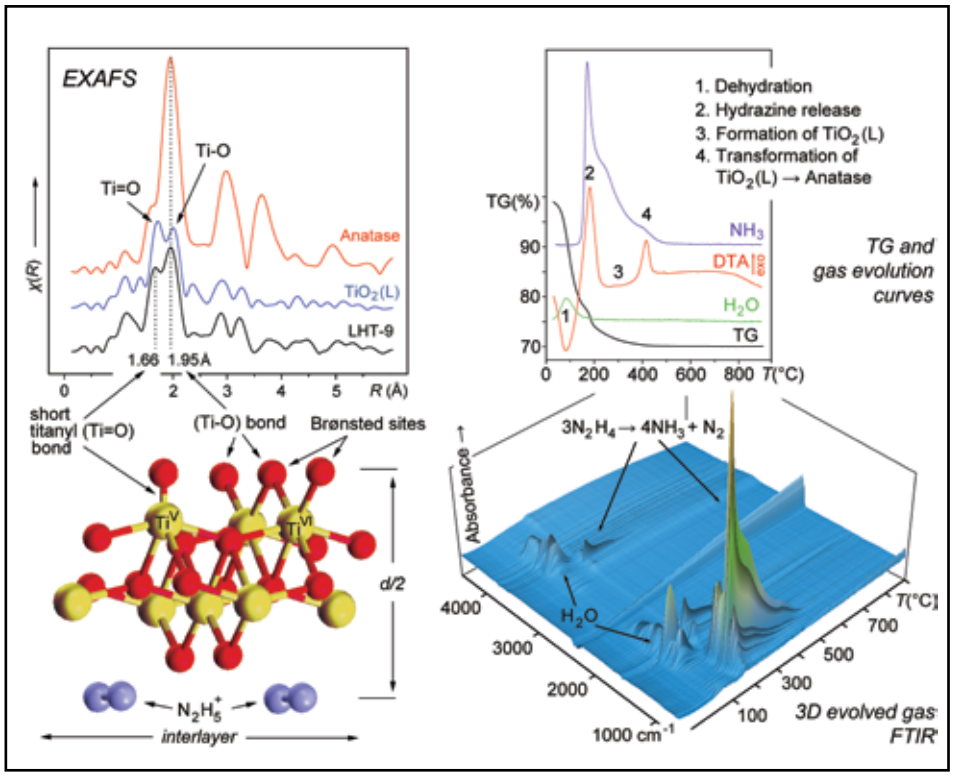

Figure 2

Left: Suggested positions of five- and six-fold coordinated Ti sites, titanyl bonds and Brønsted acid sites in the crystal structure of layered hydrazinium titanate, LHT-9. Ti-K FT-EXAFS of LHT-9 and of a new layered polymorph of titanium dioxide, TiO_2(L). The spectrum of anatase is shown for comparison. Right: Thermal transformations of LHT-9, including differential thermal analysis (DTA) and thermogravimetric (TG) curves (top) and a 3D view of the evolved gas Fourier-transform infrared (FTIR) spectrum (bottom).

sheets significantly contributes to the overall adsorption activity of this material. The occurrence of Brønsted acid sites (Fig. 2) located at the bridging Ti-O-Ti oxygen atoms is a well known feature of layered titanates.

Our EXAFS studies (Fig. 2), performed at beamline A1 of DORIS III, clearly demonstrate yet another structural surface feature of LHT-9 and its layered derivatives: The coexistence of two types of titanium-oxygen bonds attributed both to a six-fold (octahedral) coordination of Ti (~1.95 Å) and the occurrence of titanyl groups with a short (~1.65 Å) Ti = O bond. The latter (being ascribed to five-fold coordinated titanium) have never been formerly observed in EXAFS spectra of titanium dioxide nanomaterials. On the other hand, XANES studies suggested the existence of a five-fold coordination of Ti in layered titanates and nano-anatase [3,4]. One can presume that titanyl groups in LHT-9 are related to a local truncation of octahedral Ti bonds adjacent to vacant titanium positions in titanate sheets (Fig. 2) and therefore can be considered as an inherent non-periodic structural feature of all defect lepidocrocite-type titanates. Noteworthy is that the occurrence of titanyl groups is also observed in EXAFS spectra of other layered derivatives of LHT-9, for example, in a new polymorphic modification of titanium dioxide, TiO_2(L) (Fig. 2) which likely possesses layered lepidocrocite-type structure.

TiO_2(L) is formed in the course of complex thermal decomposition of LHT-9 (Fig. 2) and is easily transformed into anatase-type TiO_2 upon subsequent heating. Therefore, multistage thermal transformations of LHT-9 add additional variability to the functionality of nanohybrid titanate, and along with its polyfunctional chemical behaviour allow to construct a diversity of new titanium dioxide nanomaterials.

Contact: Sergey N. Britvin, sbritvin@gmail.com

Authors

Sergey N. Britvin[1,2], Andriy Lotnyk[3,4], Lorenz Kienle[3], Sergey V. Krivovichev[1,2], Wulf Depmeier[5]

1. Department of Crystallography, Geological Faculty, Saint-Petersburg State University, Universitetskaya Nab. 7/9, St. Petersburg 199034, Russia
2. Nanomaterials Research Center, Kola Science Center of Russian Academy of Sciences, Fersman Street 20, 184200 Apatity, Murmansk Reg., Russia
3. Institute for Material Science, Synthesis and Real Structure, University Kiel, Kaiserstraße 2, 24143 Kiel, Germany
4. Leibniz Institute of Surface Modifications, Permoserstraße 15, 04318 Leipzig, Germany
5. Institute for Geosciences, University Kiel, Olshausenstraße 40, 24118 Kiel, Germany

Original publication

"Layered Hydrazinium Titanate: Advanced Reductive Adsorbent and Chemical Toolkit for Design of Titanium Dioxide Nanomaterials", Journal of the American Chemical Society 133, 9516–9525 (2011).

References

1. **D. Portehault, C. Giordano, C. Sanchez, and M. Antonietti, "Nonaqueous Route toward a Nanostructured Hybrid Titanate", Chem. Mater. 22, 2125–2131 (2010).**
2. **T. Sasaki, F. Kooli, M. Iida, Y. Michiue, S. Takenouchi, Y. Yajima, F. Izumi, B. C. Chakoumakos, and M. Watanabe, "A Mixed Alkali Metal Titanate with the Lepidocrocite-like Layered Structure. Preparation, Crystal Structure, Protonic Form, and Acid-Base Intercalation Properties", Chem. Mater. 8, 777–782 (1996).**
3. **F. Farges, G. E. Brown, Jr., and J. J. Rehr, "Ti K-edge XANES studies of Ti coordination and disorder in oxide compounds: Comparison between theory and experiment", Phys. Rev. B 56, 1809–1819 (1996).**
4. **A.-M. Flank, P. Lagarde, J.-P. Itié, A. Polian, and G. R. Hearne, "Pressure-induced amorphization and a possible polyamorphism transition in nanosized TiO_2: an x-ray absorption spectroscopy study", Phys. Rev. B 77, 224112 (2008).**

Discovery of colloidal quasicrystals.

Micellar tilework – a mosaic in colloidal solutions

Micelles are known to self-assemble into ordered structures in aqueous solution. Such lyotropic systems so far all showed classical crystallographic symmetries. Using small-angle X-ray scattering for the first time micellar phases with exceptional 12-fold and 18-fold diffraction symmetries were observed. Such diffraction symmetries are typical for quasicrystalline phases. A 18-fold symmetry has never been reported before for any material. Water based colloidal quasicrystals open a new route to advanced photonic band gap materials.

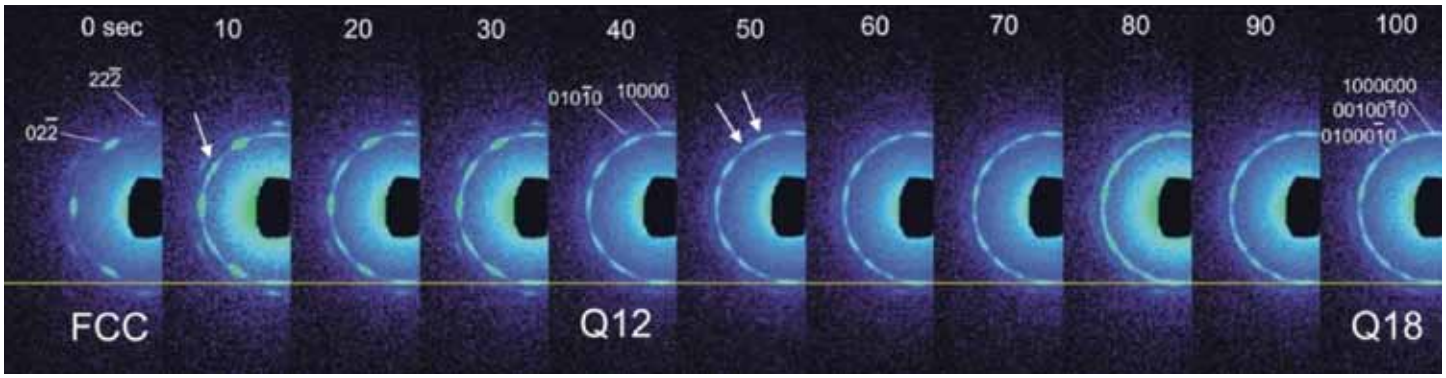

Figure 1

Time-resolved small-angle scattering pattern (BW4 at DESY) showing the temperature-induced transition from FCC phase to the Q12 and Q18 phases. The diffraction patterns were recorded in 10 sec. per frame. The transition into the quasicrystalline phases proceeds by splitting of reflections, as indicated by the arrows. The reflections for the quasicrystals are indexed on a set of five reciprocal base vectors (generalized Miller indices). The figure is taken from [S. Fischer *et al.*, Proc. Natl. Acad. Sci. 108, 1810-1814 (2011)]

The formation of micelles by association of amphiphilic molecules in aqueous solutions is one of the simplest examples for self-assembly found in nature. Micelles are commonly used in washing detergents, for the solubilisation of pharmaceuticals as well as for the preparation of advanced materials [1]. Typically, above a micelles concentration of 10 % an order-disorder phase transition occurs, where the micelles self-assemble into liquid crystals. In the case of spherical micelles the most common structure types are of cubic symmetry with space groups $Fm\bar{3}m$ (face-centred cubic, FCC) or $Im\bar{3}m$ (body-centred cubic, BCC).

We have investigated in detail the liquid crystalline phase behaviour of polymeric micelles in the concentration range from 10 % to 25 % by SAXS at beamline BW4. Shear orientation was used to obtain large monodomain samples of centimetre dimensions.

When investigating the phase behaviour of the micelles near the order–disorder transition we discovered phases with unusual diffraction patterns of 12- (Q12) and 18-fold (Q18) rotational symmetry. These diffraction symmetries are forbidden for all of the known 230 periodic lattice space groups. Such symmetries are typical for quasicrystals. Quasicrystals were first discovered 1984 by Shechtman on Al-Mn-alloys [2]. Quasicrystals have a long-range order, but are not periodic. They are most commonly found in binary and ternary metallic alloys, and recently also in binary nanoparticle mixtures. The

existence of colloidal quasicrystals has been theoretically predicted for colloids with soft interaction potentials by Denton and Löwen [3]. Such quasicrystals are stable at low temperatures in a range of concentrations between the disordered state and close-packed crystals.

To get further insight into the topological changes during the phase transitions from an FCC-phase to the quasicrystalline phases, time resolved microfocus SAXS experiments were performed (Fig.1). A shear-oriented micellar solution of 15 % was cooled from 20°C to 10°C. Diffraction patterns were recorded in 10 second per frame. At the beginning the characteristic diffraction pattern of a FCC-phase with its 6-fold diffraction symmetry was observed. After 10 seconds, a second set of six strong reflections (6_2) has appeared between the six 220 reflections (6_1) leading to a 12-fold diffraction pattern. This signals the transition into the Q12 phase. After 40 seconds the Q12 phase was fully developed. After 50 seconds a splitting of the six (6_1) reflections were observed (see arrows). This indicates a 18-fold diffraction symmetry corresponding to a Q18 phase. The data evaluation suggests that the transition from FCC phase to Q12 and Q18 phases proceeds via rearrangements of micelles in the (111) layers of the FCC phase. Figure 2 shows the diffraction patterns of the Q12 and Q18 phase and there corresponding tilling patterns.
Our results demonstrate the first example of quasicrystals that are spontaneously formed by micellar self-assembly in colloidal solutions. As they are water-based one-component quasicrystals, they are physically and chemically very simple systems. Quasicrystals with 18-fold diffraction symmetry have never been reported before for any material.
The discovery of these new quasicrystals in a chemically simple aqueous micellar system is remarkable. It opens the way to new advanced products like photonic band gap arrays produced by cost-effective and straightforward water based chemistry [4-5].

Contact: Jan Perlich, jan.perlich@desy.de
Sabine Rosenfeldt, sabine.rosenfeldt@uni-bayreuth.de

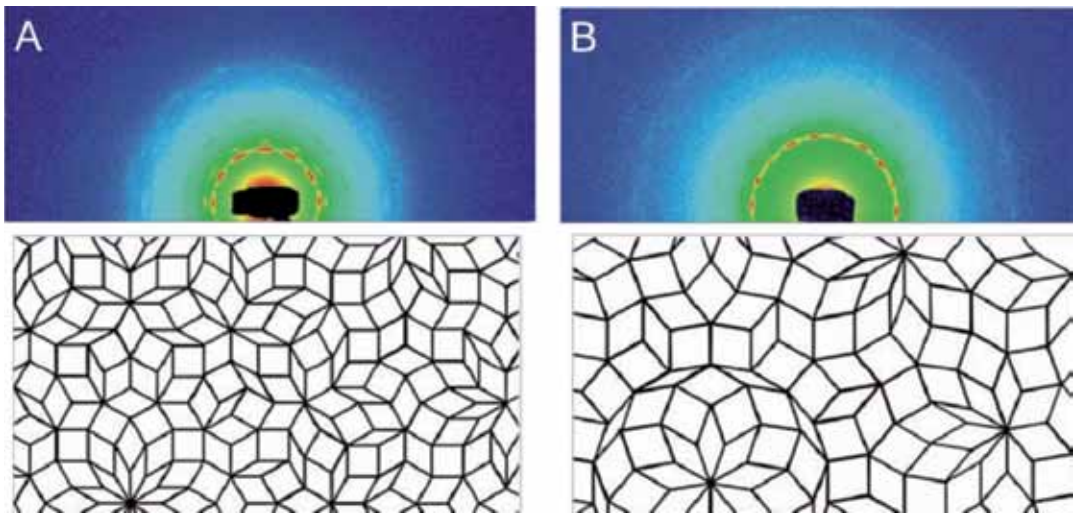

Figure 2
Diffraction image of a colloidal quasicrystal with 12-fold symmetry (A) and 18-fold symmetry (B) with the corresponding tiling patterns underneath. Each pattern is formed by four differently shaped tiles.

Authors

Steffen Fischer[1], Alexander Exner[1], Kathrin Zielske[1], Jan Perlich[2], Sofia Deloudi[3], Walter Steurer[3], Peter Lindner[4], Stephan Förster[5]

1. Institut für Physikalische Chemie, Universitat Hamburg, 20146 Hamburg, Germany,
2. DESY, Notkestrasse 85, 22603 Hamburg, Germany
3. Laboratory of Crystallography, Department of Materials, Eidgenössiche Technische Hochschule Zürich, CH-8093 Zürich, Switzerland
4. Institut Laue Langevin, F-38042 Grenoble Cedex 9, France
5. Physikalische Chemie I, Universität Bayreuth, Universitätsstrasse 30, 95440 Bayreuth, Germany

Original publication

Colloidal quasicrystals with 12-fold and 18-fold diffraction symmetry, Proc. Natl. Acad. Sci. 108, 1810-1814 (2011).

References

1. **S. Förster, T. Plantenberg, "From self-organizing polymers to nanohybrid and biomaterials", Angew. Chem. Int. Ed. 41, 688–714 (2002).**
2. **D. Shechtman, I. Blech, D. Gratias, J. W. Cahn, "Metallic phase with long-range orientational order and no translational symmetry", Phys. Rev. Lett. 53, 1951 (1984).**
3. **A. R. Denton, H. Löwen, "Stability of colloidal quasicrystals", Phys. Rev. Lett. 81, 469–472 (1998).**
4. **M. E. Zoorob, M .D. B. Charlton, G. J. Parker, J. J. Baumberg, M. C. Netti, "Complete photonic bandgaps in 12-fold symmetric quasicrystals", Nature 404, 740–742 (2000).**
5. **S. C. Glotzer, M. Engel, "Materials science: Complex order in soft matter", Nature 471, 309–310 (2011).**

Porous α-Fe_2O_3 for application in thin film microbatteries.

Do nanocrystallinity and mesopore cavities make a difference?

Combining sol-gel chemistry with simple polymer templating strategies enables the production of α-Fe_2O_3 thin films with a distorted cubic network of uniform 15 nm diameter pores and tunable nanocrystalline domain sizes. These materials are well-defined at both the nanoscale and the microscale after annealing in air at 550 °C, as confirmed by grazing-incidence small-angle X-ray scattering (GISAXS), X-ray photoelectron spectroscopy (XPS) and time-of-flight secondary ion mass spectrometry (TOF-SIMS). Electrochemical studies further show the benefits of producing a nanocrystalline material with interconnected porosity. Mesoporous α-Fe_2O_3 thin films not only exhibit enhanced lithium ion storage capabilities compared to bulk α-Fe_2O_3 but also show excellent cycling stabilities.

α-Fe_2O_3 is a binary transition metal oxide that has widespread use in applications, such as catalysis, sensing, and as non-toxic pigment. Even though it is a redox-active material, bulk versions of α-Fe_2O_3 have not proven to be of much interest for lithium ion battery applications because of poor cycling behavior and modest reaction kinetics. However, recent developments have clearly shown that when the grain size is reduced from microscale to nanoscale, the charge storage characteristics can be enhanced by suppressing the irreversible phase transformations that are observed in microcrystalline α-Fe_2O_3 upon lithiation.

In recent years, it has been shown that polymer templating strategies are efficient routes to produce metal oxides with both a mesoporous morphology and a nanocrystalline framework [1,2]. The formation of these materials relies on the solution phase coassembly of sol-gel precursors with a structure-directing agent to produce long-range periodicities reminiscent of lyotropic liquid crystalline phases [3,4]. The corresponding thin films can be achieved by the same coassembly methods but using an evaporation-induced self-assembly (EISA) process [5].

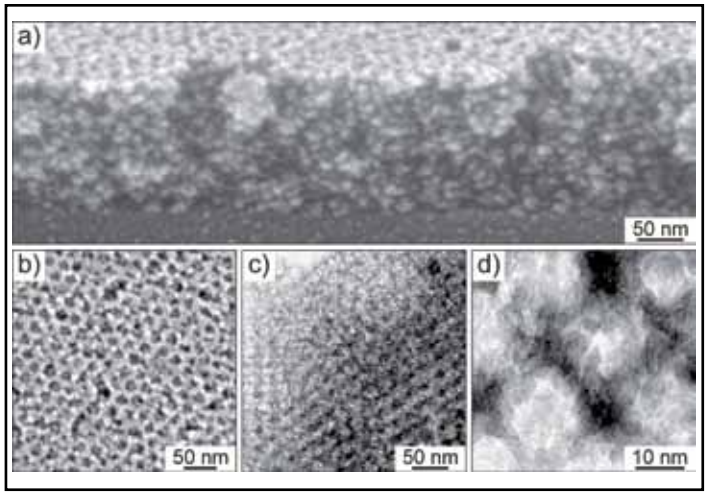

Figure 1

Morphology of self-assembled α-Fe_2O_3 thin films heated to 550 °C in air. (a) Cross-sectional SEM image showing that the distorted cubic pore structure persists throughout the films. (b) Top view SEM image confirming the absence of a sealing layer at the solid-air interface. (c,d) Low- and high-magnification TEM images showing pores averaging 15 nm in diameter.

The sol-gel derived α-Fe_2O_3 thin films studied in this work were produced using an EISA process. In the synthesis, a poly(ethylene-co-butylene)-block-poly(ethylene oxide) diblock copolymer, also referred to as KLE, served as the structure-directing agent. KLE has been shown to be particularly suitable for the preparation of large-pore mesoporous thin films with nanocrystalline walls [6]. Part of the reason for this is that KLE produces materials with sufficiently thick walls that allow for uniform nucleation and growth of the crystalline phase while retaining nanoscale porosity/periodicity.

To probe both the top surface and the porous interior of the KLE-templated α-Fe_2O_3 thin films, various microscopy techniques were used. Figure 1 shows transmission electron microscopy (TEM) and scanning electron microscopy (SEM) images of a nanocrystalline sample. These data reveal a distorted cubic network of open pores averaging 15 nm in diameter.

More quantitative information on the nanoscale structure was obtained by GISAXS and conventional SAXS experiments in transmission mode. These measurements were carried out on beamline BW4 at DORIS using a MarCCD area detector and a sample-detector distance of 1820 mm. Figure 2 shows GISAXS patterns collected on thin films heated to different annealing temperatures. It is evident from these data that KLE-templated Fe_2O_3 in fact exhibits a distorted cubic pore-solid architecture with comparatively low preferred orientation relative to the substrate. The elliptical shape of the GISAXS patterns further indicates a large unidirectional lattice con-

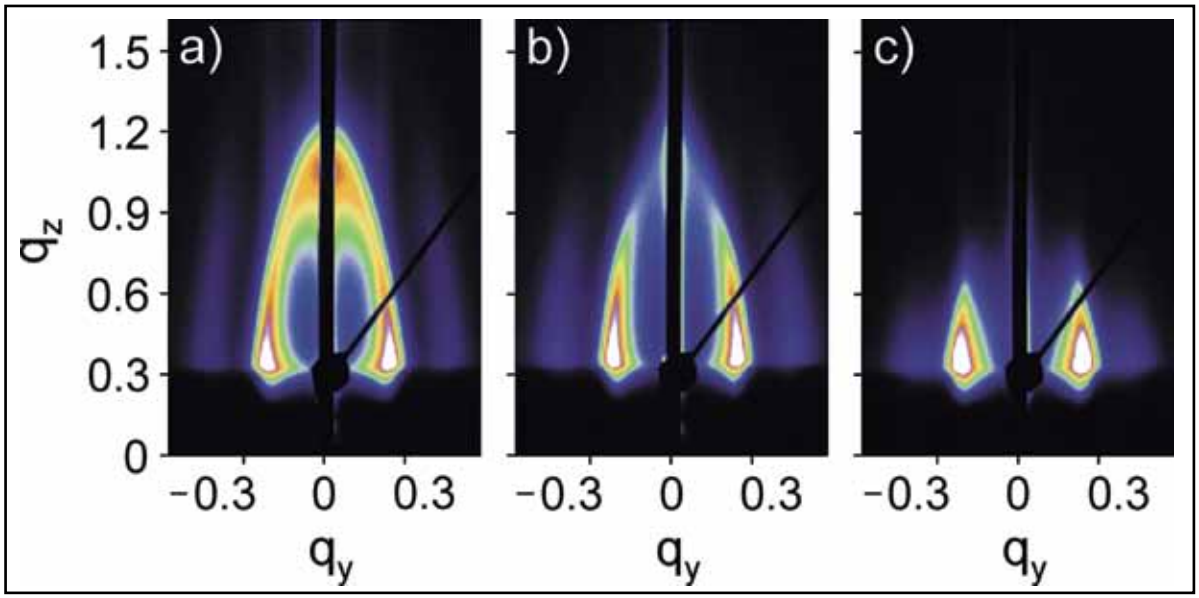

Figure 2

Synchrotron-based GISAXS on self-assembled Fe_2O_3 thin films heated to different annealing temperatures of 250 °C (a), 450 °C (b), and 600 °C (c). GISAXS patterns were collected at an angle of incidence β of 0.2°. Scattering vector q components are given in nm^{-1}.

traction, which is associated with continuous pore transformation from spherical to oblate. Upon heating the samples to 600 °C, a loss of out-of-plane scattering is observed. This loss is due to both the small number of repeat units normal to the plane of the substrate and to the growth of the nanocrystalline domains in the pore walls; the crystallization begins at ~ 400 °C.

Overall, the structure and morphology results showed that the obtained α-Fe_2O_3 thin films are homogeneous at both the nanoscale and the microscale after annealing at elevated temperatures. In addition, XPS, TOF-SIMS, and Raman studies indicated that they can be produced in phase-pure form and contain only minor defects.

To examine the redox processes present in KLE-templated α-Fe_2O_3, both cyclic voltammetry and galvanostatic charge/discharge experiments were carried out. These measurements showed the benefits of combining a mesoporous morphology with nanocrystalline thin films to achieve enhancement in electrochemical charge storage. Mesoporous α-Fe_2O_3 thin films with an average crystallite size of 14 nm are not only able to reversibly accommodate significant amounts of lithium ions but can also maintain stable cycling performance at high rates. These results are exciting and indicate that porous versions of α-Fe_2O_3 show promise as anode materials for rechargeable lithium ion batteries.

Contact: Torsten Brezesinski, torsten.brezesinski@phys.chemie.uni-giessen.de

Authors

Kirstin Brezesinski[1], Jan Haetge[1], John Wang[2], Simone Mascotto[1], Christian Reitz[1], Alexander Rein[1], Sarah H. Tolbert[3], Jan Perlich[4], Bruce Dunn[5], and Torsten Brezesinski[1]

1. Institute of Physical Chemistry, Justus-Liebig-University Giessen, Heinrich-Buff Ring 58, 35392 Giessen, Germany
2. HRL Laboratories, LLC, Malibu, CA 90265, USA
3. Department of Chemistry and Biochemistry, University of California at Los Angeles, CA 90095, USA
4. DESY, Notkestrasse 85, 22603 Hamburg, Germany
5. Department of Materials Science and Engineering, University of California at Los Angeles, CA 90095, USA

Original publication

"Ordered mesoporous α-Fe_2O_3 (hematite) thin-film electrodes for application in high rate rechargeable lithium batteries", Small 7, 407–414 (2011).

References

1. **P. D. Yang, D. Y. Zhao, D. I. Margolese, B. F. Chmelka, and G. D. Stucky, "Block copolymer templating syntheses of mesoporous metal oxides with large ordering lengths and semicrystalline framework", Chem. Mater., 11, 2813–2826 (1999).**
2. **C. Sanchez, C. Boissiere, D. Grosso, C. Laberty, and L. Nicole, "Design, synthesis, and properties of inorganic and hybrid thin films having periodically organized nanoporosity", Chem. Mater., 20, 682-737 (2008).**
3. **C. T. Kresge, M. E. Leonowicz, W. J. Roth, J. C. Vartuli, and J. S. Beck, "Ordered mesoporous molecular-sieves synthesized by a liquid-crystal template mechanism", Nature 359, 710–712 (1992).**
4. **U. Ciesla and F. Schuth, "Ordered mesoporous materials", Micropor. Mesopor. Mat., 27, 131–149 (1999).**
5. **C. J. Brinker, Y. F. Lu, A. Sellinger, and H. Y. Fan, "Evaporation-induced self-assembly: nanostructures made easy ", Adv. Mater., 11, 579-585 (1999).**
6. **J. Haetge, P. Hartmann, K. Brezesinski, J. Janek, and T. Brezesinski, "Ordered large-pore mesoporous $Li_4Ti_5O_{12}$ spinel thin film electrodes with nanocrystalline framework for high rate rechargeable lithium batteries: relationships among charge storage, electrical conductivity, and nanoscale structure", Chem. Mater., 23, 4384-4393 (2011).**

New opportunities for anti-tuberculosis drug development.

Multi-functional proteins

Tuberculosis kills millions of people every year worldwide and understanding the lifecycle and mechanisms of the causative agent, Mycobacterium tuberculosis, is crucial to tackle this disease. Structural studies on an enzyme with bisubstrate specificity present possible opportunities for drug development. Whereas most organisms utilise two specific single-substrate enzymes for histidine and tryptophan biosynthesis, in several actinobacteria including M. tuberculosis, both reactions are catalysed by one bisubstrate enzyme (PriA). The catalytic mechanism observed in M. tuberculosis is organism-specific and could be exploited as a drug target.

Tuberculosis is an infectious disease caused by the bacteria Mycobacterium tuberculosis, and kills an estimated 1.6 million people every year making it one of the largest threats to human health worldwide. The current treatment involves a long course of antibiotics but with the increasing emergence of multi drug resistant strains this is becoming less and less effective. Obviously long courses of antibiotics are costly and difficult to implement in regions where a health service infrastructure is not well established. The need for novel treatment has never been more urgent. Furthermore research shows that the lifecycle of the bacteria is more complex than originally thought – it can remain latent, and even undetectable, in the human body for many years, and only become active when the immune system becomes weakened, such as in HIV patients where tuberculosis is a frequent cause of death. Understanding how the bacteria live in the host and how it attacks the immune system is crucial to be able to combat this disease.

Mycobacterium tuberculosis is a member of a group of bacteria known as the actinobacteria and has been a major research interest at EMBL Hamburg for many years. The expertise of the Wilmanns' group at EMBL Hamburg has been in resolving the structure and function of proteins and enzymes of the bacteria with the use of structural biology techniques such as X-ray crystallography.

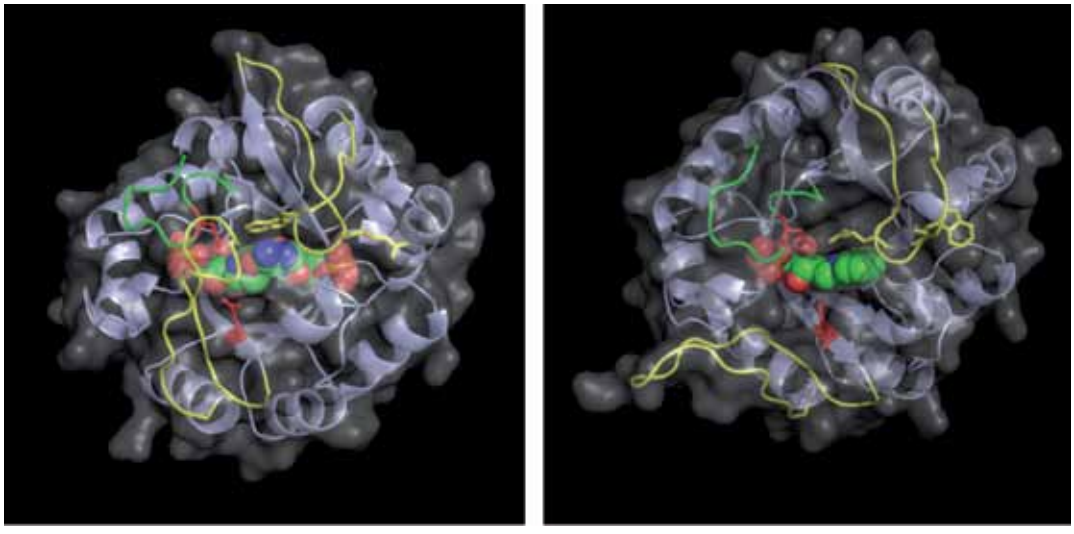

Figure 1

Mycobacterium tuberculosis' enzyme PriA has the unique ability to alter its active site – the pocket at the centre of the 3D structure shown – depending on which of the two molecules it is interacting with. The image on the left shows PriA (indicated by coloured spheres) involved in histidine biosynthesis. Tryptophan biosynthesis is shown on the right. The two loops shown in yellow are mainly responsible for the selective binding of the two different biosynthesis intermediates and fold accordingly into different conformations.

In the current study we identified an enzyme that is able to catalyse reactions on two different molecules or substrates. In most organisms, cells need two specific enzymes, known as HisA and TrpF to produce two essential amino acids – histidine and tryptophan. In most bacteria with this biosynthesis pathway, two different genes, hisA and trpF, encode these enzymes [1]. In most of the known actinobacteria genomes however, the trpF gene appears to be missing. Instead, a hisA like gene, known as priA, has been shown to encode an enzyme (PriA) with bisubstrate specificity in members of this group [2]. In the absence of structural data, the molecular mechanism by which the PriA enzyme catalyses both reactions was however not known.

We were able to solve the three dimensional structure of PriA. We found that it is has the unexpected ability to form two different active site structures which adapt to the histidine and tryptophan biosynthesis substrates. It does this by forming a reaction specific active site, or by undergoing a so called substrate induced metamorphosis to form a different active site. This mechanism of bisubstrate specific binding has never been observed before and appears to be unique for Mycobacterium tuberculosis and related organisms from the actinobacteria phylum. Considering that the two substrates differ in molecular weight by a factor of about two, and that the active sites of HisA and TrpF differ substantially in size, the bisubstrate specific binding of PriA seems quite remarkable. Comparison of structural data suggests that a high level of active site loop flexibility is a key parameter for bisubstrate specificity, as shown in Fig. 1. Nevertheless, a comparison of catalytic efficiency of both the single substrate enzymes HisA and TrpF and that of the bisubstrate specific PriA shows reduced activity as a result of decreased substrate affinity in PriA. The question whether this negative tradeoff in PriA bisubstrate specificity reflects evolutionary ancestry or evolutionary adaptation to specific living conditions [3], will have to wait further studies of other bacterial species without a trpF gene.

Since this bisubstrate specific binding mechanism is unique to these bacteria, we believe this could be an important opportunity for drug development studies in Mycobacterium tuberculosis. A drug which inhibits this organism-specific enzyme activity should not affect the host cells, or other bacteria living in or on humans. To support this we also screened 20,000 small molecule compounds and found a handful which inhibited both PriA-catalysed reactions, but had no influence on “normal” TrpF activity.

Contact: Matthias Wilmanns, wilmanns@embl-hamburg.de

Authors

Anne V. Due [a,1,2], Jochen Kuper [a,1,3], Arie Geerlof [a,4], Jens Peter von Kries [b], and Matthias Wilmanns [a]

a. European Molecular Biology Laboratory, Hamburg Unit, Notkestrasse 85, 22603 Hamburg

b. Leibniz-Institute for Molecular Pharmacology (FMP), Robert-Rössle-Strasse 10, 13125 Berlin

1. A.V.D. and J.K. contributed equally to this work

2. Present address: The Scripps Research Institute, 10550 North Torrey Pines Road, La Jolla, CA 92037, USA

3. Present address: Rudolf Virchow Center for Biomedical Research, Versbacher Strasse 9, 97078 Würzburg

4. Present address: Helmholtz Center Munich, Institute of Structural Biology, Ingolstädter Landstrasse 1, 85764 Neuherberg

Original publication

Proceedings of the National Academy of Sciences 108(9), 3554 (2011)
“Bisubstrate specificity in histidine/tryptophan biosynthesis isomerase from Mycobacterium tuberculosis by active site metamorphosis”

References

1. **G. Xie, N.O. Keyhani, C.A. Bonner, R.A. Jensen, “Ancient origin of the tryptophan operon and the dynamics of evolutionary change”, Microbiol. Mol. Biol. Rev. 67, 303 (2003)**
2. **F. Barona-Gomez, D. A. Hodgson, “Occurrence of a putative ancient-like isomerase involved in histidine and tryptophan biosynthesis”, EMBO Rep. 4, 296 (2003)**
3. **R. A. Jensen, “Enzyme recruitment in evolution of new function”, Annu. Rev. Microbiol. 30, 409 (1976)**

Common architecture of nuclear hormone receptor complexes.

Small angle X-ray scattering provides snapshots of functional states

Small angle X-ray scattering (SAXS) enables the analysis of the overall structures of highly complex biological systems in solution under conditions closely resembling the native environment. The SAXS studies of the functional states of proteins and complexes require measurements of many different samples under varying conditions to be performed with high accuracy and reproducibility. Recent developments at EMBL Hamburg facilitated a comprehensive analysis of the nuclear hormone receptor (NHR) proteins in complex with DNA. NHRs are highly important proteins controlling numerous physiological processes through the regulation of gene expression. In this study the binding of DNA to several NHRs was structurally characterized under various conditions and in complexes with different DNA fragments. The resulting structures of these complexes showed elongated, asymmetric shapes with a hinge region, which establish and maintain the integrity of the entire protein structure. The study provides a structural basis for understanding the role of DNA in the spatial organisation of NHR heterodimers in complexes with coactivators.

Small angle X-ray scattering (SAXS) is a low resolution structural method for investigations of biological macromolecules in solution. The development of data analysis and model building strategies over the last few years has allowed reliable three-dimensional shape reconstructions from experimental SAXS data [1]. The novel methods of SAXS data interpretation can also take into account additional information available from high resolution structural techniques (e.g. protein crystallography or nuclear magnetic resonance), biochemical methods and bioinformatics [2]. SAXS is especially valuable for biological solutions, where the method enables the analysis of functional states of proteins, protein-protein and protein-DNA complexes. These studies require measurements of many different protein samples with high accuracy and high reproducibility. At the EMBL Hamburg Unit, hardware and software for rapid and reliable SAXS data collection and analysis have been developed including an automated sample changing robot [3], and a data processing and analysis pipeline at the SAXS beamline X33 (storage ring DORIS III) [4]. These advances allow high precision experiments to be rapidly performed on macromolecular samples under varying conditions, followed by on-line construction of the structural models.

The advanced SAXS data collection and interpretation methods are actively applied in numerous collaborative projects at the EMBL SAXS beamline at DORIS III. One of the most striking recent applications is a comprehensive study of nuclear hormone receptors (NHRs), conducted in collaboration with scientists from the CNRS and University of Strasbourg, Illkirch, France. NHRs are a class of proteins that con-

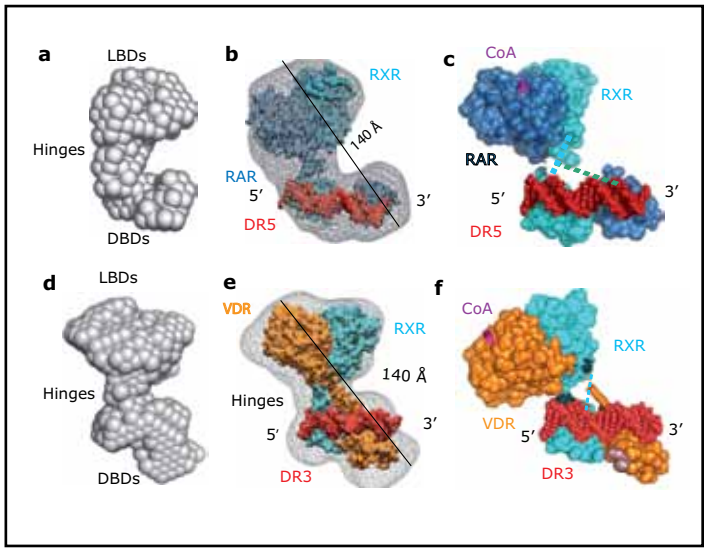

Figure 1

Solution structure of two NHR complexes with DNA (red). (a) Ab initio SAXS envelope of RXR-RAR with DNA generated by DAMMIN (b) More detailed rigid-body refined quasi atomic model in the ab initio SAXS envelope and (c) the model with the best agreement to the experimental data. (d) Ab initio envelope of RXR–VDR with DNA generated by DAMMIN and (e) quasi atomic model refined by rigid-body in the ab initio envelope. (f) Refined model of RXR–VDR with DNA showing the best agreement to the experimental data. The coactivator (CoA) bound to the NHR proteins is shown in purple. Both NHR structures show a common overall conformation of the different domains.

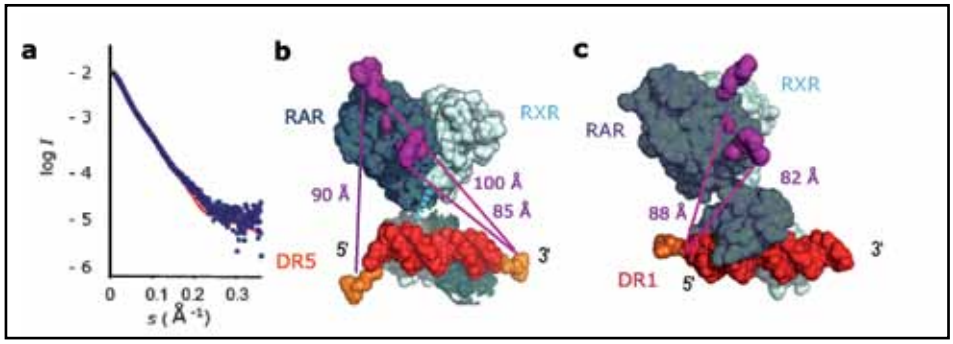

Figure 2

Validation of the SAXS models with results from FRET. (a) Comparison of the experimental SAXS curve (dots) with the corresponding fit for the refined SAXS model (red line). (b,c) Relative positions of the different domains analysed by FRET. The refined SAXS models of RXR–RAR and RAR–RXR both in complex with DNA agree with the measured distances from the FRET analysis.

trol many physiological processes by the regulation of gene expression [5]. They have a complicated structural organization consisting of DNA binding domains (DBDs) and ligand binding domains (LDBs). The former domains specifically recognize DNA sequences, whereas the latter form homo- or heterodimers, which serve for the modulation of the activity of the NHRs by binding of coactivators such as the steroid receptor coactivator-1 (SRC-1). In the present study a total of 14 NHRs and their complexes with DNA were measured under different conditions and coactivators. Already in the ab initio low resolution shapes of NHRs one can clearly recognize the domain structure of the complexes (bead models in Fig. 1). The results of the automated ab initio SAXS analysis were further combined with available high resolution crystal structures of the individual DBDs and LDBs (called RXR-RAR, PPAR-RXR and RXR-VDR). The obtained models reveal a common modular organisation with distinct DBD region containing the bound DNA, the LBD region and a variable N-terminal domain (Fig. 1, upper panel). Interestingly, a recent high resolution crystal structure of PPAR-RXR in complex with DNA, which is the first crystal structure of a DNA-bound NHR (Protein Data Bank code 3DZY [6]) shows a much more compact conformation, which is inconsistent with the SAXS models but also with the experimental SAXS data. Additional information about inter- and inner molecular distance was obtained by fluorescence resonance energy transfer (FRET) measurements of labelled samples. The distances obtained in the FRET experiments (Fig. 2) were fully compatible with the asymmetric elongated structures from SAXS suggesting that the closed conformation of the PPAR-RXR in the crystal could be caused by the crystal packing forces. Further, the more detailed analysis including the inner molecular distances information obtained by FRET confirms that the LBDs are in a crossed orientation with respect to the DBDs on the DNA, which was found to be a common architectural feature of all NHR–DNA complexes. The opening of the NHR is facilitated by binding of the coactivators, which maintain the extended conformation as a functional state in the NHR regulatory process.

The study of the NHR-DNA complexes underlines the potential of SAXS as a structural method, and the importance of a multidisciplinary approach in the studies of biological macromolecules. The possibilities for such comprehensive structural studies will be further boosted at the new high brilliance BioSAXS beamline P12 of the EMBL Hamburg at PETRA III, providing yet more precise data with much less material and at much shorter times. All techniques and methods developed at the DORIS III X33 beamline are adapted to the high performance of the new beamline and, as of autumn 2011, are already available for the users.

Contact: Dmitri I. Svergun, d.svergun@embl-hamburg.de

Authors

Natacha Rochel[1–4], Fabrice Ciesielski[1–4], Julien Godet[4–6], Edelmiro Moman[1–4], Manfred Roessle[7], Carole Peluso-Iltis[1–4], Martine Moulin[8], Michael Haertlein[8], Phil Callow[8], Yves Mély[4–6], Dmitri I. Svergun[7], Dino Moras[1–4]

1. Institut de Génétique et de Biologie Moléculaire et Cellulaire, Illkirch, France
2. Institut National de Santé et de Recherche Médicale U964, Illkirch, France
3. Centre National de Recherche Scientifique UMR 7104, Illkirch, France
4. Université de Strasbourg, Illkirch, France
5. Laboratoire de Biophotonique et Pharmacologie, Faculté de Pharmacie, Illkirch, France
6. Centre National de Recherche Scientifique UMR 7213, Illkirch, France
7. European Molecular Biology Laboratory, Hamburg Outstation, Hamburg, Germany
8. Institut Laue-Langevin, Grenoble, France

Original publication

"Common architecture of nuclear receptor heterodimers on DNA direct repeat elements with different spacings", Nature Structural & Molecular Biology 18, 564 (2011).

References

1. **H. D. Mertens and D. I. Svergun, "Structural characterization of proteins and complexes using small-angle X-ray solution scattering", J Struct Biol, 172(1): 128-41 (2010).**
2. **M. V. Petoukhov and D. I. Svergun, "Global Rigid Body Modeling of Macromolecular Complexes against Small-Angle Scattering Data", Biophys. J., 89(2): 1237-1250 (2005).**
3. **A. R. Round, D. Franke, S. Moritz, R. Huchler, M. Fritsche, D. Malthan, R. Klaering, D. I. Svergun, and M. Roessle, "Automated sample-changing robot for solution scattering experiments at the EMBL Hamburg SAXS station X33", Journal of Applied Crystallography, 41: 913-917 (2008).**
4. **M. V. Petoukhov, P. V. Konarev, A. G. Kikhney, and D. Svergun, "ATSAS 2.1 - towards automated and web-supported small-angle scattering data analysis", Journal of Applied Crystallography, 40: S223-S228 (2007).**
5. **D. M. Lonard, R. B. Lanz, and B. W. O'Malley, "Nuclear receptor coregulators and human disease", Endocr Rev, 28(5): 575-87 (2007).**
6. **V. Chandra, P. Huang, Y. Hamuro, S. Raghuram, Y. Wang, T. P. Burris, and F. Rastinejad, "Structure of the intact PPAR-gamma-RXR-alpha nuclear receptor complex on DNA", Nature, 456: 350-356 (2008).**

Serial femtosecond crystallography.

Structure in the blink of an eye (DESY in-house research performed at the LCLS)

With bright pulses of light packing a second's worth of the energetic output of a synchrotron into an unimaginably short burst, hard X-ray free electron lasers can challenge the conventional limits of macromolecular crystallography. Tiny crystals, between 100 nm and 2 µm in size, of a large membrane protein complex have been probed to a resolution of 8.5 Å using the Linac Coherent Light Source (LCLS) at the Stanford Linear Accelerator Center (SLAC) in California, USA. An international collaboration of over eighty people, with scientists from the Center for Free-Electron Laser Science (CFEL) taking a central role, demonstrated the early potential of this technique.

Almost half a decade before the availability of any X-ray free-electron laser, researchers had already realised that the very high dose rates delivered by their short and intense pulses might be a suitable strategy for reducing the amount of damage suffered by a specimen during its irradiation, allowing much smaller crystals to be examined than previously thought possible [1]. The principle is simply that the minuscule duration of the X-ray pulse would not allow for any of the normal atomic rearrangements occurring due to damage to proceed to a significant extent. Although the dose given to the specimen might be far in excess of what it could normally tolerate, the X-ray pulse is over – and therefore the information useful for structure solution already measured – before the specimen is destroyed. The validity of this approach was demonstrated in 2005 with a two dimensional specimen using FLASH [2], and it has now been applied directly to macromolecular crystallography.

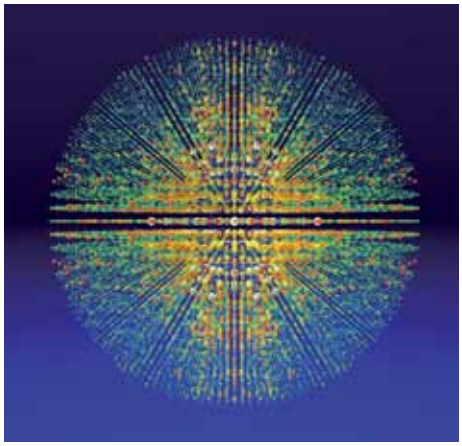

Figure 2

Three dimensional visualisation of diffraction intensities determined by combining over 15,000 individual single-shot diffraction patterns acquired using LCLS.

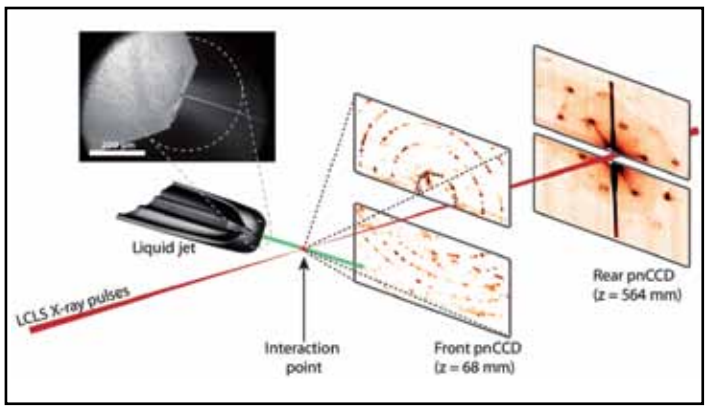

Figure 1

Experimental setup for serial femtosecond crystallography. First published in Nature 470, 73 – 78 (2011).

Small crystals between 100 nm and 2 µm in size of photosystem I, a large protein complex involved with photosynthesis in plants, were placed in the path of the LCLS's beam using a gas dynamic virtual nozzle [3], which allowed them to remain fully hydrated in their mother liquor right up until the point they were hit by the X-ray pulses. Each crystal was hit by a single X-ray pulse, forming a single diffraction pattern before being destroyed in a burst of plasma. The diffraction patterns were read out by two pnCCD detectors as shown in Figure 1. The detector closest to the interaction region recorded scattering to large angles corresponding to a resolution of 8.5 Å, while the other detector recorded lower angle scattering showing detail of the structure of the first few diffraction orders. From the patterns on the far detector, the shapes of the crystals themselves could be reconstructed using the normal algorithms of diffractive imaging, allowing their sizes to be measured.

The patterns on the near detector were similar in nature to those obtained in conventional macromolecular crystallography, and could be processed in largely the same way by the normal procedures of indexing (orientation determination) and peak intensity measurement followed by merging the measurements from a large number of patterns – over 15,000 in this initial proof of concept, and over 100,000 in later experiments. Fully automated processing using specialised software developed in the Coherent Imaging Division of CFEL at DESY [4] combined the intensities from all the patterns by a "Monte Carlo" merging process [5], leading to a three-dimensional dataset visualised in Figure 2. The dataset could be processed further using standard macromolecular crystallography software to produce an electron density map (Fig. 3) which clearly resolved the key features of the huge protein complex, such as its trans-membrane helices, its chlorophyll molecules and iron-sulphur clusters.

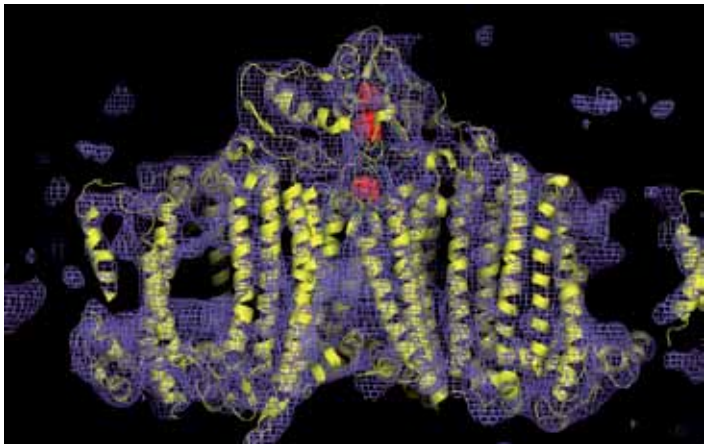

Figure 3

Electron density map of photosystem I calculated using the LCLS diffraction data. First published in Nature 470, 73 – 78 (2011).

Intense research following this proof of concept aims to achieve much higher resolution, and attention is now turning to the possibility of studying chemical reactions in a time-resolved manner using a "pump-probe" technique. Since each crystal is used only once, even reactions which ultimately lead to the destruction of the crystal could be studied. Further developments will improve the liquid jet technology and the data processing algorithms to reduce the amount of time and the quantity of protein crystals required to solve a structure, perhaps allowing chemical reactions to be studied with greater clarity.

Contact: Thomas A. White, thomas.white@desy.de

Authors

Henry N. Chapman[1,2], Petra Fromme[3], Anton Barty[1], Thomas A. White[1], Richard A. Kirian[4], Andrew Aquila[1], Mark S. Hunter[3], Joachim Schulz[1], Daniel P. DePonte[1], Uwe Weierstall[4], R. Bruce Doak[4], Filipe R. N. C. Maia[5], Andrew V. Martin[1], Ilme Schlichting[6,7], Lukas Lomb[7], Nicola Coppola[1, now 21], Robert L. Shoeman[7], Sascha W. Epp[6,8], Robert Hartmann[9], Daniel Rolles[6,7], Artem Rudenko[6,8], Lutz Foucar[6,7], Nils Kimmel[10], Georg Weidenspointner[11,10], Peter Holl[9], Mengning Liang[1], Miriam Barthelmess[12], Carl Caleman[1], Sébastien Boutet[13], Michael J. Bogan[14], Jacek Krzywinski[13], Christoph Bostedt[13], Saša Bajt[12], Lars Gumprecht[1], Benedikt Rudek[6,8], Benjamin Erk[6,8], Carlo Schmidt[6,8], André Homke[6,8], Christian Reich[9], Daniel Pietschner[10], Lothar Strüder[6,10], Günter Hauser[10], Hubert Gorke[15], Joachim Ullrich[6,8], Sven Herrmann[10], Gerhard Schaller[10], Florian Schopper[10], Heike Soltau[9], Kai-Uwe Kühnel[8], Marc Messerschmidt[13], John D. Bozek[13], Stefan P. Hau-Riege[16], Matthias Frank[16], Christina Y. Hampton[14], Raymond G. Sierra[14], Dmitri Starodub[14], Garth J. Williams[13], Janos Hajdu[5], Nicusor Timneanu[5], M. Marvin Seibert[5, now 13], Jakob Andreasson[5], Andrea Rocker[5], Olof Jönsson[5], Martin Svenda[5], Stephan Stern[1], Karol Nass[2], Robert Andritschke[10], Claus-Dieter Schröter[8], Faton Krasniqi[6,7], Mario Bott[7], Kevin E. Schmidt[4], Xiaoyu Wang[4], Ingo Grotjohann[3], James M. Holton[17], Thomas R. M. Barends[7], Richard Neutze[18], Stefano Marchesini[17], Raimund Fromme[3], Sebastian Schorb[19], Daniela Rupp[19], Marcus Adolph[19], Tais Gorkhover[19], Inger Andersson[20], Helmut Hirsemann[12], Guillaume Potdevin[12], Heinz Graafsma[12], Björn Nilsson[12] and John C. H. Spence[4]

1. Center for Free-Electron Laser Science, DESY, Notkestrasse 85, 22607 Hamburg, Germany
2. University of Hamburg, Luruper Chaussee 149, 22761 Hamburg, Germany
3. Department of Chemistry and Biochemistry, Arizona State University, Tempe, Arizona 85287-1604, USA
4. Department of Physics, Arizona State University, Tempe, Arizona 85287, USA
5. Laboratory of Molecular Biophysics, Department of Cell and Molecular Biology, Uppsala University, Husargatan 3 (Box 596), SE-751 24 Uppsala, Sweden
6. Max Planck Advanced Study Group, Center for Free-Electron Laser Science, Notkestrasse 85, 22607 Hamburg, Germany
7. Max-Planck-Institut für Medizinische Forschung, Jahnstrasse 29, 69120 Heidelberg, Germany
8. Max-Planck-Institut für Kernphysik, Saupfercheckweg 1, 69117 Heidelberg, Germany
9. PNSensor GmbH, Otto-Hahn-Ring 6, 81739 München, Germany
10. Max-Planck-Institut Halbleiterlabor, Otto-Hahn-Ring 6, 81739 München, Germany
11. Max-Planck-Institut für Extraterrestrische Physik, Giessenbachstrasse, 85741 Garching, Germany
12. DESY, Notkestrasse 85, 22607 Hamburg, Germany
13. LCLS, SLAC National Accelerator Laboratory, 2575 Sand Hill Road, Menlo Park, California 94025, USA
14. PULSE Institute, SLAC National Accelerator Laboratory, 2575 Sand Hill Road, Menlo Park, California 94025, USA
15. Forschungszentrum Jülich, Institut ZEL, 52425 Jülich, Germany
16. Lawrence Livermore National Laboratory, 7000 East Avenue, Mail Stop L-211, Livermore, California 94551, USA
17. Advanced Light Source, Lawrence Berkeley National Laboratory, Berkeley, California 94720, USA
18. Department of Chemistry, Biochemistry and Biophysics, University of Gothenburg, SE-405 30 Gothenburg, Sweden
19. Institut für Optik und Atomare Physik, Technische Universität Berlin, Hardenbergstrasse 36, 10623 Berlin, Germany
20. Department of Molecular Biology, Swedish University of Agricultural Sciences, Uppsala Biomedical Centre, Box 590, S-75124 Uppsala, Sweden
21. European XFEL GmbH, Notkestrasse 85, 22607 Hamburg, Germany

Original publication

"Femtosecond X-ray protein nanocrystallography", Nature 470, 73 – 78 (2011).

References

1. **R. Neutze et al., "Potential for biomolecular imaging with femtosecond X-ray pulses", Nature 406, 752 – 757 (2000).**
2. **H. N. Chapman et al., "Femtosecond diffractive imaging with a soft-X-ray free-electron laser", Nature Physics 2, 839 – 843 (2006).**
3. **D. DePonte et al., "Gas dynamic virtual nozzle for generation of microscopic droplet streams", J. Phys. D 41, 195505 (2008).**
4. **T. A. White et al., "CrystFEL: A software suite for snapshot serial crystallography", J. Appl. Cryst., submitted (2011).**
5. **R. A. Kirian et al., "Femtosecond protein nanocrystallography — data analysis methods", Optics Express 18, 5713 (2010).**

Coherence properties of an X-ray free-electron laser.

Marching photons
(DESY in-house research performed at the LCLS)

Single shot measurements of the coherence properties of femtosecond X-ray pulses generated by the first hard X-ray free-electron laser, the Linac Coherent Light Source (LCLS), were performed at 780 eV photon energy via the classical Young's double pinhole experiment. We determined a transverse coherence length of 17 µm in the vertical direction and a temporal coherence time of 0.55 fs. The total degree of transverse coherence was found to be 56 %. We find that the X-ray pulses can be adequately described by two transverse coherent modes in each direction. This leads us to the conclusion that 78 % of the total power is contained in the dominant mode.

The intense, coherent and ultra-short X-ray pulses produced by X-ray free-electron lasers (XFEL) promise important new insights in biology [1-3] , condensed matter physics [4], and atomic physics [5]. Spatial coherence is essential for applications such as coherent X-ray diffractive imaging, X-ray holography and X-ray photon correlation spectroscopy.

One of the most widely used methods for characterization of coherence is the double pinhole experiment, known as Young's experiment [6], where two small pinholes separated by a certain distance are illuminated. The visibility of the resultant interference pattern is a measure of the correlation within the wavefield incident at the two pinholes – that is, the transverse coherence of the illuminating beam. An analysis of the contrast of these interference fringes, as a function of their distance from the centre of the diffraction pattern, can also yield a measurement of the temporal coherence.

The experiment was conducted at the soft X-ray research (SXR) instrument of the LCLS [7]. A sketch of the experiment is shown in Fig. 1. The duration of a single pulse was about 300 fs and the average energy was about 1 mJ per pulse. At the sample position, the beam was focused to a size of 5.7 ± 0.4 µm (FWHM) in the horizontal and 17.3 ± 2.4µm (FWHM) in the vertical direction by a pair of bendable Kirkpatrick-Baez (KB) mirrors. A multiple aperture array with varying pinhole separations in the range from 2 µm to 15 µm was positioned in the focus of the beam inside the Resonant Coherent Imaging (RCI) end-station (Fig. 1). After each shot on the sample, the array was moved to an unexposed sample position. To accumulate statistics, each pinhole configuration was measured several times giving 110 patterns in total. Interference patterns were recorded by a Charge Coupled Device (CCD) detector, positioned 80 cm downstream from the apertures (Fig. 1).

The analysis was performed by fitting a theoretical expression to each measured diffraction pattern (see Fig. 1 (b)). The modulus of the effective complex degree of coherence $|\gamma_{12}^{eff}|$ at a particular pinhole separation was determined for each shot (Fig. 2). A Gaussian fit through the 'best' shots (those that provided the highest degree of coherence and shown as black squares in Fig. 2) gives an upper estimate for the transverse coherence length, l_c = 16.8 ± 1.7 µm, of the focused

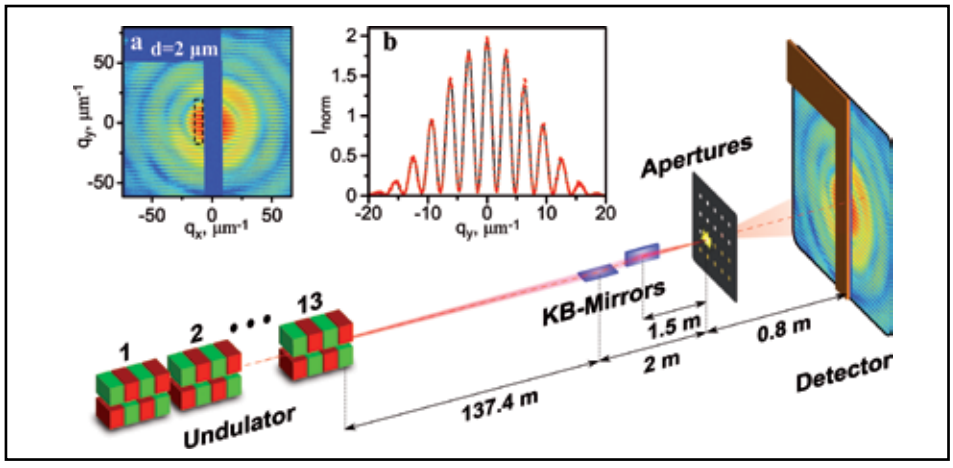

Figure 1

A sketch of the experiment showing thirteen undulator modules, a set of KB-mirrors focusing the beam on a sample frame and the detector, protected from the direct beam by a beamstop. The inset shows a typical measured diffraction pattern (a) and a line scan (b) of the interference fringes on the right edge of the marked region in (a). The experimental data (red dots) and results of the theoretical fit (black lines) are shown.

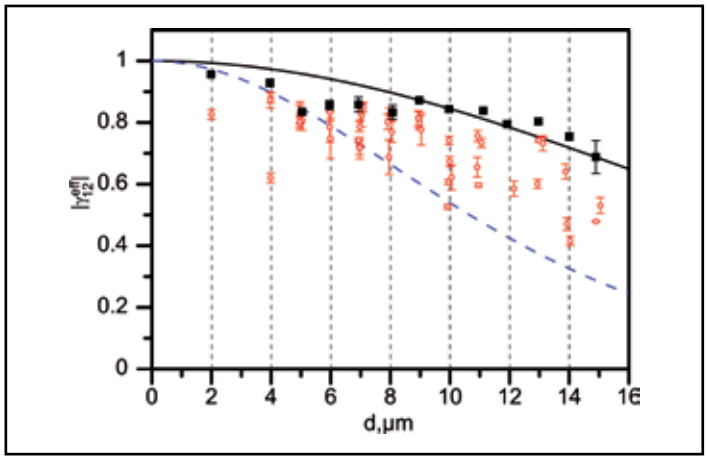

Figure 2

The modulus of the effective complex degree of coherence $|\gamma_{12}^{eff}|$ as a function of the pinhole separation. The experimental values determined from the fitting procedure are shown by red circles. A Gaussian function (black line) has been fit to the best shot values (black squares) which gives a coherence length of 16.8±1.7 μm. The blue dashed line shows the decrease in the value of $|\gamma_{12}^{eff}|$ due to the maximum measured offset between the position of the apertures and the incident beam.

LCLS beam in the vertical direction. The variation of the effective degree of coherence between different pulses for the same pinhole separation (see Fig. 2) was primarily attributed to the uncertainty in the position of the incoming beam with respect to the centre of the pinhole pair.

From the determined transverse coherence length and the size of the LCLS beam we estimate a degree of coherence of the full beam to be 0.56 ± 0.12, provided the coherence properties in the vertical and horizontal direction are the same. This value is comparable with the value obtained in simulations [8] for similar LCLS parameters. Applying a coherent mode decomposition, we further estimate that 78 ± 8 % of the total FEL beam power is concentrated in the dominant "TEM_{00}" mode. This value is substantially higher than at any existing X-ray source at that wavelength.

Some of the pulses that illuminated apertures with larger pinhole separations were extremely bright, which allowed the determination of the fringe visibility up to the edge of the detector and provided a measurement of the temporal coherence for individual femtosecond pulses. For each selected pulse the visibility $|\gamma_{12}^{eff}(\tau)|$ as a function of τ was fit by a Gaussian. An average of the determined values yields a temporal coherence time, $\tau_c \approx 0.55 \pm 0.12$ fs (rms). This value agrees well with the typical average spectrum of the LCLS beam at that energy [9].

In conclusion, we have measured the coherence properties of the LCLS using the focused X-ray beam at a photon energy of 780 eV. We foresee that this single shot methodology for the coherence measurement of high-power, pulsed X-ray sources developed in this work can be extended to investigate the performance of the LCLS in different conditions of operation. Finally, understanding the high degree of coherence at XFEL sources – as demonstrated in this work – provides a solid foundation for future coherence-based experiments that exploit these bright, coherent X-ray beams.

Contact: Ivan A. Vartaniants, Ivan.Vartaniants@desy.de

Authors

I. A. Vartanyants[1,2], A. Singer[1], A. P. Mancuso[1,6], O. M. Yefanov[1], A. Sakdinawat[3], Y. Liu[3], E. Bang[3], G. J. Williams[4], G. Cadenazzi[5], B. Abbey[5], H. Sinn[6], D. Attwood[3], K. A. Nugent[5], E. Weckert[1], T. Wang[4], D. Zhu[4], B. Wu[4], C. Graves[4], A. Scherz[4], J. J. Turner[4], W. F. Schlotter[4], M. Messerschmidt[4], J. Lüning[7], Y. Acremann[8], P. Heimann[9], D. C. Mancini[10], V. Joshi[10], J. Krzywinski[4], R. Soufli[11], M. Fernandez-Perea[11], S. Hau-Riege[11], A. G. Peele[12], Y. Feng[4], O. Krupin[4,6], S. Moeller[4], W. Wurth[13]

1. Deutsches Elektronen-Synchrotron DESY, Notkestrasse 85, 22607 Hamburg, Germany
2. National Research Nuclear University, "MEPhI", 115409 Moscow, Russia
3. University of California, Berkeley, California 94720, USA
4. SLAC National Accelerator Laboratory, 2575 Sand Hill Road, Menlo Park, California 94025-7015, USA
5. ARC Centre of Excellence for Coherent X-ray Science, School of Physics, The University of Melbourne, Victoria, 3010, Australia
6. European XFEL GmbH, Albert-Einstein-Ring 19, 22761 Hamburg, Germany
7. Laboratoire de Chimie Physique - Matière et Rayonnement, UMR 7614 (CNRS), Université Pierre et Marie Curie, Paris, France
8. ETH Zürich, Laboratorium für Festkörperphysik, Schafmattstrasse 16, 8093 Zürich, Switzerland
9. Advanced Light Source, Lawrence Berkeley National Laboratory, Berkeley, California 94720, USA
10. Advanced Photon Source and Center for Nanoscale Materials, Argonne National Laboratory, Argonne, Illinois 60439, USA
11. Lawrence Livermore National Laboratory, 7000 East Avenue, Livermore, California 94550, USA
12. ARC Centre of Excellence for Coherent X-ray Science Department of Physics, La Trobe University, Melbourne, Victoria 3086, Australian Synchrotron, Clayton, 3168 Australia
13. Institut für Experimentalphysik and CFEL, University of Hamburg, Luruper Chaussee 149, 22761 Hamburg, Germany

Original publication

"Coherence Properties of Individual Femtosecond Pulses of an X-Ray Free-Electron Laser", Physical Review Letters 107, 144801 (2011).

References

1. **H. N. Chapman et al., "Femtosecond X-ray protein nanocrystallography", Nature 470, 73–77 (2011).**
2. **M. M. Seibert et al., "Single mimivirus particles intercepted and imaged with an X-ray laser", Nature 470, 78–81 (2011).**
3. **A. P. Mancuso, O. M. Yefanov, and I. A. Vartanyants, "Coherent diffractive imaging of biological samples at synchrotron and free electron laser facilities", J. of Biotechnology, 149, 229–237 (2010).**
4. **I. A. Vartanyants et al., "Coherent X-ray scattering and lensless imaging at the European XFEL Facility", Synchrotron Rad. 14, 453-470 (2007).**
5. **L. Young et al., "Femtosecond electronic response of atoms to ultra-intense X-rays", Nature 466, 56–61 (2010).**
6. **J. W. Goodman, Statistical Optics (Wiley, New York) (1985).**
7. **P. Emma et al., "First lasing and operation of an ångstrom-wavelength free-electron laser", Nature Photonics, 4, 641–647 (2010).**
8. **Y. Ding, Z. Huang, and Ocko, S., "Transverse-coherence properties of the FEL at the LCLS", Proc. of FEL2010 Conf. (Malmö, Sweden, 2010), 151.**
9. **J. N. Galayda, et al., "X-ray free-electron lasers—present and future capabilities", J. Opt. Soc. Am. B, 27, 106–118 (2010).**

Unexpected decoherence in attosecond photoionisation.

A new manifestation of electron correlation (DESY in-house research - Theory)

Attosecond science holds the promise of controlling electron motion to manipulate physical processes at the atomic level. One way of inducing electron motion is photoionisation using an attosecond laser pulse. The typical time scale of electronic motion in atoms, molecules, and condensed matter systems ranges from a few attoseconds (1 as = 10^{-18} s) to tens of femtoseconds (1 fs = 10^{-15} s) [1]. Attosecond pulses have opened the door to real-time observations of the most fundamental processes on the atomic scale like photoionisation [2], and valence electron motion driven by relativistic spin-orbit coupling [3]. The focus of our work was to answer an open fundamental question about electron control via attosecond photoionisation: Can the nonstationary state of the parent ion be described by a Schrödinger wave function, i.e., is the ion in a coherent state?

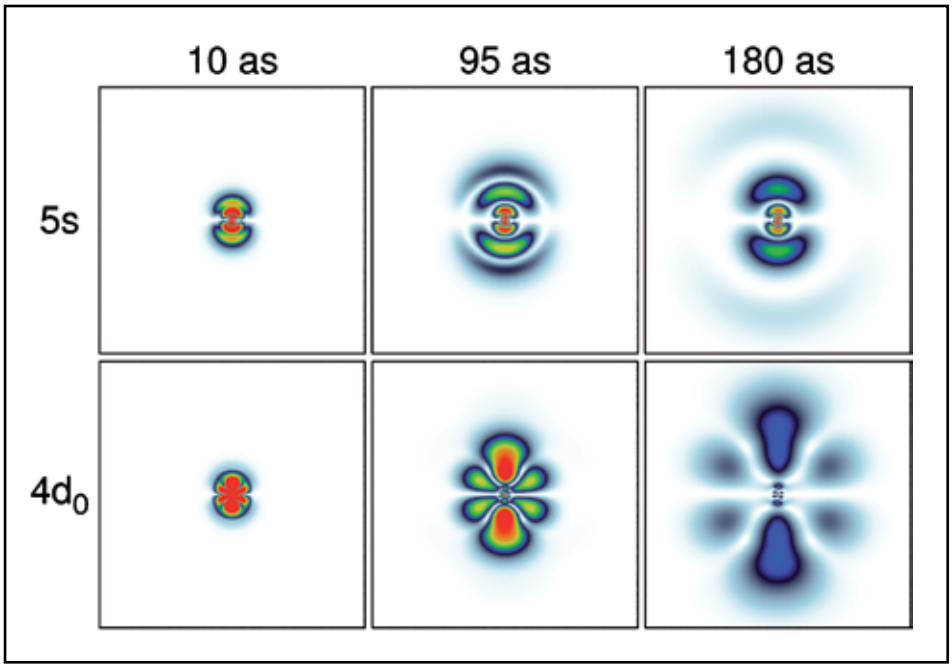

Figure 1
Probability densities of the photoelectron originating from the $4d_0$ and 5s shells of xenon are shown for different times after the ionising attosecond pulse. The pulse has a duration of 10 as, a photon energy of 136 eV, and a peak electric field strength of 25 GV/m.

Pulses with sufficiently broad coherent bandwidth can now bridge the energy splitting between valence and inner-shell electronic orbitals. One might expect that by ionising these orbitals using an attosecond pulse, a coherent superposition of the corresponding ionic eigenstates (the so-called ionisation channels) is formed. The formation of such a coherent superposition implies that the ion produced in the photoionisation process would display attosecond electronic dynamics with the maximum temporal contrast possible. While the entire system – ion plus photoelectron – is in a pure state and may be described by a wave function, the ion alone however is in a mixed state and must in general be described by a density matrix. This opens up the possibility that the state of the ion is not perfectly coherent.

In our work, we showed that the Coulomb interaction between the photoelectron and the parent ion triggers complex many-body effects, which unexpectedly enhance the entanglement between photoelectron and ion – leading subsequently to decoherence within the ion. In other words, a large bandwidth is a necessary but not a sufficient condition for producing coherent electronic wave packets in ions gener-

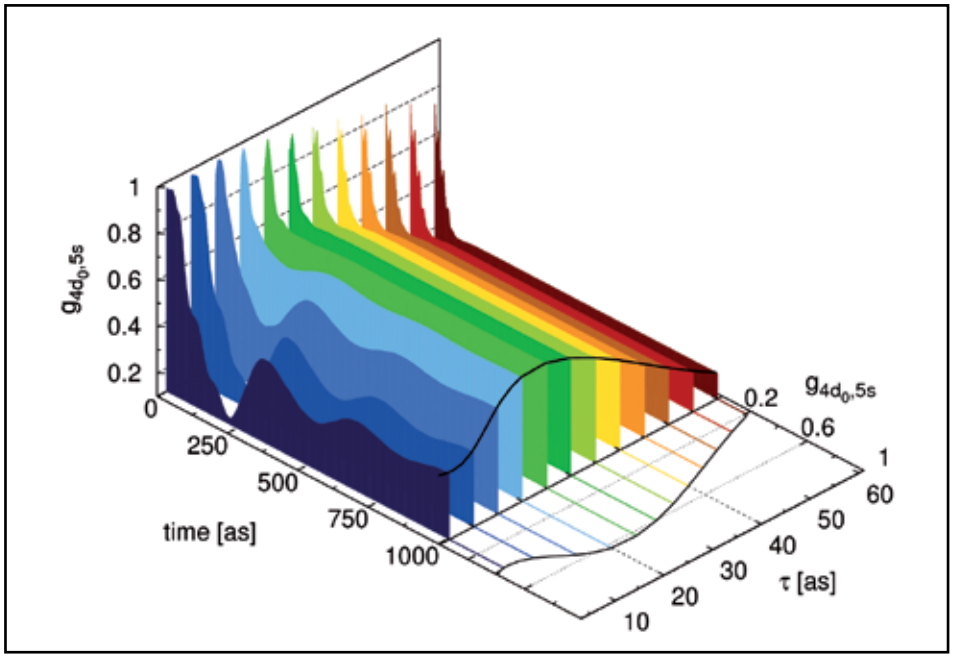

Figure 2

The time evolution of the coherence between the $4d_0$ and 5s hole states in xenon, calculated using the time-dependent configuration-interaction singles method. The photon energy is 136 eV and the pulse duration varies from 5 as to 60 as. The figure is taken from [S. Pabst, L. Greenman, P. J. Ho, D. A. Mazziotti, and R. Santra, Phys. Rev. Lett. 106, 053003 (2011)]

ated via photoionisation. However, as we also demonstrated, decoherence can be suppressed by increasing the average photon energy of the attosecond pulse, thus offering new opportunities for X-ray free-electron lasers.

In our original publication, we analysed the creation of hole states via single-photon ionisation in atoms using a single extreme-ultraviolet attosecond pulse (see Fig. 1). Our theoretical approach was based on the time-dependent configuration-interaction singles (TDCIS) approach described in Ref. [4]. TDCIS, a quantum-chemistry-inspired technique for treating the problem of interacting electrons in an external electromagnetic field, allowed us to study ionisation dynamics beyond the common single-channel approximation and to understand systematically the relevance of multiple ionisation channels during the hole creation process.

Particularly, we studied the impact of the emitted photoelectron on the remaining ion and demonstrated that the correlation between the photoelectron and the ion cannot be neglected for currently available state-of-the-art attosecond pulses. We identified so-called interchannel interactions as the driving mechanism for the enhanced entanglement between the electron and the ion.

Interchannel interactions are mediated via the excited electron and couple different ionisation channels, i.e., hole configurations, with each other. Consequently, the degree of coherence between the ionic eigenstates is strongly reduced, making it impossible to describe the subsequent electronic motion in the parent ion in terms of a pure quantum state (see Fig. 2).

Our results have far-reaching consequences beyond the atomic case. Molecules will be even more strongly affected by interchannel coupling due to the reduced symmetry and smaller energy splittings between the many-electron eigenstates of the cation. Interchannel coupling is also likely to be significant for inner-valence hole configurations in molecules, which show strong mixing to configurations outside the model space that we have employed.

Our study suggests that interchannel coupling accompanying the hole creation process will influence attosecond experiments interested in charge transfer processes in photoionised systems.

Contact: Robin Santra, robin.santra@cfel.de

Authors

Stefan Pabst[1,2], Loren Greenman[3], Phay J. Ho[4], David A. Mazziotti[3], and Robin Santra[1,2]

1. Center for Free-Electron Laser Science, DESY, Notkestrasse 85, 22607 Hamburg, Germany
2. Department of Physics, University of Hamburg, Jungiusstrasse 9, 20355 Hamburg, Germany
3. Department of Chemistry and The James Franck Institute, The University of Chicago, Chicago, Illinois 60637, USA
4. Argonne National Laboratory, Argonne, Illinois 60439, USA

Original publication

"Decoherence in attosecond photoionization", Phys. Rev. Lett. 106, 053003 (2011).

References

1. **F. Krausz and M. Ivanov, "Attosecond physics", Rev. Mod. Phys. 81, 163–234 (2009).**
2. **E. Skantzakis et al., "Tracking autoionizing-wave-packet dynamics at the 1-fs temporal scale", Phys. Rev. Lett. 105, 043902 (2010).**
3. **E. Goulielmakis et al., "Real-time observation of valence electron motion", Nature 466, 739–743 (2010).**
4. **L. Greenman et al., "Implementation of the time-dependent configuration interaction singles method for atomic strong-field processes", Phys. Rev. A 82, 023406 (2010).**

Dynamics at the liquid-vapor interface.

Watch out, liquid surface!
(DESY in-house research performed at the ESRF)

Comprehensive studies of the free surface of a model organic glass former revealed significant impact of the interface on the dynamics in the supercooled and glassy state. An enhancement of the relaxation rate was observed over a wide length-scales range – from long-wavelength surface fluctuations down to the molecular level.

The impact of the liquid-vapor interface on the nano- and macro-scale properties of amorphous materials is of great interest not only for basic science but also for industry. In our recent project, we focused on a particularly interesting problem of the influence of the free surface of the dynamic aspects of glasses. Despite numerous attempts to understand to what extent such an interface alters relaxation processes in disordered systems, this question remains still open. In fact, results published so far are highly inconclusive. For example, opposite shifts of the glass transition temperature T_g near the free surface were reported [1-4]. Also, the origin of such intriguing phenomena like surface-induced viscoelasticity [5,6] remains unclear and requires more intensive studies.

To shine more light on the relaxation near the liquid-vapor interface, we conducted comprehensive studies of the surface dynamics in a model organic glass former, dibutyl phthalate (DBP) $C_{16}H_{22}O_4$, which combines simple molecular structure with high glass forming ability. Application of two complementary surface-sensitive techniques opened us the possibility to investigate the characteristic time-scale for the relaxation τ_0 as a function of temperature T and momentum transfer q_x within the wide time-window from tens of nanoseconds to hundreds of seconds and length-scales ranging from Ångstrøm to micrometers. The slow, thermally induced fluctuations of the liquid-vapor interface has been investigated with the help of X-ray Photon Correlation Spectroscopy (XPCS), while dynamics on the molecular level in glassy dibutyl phthalate was examined using Quasi-elastic Nuclear Forward Scattering (QNFS). These experiments have been performed at the ESRF beamlines ID10A and ID18, respectively. Analysis of the XPCS data revealed well-pronounced viscoelasticity of supercooled dibutyl phthalate near its free surface. The value of the shear modulus was found to increase dramatically upon cooling. Interestingly, no evidence

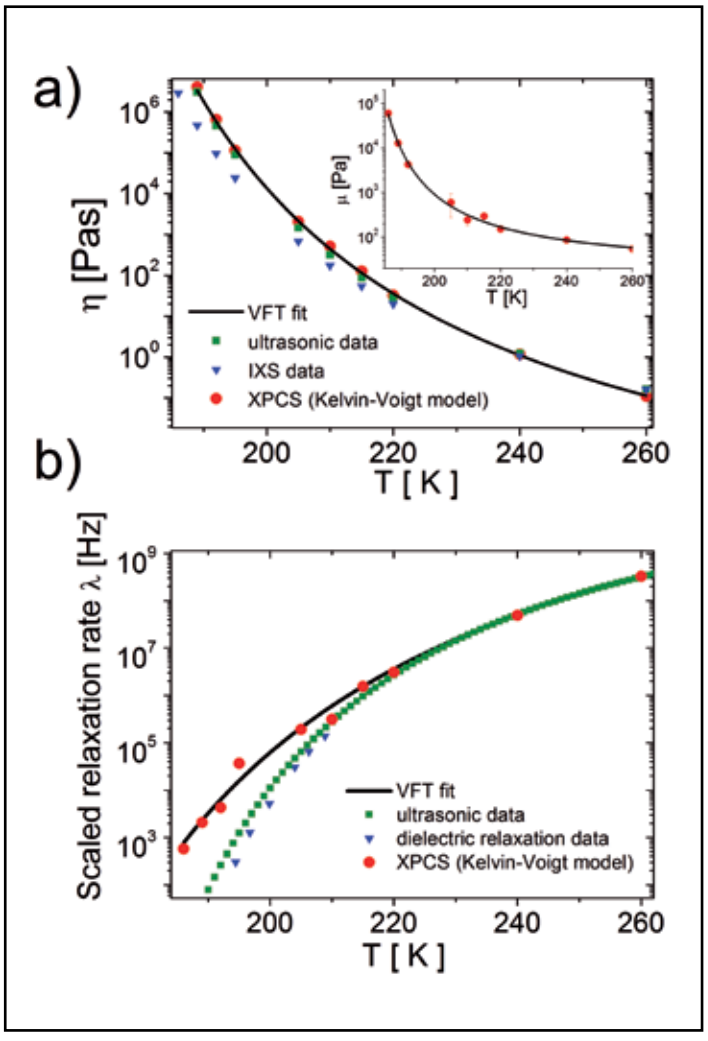

Figure 1

Fig.1 a) The viscosity η(T) and the shear modulus μ(T) (inset) near the free surface compared to the inelastic X-ray scattering [8] and the ultrasonic [7] data of a bulk dibutyl phthalate. b) The scaled relaxation rate λ calculated from XPCS data compared to Ref. [7] and the dielectric relaxation [9]. Solid lines – the Vogel-Fulcher-Tammann fits.

of the viscoelastic nature of dibutyl phthalate was reported for bulk liquid in the same temperature range [7,8]. As presented in Fig. 1a, values of viscosity η extracted from the XPCS measurements are in excellent agreement with the literature data for the bulk liquid. As a consequence of its viscoelastic nature, the relaxation rate $\lambda(T) = \mu(T)/\eta(T)$ of the surface fraction of DBP exhibits much weaker dependence on temperature and exceeds the bulk values [9] by an order of magnitude upon cooling towards T_g (Fig.1b).

The dynamics of glassy DBP was resolved by performing Mößbauer studies in the time domain under grazing incidence geometry. We studied the fast motion of the DBP molecules by monitoring the relaxation of tracers embedded into the DBP matrix. Surprisingly, values of τ_0 measured above T_g decreases upon cooling (Fig. 2). At lower temperatures, the collected data could only be explained by assuming the measured signal to be a coherent superposition of two signals with two distinct relaxation times τ_1 and τ_2. The first one matches the literature data of the supercooled bulk DBP [9] and remains constant upon further cooling. The relaxation time τ_2 corresponds to DBP in the glassy state and increases with decreasing temperature. To explain the observed data, we developed a model assuming the molecular mobility to be significantly enhanced in the vicinity of the liquid-vapor interface. In the proposed model, the relaxation time of DBP molecules depends on both temperature and distance from the interface. For supercooled dibutyl phthalate this assumption holds true for the entire probed volume. Below T_g such effect is limited to a few nanometers deep surface layer (10 - 15 nm). Molecules moving within the surface region contribute to the first signal characterized by the time-scale τ_1. The remaining part of the probed volume behaves as a bulk liquid and vitrifies at T_g, which is reflected by the presence of the second, much longer time-scale τ_2 in the recorded QNFS data.

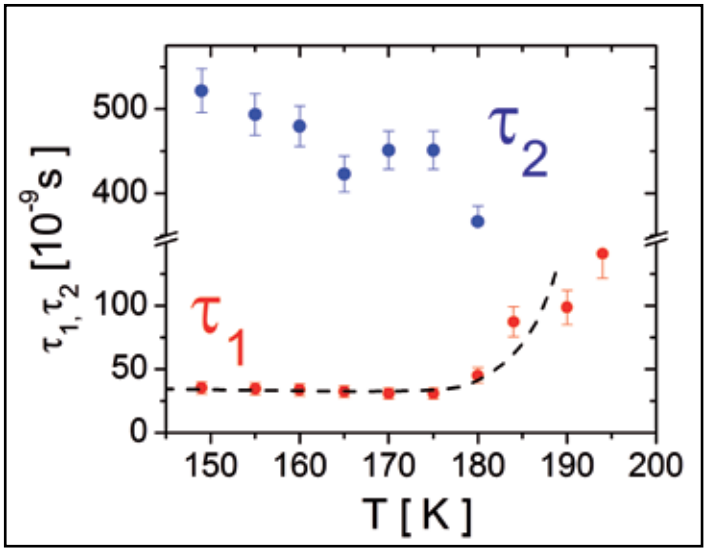

Figure 2

The relaxation times τ_1 and τ_2 extracted from QNFS data. Below 180 K, the data splits into the liquid-like branch (τ_1) and the glass-like branch (τ_2). Broken line – the multilayer model prediction of τ_1.

The outcome of both experiments points towards enhanced dynamics in the vicinity of the liquid-vapor interface. This effect is well pronounced for both supercooled and glassy DBP. Similarly to studies devoted to complex liquids [6], our data provides no evidence of the surface affecting the viscosity of the supercooled liquid and shows that the concept of elasticity induced by the free surface is valid also for simple molecular liquids.

Contact: Marcin Sikorski, sikorski@slac.stanford.edu

Authors

M. Sikorski[1], C. Gutt[1], Y. Chushkin[2], M. Lippmann[1], and H. Franz[1]

1. Deutsches Elektronen Synchrotron (HASYLAB at DESY), Notkestrasse 85, 22607 Hamburg, Germany
2. European Synchrotron Radiation Facility (ESRF), B.P. 220, 38043 Grenoble Cedex, France

Original publication

"Dynamics at the liquid-vapor interface of a supercooled organic glass former", Phys. Rev. Lett. 105, 215701 (2010).

References

1. **O. K. C. Tsui, in Polymer Thin Films, edited by O. K. C. Tsui and T. P. Russell, Series in Soft Condensed Matter (World Scientific, Singapore, 2008), p. 267.**
2. **J. L. Keddie, R. A. L. Jones, and R. A. Cory, "Size Dependent Depression of the Glass Transition Temperature in Polymer Films", Europhys. Lett. 27, 59 (1994).**
3. **G. B. DeMaggio et al., "Interface and surface effects on the glass transition in thin polystyrene film", Phys. Rev. Lett. 78, 1524 (1997).**
4. **J. A. Forrest et al., "Effect of Free Surfaces on the Glass Transition Temperature of Thin Polymer Films", Phys. Rev. Lett. 77, 2002 (1996).**
5. **H. Kim et al., "Surface Dynamics of Polymer Films", Phys. Rev. Lett. 90, 068302 (2003).**
6. **Z. Jiang et al., "Evidence for Viscoelastic Effects in Surface Capillary Waves of Molten Polymer Films", Phys. Rev. Lett. 98, 227801 (2007).**
7. **L. R. Cook et al., "Pressure and temperature dependent viscosity of two glass forming liquids: Glycerol and dibutyl phthalate", J. Chem. Phys. 100, 5178 (1994).**
8. **A. Mermet et al., "High frequency dynamics of the glass former dibutylphthalate under pressure", Phys. Rev. E 66, 031510 (2002).**
9. **P. K. Dixon et al., "Scaling in the relaxation of supercooled liquids", Phys. Rev. Lett. 65, 1108 (1990).**
10. **T. Asthalter et al., "Quasielastic nuclear forward scattering as a background-free probe of slow glass dynamics in confined geometries", Eur. Phys. J. B 22, 301 (2001)**

Research Platforms and Outstations.

Center for Free-Electron Laser Science CFEL.

Three institutions working successfully together within CFEL

Since its foundation in 2007 CFEL has grown steadily over the past four years. The total number of employed group leaders, scientists, post-docs, PhD students, technical and administrative staff exceeded one hundred in early 2011 reaching 140 by the end of the year. CFELs organizational chart includes several divisions and independent research groups provided by the partner organizations DESY, the MPG, and the UHH. DESY is in charge of three division plus one junior research group. The MPG and the UHH jointly support two divisions with three independent junior research groups. In addition, both institutions operate Advanced Study Groups (MPG-ASG and UHH-ASG) with several independent research groups.

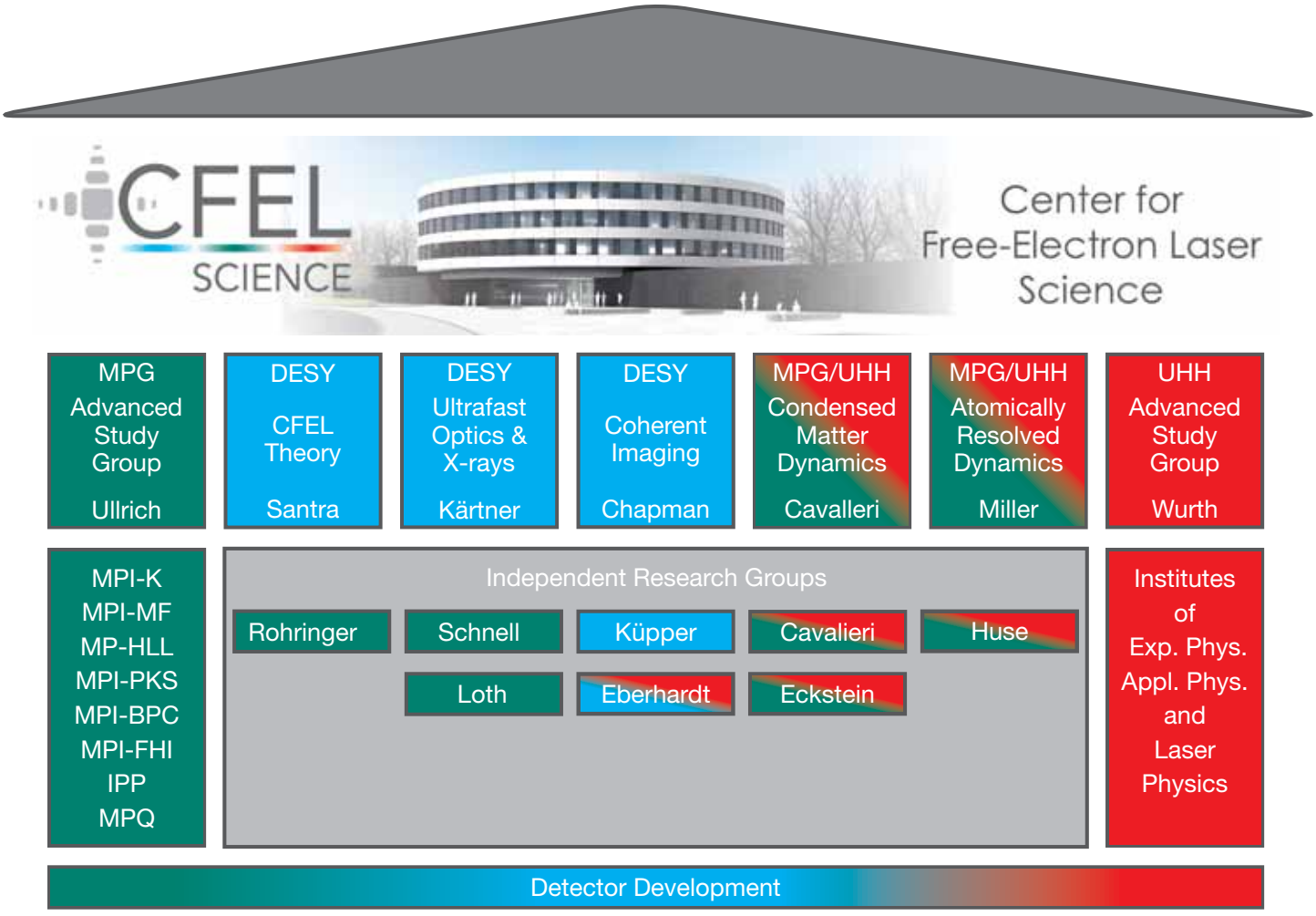

Figure 1

CFEL House – A brief chart of the organizational structure of the groups and institutions that are joining forces in the Center for Free-Electron Laser Science in Hamburg.

Figure 2
The CFEL construction site on 13 December 2011. Right: a view into the interior of the main building.

The new CFEL building across from PETRA III has taken on its final shape. The outside shell was closed just in time for the winter and over 60 workers are busy to finish the interior installations. All scientists are looking forward to moving into it in 2012 to set up experiments in the new laboratories. To accommodate the need for laboratory space until completion of the CFEL main building, two new laboratories were built right across the existing CFEL buildings 49 and 49a. A part of this 420 qm laboratory complex will be used by the Condensed Matter Division of Andrea Cavalleri and the MP independent research group for the dynamics of nanoelectronic systems of Sebastian Loth. More than half of the complex will feature a shared laser laboratory for the cooperation of the Ultrafast Optics and X-Rays Division of Franz Kärtner with the European XFEL laser group of Max Lederer.

As CFEL unites researchers from DESY, the MPG, and UHH under one roof, the idea of a CFEL internal symposium was realized for the first time with over 90 scientists attending the event Friday, 18th to Sunday 20th of March 2011. This symposium featured 21 scientific talks, a poster slam and a long lasting poster session.

CFEL hosted successfully the first Ultrafast X-Ray Summer School (UXSSS 2011) in Hamburg, featuring a highly interdisciplinary program with topics ranging from accelerator physics to molecular biology. This summer school has been taking place on a yearly basis at the PULSE institute at SLAC National Accelerator Laboratory before and was now for the first time organized in Hamburg by Robin Santra, head of the CFEL Theory Division. It was financially supported by the VolkswagenStiftung and will be back in Hamburg in the year 2013.

The DESY activities within CFEL were expanded this year with the official start of Franz Kärtner (DESY & MIT) and with the arrival of Wolfgang Eberhardt who joined DESY and the UHH-ASG. The International Max Planck Research School for Ultrafast Imaging and Structural Dynamics (IMPRS-UFAST) enrolled the first doctoral students for the winter semester 2011/2012. This school is supported by all CFEL divisions and offers

Figure 3
The laser set-up (CFEL's Controlled Molecule imaging group) for Coulomb explosion of aligned and oriented molecules.

students unique training opportunities in the field of ultrafast imaging with a view to exploring structural changes of atoms, molecules, condensed, biological, or warm dense matter on femtosecond time scales.

In the past year, the CFEL Theory Division has been making scientific progress in several areas: 1) Development of the XATOM program package for studying and predicting the behaviour of arbitrary atomic species exposed to high-intensity X-ray pulses; 2) Development of the XCID program package for studying electron correlation and coherence effects in time-resolved photoionization. An application of XCID is presented in the Research Highlights section of this report; 3) Computational research in connection with coherent diffractive imaging using X-ray FELs.

Two landmark papers from the Coherent Imaging Division were published this year in Nature, one introducing the new field of femtosecond-pulse serial crystallography (see Research Highlights) and the other demonstrating single-particle diffractive imaging of virus particles. These experiments were carried out at LCLS as part of an international consortium led by CFEL. The research program in coherent imaging has been continued by extending the technique both to hard X-ray wavelengths and the so-called water window, measuring photo-induced reactions, and developing new imaging modalities for single particles. The newly started Controlled Molecule Imaging Group of Jochen Küpper carried out novel photoelectron imaging experiments on aligned and oriented molecules at FLASH and LCLS and built up a laboratory for studying state-, size-, and isomer-selected, 3D aligned and oriented molecular beams.

The Ultrafast Optics and X-Rays Division under the leadership of Franz Kärtner started in 2011. Approximately ten students, postdoctoral and senior researchers including two MIT students are working on the DESY campus. The group continues operation at the MIT Research Laboratory of Electronics, with several researchers from DESY visiting, and has made progress in two areas important to next generation light sources: 1) scalable high energy, sub-cycle pulse synthesis with full waveform control for strong-field physics and particle acceleration; 2) demonstration of ultralow jitter femtosecond laser systems enabling large-scale timing distribution and synchronization in accelerators and light sources at the attosecond level. In June 2011, the Extreme Timescales Group (ETG) led by Adrian Cavalieri within the Condensed Matter Division made the first simultaneous, non-invasive measurement of the FEL pulse structure and arrival time at FLASH. Full temporal characterization of the FEL pulse is widely recognized as one of the primary technical limitations preventing full utilization of 4th generation X-ray sources. To achieve this groundbreaking result, the experiments were performed by an international collaboration headed by Adrian Cavalieri's ETG that included the SLAC National Accelerator Laboratory, European XFEL, and DESY. The measurements were made by adapting techniques from attosecond spectroscopy. At FLASH, single-shot measurements were made using a high intensity laser-based single-cycle THz pulse to "streak" photoelectrons ejected from helium by the FEL pulse. The full single-shot temporal information can then be extracted directly from each streaked photoelectron spectrum.

The Atomically Resolved Dynamics Division celebrated the inauguration of their Relativistic Electron Gun for Atomic

Exploration (REGAE) 7th October. This facility was established within a unique collaboration between DESY, the MPG, and the UHH. Pulses of less than 10 fs with bunch numbers up to more than 10^6 electrons are now possible with a spatial coherence of more than 30 nm at the sample position. This new source greatly advances our abilities to image atomic motions during structural transitions. At the molecular level, we can now observe the primary events governing chemistry and biology with much better "lighting". Another division activity by the Ultrafast Molecular Dynamics group of Nils Huse aims at establishing a program for transient soft X-ray spectroscopy of liquids and solvated molecules at PETRA III to study chemical processes in solution. This endeavor will develop and complement future experiments at FLASH and other coherent X-ray sources.

The development of innovative concepts for accelerator-based light sources is one of the focus areas of research within the UHH-ASG. Last year two new groups have been established in this area with the appointment of Florian Grüner as full professor and Juliane Rönsch-Schulenburg as a junior research group leader who will work on the new area of laser-plasma acceleration and on ultrashort electron bunches, respectively. Michael Rübhausen and Henry Chapman have joined forces in a new DFG research unit on ultrafast electron dynamics at transition metal centres in biological systems. One of the research highlights achieved at FLASH has been a time-resolved soft X-ray scattering study on the femtosecond dynamics across the Verwey transition in magnetite performed in a collaboration with groups from Berlin, Cologne, Stuttgart and Stanford.

The MPG-ASG has continued their successful FEL activities by exploring structural dynamics in small to medium-sized molecules and radiation damage in biological systems using their CAMP instrument. Furthermore, the ASG extended its scope toward multi-parameter experiments in solid state physics to study the relaxation of hot electrons as they interact with the coherent motion of atoms by employing simultaneously time-resolved X-ray emission spectroscopy and X-ray diffraction. The ASG's measurements probe the redistribution of electrons in the conduction band and reflect directly the evolution of the non-equilibrium distribution function. Recently, the ASG was instrumental in successfully commissioning a CAMP-like instrument at the SACLA free-electron laser in Japan. Furthermore, a novel broadband rotational spectrometer has been set up within Melanie Schnell's newly established independent research group dedicated to structure and dynamics of cold and controlled molecules within the MPG ASG. The experiments are aiming at studying molecular recognition forces at play on a molecular level, complementing ongoing experiments with coherent light sources such as FLASH.

The seven divisions have published over 75 peer reviewed papers in 2011 reflecting the overall scientific success of the CFEL Science cooperation between the three partners DESY, MPG, and UHH.

Contact: Ralf Köhn, ralf.koehn@cfel.de

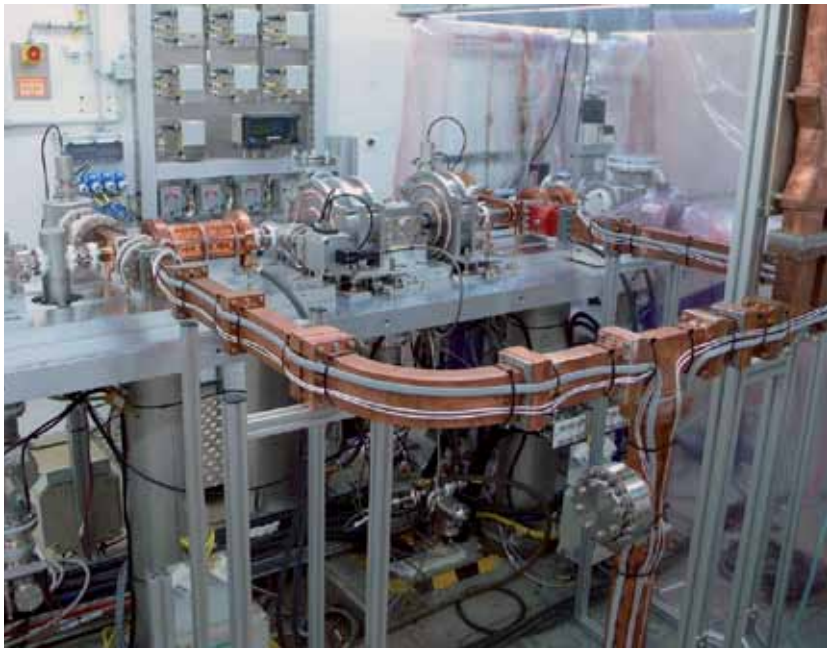

Figure 4

Official inauguration of the Relativistic Electron Gun for Atomic Exploration (REGAE) under the motto: "Molecular Movies" now with REGAE music.

Left: REGAE, right: Cutting the ribbon (from left to right: K. Flöttmann, H. Dosch, H. Graener, R. Brinkmann, R. J. D. Miller).

DESY NanoLab.

Strengthening research in Photon Science

Research in all fields of natural sciences progresses towards the manipulation of matter on smaller and smaller length scales as well as on shorter and shorter time scales. It is commonly accepted that the need for analytical tools to interrogate functional nanostructures on a molecular level and under environmentally and technologically relevant conditions will rise steeply in the next decades. The development of photon sources at DESY accompanies this evolution: The user facilities PETRA III and FLASH at DESY provide beams of outstanding brilliance for the investigation of nanoscale structures with very high spatial and temporal resolution. To exploit these experimental opportunities most efficiently and to establish a forefront nanoscience program at DESY, on-site facilities for preparation, characterization and manipulation of nanoscale structures are needed, located close to the photon sources. Moreover, a vital user community in nanosciences will be attracted if a strong in-house research program in this field is established at DESY. In order to start and support such a development, DESY plans the installation of a dedicated laboratory for research in nanosciences in close proximity to PETRA III and FLASH. This laboratory, currently referred to as DESY NanoLab, will be implemented within the frame of a new DESY photon science building on site. It will provide instruments and infrastructure to prepare and characterize nanostructured or micrometer size samples in connection with experiments performed at PETRA III and/or FLASH. Users of these facilities will have access to these instruments on a short-term basis (for relatively simple preparation and characterization tasks) or on a long-term basis for projects that are accepted after proposal evaluation.

Besides user support, the additional mission of the NanoLab is to establish and strengthen in-house research activities in selected fields of nanoscience that benefit from the unique experimental possibilities at PETRA III and FLASH. The interconnection of the NanoLab with the photon sources at DESY will enable new synergies within the nanoscience community and generate emerging research areas with a great potential for innovative developments.

The architectural planning for the new building has been started in 2010. The current layout within the planning phase of “urban development” (German: “städtebauliche Entwicklung”) is shown in Fig. 1. The building complex including the NanoLab will consist of modules that are constructed in separate phases. Partner in the first construction phase is the Helmholtz-Zentrum Geesthacht (HZG), operating the German Engineering Materials Science Centre (GEMS) in a dedicated part of the building. Long-term partners of DESY will be able to join the NanoLab and contribute to further modules of the building.

The new photon science building will be located on an approx. 5000 m^2 large area to the west of building 25f to which it will be connected. In the first construction phase (light blue areas in Fig. 1) the new DESY photon science building together with building 25f will form a U-shaped building complex. It will enclose an atrium of almost 600 m^2 floor space with a glazed roof and wall, providing a stimulating atmosphere for communication and social life, integrating an extended version of the cafeteria in 25f. The atrium of the new photon science building will be used for instance for poster sessions and exhibitions.

The first construction phase encompasses about 2000 m^2 usable floor space for offices and 1000 m^2 for laboratories. The laboratory floor space includes about 300 m^2 with special vibration insulation for sensitive instruments and sample preparation procedures. It will be located in the basement of the building part that runs parallel to 25f. Construction activities for the first phase are planned to start in spring 2013. In later phases the new DESY photon science building can be extended by comparable laboratory and office floor spaces (dark blue areas in Fig. 1), whereupon even a lecture hall with about 150 seats might be integrated.

It is foreseen that the instrumentation in the NanoLab comprises, in the first phase, instruments like high-resolution scanning electron microscopes, atomic force microscopes as well as UHV chambers for deposition, growth and analysis of samples. In later stages it is envisioned to add advanced lithography techniques, focused ion beam processing of samples with nanomanipulation and more. Synergies will be explored and coordinated with instruments that are operated by HZG, CFEL, CSSB and the University of Hamburg (Bahrenfeld Campus).

Contact:
Ralf Röhlsberger, ralf.roehlsberger@desy.de
Lindemar Hänisch, lindemar.haenisch@desy.de

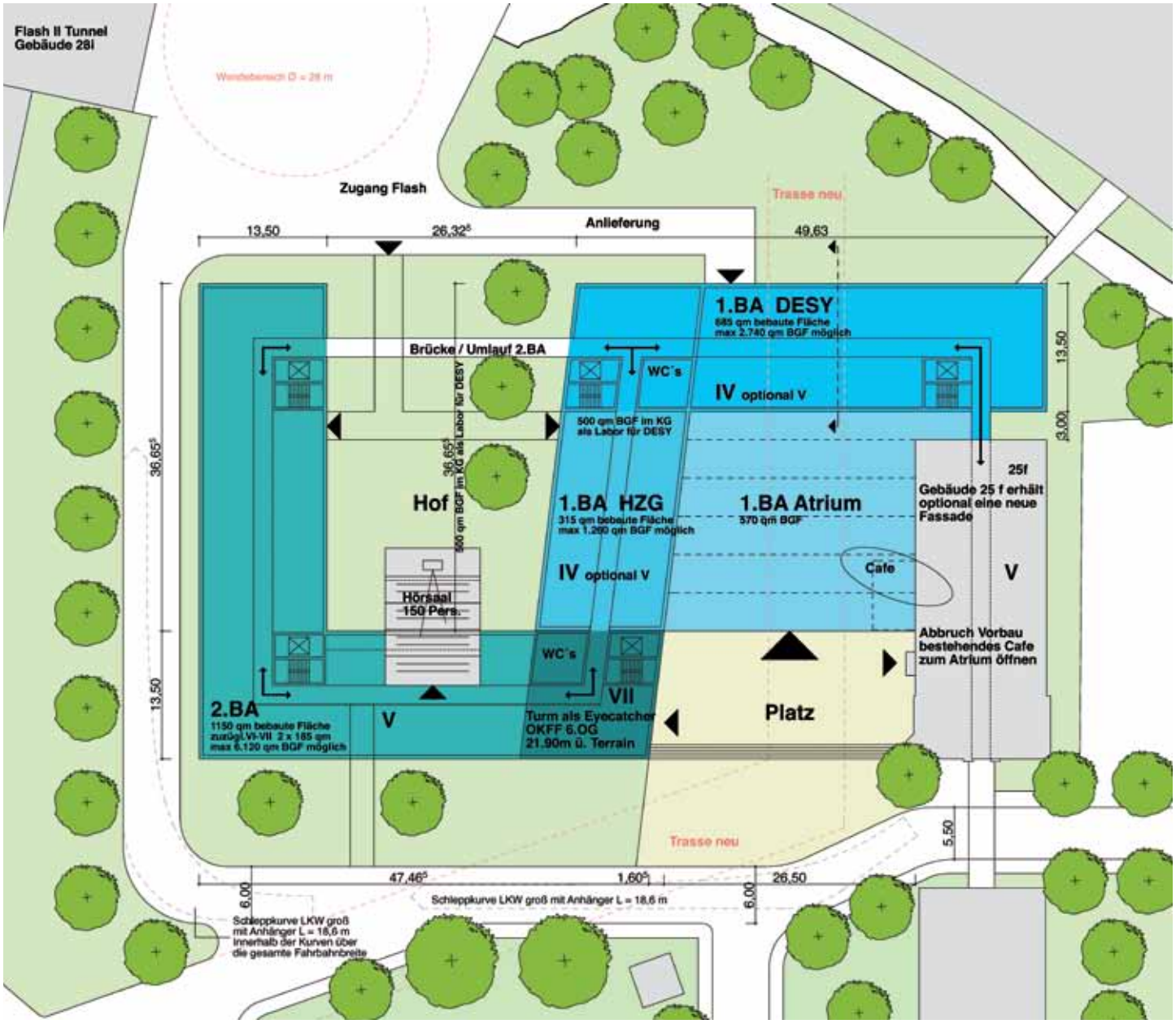

Figure 1

Layout of the new DESY photon science building at the current stage of planning (Nov. 2011). Light blue areas belong to the first construction phase to be started in 2013, dark blue areas belong to later construction phases. (Concept: planpark architekten, Hamburg)

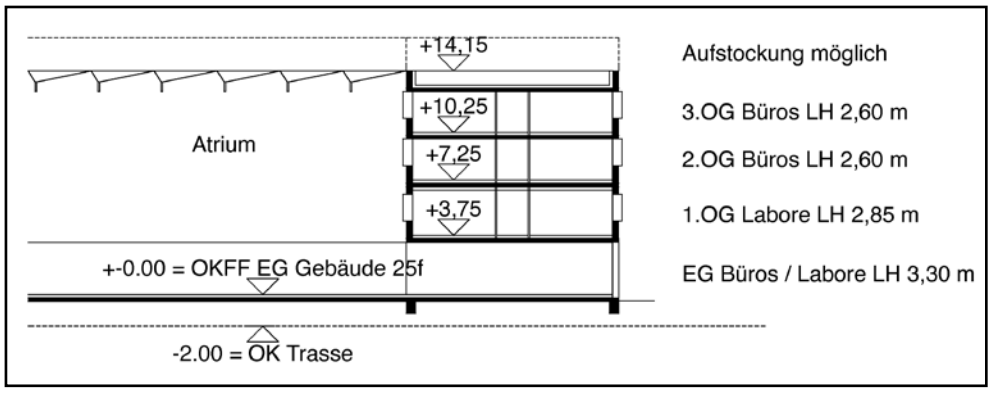

Figure 2

Cross-sectional view of the new DESY photon science building, hosting the NanoLab. (Concept: planpark architekten, Hamburg)

CSSB
Centre for Structural Systems Biology.

New chances for infection biology at DESY

The year 2011 has been one of decisive progress for the CSSB. The vision of a "Centre for Structural Systems Biology" on the DESY campus foresees a new interdisciplinary Centre where research groups from universities and other scientific institutions work together on key problems in infection biology. This field is particularly well represented in Northern Germany, where a number of scientists and institutions with outstanding international reputation are active in infection research.

The CSSB will host research groups from various disciplines and enable an optimized exploitation of the huge analytical potential offered by the extremely brilliant light sources located in Hamburg on the DESY campus. The combined use of large photon sources, laboratory infrastructure and theoretical methods allow, at least in principle, the systematic analysis and modelling of structure and dynamics on all relevant scales of the biological systems of interest. Scientists working at CSSB can extend their object of study from the very short distances and times involved in atomic processes to the much larger dimensions and longer time intervals relevant for the dynamics of large biomolecules, viruses or even more complex systems. They have the possibility to enlighten all the aspects of a complicated architecture like a living cell and to understand in detail the many different interactions enabling the cell to function. Through a truly interdisciplinary approach and the full use of world-leading research infrastructures at PETRA III, FLASH and the future European XFEL, the scientists at CSSB can overcome the traditional barriers among disciplines and achieve completely novel perspectives.

This ambitious project was supported by the politicians of the German Federal Government and of the Federal States of Hamburg and Lower Saxony, with the perspective participation of Schleswig-Holstein. In January 2011 the responsible Science Ministers convened in Hamburg and signed the agreement laying the groundwork of the CSSB, ensuring the funding of the building.

In the following months, a task force consisting of representatives of all interested institutions prepared the Cooperation Agreement which has been already approved and is currently being signed by all partners. The Agreement comprises a description of the commitment of the partners in terms of funding of research groups, contribution to equipment and to the operational costs for the first phase.

Figure 1

The German Federal Science Minister Annette Schavan (centre) with her two colleagues from Lower Saxony Dr. Johanna Wanka (left) and Hamburg Dr. Herlind Gundelach (right) after signing the CSSB Cooperation Agreement.

The partner institutions are:

- Helmholtz-Zentrum für Infektionsforschung Braunschweig
- Universität Hamburg
- Universitätsklinikum Hamburg Eppendorf
- Forschungszentrum Jülich
- Heinrich Pette Institut Hamburg
- Bernhard Nocht Institut Hamburg
- Medizinische Hochschule Hannover
- European Molecular Biology Laboratory
- Deutsches Elektronen Synchrotron DESY

The first research groups at CSSB will concentrate on structural biology, cryo-electron-microscopy and -tomography, bio-imaging as well as protein-protein-networks. A junior research group has already been installed. The search for another W2 position has been started and the announcement for three W3 positions is in preparation. Negotiations with the Swedish Research Council aiming for the establishment of a German-Swedish junior research group are under way.

The planning of the CSSB laboratory and office building has already started. It will encompass 9250 m² total surface and offer space for 10 in-house research groups and 3 - 4 guest groups, including 750 m² laboratory space. Various facilities like library, seminar rooms and a cafeteria are also foreseen. The next step will be the call for tender for detailed architectural planning. After completion of the necessary procedure for the approval of the construction, the CSSB will be built on the DESY campus in the vicinity of PETRA III and the EMBL buildings.

Contact: Edgar Weckert, edgar.weckert@desy.de

EMBL Hamburg Unit.

Structural Biology Services and Research with Synchrotron Radiation

The EMBL Hamburg Unit is a major provider of research services in structural biology, specifically for synchrotron radiation beamlines, preparation and crystallisation of biological samples, and the provision of remote software services. Most of the recent activities have been geared towards the completion of construction, commissioning and start up of operation at EMBL's integrated research facilities at the PETRA III synchrotron on the DESY Campus. EMBL Hamburg is now starting operation of three beamlines at PETRA III – two for macromolecular crystallography (MX) and one for Small Angle X-ray Scattering (SAXS) for biological applications. Alongside the beamlines, external researchers have access to experimental laboratory facilities for sample preparation and characterisation, and high throughput crystallisation as well as facilities for data processing and evaluation – all under one roof and in immediate proximity to the EMBL beamlines. Details on the quantity of services are listed in Table 1.

Table 1: Research Services		01-10/2011	01-12/2010
EMBL beamlines	No. of user visits	259	409
	No. of projects	244	261
	No. of external research groups	168	181
EMBL software	No. of users	4493	5008
	No. of external research groups	2209	2467
EMBL crystallisation	No. of users	36	25
	No. of crystallisation plates	381	390

For all three EMBL beamlines at PETRA III, the basic infrastructures (control electronics, control software, vacuum systems, cryogenic systems, media) are now operational. The optical elements (monochromators, horizontally deflecting mirrors to separate the two MX stations situated in the same sector at canted undulators) are in place, except the adaptive focusing mirror systems with Kirkpatrick-Baez geometry, which are expected to be installed by the end of 2011. For the three experimental stations, most of the components (beam conditioning units, multi-degree-of-freedom experimental tables, diffractometers, automatic sample delivery) are being implemented as well.

For two of the three EMBL beamlines at PETRA III, the commissioning of the endstations has recently begun. On the Bio-SAXS beamline (P12) an important milestone was set by the first research experiments in June 2011, performed on large viral particles and metal nanoparticles coated by biologically active shells. The data collected (Figure 1) were of high quality due to the excellent beam and detector properties (Pilatus-2M pixel detector). Several other test experiments from external groups, including the P12 partner from the Helmholtz-Zentrum Geesthacht, also yielded highly promising data. The beamline is operated from an in-house developed Beamline Meta Server which allows automated and remote data collection and analysis. A new robotic SAXS sample changer, which has been developed in collaboration with EMBL Grenoble and the ESRF allows the transfer of micro-volume solutions (Figure 2). With the present condition of the beamline (without focussing mirrors), data collection of up to 30 samples per hour has been achieved.

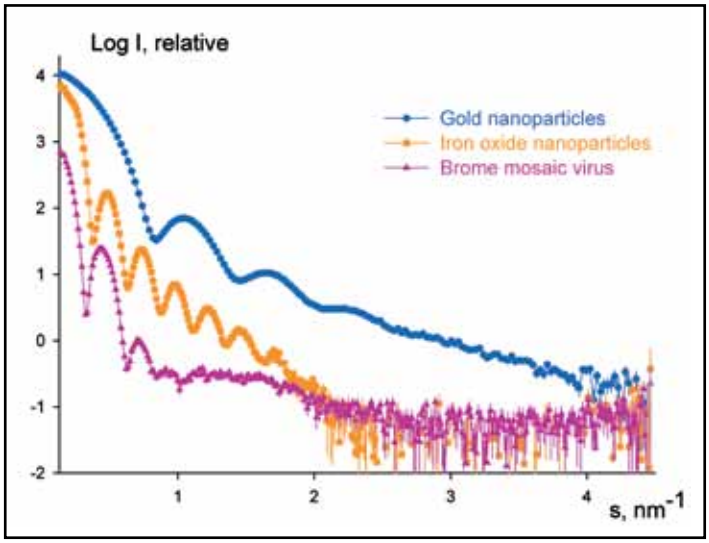

Figure 1

The radially averaged and solvent-subtracted experimental SAXS data obtained by the first external user group at the P12 beamline. The logarithm of the scattering intensity is displayed as a function of the momentum transfer $s = 4\pi \sin\theta/\lambda$, where 2θ is the scattering angle and λ=0.1 nm is the X-ray wavelength. The scattering patterns are appropriately displaced along the logarithmic axis for better visualisation.

On the macro-crystallography beamline MX2 (P14), designed for microfocus applications in MX, a novel goniostat with a vertical rotation axis and a Rayonix 225HE CCD detector have been installed. The goniostat has been developed in close collaboration with EMBL Grenoble and MAATEL (Voreppe, France) and will allow a mechanical precision below 1 µm, to make full use of the small beam sizes achievable on MX2 (Figure 3). To date, the beamline has been used for a series of successful test experiments, which for instance allowed X-ray structure determination of crystals as small as 20 µm. On the macro-crystallography beamline MX1 (P13), the beam has been passed across the deflecting mirrors. First diffraction experiments are planned before the end of 2011 after extending the vacuum system into the experimental hutch.

The Sample Preparation and Characterisation (SPC) laboratory for biological macromolecules and automated crystallisation facilities has been relocated next to the PETRA III beamlines (Building 48e). It now offers automated crystallisation at two different temperatures, automatic imaging, and various specialised protocols for optimisation of crystallisation conditions. The SPC offers a variety of approaches to assess the quality of the macromolecule samples prior to beamline data acquisition. At present, the facility is equipped with a MALDI-TOF mass spectrometer to analyse the composition of samples, and instruments to test thermostability and dispersity. An integrated system for online sample purification and sample quality assessment is developed on the BioSAXS beamline in collaboration with Malvern Instruments.

Figure 3

Prototype of a high precision diffractometer with a mini-kappa goniostat mounted on a vertical rotation axis. Development in collaboration with EMBL Grenoble and MAATEL (Voreppe, France).

Figure 2

BioSAXS sample changer on beamline P12, developed in collaboration with EMBL Grenoble and the ESRF.

In addition to the emerging activities of EMBL@PETRA III, EMBL has continued limited operation at the DORIS III beamlines X33 (SAXS) and X11, X12, and X13 for MX applications.

EMBL is also engaged in providing additional support to external users through the so-called I3 scheme by the European Commission. Until August 2011, EMBL was a member of the ELISA project (coordinated by Elettra, Trieste). We are also a member of the P-CUBE project (coordinated by the University of Zurich), which will run until 2013, and focuses on the support of activities in the field of protein sample crystallisation and characterisation. In September 2011, EMBL became the coordinator of a new project named BioStruct-X, which focuses on X-ray based methods in structural biology. In terms of future perspectives, EMBL is also a core partner of the ESFRI project INSTRUCT, which is expected to coordinate relevant future research activities in structural biology.

The provision of advanced training to scientists at all levels is one of EMBL's central goals, and this year's calendar included

a variety of courses and workshops. At the beginning of the year, EMBL welcomed students from across the Hamburg region to the PDBe Roadshow – a workshop offering hands-on user training in bioinformatic tools. EMBL Hamburg's biannual lecture series on Biophysical Methods with expert speakers from Hamburg and other EMBL institutes took place in October and November and also attracted students from across the region. Following on from the success of last year, EMBL Hamburg joined forces with colleagues at EMBL-EBI (European Bioinformatics Institute) for a second EMBO Practical Course on Computational aspects of protein structure determination and analysis: from data to structure to function, held at the EBI in November. Over the next few years, additional courses and workshops will also be added to the EMBL calendar within the framework of the INSTRUCT and BioStruct-X projects.

EMBL is a partner of the future Centre for Structural Systems Biology (CSSB) and actively involved in the CSSB task force, aiming for coherent research excellence of the future CSSB. The intended research profile of the EMBL group at CSSB will focus on combining challenging structural biology, by taking advantage of EMBL's core expertise in MX and SAXS, and systems biology-oriented approaches on projects with high relevance in infection biology. An additional goal of our institute is to integrate present and future on-campus research infrastructures into the CSSB.

This year, EMBL has also become increasingly involved in future XFEL activities in life sciences. We have responded to a call of proposals for future projects at the European XFEL. To facilitate this process, a Memorandum of Understanding was signed by the European XFEL GmbH and EMBL on 12 September, 2011 (Fig. 4). EMBL is keen to provide its specific expertise both in the fields of future research activities and provision of infrastructures in the life sciences.

Figure 4

Signing of the Memorandum of Understanding: Karl Witte (European XFEL Administrative Director), Massimo Altarelli (Chairman of the European XFEL Management Board), Iain Mattaj (Director General of EMBL), and Matthias Wilmanns (Head of EMBL Hamburg).

EMBL's recent research and technology development activities were largely associated with the construction and commissioning of the new beamlines at PETRA III. Additional key activities have been further in-house developments of software packages for automated data interpretation of SAXS and MX, as well as activities on challenging structural biology projects. Highlights from 2011 focus on two publications: on the discovery of the molecular basis of unprecedented bisubstrate activity in an enzyme from Mycobacteria tuberculosis (Due et al., published in Proceedings of the Natl. Academy USA); and a SAXS-study on the architecture of a nuclear receptor (Rochel et al., published in Nature Molecular Structural Biology). Details of these papers are to be found in the Highlights section of this report.

Contact: Matthias Wilmanns, matthias.wilmanns@embl-hamburg.de

Max-Planck Unit for Structural Molecular Biology.

Saying goodbye – and looking back to a success story!

After 25 years of structural biology research at DESY, the year 2011 marks the formal end of the MPG-ASMB lab (Arbeitsgruppe für strukturelle Molekularbiologie). In the future, the activities of the MPG will be carried out within the framework of CFEL and the anticipated foundation of a new Max-Planck-Institute. Since its establishment in 1986 the mission of the ASMB lab was to pursue basic research on the structure of biological molecules, using the unique facilities at DESY FS. The creation of the ASMB was made possible by a special grant of the BMFT (now BMBF) and administered initially through 3 host Max-Planck-Institutes (MPI for Molecular Genetics Berlin, MPI for Biochemistry München, and MPI for Medical Research Heidelberg), who chose the three group leaders Ada Yonath (AY), Hans-Dieter Bartunik (HDB), and Eckhard Mandelkow (EM). Their research focus was the structure of the ribosome, the universal protein factory of cells (AY), the structural basis of enzyme reactions (HDB), and the structure of the cytoskeleton and neurodegenerative diseases (EM). In retrospect, the research was remarkably successful in all areas, as evidenced by several prestigious scientific awards, notably the Nobel Prize in Chemistry to Ada Yonath in 2009. Highlights of this period were the high-resolution structure of the ribosome complex (containing multiple protein and RNA molecules, Ada Yonath and colleagues), the structure of the proteasome (the multi-enzyme protein degradation complex, Hans-Dieter Bartunik in collaboration with Robert Huber's group at the MPI for Biochemistry München), the structures of kinesin motor proteins and Tau proteins and their involvement in Alzheimer neurodegeneration (by the groups of Eckhard and Eva Mandelkow). Throughout these 25 years as guest, the ASMB lab enjoyed the generous support of the host institution DESY. It was an excellent model for the collaboration between different institutions which laid the basis for the success in scientific discovery. The following paragraphs summarize recent progress in two areas, the reaction mechanism of an enzyme of the MAO family (Bartunik) and structural transitions of Tau proteins (Mandelkow), both important for nerve cell function and degeneration.

MAO-like enzymes (Monoamine oxidase-like enzymes): Processes catalysed by enzymes generally proceed through a number of reaction states, which are short-lived and associated with changes in conformation. Crystal structural analysis of intermediates of such reactions is often limited to stable dead-end complexes mimicking productive states. In the case of the flavoenzyme 6-hydroxy-L-nicotine oxidase (6HLNO), we were able to follow the complete reaction cycle of nicotine degradation in a series of high-resolution crystal structures (Kachalova et al., 2010; 2011). 6HLNO catalyses the dehydrogenation of the pyrrolidine moiety of 6-hydroxy-L-nicotine and subsequent hydration of an intermediate product, which opens the pyrrole ring to yield the final pseudooxynicotine product (Fig. 1a). The substrate, which was diffused into the enzyme crystal under anaerobic conditions, was observed to bind at the active site close to the isoalloxazine ring of the flavin adenine dinucleotide cofactor (Fig. 1b). Upon initiation of the enzymatic reaction by exposure to oxygen, dehydrogenation of the tertiary amine substrate associated with reduction of the flavin was observed.

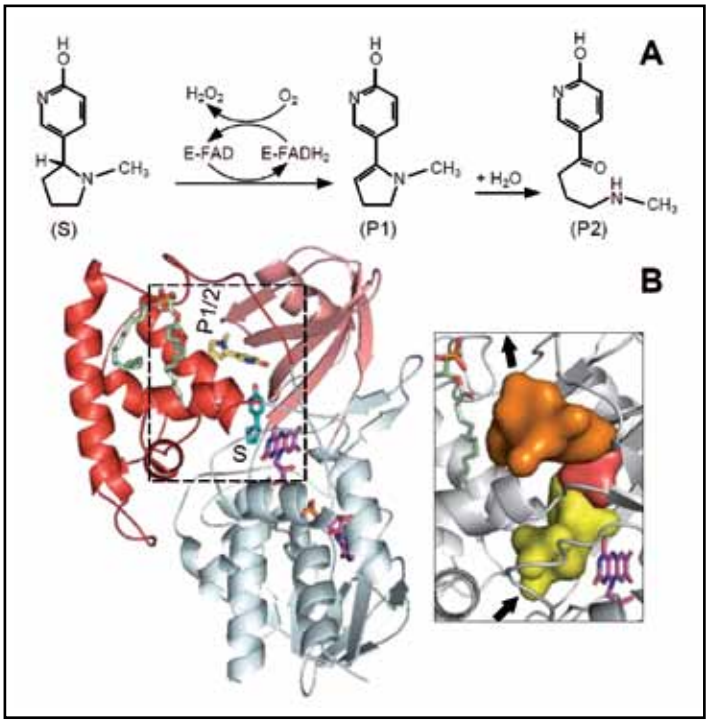

Figure 1

(a) Reaction catalysed by 6HLNO. The intermediate product P1 is formed upon dehydrogenation of the pyrrolidine moiety. Enzymatically assisted hydrolysis opens the pyrrole ring of P1 and results in the final ketone product P2. (b) Crystal structure of 6HLNO with substrate (S) and product sites (P1/2). S is bound in the solvent-inaccessible active-site cavity (yellow). Upon gated transfer through a channel (red), the products P1 and P2 bind at the exit cavity (brown). Arrows indicate possible paths of substrate entry and product P2 exit (Adapted from Kachalova et al., 2011).

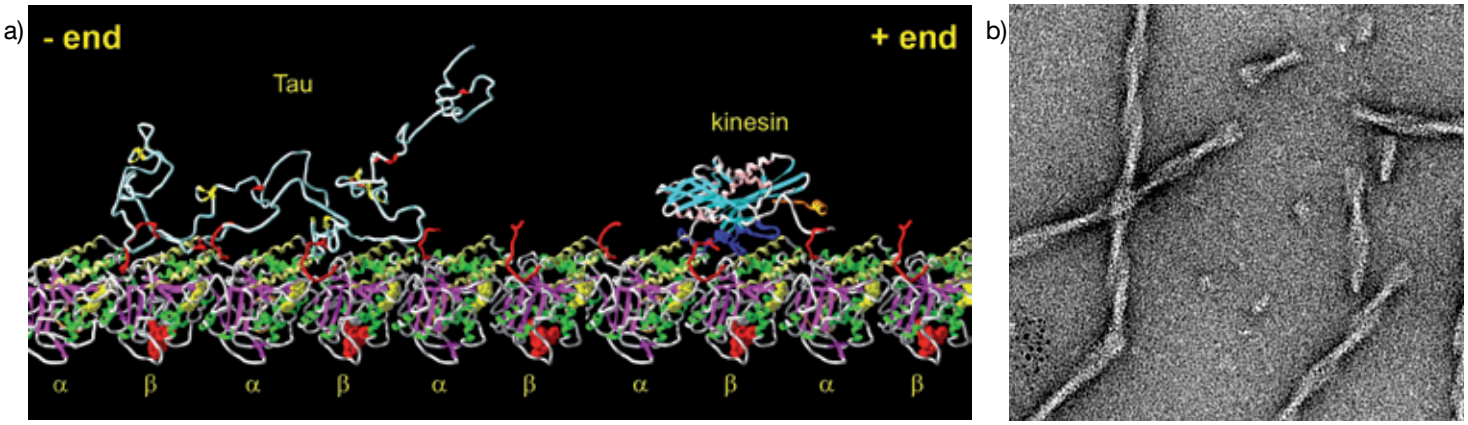

Figure 2

(a) Structural model of microtubules and their interacting proteins kinesin (a motor protein) and Tau. Kinesin (upper right) and the microtubule protofilament (string of tubulin subunits, lower half) consist of well-folded proteins with defined secondary structure, whereas Tau (upper left) is mostly unfolded and flexible. (b) Electron microscopic image of aggregated Tau protein, forming abnormal filaments in neurons affected by Alzheimer disease.

The intermediate methylmyosmine product rapidly departs from the active site and moves by gated transfer to a remote cavity close to the enzyme surface. Enzymatically assisted hydrolysis to the final product occurs at the second site, followed by release to the solvent. The presence of the product in the second site does not prevent binding of a new substrate to the active site, which shows that substrate access and product release follow different paths within the enzyme molecule. The possible binding of substrate both to the oxidized and reduced enzyme was confirmed by kinetic assays of 6HLNO activity (collaboration with Andrew Holt, Univ. Alberta, Edmonton, Canada). The enzymatic reaction is stereospecific, and further studies involving the D-stereoisomer, which acts as an inhibitor, provided a structural basis for explaining chiral selection.

The reaction mechanism is of general relevance for flavin amine oxidases, which play a role in cellular processes as diverse as metabolic degradation and chromatin remodelling. 6HLNO is a member of the monoamine oxidase (MAO) family of enzymes. In sequence and structure, 6HLNO is a close neighbour of human MAO-A and MAO-B, which play central roles in the control of the concentration of neurotransmitters in cells and represent targets for the treatment of neurological diseases including Parkinson, Alzheimer and mental disturbances.

Tau protein and neurodegeneration: Recent years have seen a surge of interest in the protein “Tau” because of its role in several neurodegenerative diseases such as Alzheimer disease. Tau’s normal function is to regulate the stability of microtubules, the “tracks” of intracellular transport by “motor proteins” in axons, the long extensions of nerve cells (Fig. 2a). In the disease state, Tau becomes chemically modified, detaches from microtubules, and forms insoluble aggregates, the “neurofibrillary tangles” (Fig. 2b). We have studied the structural changes in Tau in the transition from normal to aggregation-prone states. One enigma is that Tau is a “natively unfolded” protein which lacks a defined structure and is highly soluble, unlike the proteins it interacts with (tubulin, kinesin, Fig. 2a). A combination of X-ray crystallography, SAXS, and NMR spectroscopy has revealed the structural features of Tau, motor proteins, and modifying enzymes (protein kinases) (collaborations with D. Svergun, EMBL Hamburg and C. Griesinger, M. Zweckstetter, MPI Göttingen). The key to pathological aggregation is encoded in a simple structural principle, the beta-structure in two short hexapeptide motifs within the Tau molecule. Self-assembly of these motifs leads to aggregation (Fig. 2b), even though the majority of the protein retains its unfolded structure. Cell and animal models of Tau pathology revealed that the residual beta-structure is also crucial for the degeneration of nerve cells. Consequently, one of the current efforts is aimed at developing compounds which prevent aggregation (“beta busters”) and thus slow down or reverse the disease process. In the future, this work will be continued at the DZNE (Deutsches Zentrum fur neurodegenerative Erkrankungen, Bonn) which is like DESY a member of the Helmholtz Gemeinschaft.

Contact: Eckhard Mandelkow, mandelkow@mpasmb.desy.de

References

1. G. S. Kachalova, G. P. Bourenkov, T. Mengesdorf, S. Schenk, H. R. Maun, M. Burghammer, C. Riekel, K. Decker, and H.D.Bartunik, “Crystal structure analysis of free and substrate-bound 6-hydroxy-L-nicotine oxidase from Arthrobacter nicotinovorans”, J. Mol. Biol. 396, 785–799 (2010).

2. G. S. Kachalova, K. Decker, A. Holt, and H. D. Bartunik, “Crystallographic snapshots of the complete reaction cycle of nicotine degradation by an amine oxidase of the monoamine oxidase (MAO) family”, Proc. Natl. Acad. Sci. USA 108, 4800–4805 (2011).

3. B. Bulic, M. Pickhardt, E.-M. Mandelkow, E. Mandelkow, E., “Tau protein and tau aggregation inhibitors”, Neuropharmacol. 59, 276–289 (2010).

4. A. Shkumatov, S. Chinnathambi, E. Mandelkow, D. I. Svergun, “Structural memory of natively unfolded tau protein detected by Small-Angle X-ray Scattering”, Proteins 79, 2122–2131 (2011).

5. X. Li, Y. Kumar, H. Zempel, E.-M. Mandelkow, J. Biernat, E. Mandelkow, “Novel diffusion barrier for axonal retention of Tau in neurons and its failure in neurodegeneration”. EMBO Journal [Epub ahead of print] (2011).

Helmholtz-Zentrum Geesthacht Outstation at DESY.

GEMS has found a new home

The German Engineering Materials Science Centre (GEMS), operated by the Helmholtz-Zentrum Geesthacht (HZG) on the DESY site, has continued to successfully provide the high-brilliance X-rays from the DESY synchrotron radiation sources DORIS III and in particular PETRA III to the engineering materials science community. In 2011, GEMS could further improve the support for users with the help of HZG scientists having moved from Geesthacht to the new provisional GEMS building 221 (Fig. 1). The planning for the new DESY photon science building, where the HZG GEMS as well as the DESY NanoLab activities will be integrated, is well advanced, and the final move to new space for offices and in particular for laboratories is envisaged for 2014. This will add a new quality to sample preparation, in and ex situ instrumentation and data analysis facilities.

The visibility of GEMS in the international engineering materials science community could further be increased in 2011. GEMS organised the 6th International Conference on Mechanical Stress Evaluation by Neutrons and Synchrotron Radiation (MECA SENS VI, www.mecasens2011.de) and the International Summer School “Application of Neutrons and Synchrotron Radiation in Engineering Materials Science” (www.hzg.de/mw/summerschool). Guided tours of the GEMS facilities on the DESY site and practical training sessions during the school demonstrated the potential of the GEMS instrumentation to senior scientists, postdocs and PhD students.

The GEMS beamlines at DESY are in smooth user operation or are being commissioned; the detailed status is outlined below.

Routine user operation with experiments in the hard X-ray regime was continued at the HZG beamline HARWI II at DORIS III. About 200 days of beamtime were offered to the user groups. The dilatometer, which has been in operation since 2009 at this beamline, enjoys great popularity. Meanwhile, five external and two HZG-internal groups have used this instrument, and its quenching unit is in normal user mode. The differential scanning calorimetry (DSC) unit of the dilatometer instrument has also been tested and will first be offered to the users in autumn 2011. The deformation and compression unit is in commissioning mode and will be regularly available at the beginning of 2012. Moreover, a couple of minor and major improvements of both hardware and software of the HARWI II diffractometer and sample environments have been realised.

Figure 1

The provisional GEMS office container (bldg. 221) next to HARWI II (bldg. 25c).

The High-Energy Materials Science Beamline (HEMS, P07 at PETRA III) for research with high-brilliance hard X-rays went into regular user operation at the end of May 2011 for two of its four experimental stations EH2 and EH3. In EH2 (operated by DESY), a rail-system for various detector geometries was implemented and the beam tilting device was successfully commissioned by our DESY colleagues. In EH3, a pilot experiment for in situ chipping-off experiments by colleagues from the Technical University of Berlin made for the first time full use of the instrument’s extraordinary capabilities in August 2011, combining a load capacity of 1 t with a positioning resolution

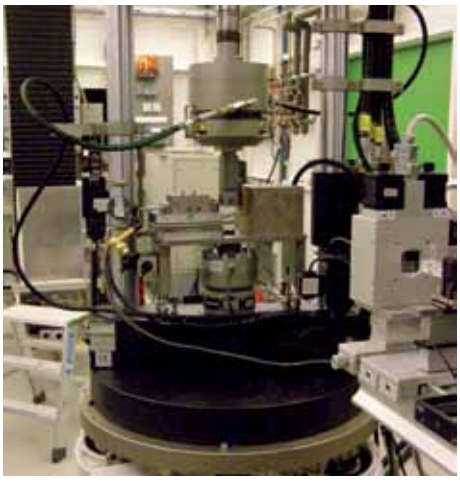

Figure 2

In situ chipping off steel inside the 100 kN HZG stress rig from Instron, positioned on the high-load hexapod in EH3.

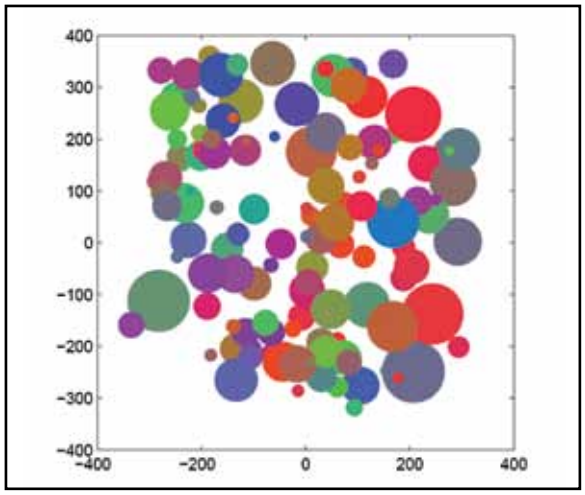

Figure 3

First centre-of-mass grain map of undeformed Al at 60 keV – 14 cuts á 50 µm, measured with a beam size of 0.05 x 1.0 mm². 128 indexed grains are shown as spheres with diameters reflecting relative volumes and colours corresponding to orientation (position accuracy 30 µm, orientation accuracy 0.15°, relative error of volume 35 %, courtesy J. Oddershede).

of 1 µm. Steep residual stress gradients in steel deformed by a knife edge using a 100 kN stress rig from Instron were measured with a spot size of 10 x 10 µm² (see Fig. 2).

In EH4, several components of the micro-tomography system were commissioned (first test tomogram in April 2011). Test experiments together with friendly users were scheduled for November and December 2011; regular user experiments are foreseen for 2012. The design of the 3D-XRD (=3-Dimensional X-Ray Diffraction) strain and stress mapper was completed, all components have been ordered or are already delivered. First test experiments for grain mapping were carried out, resulting in the first grain map taken at HEMS (May 2011, Fig. 3). The dedicated 3D-XRD strain mapper will become operational in 2012. The side station / test facility EH1 received an instrumental upgrade for sample positioning and turned out to be an extremely valuable fast-access experimental station for HZG in-house research (texture, residual stresses and in situ phase analysis with the abovementioned dilatometer) and student training with several groups from the universities of Kiel and Clausthal.

The best focus reached at HEMS so far was smaller than 3 x 35 µm² at 80 keV with Al compound refractive lenses (CRL) and the maximum flux 2 x 10^{11} photons/s mm² at 80 keV at mid-position of the beamline in EH2. Several industrial users performed experiments at HEMS, taking advantage of the possibility to measure residual stresses with a depth resolution < 0.8 mm (in beam direction) in the bulk of industrial components by using conical slits.

At the Imaging Beamline (IBL, P05 at PETRA III), the first half of 2011 was dedicated to the set-up and commissioning of the double crystal monochromator (DCM). Initial tests led to the first beam in the experimental hutches EH1 and EH2. Unfortunately, the DCM soon had several problems concerning the positioning and the vacuum which led to a considerable delay

Figure 4

The impressive monolithic granite basis of the nanotomography set-up installed at IBL.

in the beamline commissioning. A big effort was the installation of the basic parts of the nanotomography setup in the experimental hutch EH1 of IBL (see Fig. 4). Furthermore, a double multilayer monochromator (DMM) is currently in the design phase; delivery is planned for the end of 2012. First users for tomography experiments are expected in 2012. Commissioning of the nanotomography setup is planned for the beginning of 2012.

Main user activities of the HZG tomography team in 2011 took place at the DORIS III beamlines BW2 (1/4 of the beamtime available) at lower photon energy and at HARWI II at higher energies, the latter with optional differential phase contrast (DPC). The first one of identical sample changers for all tomography stations was commissioned at HARWI II and demonstrated the potential for an even more efficient use of beamtime.

HZG together with EMBL commissioned the PETRA III small-angle scattering beamline BioSAXS (P12). The first X-ray beam reached the optics hutch in December 2010, a collimated beam (1.0 x 0.85 mm²) the experimental hutch in March 2011. An automatic sample chamber for aqueous samples has been put in operation for first scattering measurements on surfactant solutions. The operation of the instrument in „friendly user" mode has started in September 2011. The required sample volume is only 10 µL. The phase transition from a vesicle-like system to a sponge phase, with the potential application as drug-delivery nanoparticles, was followed by SAXS. Focusing mirrors will soon be delivered such that experiments with focused beam are planned for spring 2012.

The Helmholtz-Zentrum Geesthacht Outstation at DESY is planning to continue to offer instrumentation for complementary and versatile synchrotron radiation applications in materials science (scattering and imaging) by using X-ray beams in a wide energy range and of various sizes also after the DORIS III shutdown. In the current scenario, the HARWI II diffraction part will move to the damping wiggler beamline in Hall North of the PETRA III extension. For the large-beam tomography instrument a place in Hall East is under discussion.

Contact: Martin Müller, martin.mueller@hzg.de
Andreas Schreyer, andreas.schreyer@hzg.de

University of Hamburg on the DESY site.

University and DESY - Strong partners for Photon Science

Photon Science is one of the major research areas of the University of Hamburg. The collaboration with DESY and the research with synchrotron radiation have a long tradition which goes back to the early days of synchrotron radiation research at DESY, where members of the Institute of Experimental Physics have been actively involved in the first experiments. Recently, DESY and the University of Hamburg have established PIER – a **P**artnership for **I**nnovation, **E**ducation and **R**esearch – to tighten the links between the two institutions even more (www.pier-campus.de). The four key scientific areas of this partnership are Particle- and Astroparticle Physics, Nanoscience, Life Sciences and of course Photon Science.
Groups from the University are actively involved in developing and running beamlines as well as building instrumentation for experiments at DESY. One focus area are endstations at PETRA III in the framework of the BMBF collaborative research ("Verbundforschung"): A low temperature cryostat with integrated 7 Tesla-magnet for X-ray Absorption Spectroscopy (Fig. 1) is now in operation and cooling tests have demonstrated a base temperature below 50 mK (group of Wilfried Wurth). First experiments with the cryostat at the variable polarization XUV beamline P04 will hopefully be performed at the beginning of next year. Michael Martins is leading an effort to build an ion-storage ring for spectroscopy (PIPE) at P04 which is also close to completion (Fig. 2) and Robert Johnson is involved in the hard X-ray photoemission project at beamline P09. Research in structural biology is performed in a collaboration between the University of Hamburg (Christian Betzel, Institute for Biochemistry and Molecular Biology) and the University of Lübeck (Rolf Hilgenfeld, Institute for Biochemistry) in the Laboratory for Structural Biology of Infection and Inflammation on the DESY site. This research field will be considerably expanded in the future with the new Centre for Structural Systems Biology (CSSB), where the University of Hamburg is one of the partners. Apart from the new activities at PETRA III, the University stills runs a very active research program at DORIS III including, for example, the chemical crystallography activities at beamline F1 (Ulrich Bismayer).
University groups are heavily involved in research at FLASH. They are major partners in the first BMBF priority program ("Forschungsschwerpunkt") in condensed matter research FSP-301 "FLASH: Matter in the Light of Ultra Short and Extremely Intense X-ray Pulses" coordinated by Wilfried Wurth. The FSP-301 is now in the second three-year funding period. Projects from the University of Hamburg are, among others, the instrumental effort to build new spectrometers for photoelectron spectroscopy (Wilfried Wurth together with the University of Kiel), the upgrade of the new VUV Raman spectrometer (Michael Rübhausen), a project on nonlinear X-ray physics

Figure 1

The low-temperature cryostat at P04

Figure 2

The PIPE ion-storage ring at beamline P04 in the PETRA III experimental hall

with sub-10 fs time and sub-30 µm spatial resolution (Markus Drescher), and an instrument for time-resolved coherent imaging of magnetic nanostructures which is developed for use at PETRA III and FLASH (by Hans-Peter Oepen from the Institute of Applied Physics together with Gerhard Grübel from DESY). An area where the University is also particularly strong is the research on an innovative concept for accelerator based light sources. The seeding experiment "sFLASH" (Markus Drescher and Jörg Roßbach) is now in the test phase. In the framework of the FSP-301 Jörg Roßbach and his coworkers are pursuing two projects where the focus is on the creation of extremely short X-ray pulses at FLASH (sub-10 fs), either through seeding with high harmonic laser sources or through the production and manipulation of ultrashort electron bunches and the monitoring tools needed for these bunches. With the recent appointment of Florian Grüner and his work in laser-plasma accelerators the University has expanded its activities in accelerator physics in strong collaboration with DESY.

The Center for Free-Electron Laser Science (CFEL), which was founded by the University of Hamburg together with DESY and the Max-Planck Society to foster interdisciplinary science with free-electron laser sources, is now fully operational. Its new building will be finished in spring next year, as outlined in detail in the CFEL contribution to this report.

Research groups from the University and their partners from DESY, European XFEL and the Max-Planck Society have successfully applied for a DFG Collaborative Research Centre (SFB 925) on "Light Induced Dynamics and Control of Correlated Quantum Systems" (speaker: Klaus Sengstock) which started in July this year. In addition an application for the foundation of a Cluster of Excellence – "Hamburg Centre for Ultrafast Imaging: Structure, Dynamics and Control of Materials on the Atomic Scale" (speaker: Dwayne Miller) – has been submitted within the framework of the Federal and State Excellence Initiative.

At the same time, academic education is pursued in collaboration between DESY Photon Science and the Department of Physics of the University. Examples are a joint master course in X-ray physics, which is by now well established, and the multidisciplinary approach in the graduate training program (Graduiertenkolleg) GRK 1355 "Physics with new advanced coherent radiation sources", dedicated to the development, characterization and application of modern sources for light and matter waves. Recently, an International Max-Planck-Research School for "Ultrafast Imaging and Structural Dynamics" has been established by the Max-Planck Society (speaker: Dwayne Miller, Joachim Ullrich) with involvement of the University of Hamburg, DESY, CFEL and European XFEL providing new exciting opportunities for graduate students in Photon Science on campus.

Contact: Wilfried Wurth, wilfried.wurth@desy.de

Light Sources.

DORIS III.

Preparing for the finish

In view of the upcoming end of synchrotron radiation (SR) research at DORIS III in 2012, every effort was made to ensure a smooth and efficient operation for user experiments throughout the remaining period. The demand for beamtime at DORIS III beamlines persists at a high level and all instruments currently in operation will be available until shutdown. The only exception is beamline BW6 which had been operated by the Max-Planck Unit for Structural Molecular Biology in Hamburg for many years. This activity has ended and the BW6 instrument has been shut down.

During the winter break 2010/11, the long straight section of the storage ring was considerably modified for the installation of the OLYMPUS detector, which is going to be used for a particle physics experiment at DORIS III in 2012. This reconstruction was completed on time and during the following machine commissioning it was verified that the storage ring can be switched without difficulty between operational modes for synchrotron radiation at 4.5 GeV and for particle physics at 2 GeV. SR user experiments started again on 1st March, according to schedule.
In the four weeks long summer shutdown, the straight section was opened again for the final installation of the OLYMPUS detector. After an extensive testing phase with beam, SR user operation resumed as planned mid of August.

The overall DORIS III operation in 2011 was reliable except for two interruptions in May due to problems with a dipole chamber and a vacuum valve. Over the whole year, a total of 5300 h with an availability better than 90.4 % has been delivered for SR user operation.

Although already last year a record number of research proposals for experiments at DORIS III was submitted, there was an additional unexpected increase of the number of submissions in 2011. In total, 415 new proposals for experiments at DORIS III beamlines were accepted, whereof 46 proposed combined experiments at DORIS III and PETRA III beamlines. These numbers do not include proposals for structural biology research at EMBL beamlines.

This corresponds to a significant increase of 60 %, which may be related to the fact that, due to the planned end of SR operation in mid-October 2012, it was the last round of proposal submission for experiments at DORIS III. The number of proposals submitted by international research groups was 44 % of the total.

In 2011, a number of very interesting publications resulted from experiments performed at DORIS III instruments, examples of which are presented in the Research Highlights section of this report. Much attention, also from the media, received themes concerning cultural heritage. The well attended public lectures during the Users' Meeting in January 2011 (Fig. 1) presented a selection of the work done in this area at DORIS III.

Contact: Wolfgang Drube, wolfgang.drube@desy.de

Figure 1
The announcement of the public lectures on cultural heritage themes.

Alte Kunstschätze in neuem Licht.

Öffentliche Vorträge bei DESY
Donnerstag, 27. Januar 2011

Deutsches Elektronen-Synchrotron DESY
Notkestraße 85, 22607 Hamburg
Hörsaal, Gebäude 5

Moderne Untersuchungsmethoden mit brillanten Lichtquellen ermöglichen neuartige Einblicke in die Techniken und Materialien alter Meister.

Programm

14:00 Begrüßung: Edgar Weckert (DESY), **Wolfgang Drube** (DESY)

Moderation: Koen Janssens (Universität Antwerpen, Belgien)

14:20 Kulturgut im Röntgenlicht
Joris Dik (Technische Universität Delft, Niederlande)

15.00 Synchrotron-based research at the J. Paul Getty Museum
Marc Walton (Getty Conservation Institute, Los Angeles, USA)

15.40 Kaffeepause

16:15 Visualisierung übermalter Gemälde mit Röntgenfluoreszenz
Matthias Alfeld (Universität Antwerpen, Belgien)

16:45 Metalle erzählen - von gelöschten Schriften und neolithischer Beilherstellung
Leif Glaser (DESY)

17:15 Möglichkeiten der Kulturgutanalyse an DESY Lichtquellen
Karen Appel (DESY)

17:45 Schlusswort

HELMHOLTZ GEMEINSCHAFT | Universiteit Antwerpen | TU Delft

Organisiert in Zusammenarbeit mit der Universität Antwerpen (Belgien) und der Technischen Universität Delft (Niederlande).

Kontakt:
DESY PR, Telefon: 040/8998 3613
E-Mail: desypr@desy.de

Webseite: hasylab.desy.de/usersmeeting

Beschleuniger | Forschung mit Photonen | Teilchenphysik

Deutsches Elektronen-Synchrotron
Ein Forschungszentrum der Helmholtz-Gemeinschaft

DESY

FLASH.

The calm before the storm

In 2011, until the start of the shutdown in September, the focus at FLASH was on user operation. During the third user period at FLASH – out of 8834 hours from September 2010 to September 2011 – 56 % (4955 h) of beamtime were dedicated to the 29 user experiments, which were approved out of 75 proposals by the FLASH project review panel in December 2009. In addition, time was reserved for machine studies (37 %), maintenance (3 %), and a two weeks shutdown over Christmas 2010 (4 %). Most of the machine study time has been devoted to improvements of the FEL performance and to set up and advance photon beamlines and diagnostics. Part of the study time (about 15 %) has been reserved for general accelerator physics studies and developments related to future projects, in particular the European XFEL and the International Linear Collider. During the third user period, in total 3740 hours of FEL radiation were delivered to the users (Fig. 1). This corresponds to 75 % of the overall time dedicated to user runs, and 97 % of the beamtime originally scheduled for the experiments

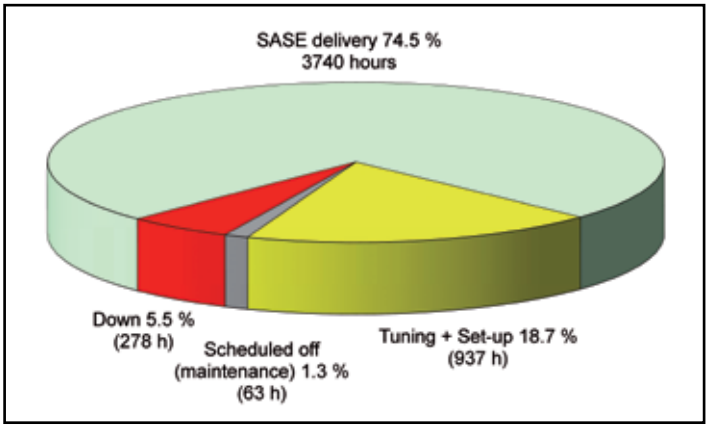

Figure 1

FEL beam delivery during the user beam time blocks in the third user period from September 2010 to September 2011.

(since losses of beamtime could mostly be compensated by contingency shifts). Due to the vast range of requested parameters, such as wavelength, pulse length and pulse pattern, 19 % of time during the user runs was used for set-up and tuning of the machine. The uptime of the FLASH accelerator during the user runs was 94 %.

During the third user period more than 30 different wavelengths between 4.7 nm and 45 nm were provided to the experiments. Interests are quite uniformly divided into one third short wavelength operation below 10 nm, one third near 13.5 nm and one third long wavelength operation above 20 nm. Equally varied were the delivered bunch train patterns with nearly 50 % single bunch operation and slightly above 50 % multi-bunch operation with different bunch to bunch spacing, all at a bunch train repetition rate of 10 Hz. A new record could be achieved at FLASH: At 6.9 nm and in a multi-bunch operation of 300 bunches at 1 MHz spacing an average power exceeding 300 mW was reached (Fig. 2). A similar performance was also obtained at 4.7 nm. With regard to the pulse duration, about one fourth of the experiments required very short pulses below 50 femtoseconds. Thus, online techniques to determine the pulse length on a shot-to shot basis take on a strong new focus in the machine and photon diagnostic program.

Early in the third user period, in September 2010, the electron beam energy was successfully increased to 1.25 GeV and lasing in the water window at a wavelength of 4.12 nm in the fundamental was achieved as described in Photon Science 2010 report. Since the original FLASH design intended a beam energy of 1 GeV and thus wavelengths above 6 nm, the majority of the beamlines were designed for the 6 – 80 nm range and use carbon coated silicon mirrors. Thus, they generally do not transport radiation in the water window between the oxygen K(1s) absorption edge (λ = 2.3 nm or 543 eV) and the carbon K edge (λ = 4.37 nm or 284 eV) that well. At BL2 in the unfocused branch, the mirrors have nickel as a second coating and a first proof-of-principle in-house experiment could hence be performed at 4.3 nm. It showed that short wavelength radiation can be transported to the end station at BL2 with a good transmission of 45 %. Following this success, an upgrade of the focused branch of beamline BL2 with a nickel coated ellipsoidal mirror (instead of the present carbon coating) is planned for the following shutdown in early 2013.

Figure 3

Top: The FLASH tunnel after the start of the FLASH II construction (September 2011). Bottom: Artists view of the FLASH II and FLASH experimental halls as well as the PETRA III North extension (from left to right). (Courtesy Architekturbüro Renner Hainke Wirth)

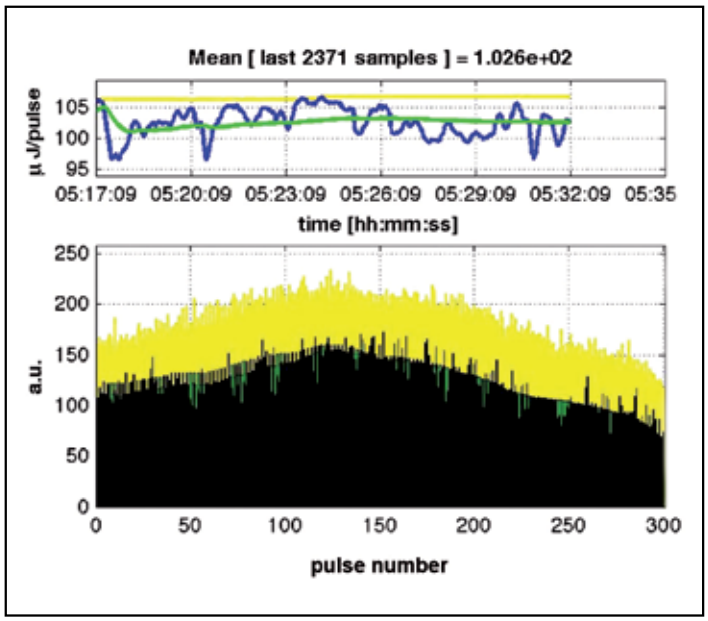

Figure 2

FEL pulse train of 300 pulses with 1 MHz repetition rate at 6.9 nm.
Top: The blue trace shows the bunch train averaged photon pulse energy in μJ determined by means of a calibrated gas monitor detector; the yellow trace is the peak value while the green shows the signal averaged over longer times within the data acquisition period. Bottom: The black histogram is a pulse resolved snap-shot of one individual pulse train, the yellow histogram depicts the peak values during the acquisition period and the green histogram is a time average.

FLASH II – Extension of the FLASH Facility

Major changes are again in store for FLASH in the next few years. The civil construction for the second undulator beamline – FLASH II – has started requiring a 3.5 months shutdown of FLASH which started in autumn 2011 and a 1.5 months shutdown of PETRA III in early 2012. Following these shutdowns, FLASH II work can press ahead without major disruption of FLASH and PETRA III operation during 2012. A second FLASH shutdown is scheduled for early 2013, when the existing FLASH accelerator is connected to the new FLASH II undulator beamline. A goal is to complete the FLASH II tunnel and install its major components until spring 2013.

In addition to the SASE (self-amplified spontaneous emission) mode that is used in FLASH, HHG (high harmonic generation) seeding is foreseen for FLASH II. The pilot project, sFLASH, to establish direct HHG seeding at FLASH is in the commissioning phase. During the 2011 shutdown the HHG source and the XUV seed transport beamline are modified in order to enhance the available seed power. It is expected that seeded FEL pulses will have superior characteristics in terms of short pulse operation and longitudinal coherence compared to the standard SASE mode. In summary, a storm of upgrades is forecasted for FLASH in the next years with many new opportunities for exciting science to come.

Contact: Josef Feldhaus, josef.feldhaus@desy.de (FLASH)
Elke Plönjes, elke.ploenjes@desy.de (FLASH)
Bart Faatz, bart.faatz@desy.de (FLASH II)

PETRA III.

The first full year of operation

2011 was the first year with full-time user operation of PETRA III. The PETRA III project was formally finished successfully on 31st December 2010. Currently six beamlines (P01, P03, P07, P08, P09, and P10) are scheduling users via the DESY DOOR system. Four more beamlines are serving friendly users (P02, P06, P12, and P14); these beamlines were included in the call for proposals in fall 2011. The remaining four beamlines are still commissioning some of their components.

Storage ring

The operation for users started in March, was interrupted by a five weeks shutdown to allow for cable work in preparation of FLASH II and ended on 21st December. In total 4300 hours have been delivered to the scientific community. The reliability reached 93.6 % on average with a high of 97.6 % in the fourth run in August.

The storage ring has reached almost all design parameters. For users the design current of 100 mA is now delivered routinely in most filling patterns as shown in Fig. 1. Due to problems with the RF fingers the single bunch current is still limited to 2 mA limiting the total current in 40 bunch mode to 80 mA. Top-up operation is standard now with a minimum current fluctuation of 0.3 % (in 240 bunch filling mode). Beam stability values in the range of 100 nm or 100 nrad have been achieved and maintained over days. The availablility of the machine in 2011 is summarised in Fig. 2.

In July the second module of the P01 undulator was installed, resulting now in a 10 m device. After some alignment the full performance was obtained with complete overlap of the central-cones of the two modules and an increase in monochromatic flux of 100 %.

First steps have also been performed in the commissioning of the APPLE II undulator of P04 with full current beam. Up to now no major difficulties have been encountered using the device in circular polarized mode.

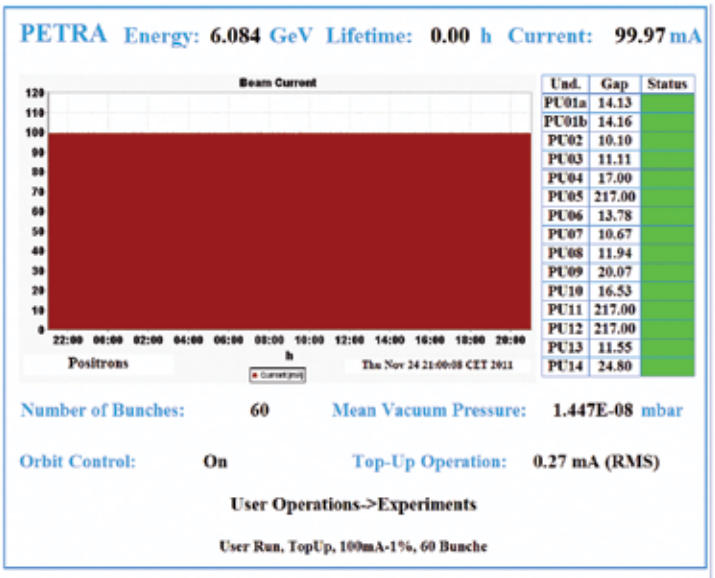

Figure 1

History of PETRA III beam current showing 24 hours of top-up operation at 100 mA.

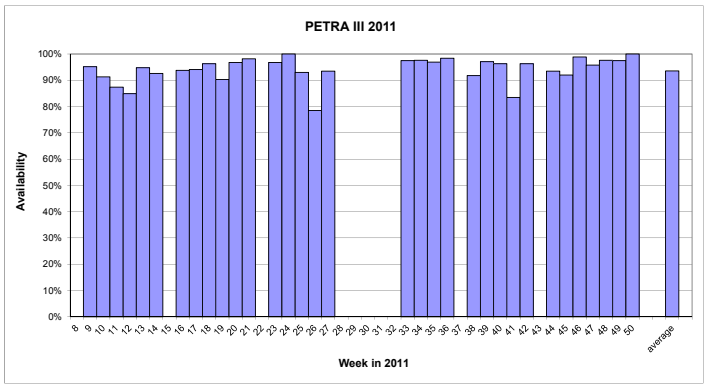

Figure 2

Availability of PETRA III in 2011. The last bar on the right indicates the average which amounts to 93.6 %.

Beamlines and experiments

Great progress has also been made in improving the performance of monochromators. In particular for beamlines with long lever arms (60 m and more) the specifications are extremely ambitious. The stability of the high-heat load double crystal monochromators of P10 has been optimized to the 30 nrad range by using a channel-cut crystal. Although the tuning range is limited this will be an option the reach even higher performance. A second big step was made at the side-station monochromators of P02 which was complemented by piezo actuators to allow for feedback operation.

In several beamlines mirrors for suppressing higher harmonics and to steer the X-ray beam have been installed. They perform as expected with reflectivities in the high 90 % regime.

In sector 3 (variable polarization soft X-rays) the heart of the grating monochromator, a holographically produced laminar varied-line-spacing (VLS) grating was installed in one of the pre-mirror plane-grating units (PMPGU) in late summer 2011. Prior to this event the PMPGU was extensively commissioned in order to verify the sub-0.02 arcsec angular stability of the grating axis. The first monochromatic beam was introduced into the beamline on 30 September. It became immediately apparent that the beamline is able to deliver the expected high photon flux into a very well collimated soft X-ray beam. On 21 October we could observe – using a prototype of the beamline online diagnostic unit – the first scan of the 1s->pi* resonance of molecular nitrogen with indications of vibrational resolution, which is somewhat remarkable taking into account that we have presently to use a simple polished solid aluminium block instead of the Si single-crystal block of the final mirror. Therefore we look forward to a really big push of the resolving power towards design values once the internally cooled Si mirror is delivered early 2012 and subsequently brought into operation together with the second grating which arrived in October. In the meantime commissioning of the beamline will continue including first test experiments.

Great progress has been made in the delivery of nanometer sized beams. Mostly P10 (in collaboration with University of Göttingen) and P06 (collaboration with Technical University Dresden and Paul-Scherrer-Institute, Switzerland) have achieved spot sizes of 10 nm and 21 nm, respectively. These beams were used to image bacteria or trace element distributions in plants or minerals.

Results of a first study performed in a collaboration of the P02 team with the Geo-Forschungszentrum Potsdam illustrate the potential of combining synchrotron X-ray diffraction and Brillouin Spectroscopy to study the elastic properties of matter at extreme conditions. In the near future, these complimentary techniques will both be available at PETRA III. Both in-situ studies using a spectrometer at the beamline and off-line studies in the nearby laser laboratory are currently commissioned. In a further test experiment by D. Andrault on SiO2-Stishovite at P02 the laser heating system set-up in collaboration with Frankfurt University achieved temperatures of 4000K at a pressure of more than 100 GPa.

In the last call for proposals for the eight active PETRA III beamlines resulted in a dramatic increase in the request as depicted in Fig. 3. All beamlines are now overbooked and numbers are expected to increase even further in the calls to come.

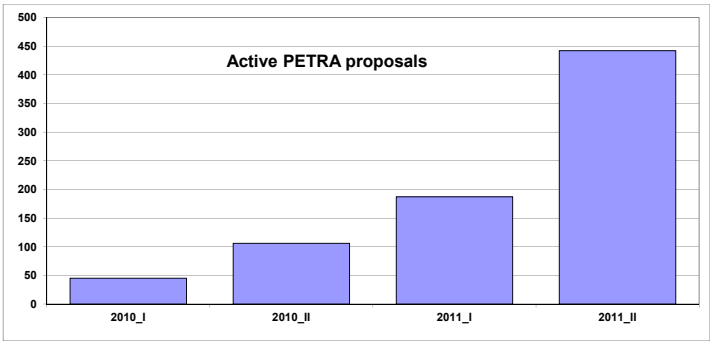

Figure 3

Number of active PETRA III proposals. Each proposal is valid for one year (i.e. 2 terms).

Contact: Hermann Franz, hermann.franz@desy.de
Klaus Balewski, klaus.balewski@desy.de

PETRA III Extension - Adding ten more beamlines

As the scheduled shutdown of the DORIS III facility in October 2012 is approaching, the planning of the PETRA III extension is progressing fast. Within the scope of this project a new experimental hall on either side of the large PETRA III hall (North and East) will be built making use of the respective long straight section and part of the adjacent arc. Each hall will accommodate 5 independent beamlines. The northern straight section accommodates one of the two 40 m long damping wiggler arrays producing an extremely hard and powerful X-ray beam which will be the source for one of the beamlines. The long straight in the east will be used for additional insertion devices.

In each of the arc sections, about 50 m of the machine lattice will be modified to replace the long PETRA III dipole magnets by two double bent achromat (DBA) cells, each providing a 5 m long straight section. Following the present PETRA III beamline arrangement, a canting dipole will be used to divide each DBA cell into two 2 m straights allowing separate insertion devices for two independent beamlines. For the new beamlines, a larger canting angle was chosen (20 mrad instead of 5 mrad) in order to provide more spatial flexibility for the experiments further downstream. The modified lattice provides in addition 8 short straight sections in the arcs with source properties corresponding to a high-β section at PETRA III today which make them very suitable for the use of undulators. The total beamline lengths will range from 70 m to 140 m.

PETRA III East			
beamline	**applications / instruments**	**insertion device**	**range**
P21	Swedish materials science beamline - high-energy in-situ X-ray diffraction and scattering for materials science research - large sample imaging	4 m undulator & wiggler	~50-200 keV
P22	nano X-ray spectroscopy (India-DESY collaboration) applications (to be discussed)	2 m undulator	~3-50 keV
P23	nano X-ray diffraction (Russian-German collaboration) - structure & processes in low-dimensional and nanoscale systems) - (time-resolved) nano-diffraction in complex and in-situ sample environments - low-T, high-pressure diffraction	2 m undulator	~5-50 keV
P24	chemical crystallography - single-crystal diffraction - pump-probe diffraction techniques - diffuse scattering - low temperature & non-ambient sample environments	mini-undulator	~8-40 keV
P25	P25.1 education/training/testing (to be discussed) P25.2 fixed energy side-branch (to be discussed)	mini-undulator	to be discussed
PETRA III North			
P61	P61.1 fixed-energy side branch (tentative: PDF instrument; feasibility study ongoing) ; P61.2a high-energy engineering materials science station (Helmholtz-Centre Geesthacht, HZG) P61.2b extreme conditions (large volume press)	damping wiggler (40 m)	~50-200 keV monochr. & pink beam
P62	small angle X-ray scattering WAXS, SAXS, USAXS in transmission & reflection geometry with moderate beamsize	mini-undulator	~10-25 keV
P63	X-ray micro fluorescence micro-probe applications beam size down to ~5 μm^2	mini-undulator	~3-45 keV
P64	X-ray absorption spectroscopy time-resolved studies & diluted systems bio-XAFS	2 m undulator	~3-45 keV
P65	X-ray absorption spectroscopy in-situ studies for catalysis & chemistry	mini-undulator	~4-45 keV

Five of the new beamlines will serve to continue very productive techniques which are currently being offered at DORIS III and are not yet implemented at PETRA III. Most of these beamlines will continue to use the compact UHV double-crystal monochromators which are being very successfully operated at DORIS III beamlines. However, this water-cooled “CEMO-type” monochromator has been designed for use at bending magnet beamlines and cannot cope with the extreme heatload of a full PETRA III undulator. It is therefore planned to use few-period undulators (“mini-undulators”) in combination with this monochromator. For higher energy beamlines, additional photon absorbers may be used to effectively reduce the power in the low energy regime allowing for more periods of the undulator. It should be mentioned that the use of mini-wigglers to obtain a continuous spectrum is not an option because a fixed-gap few-period device in combination with the low source emittance of a hard X-ray machine such as PETRA III results in a spatial inhomogeneity of the illuminated area on the sample as a function of photon energy. The use of tuneable mini-undulators for the DORIS III techniques will provide a considerably brighter beam for these applications at PETRA III.

PETRA III North is located next to the present FLASH facility and beamline P61 (see table for a complete list of beamlines) will be using the powerful beam from the array of 10 damping wigglers (DW) in the northern long straight section for high X-ray energy materials science applications. Using high-power filters, only the hard X-ray spectrum (> 50 keV) will be guided to the optical components. The straight branch provides space for two large in-line experimental hutches. The feasibility study of using an additional fixed-energy side branch is ongoing. The instruments in the straight branch will use monochromatic as well as pink beams in the range 50 – 200 keV. The first hutch will accommodate the engineering materials applications presently being offered by Helmholtz-Zentrum Geesthacht (HZG) at the HARWI II station while the second hutch will be focusing on extreme conditions research using a large volume press.

In the arc, there will be three mini-undulator beamlines for small angle X-ray scattering (P62), X-ray µ-fluorescence (P63) and in-situ X-ray absorption spectroscopy (P65). A second XAFS beamline (P64) will be built using a 2 m long insertion device for flux limited applications such as time-resolved absorption studies (QEXAFS), diluted systems as well as biological XAFS. The specification of this device is a critical issue because of the need to offer a reasonably broad energy spectrum for QEXAFS scanning.

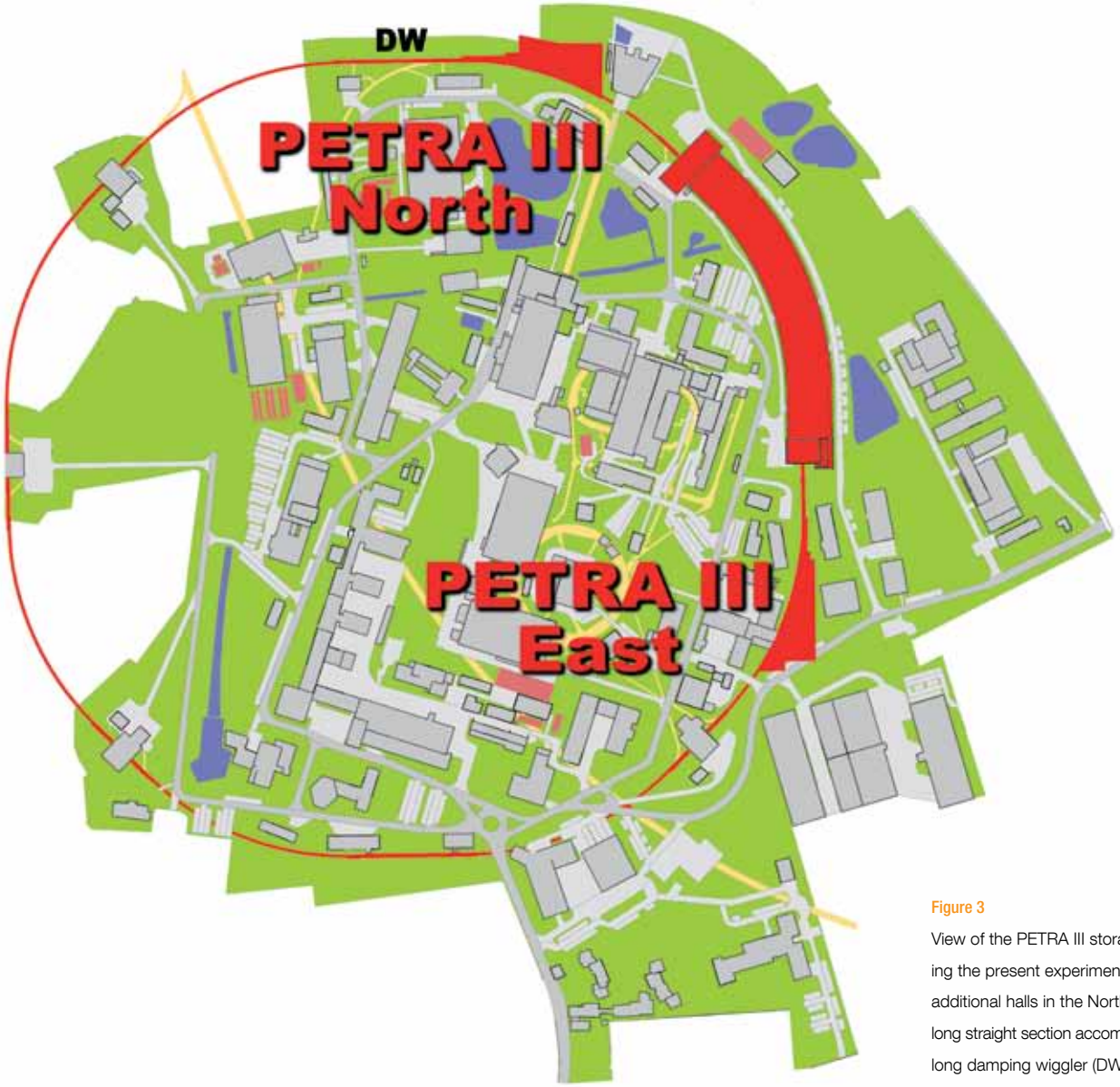

Figure 3
View of the PETRA III storage ring (red line) showing the present experimental hall and the planned additional halls in the North and East. The northern long straight section accommodates one of the 40 m long damping wiggler (DW) arrays.

In PETRA III East there will be two mini-undulator beamlines, one for chemical crystallography methods (P24) and another for education, training and testing purposes (P25). In addition, three full undulator beamlines are planned which will be built in collaboration with international partners, Sweden, India and Russia. The long straight section in the East (P21) is well suited to accommodate specialized long insertion devices such as a high-energy in-vacuum undulator and an optional additional high-k wiggler. The focus of this beamline will be on high-energy materials science applications in the range 50 – 200 keV and will be built in close collaboration with the Swedish materials science community. The two remaining short straight sections will be used to implement a nano-spectroscopy beamline (P22) and a beamline for nano-diffraction (P23) experiments.

The range of scientific applications, specification of techniques and requirements for instrument parameters are being discussed with the user community, the scientific advisory bodies and the international partners. In 2011, a second round of user workshops was held (see meeting reports in this book). Technical design reports for some beamlines will be finalized in spring next year and being discussed with international experts. The design of beamline frontend components will benefit from the work already been done for frontends of the current beamlines at PETRA III. The detailed technical design of the beamline optics and experimental area is expected to start in summer 2012.

According to the current schedule, the civil construction of the PETRA III extension will start in March 2013. During the machine modifications and the initial construction phase of the experimental halls, the storage ring cannot be operated and the user operation at PETRA III will pause. Every effort will be made to minimize this interruption. After the machine restart, the completion of the new facilities PETRA III North and East will continue in parallel. During the longer shutdown in 2013, the beamline frontends of the two XAFS beamlines will already be implemented while the remaining frontend installation will require additional short shutdowns in the following years. It is expected that the XAFS beamlines in PETRA III North will be available for users in summer 2014.

Contact: Wolfgang Drube, wolfgang.drube@desy.de
Klaus Balewski, klaus.balewski@desy.de

European XFEL.

On track building the world's most brilliant X-ray light source

The European XFEL, which will be the world's most brilliant light source for ultrashort X-ray pulses when operation starts in 2015, has successfully moved ahead in 2011. The civil construction of the facility as well as research and development of key parts for the machine have made good progress. In addition, European XFEL has been able to further strengthen its international network of research institutions and collaborations to exchange know-how and experience in the development of new technologies.

The European XFEL is one of the largest and most ambitious European research projects to date. The construction and operation of the European XFEL facility has been entrusted to a non-profit limited liability company under German law, the European X-Ray Free-Electron Laser Facility GmbH (European XFEL GmbH), which grew from 74 employees to more than 100 in 2011. At present, 12 countries are participating in the project: Denmark, France, Germany, Greece, Hungary, Italy, Poland, Russia, Slovakia, Spain, Sweden, and Switzerland. The shareholders are designated by the governments of the international partners and form the European XFEL Council, which decides on important issues related to the company and project. The main shareholder is DESY, representing Germany in the council. DESY and European XFEL collaborate on construction, commissioning, and operation of the 3.4-kilometre-long facility on the basis of a long-term agreement. Shareholders contribute the funds for the construction of the facility, either in cash or in-kind, i.e. by providing components built in their laboratories.

Half-time at civil engineering

By the end of 2011, the tunnel boring machines, TULA and AMELI, successfully completed more than 80 % of the tunnels tubes. At the beginning of August, TULA reached the injector building and finished the construction of the 2.1-kilometre-long linac tunnel, as shown in Fig.2. The smaller machine, AMELI, will continue boring until mid-2012, when it will complete the FEL tunnel segments under the Schenefeld site. In the meantime, construction of the injector building proceeded very well and the modulator hall was the second above-ground building of the facility to be completed, following the Accelerator Module Test Facility (AMTF) hall on the DESY site.

In-kind contributions and international cooperations

At present, the value of in-kind contributions accounts for about 50 % of the total project budget. At the end of 2011, more than 70 single contributions from eight partner countries have been proposed, of which 27 were already approved. Almost all contributions are related to the linac and injector complex constructed and operated by the Accelerator Consortium under DESY leadership. First components were delivered in 2011 and are currently being tested. A prototype accelerator module, which had been disassembled and then reassembled at CEA in Saclay, France, was delivered to the DESY site in Hamburg. It was mounted onto the first in-kind contribution delivered by a partner country, a test bench manufactured at the Budker Institute of Nuclear Physics (BINP) in Novosibirsk. During the autumn, the first segments of the helium transfer line required for testing the accelerator elements arrived from Poland.

In 2011, European XFEL further extended international cooperation by signing cooperation agreements with the leading Spanish high-power laser facility (CLPU) and the Brazilian synchrotron radiation laboratory (LNLS). A cooperation agreement was also signed with the University of Hamburg and a memorandum of understanding with the European Molecular Biology Laboratory (EMBL). As Europe's brightest X-ray source, the European XFEL is ideally suited for deciphering the structure and dynamics of biomolecules. In October, European XFEL joined the EU research network CRISP, a platform for 11 new international research infrastructures currently being planned or built. The cooperation is expected to contribute to the cost-effective and coordinated development of new key technologies in the relevant fields of accelerator technology, physics instrumentation and experiments, and detectors and data acquisition technologies.

Figure 1

First undulator segments from industrial production: Each five-metre-long segment contains two rows with 207 magnets and has a total mass of eight tons

Figure 2
The linac tunnel just after its completion. Tunnel builders are testing a special crane needed for the exact positioning of the 875 pre-fabricated supports for the concrete floor elements.

Other cooperations have also yielded initial tangible results: the Institute of High Energy Physics in Beijing built a prototype undulator segment that was delivered in spring 2011 and now being tested by European XFEL experts in Hamburg.

First pre-series undulators

In summer 2011, six pre-series prototype undulator segments from industrial production (four from Spain and two from Germany) which were ordered by European XFEL were delivered to Hamburg, as shown in Fig.1. After being successfully tested they will be the basis for the mass production of all 91 segments. Following measurements at SLAC and PITZ, an updated undulator layout was introduced in 2011. New parameters will lead to improved performance in the future: shorter wavelengths of down to 0.05 nanometres (previously 0.1 nm), and shorter pulses of just a few femtoseconds (previously 100 fs) will be possible to meet the needs of the future users even better.

R&D for detectors and instruments

Significant progress has been made in the development of the instruments that scientists from very different disciplines will use to carry out their research. Based on in-house developments and the knowledge gained through close association with the future user community, European XFEL scientists published conceptual design reports for four of the six instruments currently planned as well as for the beam transport systems. In the coming year, the conceptual design reports for the FXE, SPB, SQS, and MID scientific instruments will be elaborated in technical design reports scheduled for publication in 2012.
What makes the European XFEL unique is its extremely high pulse rate and peak brilliance. The X-ray pulses will be delivered in trains of 600 µs, each containing up to 2 700 pulses with a train repetition rate of 10 Hz. To leverage the unique qualities of the European XFEL, a detector R&D programme has been started to master the vast technological challenges in the fields of sensitivity, angular resolution, radiation hardness, detector area, and storage capacity. In 2011, the projects AGIPD (led by DESY), DSSC (led by MPI Halbleiterlabor) and LPD (led by Rutherford Appleton Laboratory) have passed a major review. First performance measurements with prototype sensors have been completed successfully.
European XFEL and DESY are collaborating closely in the field of photon diagnostics. The experience acquired at FLASH using gas-based monitor detectors for pulse-resolved measurement of intensity, beam position, and spectral content is particularly important. A prototype for hard X-rays has been built and will be tested using hard X-ray FEL radiation at the SPring-8 Angstrom Compact Free-electron Laser in Japan (SACLA). European XFEL is also cooperating with the P04 beam line team at PETRA III in the area of photoemission spectroscopy for future online wavelength and light polarization diagnostics. A third area of collaboration is the development of optical lasers for the experiments at FLASH and the European XFEL suitable for high repetition rates of up to 4.5 MHz and delivering very short and energetic pulses. To this end, the laser group at European XFEL has become operative and development of front-end, high-power burst-mode laser amplifiers is pursued with highest priority.

Contact: Massimo Altarelli, massimo.altarelli@xfel.eu

New Technologies and Developments.

“High-Z” pixel detectors.

Fast, efficient photon-counting detectors for hard X-ray experiments

Photon-counting pixel detectors, such as Pilatus and Maxipix, are the cutting-edge technology in a range of X-ray scattering and imaging experiments. These detectors have a “hybrid pixel” structure, where a pixelated silicon sensor is bonded to a readout chip that can independently process the signals from every pixel. The main weakness of this technology is that its use is currently limited to lower X-ray energies (typically below 25 keV), since the silicon sensor is near-transparent to high energy X-rays. By replacing the silicon with a semiconductor with a high atomic number (“high-Z”) it would be possible to extend this technology to hard X-ray experiments, and thus achieve a combination of excellent signal-to-noise performance, high quantum efficiency and high speed.

There are a range of high-Z semiconductors that could potentially be used in these photon-counting detectors, with germanium, cadmium telluride and gallium arsenide being particularly promising. However, each of these materials presents different technical challenges. Rather than committing ourselves to working with a single material, we have started collaboration projects with other institutes and companies developing different materials, so that we can quickly take advantage of whichever technology gives the best results. Additionally, working with high-Z semiconductors places special requirements on the readout chip and detector construction. We have contributed to the development of the new Medipix3 readout chip [1] and built our own prototype detector modules [2] so that these new sensors can be put to use in experiments as quickly as possible.

Germanium is widely used in detectors, and unlike other high-Z materials it is already available in large wafers of excellent quality. However, it has not previously been used in hybrid pixel detectors, for a number of practical reasons: it needs to be cooled during operation, it is relatively sensitive to high temperatures and chemical damage (which makes it difficult to bond it to a readout chip), and only a few companies and groups have the expertise needed to produce finely structured Ge detectors. In collaboration with the detector manufacturer Canberra (Lingolsheim) and Fraunhofer IZM (Berlin), a process for building germanium hybrid pixel detectors has been developed. Canberra have modified their existing strip detector technology to produce small pixels, and successfully manufactured a set of 10 test

Figure 1

CdTe pixel detector with 256 by 256 55 µm pixels, read out by a Medipix2 chip.

wafers (using cheaper optical grade germanium) with large arrays of 55 µm pixels. By using an indium bonding process at IZM, it will be possible to bond the sensors to readout chips without damage, and then operate them safely at low temperature. IZM is currently optimizing their bonding process using the test wafers. By taking advantage of this detector’s small pixel volume, and the Medipix3 readout chip’s high tolerance for leakage current, it will be possible to operate the finished detectors at relatively warm temperatures (estimated -60°C, rather than -192°C).

Another option for high-Z detectors is cadmium telluride. This is already used in single-element detectors and small arrays of large pixels, and provides high quantum efficiency even at extremely high energies. However, the largest wafer size currently available is small (3”), and the material often has nonuniformities [3]. As part of the HiZPAD consortium (an ELISA-funded collaboration between European synchrotrons and other institutes working with hard X-ray detectors) we have ordered and evaluated 1mm-thick CdTe pixel detectors based on the Medipix2 readout chip, which have a 256 by 256 array of 55 µm pixels [4]. The detector is shown in Fig. 1.

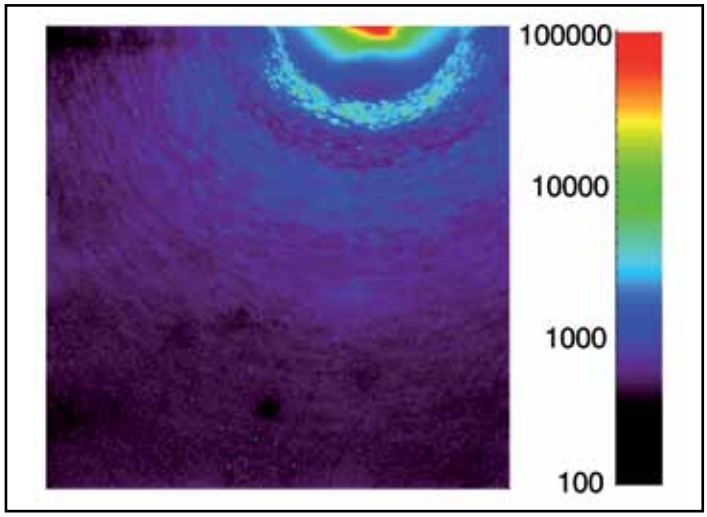

Figure 2

Image of the vicinity of the (030) Bragg peak of $LiMnPO_4$, taken during a 5s acquisition using a CdTe Medipix2 detector with 256 by 256 pixels. The logarithmic scale shows the number of counts accumulated in each pixel.

The CdTe sensor was tested on BW5 at DESY, using 100 keV beam. At this energy, 1mm-thick CdTe has an absorption efficiency of 57%. In flat-field beam tests, it was found that the detector has a number of clusters of insensitive pixels, corresponding to approximately 2000 pixels (3% of the total area). Some additional nonuniformities were seen on the sensor, due to grain boundaries in the material, but these could be successfully removed by flat-field correction.

The sensor was then used in a diffuse scattering experiment with $LiMnPO_4$ at 100 keV beam energy. By scanning the sample angle and detector position the scattered intensity was measured around the (030) Bragg peak. Fig. 2 shows the sum of 5 images (each taken for 1s), taken at a single angle and detector position. Interpolation was used to correct the insensitive pixels. A log scale is used in the figure, and it can be seen that the detector works effectively across a wide dynamic range. In this image, the background from scattered photons is approximately 100 counts, but the detector itself is sensitive to single photons. Due to these promising results, more of these CdTe sensors have been ordered.

A third collaboration project has been started, to produce gallium arsenide detectors. GaAs can operate at room temperature, and can be produced in large wafers, but it typically contains many lattice defects that degrade its detection performance. This project is a German-Russian partnership between DESY, FMF (Freiburg), KIT (Karlsruhe), JINR (Dubna) and RID Ltd. (Tomsk). The Russian partners have developed a method to improve the material qualities using chromium compensation [5]. FMF will bond the sensors to readout chips, and DESY and KIT will test the detectors and develop readout electronics.

Regardless of the sensor material used, a suitable readout chip and readout electronics are needed. DESY is a member of the Medipix3 collaboration, which is developing a new generation of readout chips that can be used in a variety of X-ray applications. DESY has contributed to the chip design by simulating different ways of implementing a “charge summing” function, which will improve the performance of high-Z sensors by compensating for charge-sharing and fluorescence within the sensor [6, 7]. We have developed a prototype detector module, LAMBDA (Large Area Medipix-Based Detector Array), which is compatible with silicon or high-Z sensors bonded to Medipix3 chips [2]. (This includes low-temperature operation with germanium.) The module has been designed to have a tileable layout, so that multiple modules can be combined to cover a large area. While the prototype module uses USB2 readout for test purposes, the finished module will take advantage of a high-speed readout board being developed by DESY FEA. Combined with the advanced features of Medipix3, this will allow the detector to work at frame rates of 2 kHz with zero dead time.

Contact: David Pennicard, david.pennicard@desy.de
Heinz Graafsma, heinz.graafsma@desy.de

References:

1. R. Ballabriga, M. Campbell, E. Heijne, X. Llopart, and L. Tlustos, “The Medipix3 prototype, a pixel readout chip working in single photon counting mode with improved spectrometric performance”, IEEE Trans. Nucl. Sci. 54 1824 (2007).
2. David Pennicard et al., “Development of LAMBDA: Large Area Medipix-Based Detector Array”, JINST 6 C11009 (2011).
3. D. Greiffenberg et al., “Characterization of Medipix2 assemblies with CdTe sensor using synchrotron radiation”, IEEE NSS conf. record, 287 – 290 (2008).
4. A. V. Tyazhev et al., “GaAs radiation imaging detectors with an active layer thickness up to 1 mm”, NIMA 509, 34-39 (2003).
5. D. Pennicard, R. Ballabriga, X. Llopart, M. Campbell, and H. Graafsma, “Simulations of charge summing and threshold dispersion effects in Medipix3”, Nucl. Instrum. Meth. A 636, 74 (2011).
6. D. Pennicard and H. Graafsma, “Simulated performance of high-Z detectors with Medipix3 readout”, JINST 6 P06007 (2011).

Collaboration:

DESY, the Medipix3 collaboration (http://medipix.web.cern.ch/medipix/), TU München, Canberra (Lingolsheim), Fraunhofer IZM, the HiZPAD consortium (http://hizpad.esrf.eu/), FMF, KIT, JINR, RID Ltd.

The Variable Line Spacing grating spectrometer at FLASH.

Spectral distributions online!

Online photon diagnostic tools that enable the determination of free-electron laser (FEL) photon beam properties like its intensity, spectral distribution or temporal structure in a non-destructive way are essential for gaining all information required for the user experiments at the beamline end. These diagnostic devices can help optimizing the FEL operation parameters and improving the interpretation of recorded data sets, respectively. Making use of two interchangeable plane diffraction gratings with variable line spacing (VLS), a spectrometer was designed and installed at FLASH which allows to measure spectral distributions over the full wavelength range (4-60 nm) of the FLASH photon pulses online [1]. The plane VLS grating reflects in grazing incidence most of the incoming radiation in 0^{th} order downstream to the experimental end-stations while 1^{st} order light is dispersed and focused onto a detector unit tangent to the focal plane of the dispersed beam (see Fig 1). In the actual detection unit scheme an intensified camera (ICCD) is used, imaging the fluorescence emitted from a Ce:YAG crystal placed in the focal plane. Following the focal curve the detector units' geometrical position gives information on the wavelength and the spectral distribution of the incoming photon pulse.

The spectrometer was cross-calibrated against the spectrometer at the end of the FLASH accelerator tunnel and the high-resolution monochromator installed at the PG beamline branch. Here a set of different known FLASH wavelengths was related to the corresponding detector position where the recorded spectra are well centered on the Ce:YAG crystal. The latter also has to be positioned correctly in the focal plane to ensure highest spectrometer resolution. In order to determine the proper detector position for a given FLASH wavelength, systematic scans of the detector unit in the two-dimensional parameter space have been performed. In addition the determined spectral linewidths of atomic absorption lines of rare gases were used for resolution optimization. These absorption lines occur as sharp dips within the natural bandwidth of the FEL spectrum as the photon beam is travelling through the gas-filled attenuator (installed in front of the VLS spectrometer).

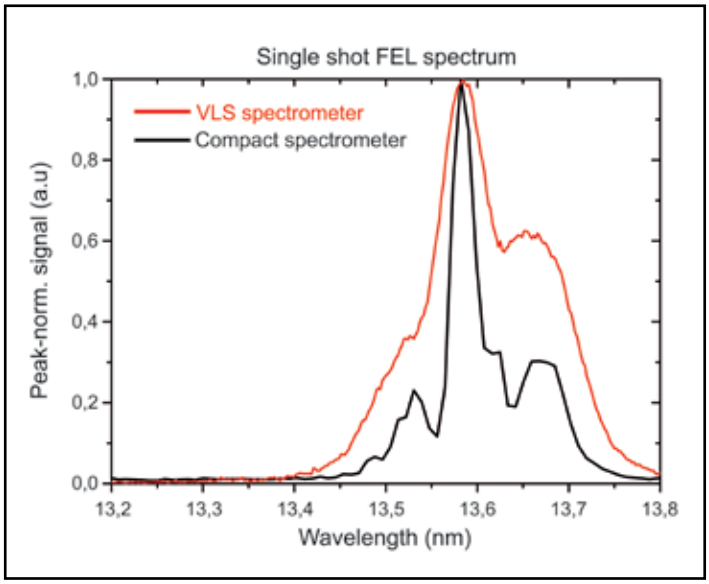

Figure 2

Comparison of a single shot FEL spectrum acquired with the VLS grating spectrometer (red) and with the compact spectrometer (black). The compact spectrometer was installed behind the users' experimental setup.

The spectrometer – although not fully calibrated at that time – was used during various user runs, recording spectra in parallel to the main experiment (see Fig. 2) and thus enabling users to include this spectral information on the FEL pulse in their data post-analysis, e.g. sort out data where the wavelength matches an atomic absorption resonance in the experiment. In addition it is also used as an online wavelength monitor by machine operators who can correct for potential wavelength drifts that way.

The implementation of the taken calibration data into the spectrometer control is about to be finished, making the device fully operational at FLASH. Shot to shot comparison with the calibrated compact spectrometer [2] which was recently commissioned at FLASH will allow to further optimize the performance and the resolution of the online VLS spectrometer.

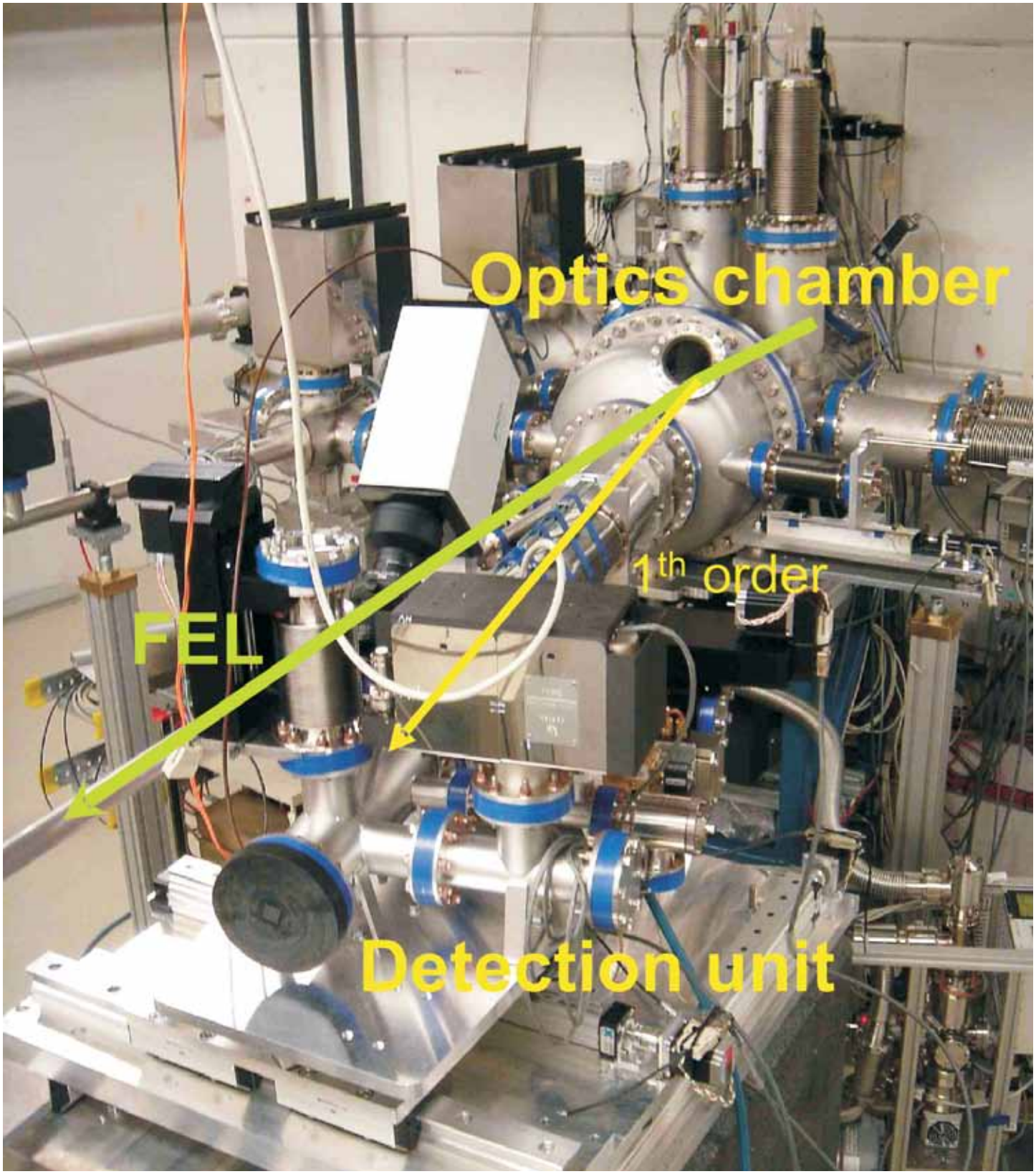

Figure 1

The VLS online grating spectrometer installed at FLASH.

Contact: Günter Brenner, guenter.brenner@desy.de
Svea Kapitzki, svea.kapitzki@desy.de

References:

1. G. Brenner et al., "First results from the online variable line spacing grating spectrometer at FLASH", NIM A 635, S99-S103 (2010).
2. F. Frassetto et al., "Compact spectrometer for photon diagnostics of the extreme-ultraviolet free-electron-laser radiation", NIM A 635, S94-S98 (2011).

The PETRA III Computing Model.

An integrated system for online control, data management and data processing

The PETRA III experiments created new computing challenges. In comparison to prior photon science facilities at DESY the PETRA III beamlines are longer, consist of more elements and use a greater variety of electronic devices. Modern 2D detectors came into operation generating high data rates that make data storage and data processing an issue. In addition, there is an increasing demand for more flexible user interfaces. This applies to scripting languages, the command line interface and graphical user interfaces. Therefore, a new online control system had to be designed and a concept for data management and data processing had to be developed. The main features of the resulting computing model are explained below.

Experiment control

The following issues have to be considered when designing an experiment control system:

- Sustainability: Modular systems with well-defined interfaces for hardware, communication and application layers can be extended and maintained by a group of programmers.
- Flexibility: User groups change frequently at the beamlines. In general, they have specific requirements for their experimental procedures. Hence, an efficient customization of the system is important to make the best use of the beamtime.
- Platform independence: Linux and Windows have to be supported. Bindings to scripting and programming languages are mandatory.
- Performance: An online control system needs sufficient bandwidth to handle motors, counters, timers, etc. However, 2D detectors, creating by far the highest data rates, do not use the control system for data transfer but access storage media directly.

Ideally an online control system is based on a product that is supported by an international community. Resources are saved by sharing the software among the partners. The communication inside the collaboration about new ideas and experiences is of equal importance. Finally, collaborations are the only way to develop common user interfaces which are so important for travelling scientists.

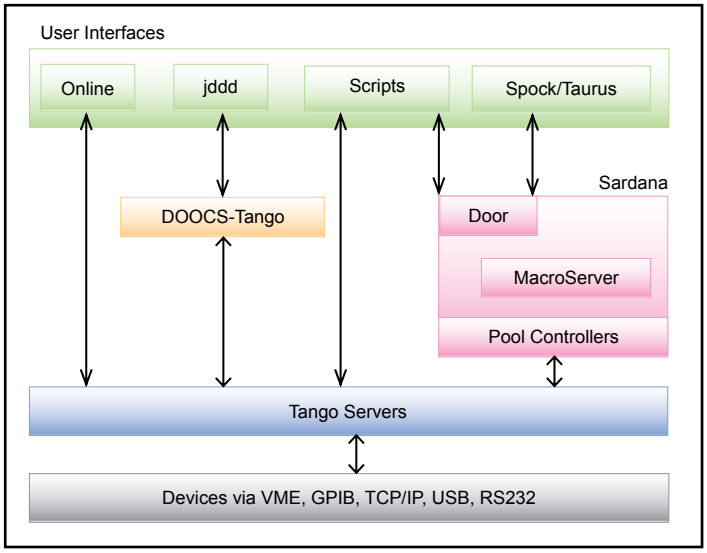

Figure 1

The main components of the experiment control system.

Figure 1 gives a schematic view of the PETRA III experiment control system. It consists of several layers: the hardware busses, the network-communication and the clients. Devices are connected via: VME, GPIB, TCP/IP, USB and RS232. Tango [1] exports the devices to the network. Clients can communicate directly to the Tango device servers or make use of the additional functionality provided by the Sardana [2] framework.
Online is a general purpose experiment control program that operated many DESY beamlines for a long time. It has been made Tango-compliant for the experiments at PETRA III. Online has a command line interface, a binding to Perl and a graphical user interface.
Python scripts using PyTango [3] have been written by scientists shortly after the PETRA III operation began. PyTango is a Python module which exports the complete c++ Tango API to Python. jddd [4] applications exist for every beamline. They display selected variables for a quick overview of the whole setup. jddd has a hierarchical structure with several expansion levels which makes it possible to organize the displayed information in a convenient way.

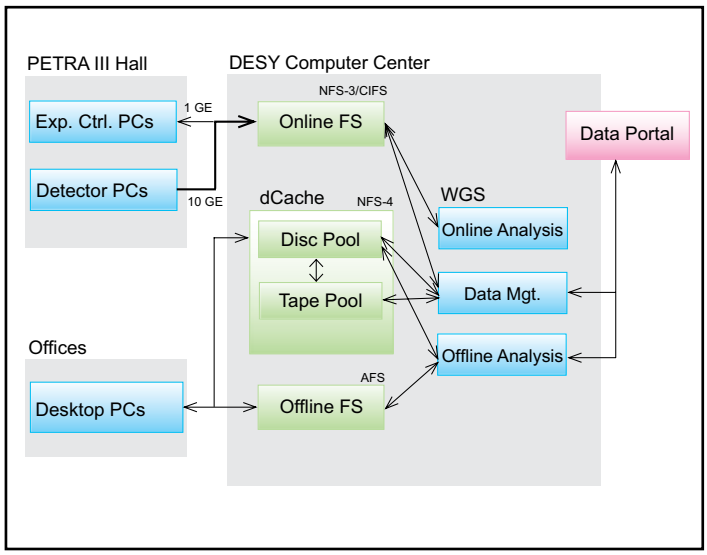

Figure 2

Data flow paths.

Sardana was created at ALBA with important contributions coming from the ESRF. It is a framework consisting of the device pool, the MacroServer, Spock and Taurus. The device pool is an additional standardization layer. The MacroServer organizes the execution of procedures during measurements. Spock is a command line interface and Taurus creates graphical user interfaces. In the meantime DESY participated in this project and added some extensions. Sardana has been rolled out to the PETRA III experiment PCs. First applications are in use.
To allow users to work with data collected at different beamlines at the same or different facilities a standard data format is mandatory. NeXus [5] has been selected to be the future file format for PETRA III following the recommendations of HDRI [6] and PANDATA [7]. It will permit to aggregate data files from different sources into a portable and self-describing form.

Data management

Figure 2 gives an overview of the data flow paths. The PETRA III experiments send their data to the online file server which serves as a buffer to make the data available for near real time analysis. All data are archived in the dCache [8] tape pool. Data to be analysed are staged to the dCache disk pool. In addition there is an offline file server for storing analysis results and temporary data. A blade centre which is divided into 16 workgroup servers provides the necessary computing power. The workgroup servers are allocated to specific purposes like online analysis, data management and offline analysis. The online file server consists of 2 server systems, each one with 2 heads which allow for a takeover option. The servers are set up as raid-6 storage systems with a snapshot option of 20% of the total space. The total capacity of the online file server is 145 TB. It is divided into volumes which are assigned to specific beamlines. The file and compute services are provided by the DESY computer centre.
It is expected that certain guest groups do not have sufficient IT infrastructure at their home institutes to store and process large data volumes. DESY plans to support these scientists by providing them with storage and computing services. A data portal is currently being prepared that facilitates access to the dCache and permits the full remote management of the data, which includes the search for data and meta-data and a user controlled right management.

Conclusion

PETRA III computing integrates the activities from national and international partners. This approach saves resources and enhances the communication on the relevant topics which is crucial for the fast and continuous incorporation of new developments. Furthermore, collaborations among synchrotron radiation facilities are the precondition for establishing common user interfaces. Achieving this goal would ease the burden of our scientific users in performing measurements at different facilities. It has been demonstrated that the experiment control system is flexible enough to fulfil the current requirements and to cope with future challenges.

Contact: Thorsten Kracht, thorsten.kracht@desy.de
Teresa Núñez, maria-teresa.nunez-pardo-de-vera@desy.de
André Rothkirch, andre.rothkirch@desy.de
Frank Schlünzen, frank.schluenzen@desy.de

References:

1. Tango Control System http://www.tango-controls.org.
2. J. Klora, T. Coutinho et al., “The architecture of the ALBA Control System”, Proceedings NOBUGS (2008).
3. PyTango, http://www.tango-controls.org/static/PyTango/latest/doc/html/index.html.
4. Jddd, A Java DOOCS Data Display, http://jddd.desy.de.
5. NeXus, http://www.nexusformat.org.
6. HDRI, High Data Rate Initiative for Photons, Neutrons and Ions, http://www.pni-hdri.de/.
7. PANDATA, Photon and Neutron Data Infrastructure, http://www.pan-data.eu/.
8. dCache, http://www-dcache.desy.de.

A compact high vacuum heating chamber for X-ray scattering.

Studying structural changes

Modern synchrotron radiation sources such as PETRA III offer the possibility to study not only samples under static conditions but also allow in-situ studies of dynamic systems. Such experiments require special sample setups with full optical access to the sample by X-rays.

The compact high vacuum heating chamber was designed to allow sample heating under high vacuum conditions or gas atmospheres up to 1bar to study temperature induced phase transitions, oxidation processes as well as catalytic processes on surfaces and thin films by (grazing incidence) X-ray diffraction and X-ray reflectivity. Such chambers are usually quite bulky. The new heating chamber was designed to fit into the high precision Kohzu diffractometer at the high resolution X-ray scattering beamline P08 at PETRA III. This diffractometer has a very compact design with only 38 mm maximum space between the sample goniometer and the centre of rotation of the diffractometer. Thus, a compact design is also required for the high vacuum chamber.

The chamber is composed of four main parts: 1) the chamber body based on a DN63CF flange with four DN16CF flange connections, 2) the water cooled copper cooling shield, 3) the sample stage consisting of a copper block with a resistive heating wire, and 4) a hemispherical Beryllium dome covering the chamber. Beryllium has the lowest X-ray absorption coefficient and is therefore extremely well suited to be used as window material for X-rays. The hemispherical shape gives full access to the sample surface, which is required especially for grazing incidence X-ray diffraction experiments.

First in-situ experiments on the reduction of iron oxide thin films have successfully been performed using the high vacuum

Figure 1

Sketch of the high vacuum heating chamber.

Figure 3
Experimental hutch of the high resolution X-ray diffraction beamline P08 at Petra III

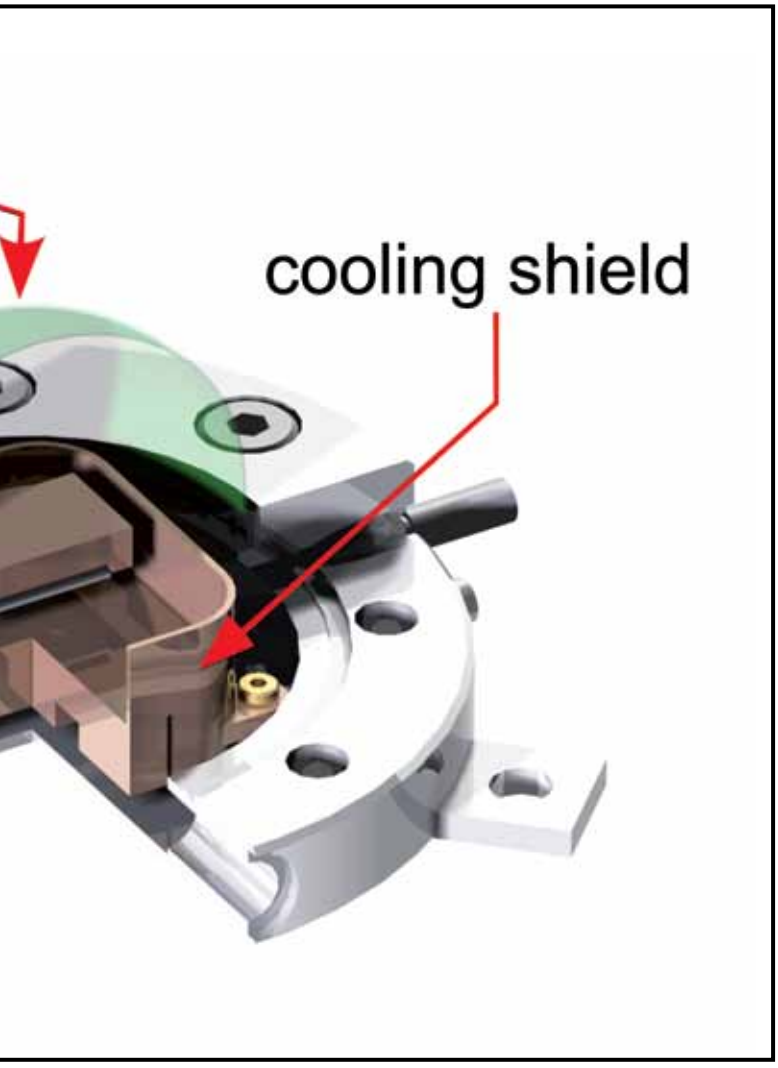

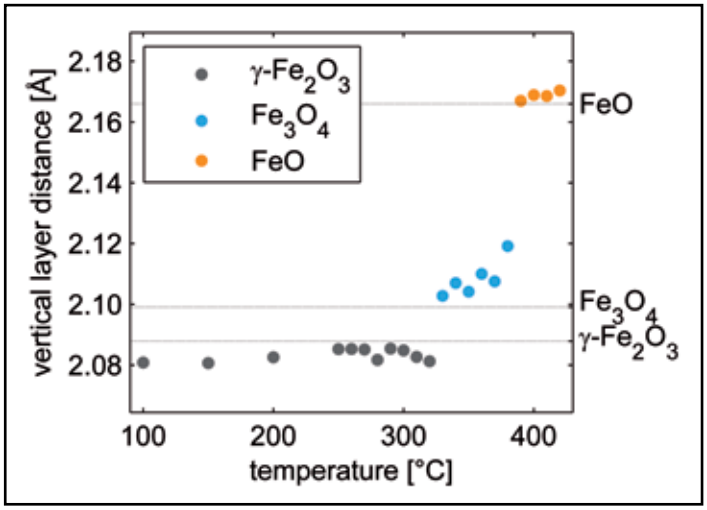

Figure 2
Evolution of the vertical layer distance during the heating of a maghemite thin film

chamber. During the heating of a maghemite (γ-Fe_2O_3) film - grown on magnesium oxide - in high vacuum, X-ray diffraction scans along the specular crystal truncation rod were performed. From these scans it was possible to obtain the evolution of the vertical atomic layer distance of the iron oxide film. The increase of the vertical layer distance indicates a reduction of the iron oxide film occurring in two steps with a first reduction from maghemite to magnetite (Fe_3O_4) around 360°C and a second reduction from magnetite to wuestite (FeO) which is completed around 410°C.
The chamber is now available for user experiments at the P08 beamline requiring a high vacuum setup.

Contact: Florian Bertram, florian.bertram@desy.de

Hard X-ray nanoprobe at PETRA III.

A scanning microscope with spatial resolution down to 10 nm

A key strength of hard X-rays is their large penetration depth in matter, allowing one to image the interior of an object without destructive sample preparation or to investigate a specimen inside a special sample environment, such as a chemical reactor or a pressure cell. In combination with tomography, the three-dimensional inner structure of an object can be reconstructed. In addition, in scanning microscopy a variety of X-ray analytical techniques can be used such as X-ray fluorescence, absorption, and diffraction techniques. In this way, the elemental composition, the chemical state of a given element, or the local nanostructure of the sample can be imaged with high resolution. X-ray microscopy finds application in many fields of science, ranging from nanotechnology, physics, and chemistry to biomedical, earth, and environmental science. X-ray microscopy techniques have greatly benefited from the ever increasing brilliance of modern synchrotron radiation sources. Therefore, PETRA III is particularly well suited to host a hard X-ray scanning microscope.

Starting 2012, the hard X-ray nanoprobe station of beamline P06 at PETRA III takes up its user operation. It was developed, built, and commissioned over the last three years in collaboration with Technische Universität Dresden. Figure 1 shows the scanning microscope that is located at the far end of the beamline about 100 m from the source. It is designed to provide a stable hard X-ray beam with lateral dimensions well below 100 nm [1]. It is based on nano-focusing refractive X-ray lenses (NFLs) [2, 3], but can also accommodate other nano optics, such as Fresnel zone plates [4] or multilayer Laue lenses [5].

The scanning microscope offers different contrast mechanisms, such as fluorescence, absorption, small- and wide-angle scattering. In addition, the instrument is well suited for coherent X-ray imaging techniques with a nanobeam [6], and ptychography is routinely available. In this latter scanning coherent diffraction microscopy technique the sample is scanned through the diffraction-limited nano beam. At each position of the scan, a far-field diffraction pattern of the sample is recorded [7].

Figure 1

Hard X-ray scanning microscope at P06 (nanoprobe station).

From these data, both the object and the illuminating beam can be reconstructed with a spatial resolution well beyond that given by the beam size [8, 9]. This is illustrated in Fig. 2 that shows a scanning micrograph of a tantalum test pattern (NTT-AT) recorded at 15.25 keV with a nano beam [lateral size 80 nm full width at half maximum (FWHM)]. A region of 2 x 2 μm^2 is scanned in steps of 50 x 50 nm^2. While Fig. 2a) depicts the Ta fluorescence map, Fig. 2b) shows the phase shift of the transmitted X-rays in the test object as reconstructed from the ptychographic data. While the focus size limits the resolution in conventional scanning microscopy, ptychographic imaging yields spatial resolutions well below the diffraction limit of the nanofocusing optic. In our microscope, ptychographic images with spatial resolutions down to about 10 nm were obtained for strongly scattering objects.

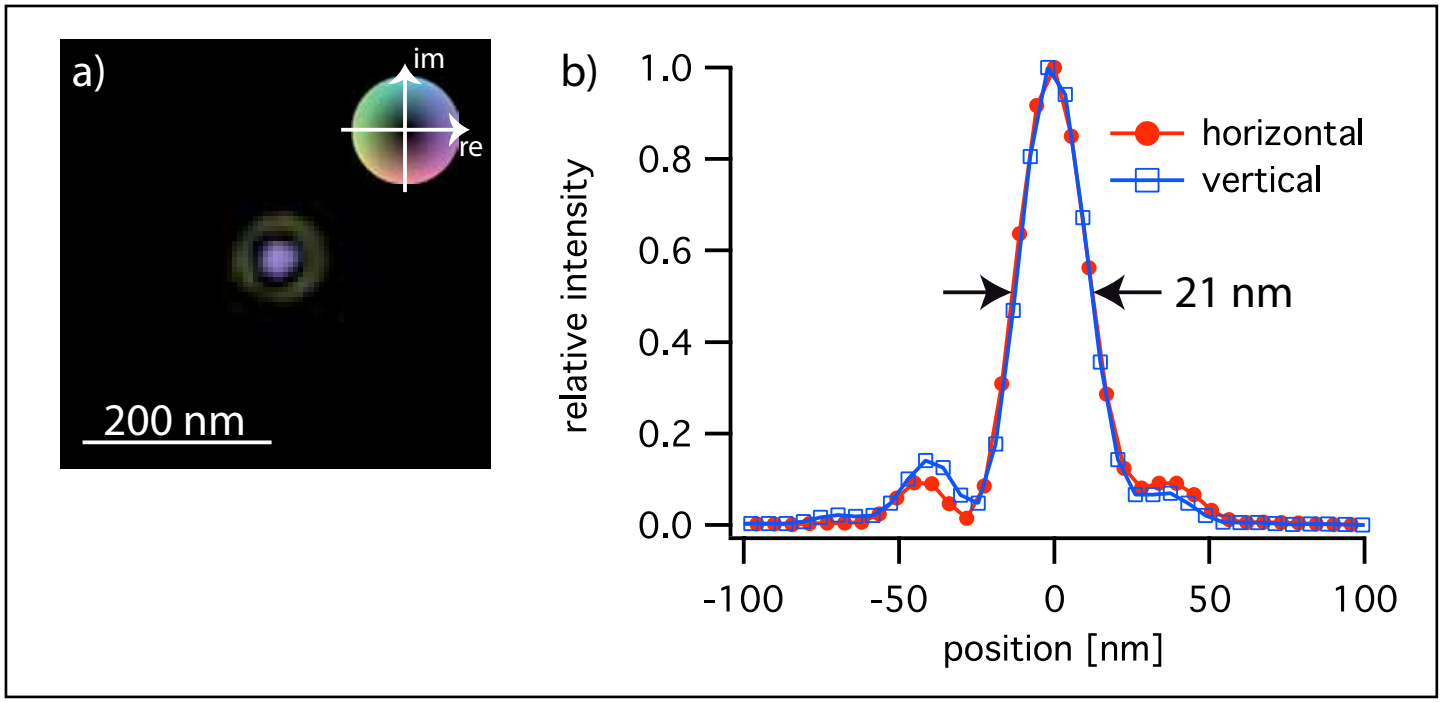

Figure 3

a) Complex X-ray wave field in the focus of a Fresnel zone plate at 10 keV. The complex phase is coded according to the colour wheel. b) Horizontal and vertical line profile of the intensity in the focus. The FWHM beam size is 21 nm.

In order to improve the spatial resolution in conventional scanning microscopy, X-ray optics with higher numerical apertures are needed. This calls for improved refractive lenses [2, 3, 10], Fresnel zone plates [4], or multilayer Laue lenses [5]. As an example, a zone-doubled Fresnel zone plate made at the Paul Scherrer Institute was tested [4] (diameter D = 150 µm, outermost zone width dn = 25 nm). It was used to focus 10 keV X-rays to a focal point about 30.3 mm behind the optic. A ptychogram of the Ta test pattern was recorded, yielding the complex wave field in the focus shown in Fig. 3a). A line profile through the intensity in the focus is shown in Fig. 3b), demonstrating a 21 nm FWHM beam size.

Contact: Christian G. Schroer, christian.schroer@tu-dresden.de
Gerald Falkenberg, Gerald.falkenberg@desy.de
Christian David, Christian.david@psi.ch.

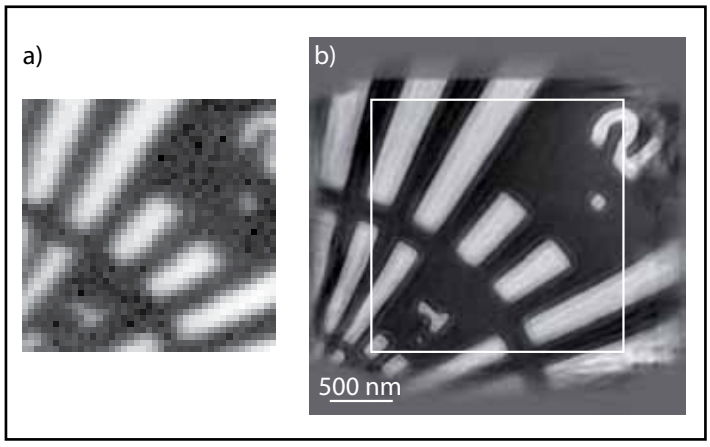

Figure 2

X-ray scanning micrograph of a test structure made of tantalum (NTT-AT).
a) Ta fluorescence map recorded over a field of view of 2 x 2 µm^2 in steps of 50 nm.
b) reconstructed ptychogram recorded simultaneously with the fluorescence data. The rectangle delineates the scanned area

References:

1. C. G. Schroer et al., Nucl. Instrum. Meth. A 616, 93 (2010).
2. C. G. Schroer et al., Appl. Phys. Lett. 82, 1485 (2003).
3. C. G. Schroer et al., Appl. Phys. Lett. 87, 124103 (2005).
4. J. Vila-Comamala et al., Ultramicroscopy 109, 1360 (2009).
5. H. C. Kang et al., Phys. Rev. Lett. 96, 127401 (2006).
6. C. G. Schroer et al., Phys. Rev. Lett. 101, 090801 (2008)
7. J. M. Rodenburg and H. M. L. Faulkner, Appl. Phys. Lett. 85, 4795 (2004).
8. P. Thibault et al., Science 321, 379 (2008).
9. A. Schropp et al., Appl. Phys. Lett. 96, 091102 (2010).
10. C. G. Schroer, B. Lengeler, Phys. Rev. Lett. 94, 054802 (2005).

FLASH beam characterization from measurement of the Wigner distribution.

Phase-space tomography yields spatial coherence

FEL applications require in some cases a beam characterization beyond standard techniques as e.g. caustic measurements, beam profiling or wavefront sensing [1]. In particular for partially coherent sources the consideration of 2nd order correlations is mandatory for reliable beam propagation or for the design of complex optical systems. Regarding the emission of SASE-type FELs, the stochastic nature of the beam generation and amplification process influences the spatial coherence properties, as predicted by theory and supported by experimental investigations [2]. However, the experiments carried out so far are based on Young's double slit experiment and investigation of the corresponding two-beam interference patterns, which is extremely time-consuming if the entire four-dimensional representation space has to be mapped. In contrast, the Wigner distribution [3], being a two-dimensional Fourier transform of the mutual intensity, can be fully reconstructed from two-dimensional intensity profiles of the beam via tomography, using refractive and/or reflective optics exclusively [4]. In particular, the 2D Wigner function can be computed from a set of standard beam profile measurements taken at several z-positions along the beam path in the vicinity of the waist [5].

Fig. 1 shows the setup employed for beam caustic measurements at FLASH BL2.

The experiment is described in detail elsewhere [6]. A carbon-coated ellipsoidal mirror focuses the beam to approximately 20 µm FWHM. Optimum alignment of the mirror was achieved by minimizing its wavefront aberration, as detected with a EUV Hartmann sensor installed in the FEL beam. The caustic sensor, a phosphorous screen imaged onto a CCD chip by a 10x magnifying microscope on a linear translation stage, senses the beam near the focal plane of the ellipsoidal mirror. Beam profile measurements were taken at 32 z positions within an interval of 124 mm evenly distributed around the beam waist and covering approximately 2.5-3 Rayleigh lengths (z_R) [7] in both axial directions.

For reconstruction of the Wigner function h each two-dimensional record is separately integrated over x and y, delivering the one-dimensional marginal distributions e.g. $I_{x,z}$. The latter are Fourier transformed ($I(x) \rightarrow \tilde{I}(w)$) and then mapped into two-dimensional sub-spaces according to $\tilde{I}_{x,z}(w_x) \rightarrow \tilde{h}_{x,z=0}(w_x, z \cdot w_x)$, for the horizontal and vertical direction, respectively. Finally, the Wigner function is obtained as $h = h_x \cdot h_y$ from the inverse Fourier transforms of the 2D sub-spaces.

Fig. 2 shows beam profiles of FLASH for five positions around the waist. Apart from the hyperbolic expansion of the diameter, the beam shows a smooth intensity distribution near the waist and obviously develops a horizontal modulation when approaching the far field region. Results of the beam parameter evaluation shown in table 1 yield an average beam propagation factor M^2 [7] of 4.14 and 2.93 as well as a global degree of coherence K [5] of 0.29 and 0.36 for horizontal and vertical direction, respectively. Furthermore, the rms wavefront aberration w_{rms} at waist was determined to approximately 0.4 nm.

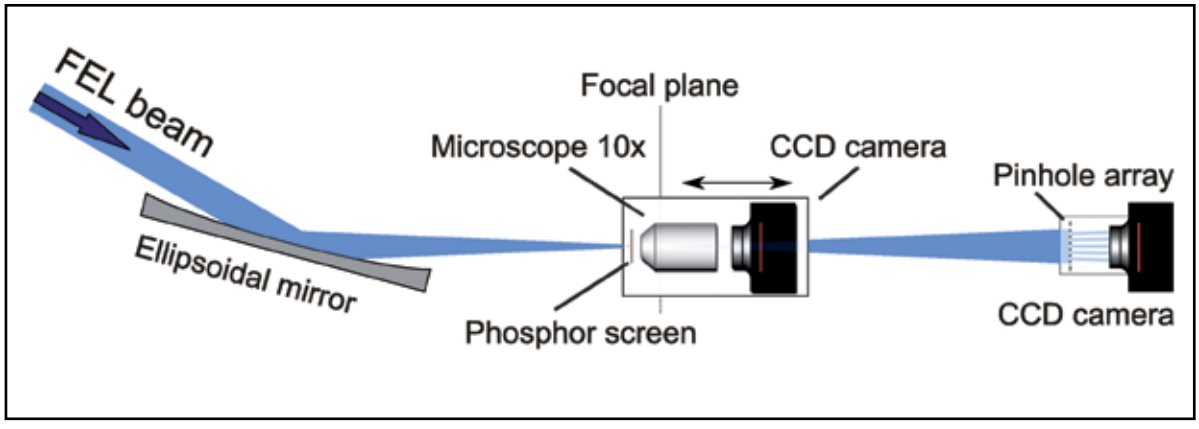

Figure 1
Experimental setup for measurement of the 2D Wigner distribution of the FLASH beam at BL2.

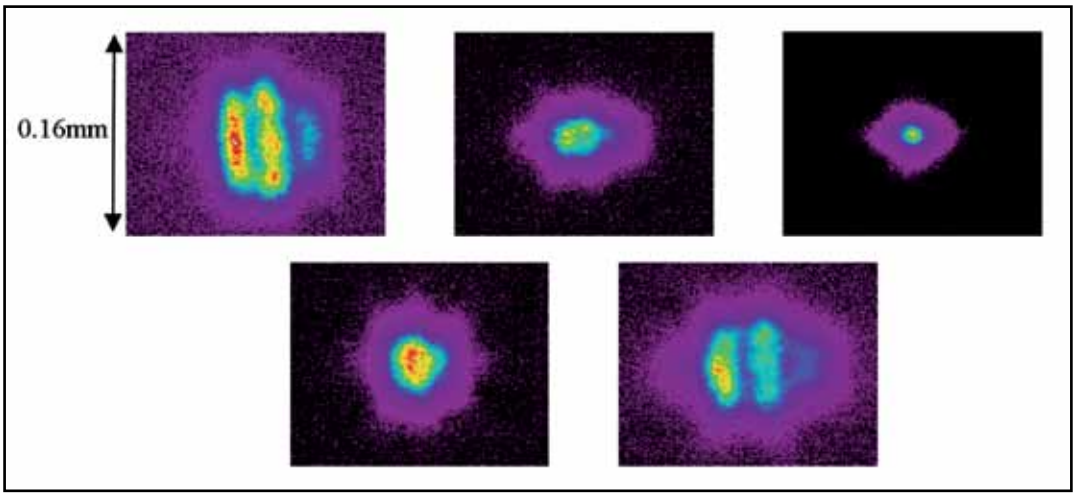

Figure 2
FLASH irradiance profiles in the vicinity of the beam waist of BL2 at five positions separated longitudinally by 30 mm.

Regarding the small value of w_{rms}, the reduced beam quality (M^2 ~ 3 - 4) is mainly a consequence of the low spatial coherence rather than being induced by wavefront aberrations, the latter being dominated by astigmatism. In concordance with the reduced global degree of spatial coherence the modal spectrum evaluated from the Wigner function contains a considerable amount of uncorrelated higher order modes (cf. Fig. 3).

M_x^2 / M_y^2	4.14 / 2.93
z_{Rx} / z_{Ry} [mm]	27.6 / 19.4
d_{0x} / d_{0y} [mm]	0.04 / 0.028
z_{0x} / z_{0y} [mm]	56.8 / 68.8
w_{rms} [nm]	0.43
K_x / K_y	0.29 / 0.36

Table 1:
Beam parameters M^2, Rayleigh range z_R, waist diameter d_0, waist position z_0, rms wavefront deformation w_{rms} and global degree of coherence K from numerical reconstruction of the Wigner distribution for FLASH.

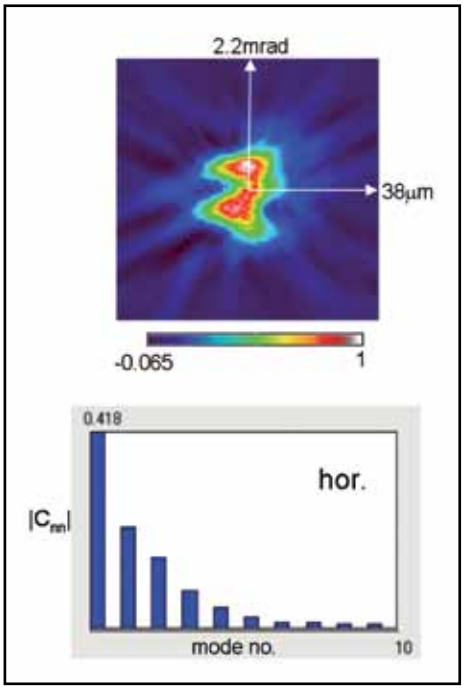

Figure 3
(above): Wigner distribution h as a function of spatial (x) and angular coordinate (u); below: spectrum of the first ten Hermite-Gaussian modes of FLASH for the horizontal direction.

The results clearly show that a valuable amount of information, especially on spatial coherence properties, can be gained from reconstruction of the Wigner distribution of an FEL beam, even for a reduced data set originally recorded for the purpose of standard beam parameter estimation only. However, this does no longer hold in the presence of considerable wavefront aberrations or more complex mode content. In those cases a proper characterization of partially coherent beams requires a full four-dimensional approach. In particular, when coherence properties of the beam are of major importance, the comprehensive information gained from four-dimensional measurements may outweigh the higher experimental effort. Taking this into consideration, more accurate measurements of the Wigner function of FLASH are planned for the future.

Contact: Bernd Schäfer, bernd.schaefer@llg-ev.de
Kai Tiedtke kai.tiedtke@desy.de

References:

1. **B. Flöter et al., "Beam parameters of FLASH beamline BL1 from Hartmann wavefront measurements", Nucl. Instr. and Meth. A, doi:10.1016/j.nima.2010.10.016 (2010).**
2. **A. Singer et al., "Transverse-Coherence Properties of the Free-Electron-Laser FLASH at DESY", PRL 101, 254801 (2008).**
3. **B. Eppich et al., "Measurement of the four dimensional Wigner distribution of paraxial light sources", in Proc. SPIE 5962-2, D1-D11 (2005).**
4. **B. Schäfer et al., "Characterization of an ArF excimer laser beam from measurements of the Wigner distribution function", New J. Phys., 13 043013 (2011).**
5. **B. Schäfer et al., "FEL beam characterization from measurements of the Wigner distribution function", Nucl. Instr. and Meth. A, doi:10.1016/j.nima.2011.07.031 (2011).**
6. **B. Flöter et al., "EUV Hartmann sensor for wavefront measurements at free-electron laser FLASH", New J. Phys. 12, 083015 (2010).**
7. **ISO 11146-1,2,3, Lasers and laser-related equipment – Test methods for laser beam widths, divergence angles and beam propagation ratios, International Organization for Standardization (ISO), Geneve (2004/2005)**

Collaboration:

DESY, Laser-Laboratorium Göttingen e.V.

Brillouin spectroscopy and micro X-ray diffraction at PETRA III.

A powerful “tandem” to determine the elastic properties of mantle minerals

Our knowledge of the structure is largely based on geophysical probes from the surface of the earth such as seismology. The arrival time of seismic waves from the source of an earthquake to the seismic stations, and the waveform (peak amplitudes) of seismograms tell us about the average viscoelastic properties and spatial arrangement of the materials that constitute the inner shells of our planet. The thorough analysis of large sets of seismograms makes it possible to construct seismic velocity models of the deep Earth interior. The interpretation of the seismic velocity models in terms of composition of the Earth is heavily dependent on our knowledge of the elastic properties of minerals at pressures and temperatures experienced in the Earth’s interior. The elastic properties can be determined by measuring Brillouin scattering in a diamond anvil cell (DAC). Such measurements provide sound wave velocities of single crystals or powders as a function of pressure when the density of the mineral from X-ray diffraction are known. Below we describe the first step to establish a “tandem” experimental setup that is being built at PETRA III and will allow scientists to independently measure both acoustic velocities using Brillouin scattering and densities using x-ray diffraction at the same experimental pressure and temperature conditions by simply transferring the DAC from the Extreme Conditions Science Infrastructure (ECSI) laser lab to the adjacent Extreme Conditions Beamline (ECB, P02.2). This powerful “tandem” combination, unique in Europe, is crucial to develop compositional models consistent with the average seismic velocities in the earth mantle. This is a joint project between the Deutsches Geo-Forschungs-Zentrum Potsdam GFZ and DESY.

Brillouin scattering is the inelastic scattering of laser light (‘photons’) by thermally activated lattice vibrations (‘phonons’). The amount of the energy shift of the inelastically scattered light compared to the elastic line position is proportional to the sound wave velocities of the sample.

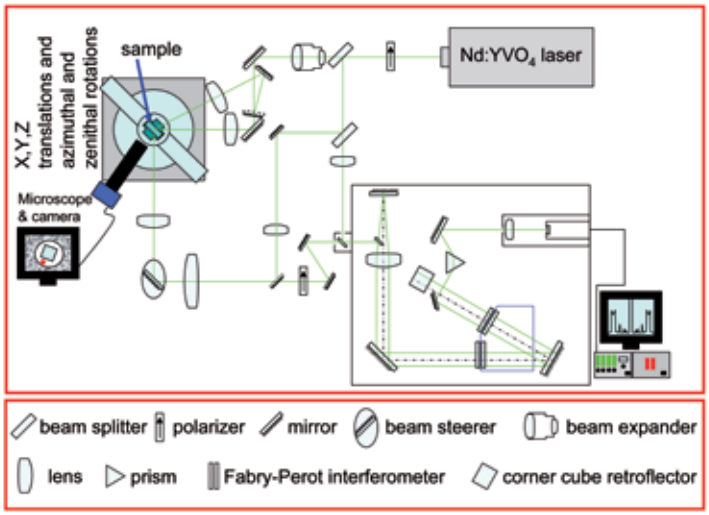

Figure 1

Schematic diagram of the Brillouin set up.

Figure 2

The new Brillouin scattering system at the laser lab of the ECS Infrastructure (ECIS) of PETRA III is based on a large diameter Eulerian cradle (400 mm) that will allow the users to perform experiments using large sample holders required when using externally heated DACs.

Fig. 1 illustrates a schematic diagram of the Brillouin set up built at PETRA III. The prominent features are the laser with an etalon, the Eulerian cradle that holds the diamond anvil cell with the sample and the 6 pass Tandem Fabry – Perot interferometer. A laser beam (Nd:YVO4 Verdi ™ by Coherent, 532 nm wavelength) is focused on the sample. The scattered light is further focused on the entrance pinhole of the Fabry – Perot interferometer.

To obtain the full elastic tensor C_{ij} from measurements of single crystals it is necessary to rotate the DAC about the χ- axis of the cradle. The Brillouin system at PETRA III is designed in such a way that two experimental geometries with 90° and 50° scattering angle are available.

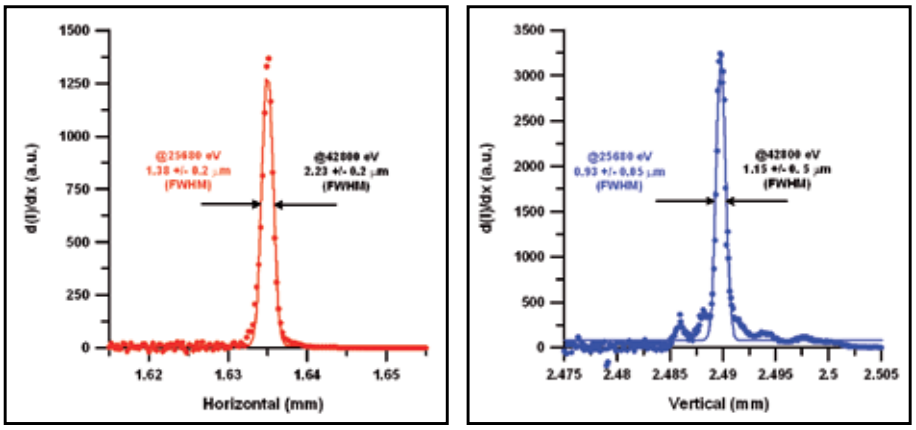

Figure 4

X-ray focus at the ECB achieved with a pair of 320 mm Kirkpatrick-Baez mirrors and without a clean-up slit.

The ECB offers the possibility to perform high pressure diffraction experiments up to multi Mbar pressure due to its small focus of 2 (H) x 1 (V) μm^2 at 42.8 keV with 6 x 10^{11} ph/sec in the focal spot and a divergence of 6 (H) and 0.6 (V) $mrad^2$ (Fig. 4). The

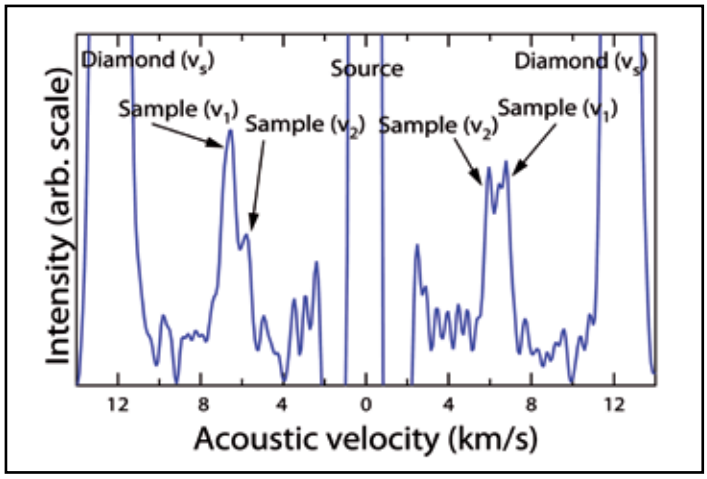

Figure 3

A first Brillouin scattering spectrum of a sample of natural clintonite loaded in the diamond-anvil cell.

combination of these experimental capabilities – optical Brillouin spectroscopy in the laser lab and X-ray diffraction on the very same sample at the ECB – will produce exciting new results on the elastic properties of material at high pressure.
The power of combining Brillouin scattering and synchrotron X-ray diffraction was recently demonstrated by two studies of nano-crystalline MgO [1,2]. In this study we conducted multiple compression experiments and measured both X-ray diffraction and Brillouin scattering at several pressures up to a maximum of 65 GPa and found clear indication that the bulk compressibility of nc-MgO is enhanced compared to bulk MgO, i.e. nc-MgO is "softer". The comparison of our new data to high-pressure sound wave velocity measurements on the same material using Brillouin spectroscopy provides insights into the distinct contributions of both the crystalline and the inter-crystalline fractions within nano materials to the overall elastic response. By using both data sets, we provide first quantitative constrains on the compressibility of the crystalline cores and the intercrystalline material to high-pressures.

The Brillouin measurements on nano-crystalline MgO were conducted on the Brillouin system located at the GFZ and X-ray diffraction at the ECB. We have recently completed the basic installation of the Brillouin scattering system at the ECSI and performed test measurements of Brillouin scattering on a single-crystal of natural clintonite [$CaMg_{2.29}Al_{0.59}Fe_{0.12}(Si_{1.2}Al_{2.8})O_{10}(OH)_2$], a calcium-rich member of the layered silicates (phyllosilicates) family, such as serpentine that plays a critical role in earthquake generation associated to the dynamic behaviour of colliding tectonic plates. The tiny 100 µm-wide crystal platelet was loaded in a Boehler-Almax DAC with a total optical access of 70°. The measurements were performed in forward symmetric scattering geometry with a scattering angle equal to 50°. The laser ran at a power of 270 mW. The spectrum in Fig. 3 shows both the shear modes of the diamonds (<vs> = 12.30 ± 0.02 km/s), and two modes of the sample v1 = 6.65 ± 0.05 km/s and v2 = 5.8 ± 0.1 km/s.

Outlook

The newly built Brillouin system has a Eulerian cradle that can accommodate wire resistive heated DACs (maximum temperature ~ 900 °C). This will allow us to explore the evolution of the elastic properties of materials to high pressures and/or high temperatures, including the effects of phase transitions. The complete Brillouin system setup will also include a laser heating system (IR solid state laser, wavelength 1064 nm, 100 W max output power) and a Raman spectroscopic setup. The Brillouin scattering system in its full capability will access temperatures in the range of 25 - 2500 °C.

Contact: Sergio Speziale, speziale@gfz-potsdam.de
Hans Josef Reichmann, hanni@gfz-potsdam.de
Hauke Marquardt, hama@gfz-potsdam.de
Hanns-Peter Liermann, hanns-peter.liermann@desy.de

References:

1. **H. Marquardt et al. "Elastic properties of MgO nanocrystals and grain boundaries at high pressures by Brillouin scattering", Phys. Rev. B, 84, 6, 064131 (2011).**
2. **H. Marquardt et al., "The effect of crystallite size and stress condition on the equation of state of nanocrystalline MgO", J. Appl. Phys, 110, 113512, (2011).**

A 2nd generation transfocator.

An automated lens changer for 1D and 2D parabolic Beryllium compound refractive lenses

Focusing devices have become standard equipment at beamlines of modern synchrotron sources. Over the last years 'transfocator' designs (automated variable lens changer) were made for 2D Beryllium compound refractive lenses [1-4]. Here, the next generation transfocator is presented. The new design makes it possible to use standard 2D lenses as well as newly designed 1D lenses together. This enables independent control over the beam shape in both transversal directions.

The Coherence Beamline P10 tries to make the full coherent flux of PETRA III available for coherent scattering experiments. It operates in low beta configuration since the resolution of coherent diffraction imaging experiments is limited by the source size. In this configuration the source sizes are 14 µm in the vertical direction and 84 µm in the horizontal direction (FWHM values) [5], i.e. the source is still strongly asymmetric by a factor of 6. The transversal coherence length ξ_t is inversely proportional to the source size σ_t, i.e. it is 6x larger in vertical direction than in horizontal one.

Matching vertical and horizontal transverse coherence length (or defining slit size) at the sample position will yield symmetric speckles, which is of advantage for certain coherent scattering experiments [6]. For this purpose it is planned to use a vertical pre-focusing device to create a vertical virtual source along the P10 beamline and to use a second lens system to create a coherently focused beam (< 100 µm^2) at the sample position. In such a focusing scheme the 2nd lens must consist of 1D and 2D lenses in order to match the focal positions in vertical and horizontal direction since the object distances of both directions are different.

Beryllium lenses are commercially available from the group of Bruno Lengeler, RWTH Aachen [7]. 2D lenses exist in many different sizes (R = 50 … 1500 µm). The actual 2D Be lens is mounted inside a high precision stainless steel disk of 12 mm diameter. The centres of the lens and the disk match to a few microns (Fig. 1b). However, the design of the 1D lens is quite different. The 1D lens is mounted in the centre of a high precision stainless steel square of 20 x 20mm^2 with the lens axis parallel to one of the frame axis (Fig. 1a). Due to the fabrication process

Figure 1

Image of a 1D Beryllium lens (left side) and image of a 2D Beryllium lens (right side). The design differs in shape and size.

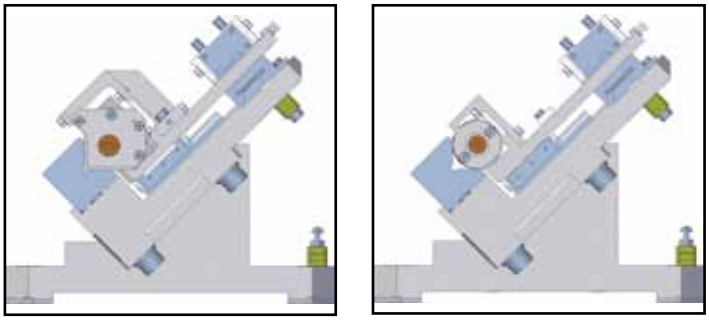

Figure 2

Design of a 1D lens stack holder (left side) and a 2D lens stack holder (right side).

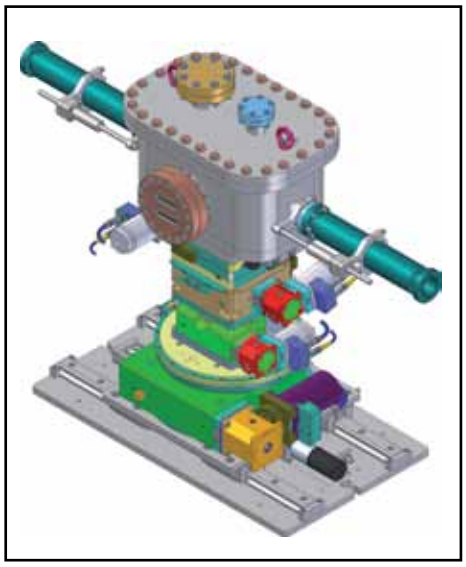

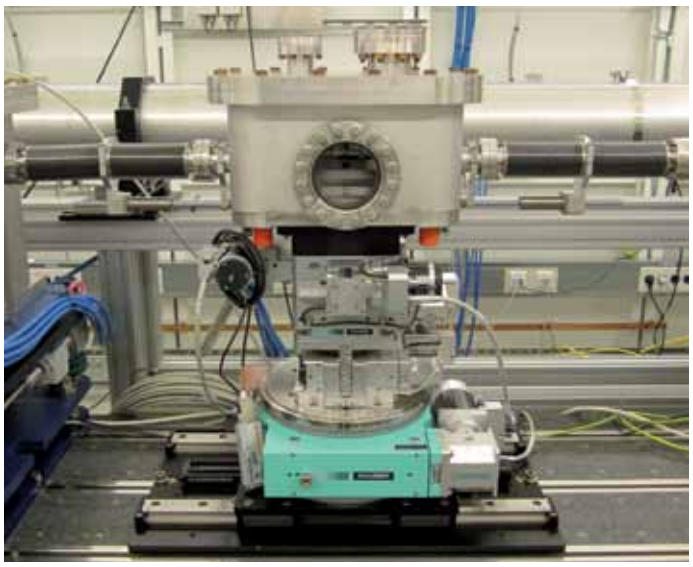

Figure 4

Design of the P10 transfocator (left side) and the actual device (right side).

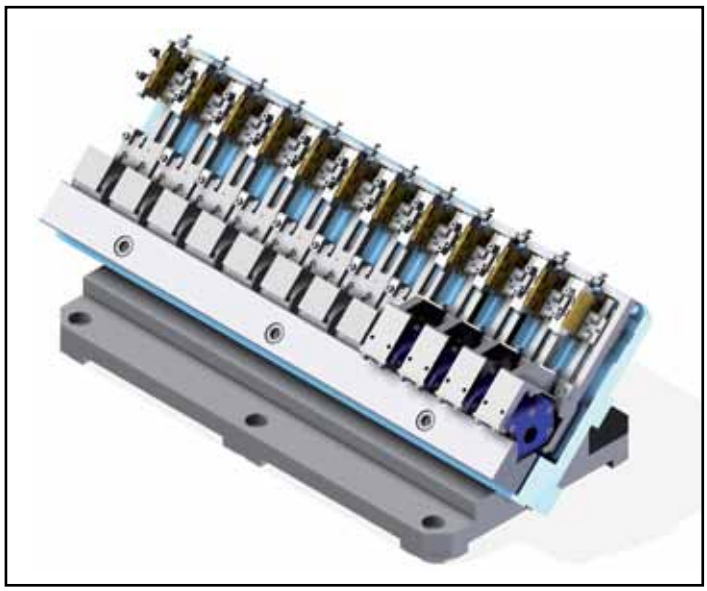

Figure 3

Design of mounting plate with piezo driven lens stack holders and high precision prism.

only a few different sizes are available (R = 500, 1000 and 1500 µm).

The original DESY 2D transfocator design mounts stacks of 2D lenses inside a high precision cylinder of 20 mm outer diameter. Each stack is driven by piezo actuators to align these different lens stacks in a 90 degree prism (the optical axis) [3]. The complete device can be aligned to the beam direction by a 4-axis tower.

The new design aligns stacks of 1D and 2D lenses with respect to one high precision 90 degree prism. It must ensure that the centres of all lenses are at the same distance from the prism. To accomplish this goal, new piezo driven stack holders for 1D lenses (Fig. 2a) were developed. Fig. 2b shows the 2D stack holder. The P10 lens consists in total of 12 independent lens stacks (8 x 2D, 4 x 1D). The prism and the 12 piezo driven stack holders are mounted on a base plate, which is rotated by 45 degrees around the beam direction to ensure that the 1D lenses are focusing either vertically or horizontally (Fig. 3). The whole design is UHV compatible and is housed inside a vacuum chamber.

A 5th motorized stage, a translation along the beam direction (± 150 mm), was added to cover continuously the full energy range from 4 - 20 keV for image distances between 1 m to 2.5 m with these highly chromatic optical elements. Fig. 4a shows the full design and Fig. 4b the actual device installed in P10-EH2.

First results of measurements at P10 look very promising. It seems that a) the lens system works as predicted (beam sizes < 20 µm^2 are easily achieved) and b) the coherence properties seem preserved in the focused X-ray beam.

Contact: Michael Sprung, michael.sprung@desy.de

References:

1. G. B. M. Vaughan et al., J. Synchrotron Rad. 18 125 (2011).
2. A. Snigirev et al., J. Phys.: Conf. Ser. 186 012073 (2009).
3. T. Schubert, Design of the CRL changers for P08 and P09
4. R. Doehrmann et al., DESY Photon Science Highlight 2009
5. Technical Design Report of PETRA III http://petra3.desy.de/sites/site_petra3/content/general/tdr/index_eng.html
6. The main reason is that detector pixels are typically square. Strongly asymmetric speckles do not match those pixels well and binning is not always an option.
7. Homepage of Bruno Lengeler group at RWTH Aachen, Germany http://www.physik.rwth-aachen.de/en/institutes/institute-iib/group-lengeler/

The Adaptive Flight Tube Setup at the PETRA III P03 beamline.

A flexible Beamline setup for a wide range of SAXS Experiments

X-ray scattering is a powerful tool to obtain information about the structure of condensed matter, from the atomic and molecular structure to the mesoscopic domain. This requires the flexibility to install experiments either in transmission or in grazing incidence geometry, to enable bulk or surface and near-surface investigations.

The high brilliance and the small divergence of the micro focused X-ray beam provided by the MiNaXS-Beamline at PETRA III, allow us to investigate fast kinetic processes in a large number of experiments such as deformation experiments, monitoring of deposition processes, chemical reactions and temperature driven kinetics. The desired q-range in micro-beam small angle X-ray scattering (μSAXS) experiments often extends to several orders of magnitude [1]. Therefore, the sample-to-detector distance must be flexible in order to adjust the detector position for the different q-ranges.

To manage this large number of experimental setups, a modular and flexible infrastructure is essential. For this reason, we installed a modular adaptive SAXS-setup at MiNaXS [2]. In order to maximize the signal-to-noise ratio, the flight path between sample and detector has to be evacuated. The basic configuration of the setup is shown in Fig. 1.

To fulfil the vacuum condition and enable rapid changes between μSAXS/WAXS and μUSAXS configurations a modular setup has been designed: It consist of two independent motor driven membrane bellow systems (sealed by Kapton windows), installed on a movable optical bench, a detector device mounted on rails and an in-vacuum beam stop positioning device with two independent beam stops. This setup allows changes of the flight tube length within a few minutes without breaking the vacuum. Sample to detector distances from 60 cm to 2.2 m (one bellow segment), or 120 cm to 5 m (two bellow segments) are possible. The beamline software controls all devices remotely. To adapt the desired q-range in an automated way it is possible to couple these three devices.

The travel range of each bellow system is 1750 mm, at a minimal length of 400 mm. That means an automated adaption of the sample to detector distance up to 5 m is possible.

A travel range of the detector device of 10 m allows for an easy positioning of the detectors even in the USAXS range. Two detectors can be mounted at the device, to measure fast kinetics or to optimize the SAXS resolution, according to the low divergence of the beamline, by using the same setup.

The optical bench can be moved along the detector device rails using air pads in case more space is required for the sample environment / the experiment setup, for example in the case of the imaging ellipsometer setup and the sputter – deposition – chamber, see Fig. 2.

To cover the WAXS regime, an additional detector-positioning device has been designed and will be available in spring 2012, see Fig. 3. With this new device, it will be possible to perform simultaneous SAXS/WAXS measurements at MiNaXS.

Contact: Ralph Döhrmann, ralph.doehrmann@desy.de

Contributions from:
R. Döhrmann, S. Gogolin, A. Buffet, S.V. Roth
Hamburger Synchrotronstrahlungslabor at DESY, Notkestr. 85, D-22607 Hamburg

References:

1. S.V. Roth et al., Rev. Sci. Instr. 77, 085106 (2006).
2. A. Buffet et al., "P03: The Microfocus and Nanofocus X-ray Scattering (MiNaXS) beamline at the PETRA III storage ring", in preparation (2011).

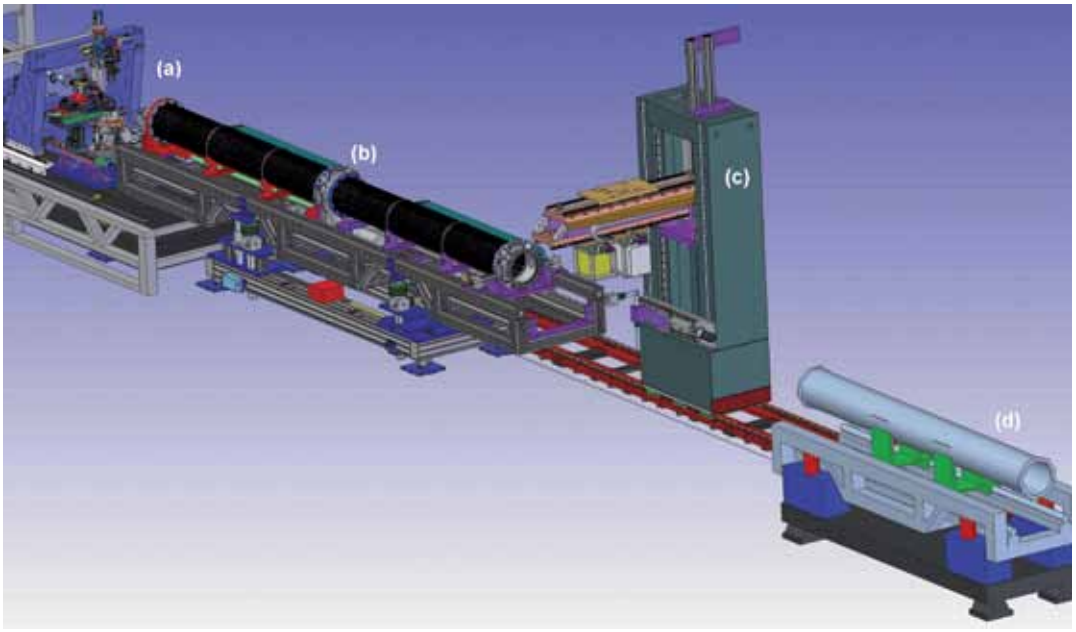

Figure 1

CAD drawing of the Adaptive SAXS- Experiment
a) Standard sample environment.
(b) The flight tube consists of two membrane bellow systems
c) Detector positioning device with two mounted detectors.
d) Additional optical bench to extend the flight path for µUSAXS experiments

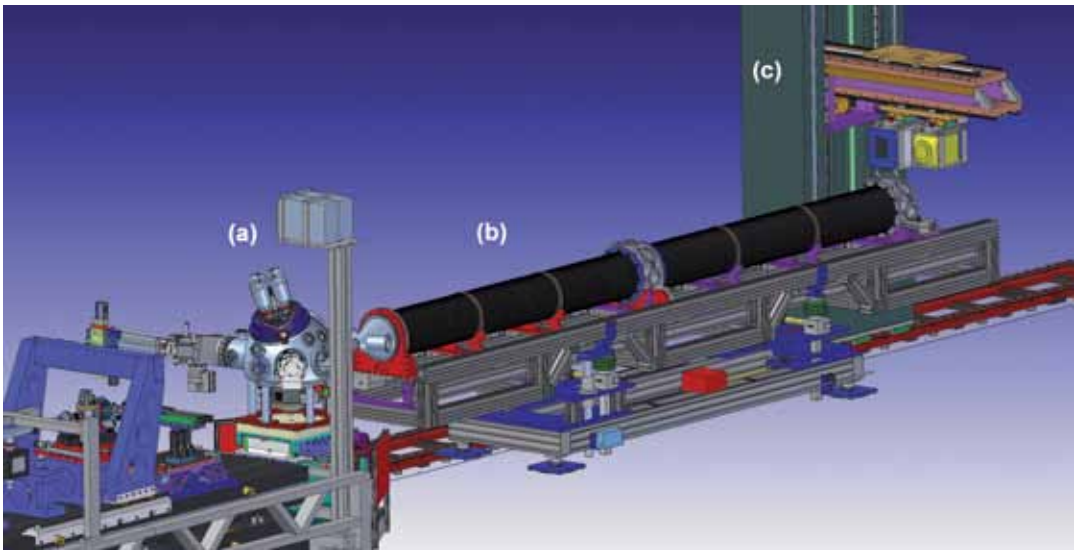

Figure 2

CAD drawing of the sputter deposition setup in µGISAXS geometry to show the possibility to install bulky equipment.
a) Sputter deposition chamber
b) The two coupled segments of the adaptive flight tube
c) SAXS Detector device with installed Pilatus 300K- and Roper detector.

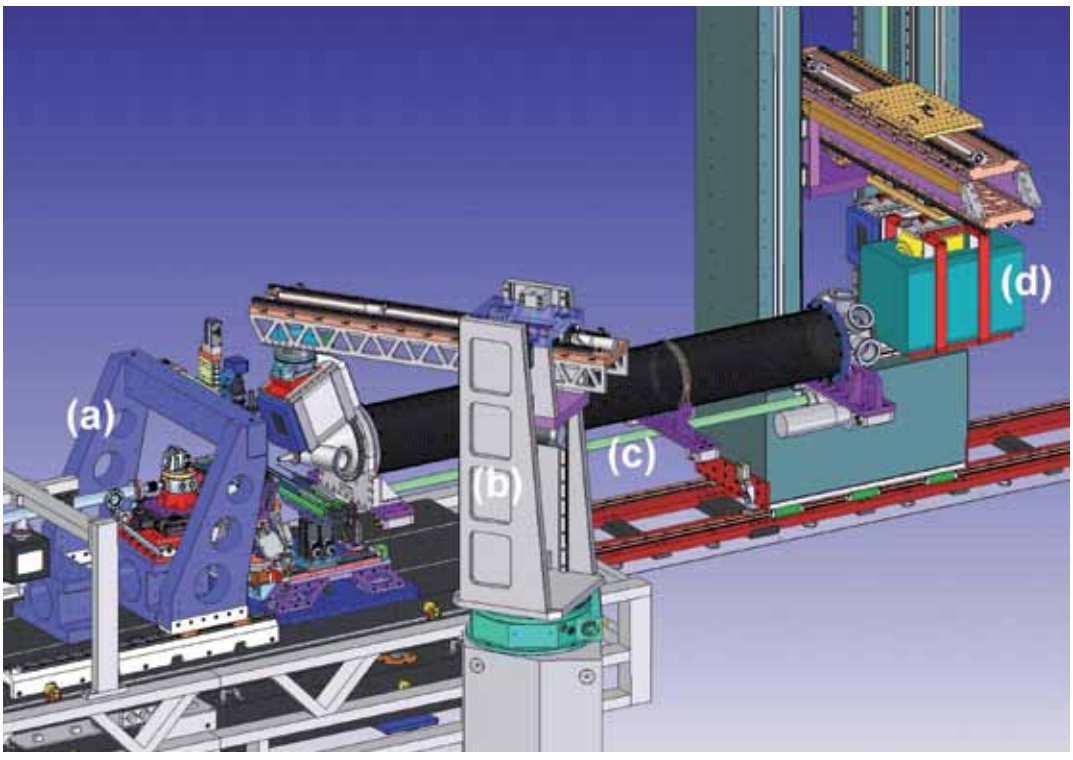

Figure 3

CAD drawing of the setup for simultaneous measurements of µWAXS and µSAXS (available in spring 2012)
a) Standard sample Setup
b) WAXS Detector positioning device with Pilatus 300K detector
c) One segment of the membrane bellow system,
d) SAXS Detector device with installed Pilatus 1M detector

Microfluidics with GISAXS at the PETRA III P03 beamline.

Investigating the dynamics

X-rays are a useful probe for the investigation of flow and processes in microfluidic systems. With the application of a reflection geometry in GISAXS (grazing incidence small angle X-ray scattering) and a specially designed fluidic cell, surface sensitive investigations are possible. The basic principle has been demonstrated with pioneering experiments at the beamline BW4 of DORIS III [1, 2]. With the highly brilliant X-ray beam of PETRA III time-resolved microfluidic experiments in GISAXS geometry become available. The necessary sample environment is developed at beamline P03 to offer the opportunity of microfluidic experiments with a so far unique time resolution.

In Fig. 1a the basic principle of a microfluidic GISAXS experiment is shown including the top part of the microfluidic cell. This cell is made of a copolymer based on cyclic olefines. The material is transparent to visible light and has a relatively low absorption at the X-ray energies used. Figure 1b shows the microfluidic set-up at beamline P03. The top part is connected to the surface to be investigated (e. g. a thin polymer film on a glass slide with a metallic clamp). The channel geometry (1 mm wide and 1.3 mm deep) enables the study of the solid-liquid interface during the continuous flow of a solution with a broad range of flow rates. The experimental set-up offers versatile investigations, such as attachment processes and layer formation of nanoparticles as shown in Fig. 1c. Thus the detachment of unwanted detrimental films from surfaces and related chemical reactions (e.g. nano-particle formation) caused by subsequent attachment to the surface can be probed. The envisaged high time resolution will allow following the corresponding kinetics.

Contacts: Stephan Roth, stephan.roth@desy.de
Stephan Förster, stephan.foerster@uni-bayreuth.de
Peter Müller-Buschbaum, peter.mueller-buschbaum@ph.tum.de
Volker Körstgens, volker.koerstgens@ph.tum.de

References:

1. **J.-F. Moulin, S. V. Roth and P. Müller-Buschbaum, Rev. Sci. Instrum. 79, 015109 (2008).**
2. **E. Metwalli, J.-F. Moulin, J. Perlich, W. Wang, A. Diethert, S. V. Roth and P. Müller-Buschbaum, Langmuir 25, 11815 (2009).**

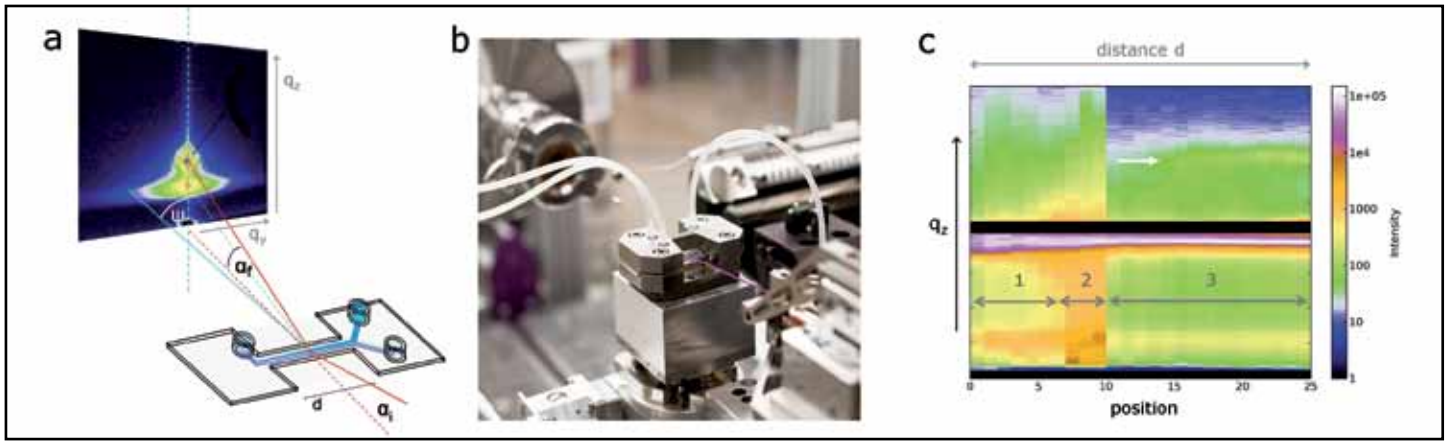

Figure 1

a) Sketch of measuring principle with microfluidic cell design. b) Experimental set-up at beamline P03; the arrow indicates the incoming focused X-ray beam. c) Example of microfluidic experiment with nanoparticles in aqueous dispersion attaching to a biopolymer film: The intensity map shows cuts along q_z at $q_y = 0$ for 25 positions along the microfluidic channel showing the initial stage of the experiment 1: dry polymer; 2: wetted polymer; 3: channel filled with dispersion; the white arrow indicates attachment of particles.

Microfluidics with microfocus SAXS at the PETRA III P03 beamline.

In-situ investigations with short residence times

Microfluidics has developed into an established experimental technology. Driven by demands in micro-bioanalytics ("lab-on-a-chip") and chemical microreactor engineering, microfluidic devices for handling liquid volumes down to picoliters have been developed. Together with the current miniaturization in X-ray optics, particularly at 3rd generation synchrotron sources like PETRA III, micron-size X-ray beams with high brilliance have become available. The combination of microfluidics with microfocus SAXS-experiments developing into a powerful experimental methodology suitable for detailed in-situ investigations with short residence times. This approach is also of advantage when precious samples are only available in very small amounts (like i.e. proteins) or when high-intensity radiation prevents a detailed characterization due to degradation effects in static experiments. In the framework of an on-going BMBF-project we are developing and establishing the production of X-ray transparent microfluidic chips using a combination of optical lithography and soft-lithography. These microfluidic devices can be set up in the microfocus X-ray beam at the MiNaXS/P03 beamline. The obtained SAXS-patterns can then be analysed using the software "Scatter" which allows the quantitative simulation of (an)isotropic scattering patterns to gain structural information about the material [1].

We were able to demonstrate how flow-induced orientation changes of wormlike block copolymer micelles (poly(butadiene)-b-poly(ethylene oxide), PB-b-PEO) within the micro-channels, can be observed and followed in-situ [2]. Furthermore, the anisotropic scattering pattern allows quantifying the orientation distribution, see figure 1. Shear-induced alignment plays an important role in material sciences as well as in technical processes such as injection molding or extrusion.

Contact: Stephan Roth, stephan.roth@desy.de
Stephan Förster, stephan.foerster@uni-bayreuth.de
Peter Müller-Buschbaum, peter.mueller-buschbaum@ph.tum.de
Volker Körstgens, volker.koerstgens@ph.tum.de

References:

1. S. Förster, L. Apostol, W. Bras, J. Appl. Crystallogr. 43, 639 (2010).
2. J. Thiele, M. Trebbin, D. Steinhauser, J. Perlich, S. V. Roth and S. Förster, in preparation.

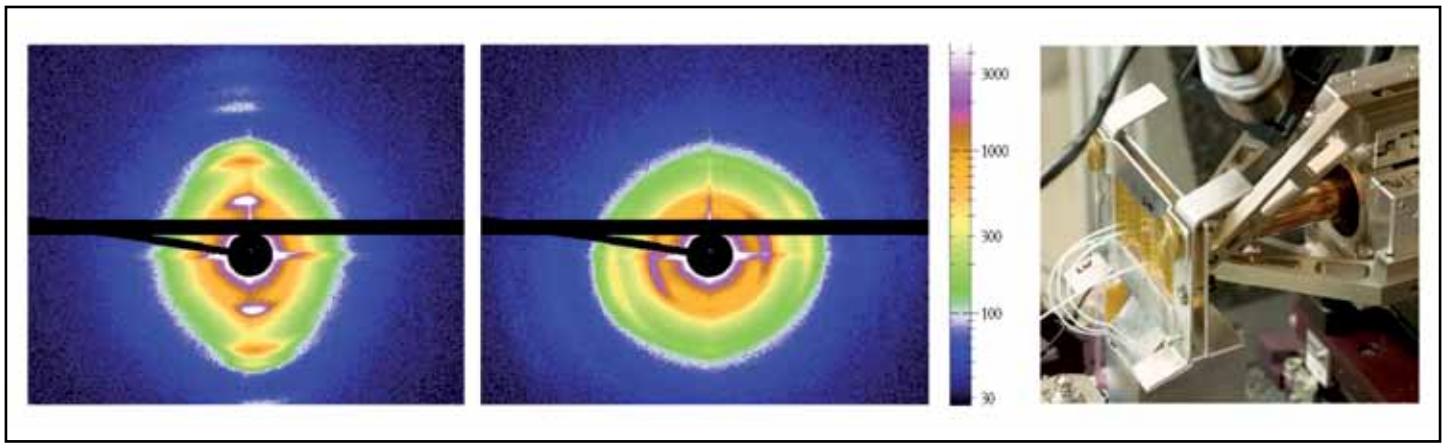

Figure 1

(Left, Middle) The precise sample positioning and a small beam size at MiNaXS/P03 allowed to reveal that the very small distance of ca. 120 µm, between channel-wall and -centre, can make a huge difference in the shear stress-induced orientation of PB-b-PEO wormlike micelles which flow in a 250 µm microchannel with a 5:1-ratio tapering. The horizontal black line is induced by a finite separation of the modules of the PILATUS 300k detector (DECTRIS). (Right) Experimental setup: microfluidic device at MiNaXS/P03.

Facts and Numbers.

Light source characteristics.

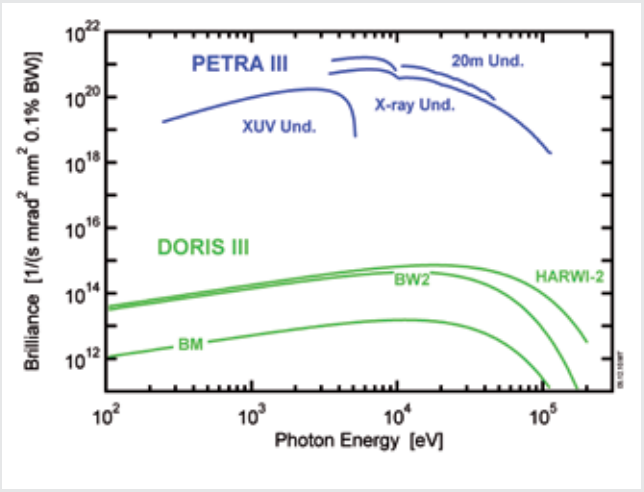

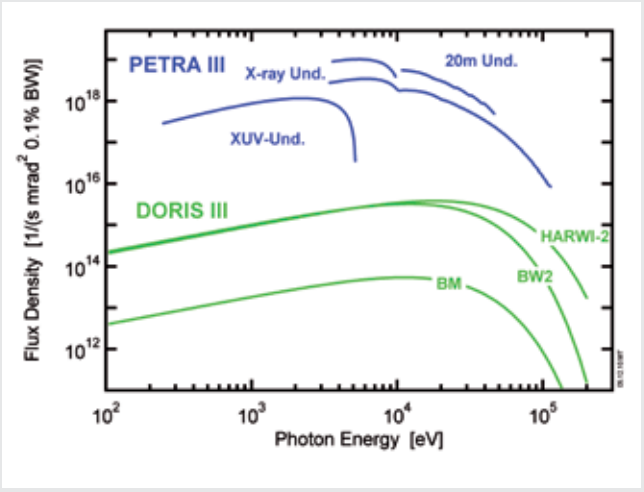

Storage ring sources

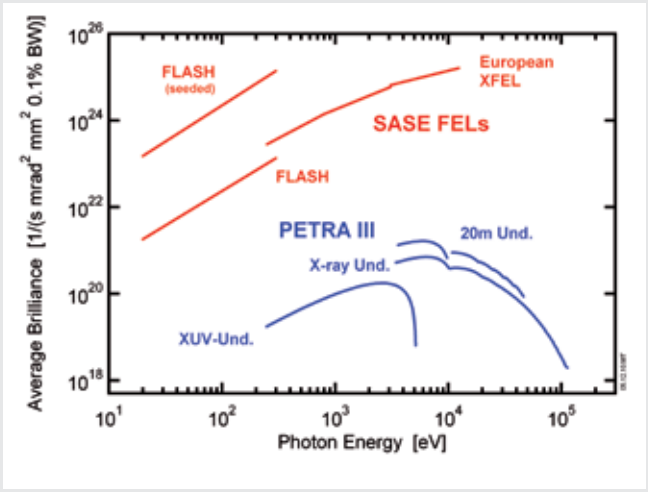

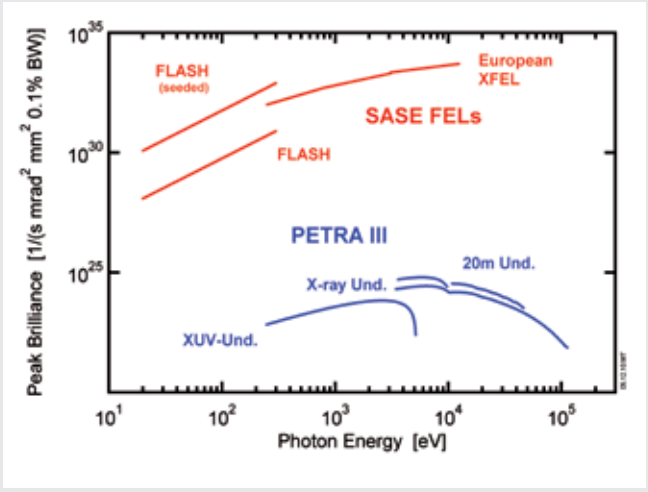

Free-electron laser sources
(in comparison with PETRA III)

Beamtime statistics 2011.

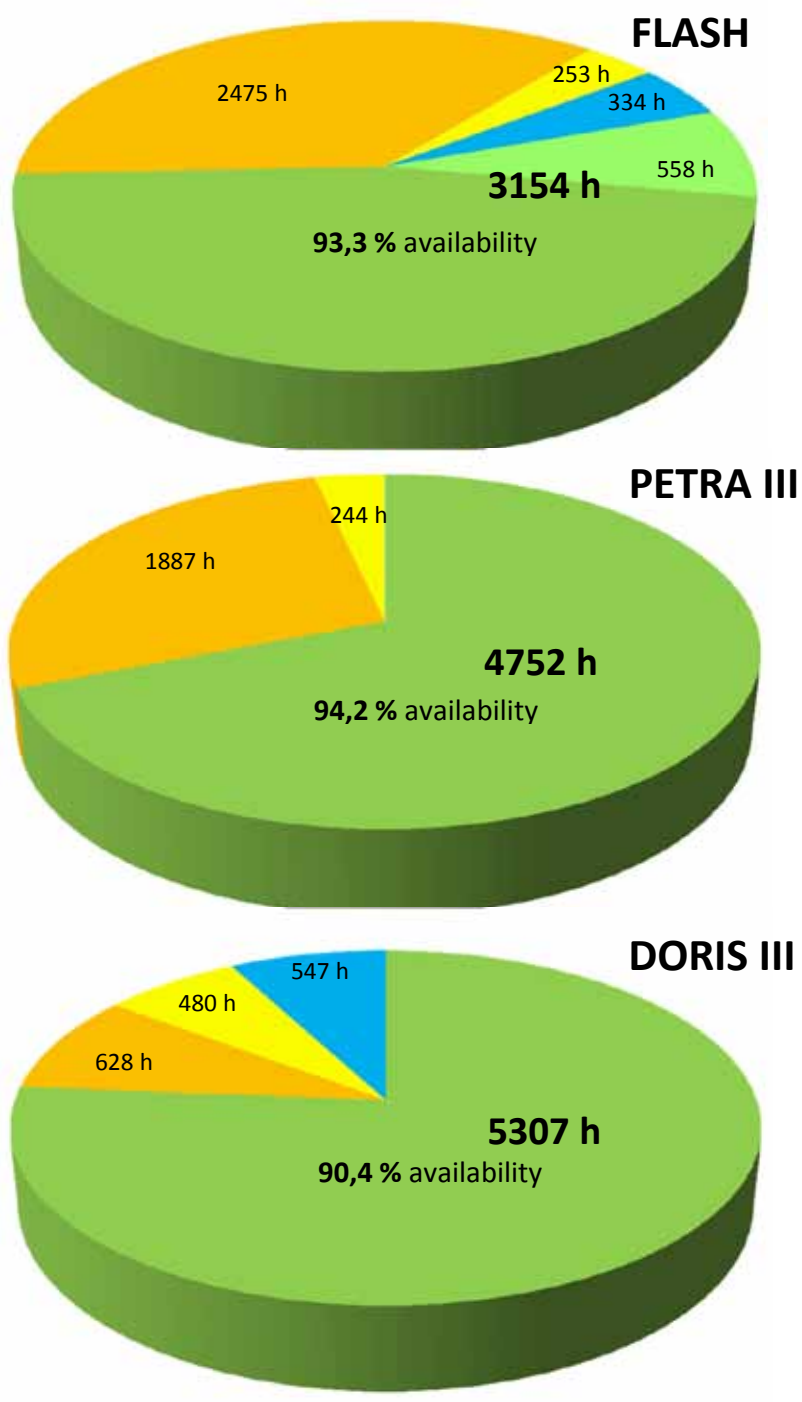

Operation periods 2011

FLASH	1/2011: 14.02.-12.09.
PETRA III	1/2011: 03.03.-11.07.
	2/2011: 15.08.-21.12.
DORIS III	1/2011: 01.03.-11.07.
	2/2011: 15.08.-21.12.

FLASH.

Beamlines and parameters

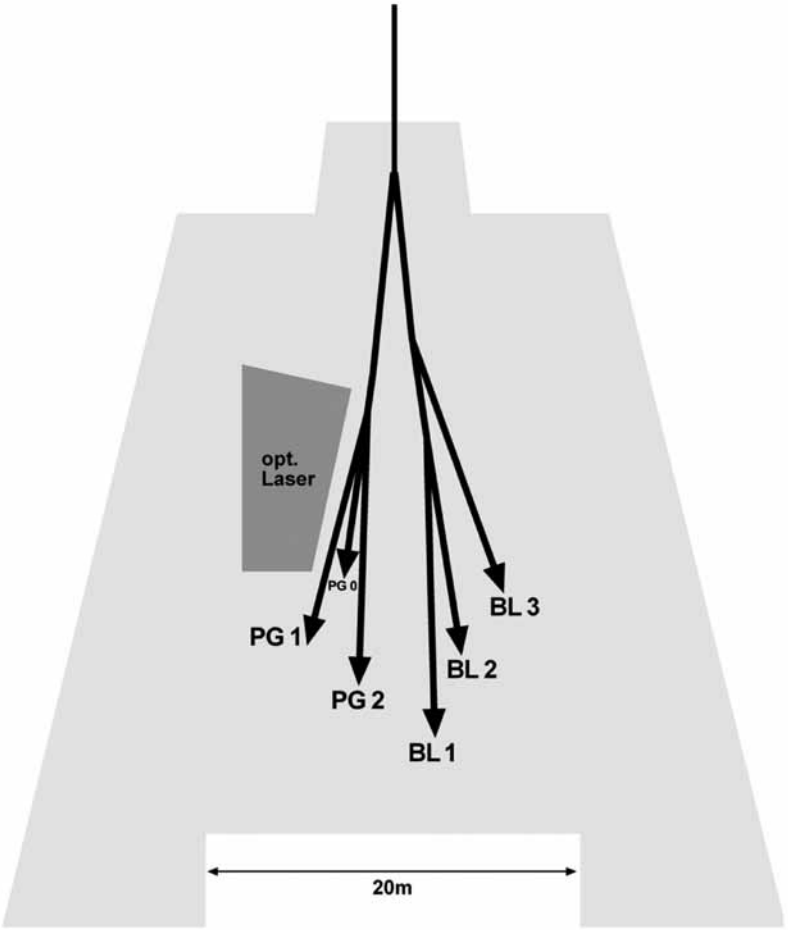

Machine parameters FLASH

Electron energy (max.)	1.25 GeV
Length of the facility	315 m
Normalized emittance	1.5 mm mrad (rms)
Emittance	0.6 nm rad (rms)
Bunch charge	0.1 – 1 nC
Peak current	2 kA
Bunches per second (typ. and max.)	300 and 3000

Lasing parameters

Photon energy (max.)	301 eV (fundamental)
Wavelength (min.)	4.12 nm (fundamental)
Pulse duration (FWHM)	50 - 200 fs
Peak power	1 - 3 GW
Bunch energy (average)	up to 400 µJ
Photons per bunch	10^{12} - 10^{13}
Average brilliance	10^{17}-10^{21} photons/sec/mm^2/mrad^2/0.1%
Peak brilliance	10^{29} - 10^{31} photons/sec/mm^2/mrad^2/0.1%

*Status 1.12.2011

FLASH beamlines and user instruments
(including instrumentation provided by university groups and funded by the BMBF „Verbundforschung“)

BL1

Focused FEL beam, 100 µm spot size	DESY
Instrumentation for the preparation of and electron and ion spectroscopy on mass-selected clusters	U Rostock
Pump-probe setup for the study of transient response of melting/ablating solids	U Duisburg-Essen
Setup for resonant soft X-ray scattering	CFEL U Oxford
Experimental system for the spectroscopic study of molecular desorption from surfaces of solids	U Münster
Single-shot cross-correlator	U Hamburg

BL2

Focused FEL beam, 20 µm spot size or unfocused beam	DESY
Instrumentation for two-colour pump probe experiments of atoms and molecules	DESY DCU Dublin European XFEL
Reaction microscope for the study of multiple ionization processes of atoms and molecules	MPI-K Heidelberg
Velocity map imaging spectrometer (electrons and ions) for atoms and molecules in strong fields	MBI Berlin AMOLF Amsterdam
Setup for angle-resolved photoelectron spectroscopy (ARPES) of atoms and molecules	FHI Berlin
Station for spectroscopy of rare gas clusters and nanoparticles	TU Berlin
Single-shot single-particle (time-resolved) diffraction imaging of nanostructures and biological samples	CFEL DESY LLNL Livermore U Uppsala
Setup for Thomson scattering spectroscopy to probe plasma dynamics in a liquid hydrogen jet	DESY LLNL Livermore U Oxford U Rostock
Instrumentation for measuring damage thresholds and optical properties of solid samples	ASCR Prague DESY IFPAS Warsaw LLNL Livermore
Setup for electron and ion spectroscopy to study multi-photon processes in gases	DESY PTB Berlin U Hamburg
XUV beam splitter with variable delay for photon diagnostics and time-resolved experiments (permanent installation)	DESY HZB U Münster
Magnetic X-ray diffraction imaging and holography	DESY HZB TU Berlin

FLASH beamlines and user instruments

BL3		
	Focused FEL beam, 20 µm spot size or unfocused beam + THz undulator radiation	DESY
	Magneto-optical trap & reaction microscope to study ultra-cold plasmas	MPI-K Heidelberg
	Setup with multilayer optics for sub-micron focusing to create and study plasmas and warm dense matter	U Belfast CFEL DESY U Oxford
	System for angle-resolved photoelectron spectroscopy (ARPES) and ion spectroscopy of metal vapors	DESY U Hamburg
	Microfocus setup for spectrometry of multi-photon processes in rare gases at extreme power densities	DESY PTB Berlin
	Split multilayer-mirror & reaction microscope for time-resolved spectroscopy of small molecules	MPI-K Heidelberg
	Microfocus setup for time-resolved imaging of rare gas clusters	TU Berlin
	Experimental station for pump-probe experiments combining μJ-level, few-cycle THz and XUV FEL pulses	DESY U Hamburg
	THz pump X-ray photo-emission probe (Mott-Detector) setup for magnetic measurements	CFEL DESY U Hamburg HZB
	Molecular beam setup to study femtochemistry via pump-probe photoelectron-spectroscopy	DESY HZB CFEL FU Berlin
PG1		
	Plane grating monochromator, microfocus (5 µm spot size)	DESY, U Hamburg
	High-resolution two-stage spectrometer for inelastic (Raman) scattering (permanent installation)	DESY U Hamburg
PG2		
	Plane grating monochromator (50 µm focus)	DESY, U Hamburg
	Setup for resonant inelastic X-ray scattering (RIXS) and photoelectron spectroscopy of solids	U Hamburg
	Electron beam ion trap (EBIT) for high-resolution spectroscopy of highly charged ions	MPI-K Heidelberg
	Ion source and trap for spectroscopic studies of the photo-fragmentation of molecular ions and radicals (permanent installation)	U Aarhus MPI-K Heidelberg
	System for angle-resolved photoelectron spectroscopy (ARPES) of solids and surfaces	U Kiel
	Setup for the study of fs-dynamics of magnetic materials	U Hamburg HZB
	XUV beamsplitter with variable delay for time resolved experiments (permanent installation)	U Hamburg
	Soft X-ray diffraction imaging system for magnetic materials and nanostructures	DESY U Hamburg U Heidelberg HZB FH Koblenz
	Spin-polarized photo-emission (Mott-Detector) chamber for the investigation of laser induced ultrafast demagnetization processes	ETH Zürich HZB DESY U Hamburg SLAC

Note: instruments are non-permanent installations unless noted otherwise

PETRA III.

Beamlines and parameters

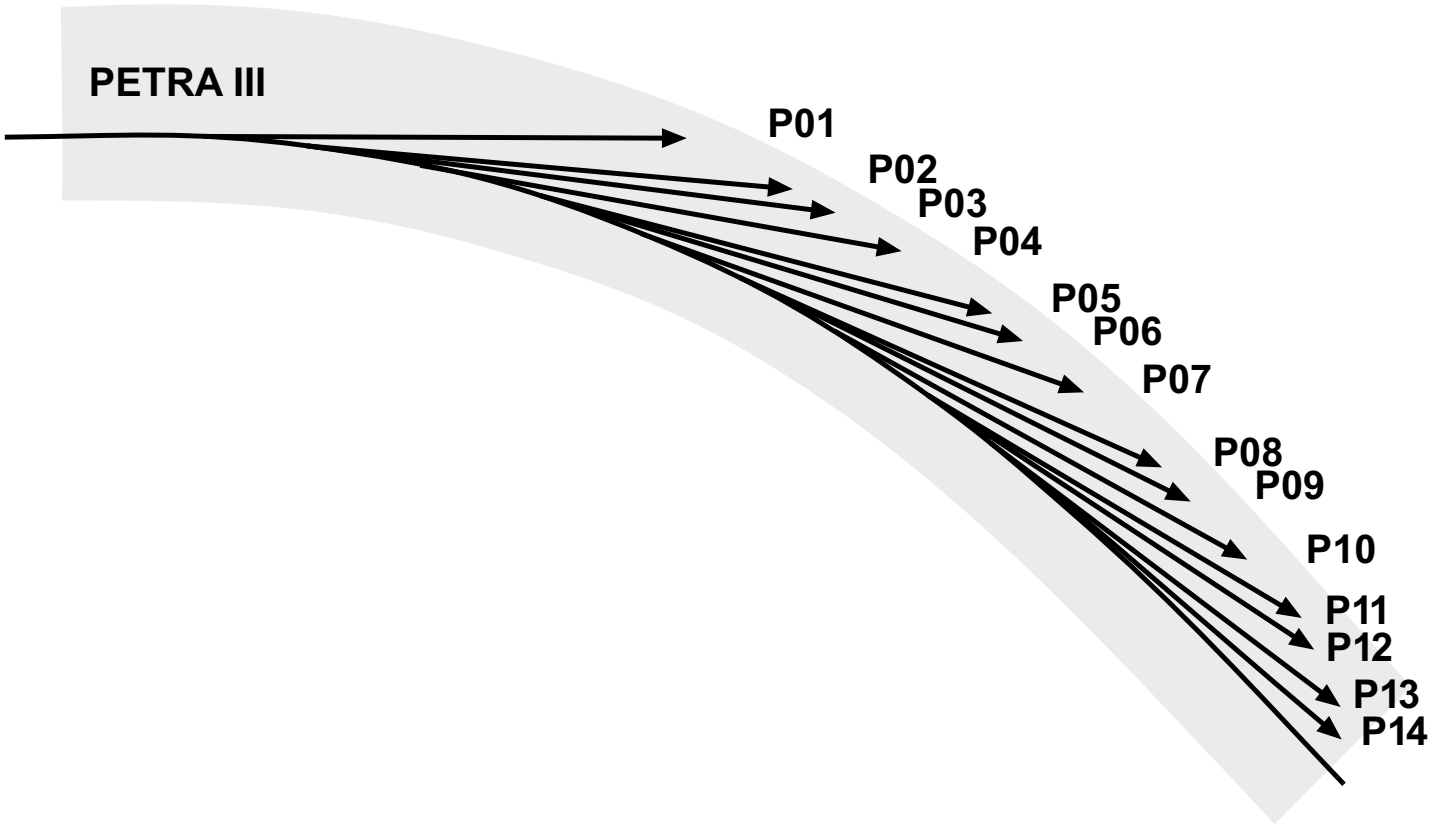

Machine parameters PETRA III

Positron energy	6.08 GeV
Circumference of the storage ring	2304 m
Number of buckets	3840
Number of bunches	240, 60, and 40
Bunch separation	32 ns, 128 ns, and 192 ns
Positron beam current	100 (80) mA (top-up)
Horizontal positron beam emittance	1.0 nmrad (rms)
Coupling factor	1%
Vertical positron beam emittance	0.01 nmrad (rms)
Positron beam energy spread	0.1% (rms)
Horizontal x vertical beam size at 5 m undulator (high β section)	141.5 x 4.9 µm
Horizontal x vertical beam size at 5 m undulator (low β section)	34.6 x 6.3 µm

PETRA III beamlines and instruments
(including instrumentation provided by university groups and funded by the BMBF „Verbundforschung“)

P01 Inelastic and Nuclear Resonant Scattering			
	10 m undulator (U32), high-ß		
	Hutch1 Nuclear resonant scattering setup Nuclear lighthouse effect spectrometer	6 – 40 keV	DESY
	Hutch2 Spectrometer for inelastic scattering with nanobeam	6 – 40 keV	DESY, TU Dortmund
	Hutch3 Nuclear resonant scattering with special sample environments: Extreme conditions and UHV	6 – 40 keV	DESY TU Kaisersl.
P02 Hard X-Ray Diffraction			
	2 m undulator (U23), high-ß		
	Hutch1 Powder diffraction side station High-resolution powder diffractometer	60 keV	DESY TU Dresden U Erlangen-Nürnberg
	Hutch2 Station for diffraction experiments under extreme conditions (high p, high T) Laser heating for the extreme conditions station	8 – 100 keV	DESY U Frankfurt
P03 Micro- and Nanobeam Wide and Small Angle X-ray Scattering (MINAXS)			
	2 m undulator (U29), high-ß		
	Hutch1 General Purpose µSAXS/WAXS station Setup for in-situ deposition experiments, AFM µGISAXS option with ellipsometer	8 – 23 keV	DESY U Hamburg TU München
	Hutch2 Setup for nanobeam Scanning-Experiments (SAXS/WAXS, GISAXS) Nanofocus endstation including in-situ deformation experiments	8 – 23 keV	DESY U Kiel
P04 Variable Polarization Soft X-rays			
	5 m APPLE undulator (UE65), high-ß		DESY
	UHV-diffractometer for elastic and inelastic resonant XUV scattering	0.2 - 3.0 keV	U Köln
	Ultra-high resolution XUV photoelectron spectrometer for in-situ real-time investigation of dynamic processes in nano structures	0.2 - 3.0 keV	U Kiel U Würzburg
	PIPE: instrument for flexible two-beam experiments to investigate mass selected ions (atoms to nano particles) with photons	0.2 - 3.0 keV	U Giessen U Hamburg FU Berlin U Frankfurt
	Soft X-ray absorption spectrometer with variable polarization at 30 mK	0.2 - 3.0 keV	U Hamburg U München
	Nano focus apparatus for spatial and time resolving spectroscopy	0.2 - 3.0 keV	U Hamburg FH Koblenz
P05 Imaging beamline			
	2 m undulator (U29), low-ß		
	Hutch1 Micro tomography setup for absorption, phase enhanced and phase contrast tomography	5 – 50 keV	HZG
	Hutch2 Nano tomography instrument combining hard X-ray microscopy and tomography	5 – 50 keV	HZG
P06 Hard X-ray Micro/Nano-Probe			
	2 m undulator (U32), low-ß		
	Hutch1 Instrument for imaging at (sub-)micrometer spatial resolution applying X-ray fluorescence, X-ray absorption and X-ray diffraction techniques	2.4 - 100 keV	DESY
	Hutch2 Instrument for imaging by coherent X-ray diffraction and X-ray fluorescence with nanoscopic resolution	5 – 50 keV	DESY KIT Karlsruhe TU Dresden

P07 High Energy Materials Science (HEMS)		
4 m in-vacuum undulator (U19), high-ß		
Hutch1 Test facility	53 / 87 keV (fixed)	HZG
Hutch2 Multi purpose diffractometer for bulk and interfaces	50 – 250 keV	DESY, U Siegen
Hutch3 Heavy-load (1t) diffractometer	50 – 250 keV	HZG
Hutch4 3D-XRD strain and stress mapper Instrument for microtomography	 50 – 250 keV	HZG HZG
P08 High-resolution diffraction		
2 m undulator (U29), high-ß		
Hutch1 High-resolution diffractometer X-ray diffractometer for liquid interfaces studies Extension for external sample environments and coherent scattering	5.4 – 30 keV	DESY U Kiel
P09 Resonant scattering / diffraction		
2 m undulator (U32), high-ß		
Hutch1 High precision diffractometer for resonant scattering and diffraction	2.4 – 50 keV	DESY
Hutch2 Heavy load diffractometer for resonant scattering and diffraction, high magnetic fields	2.4 – 50 keV	DESY U Siegen
Hutch3 High-resolution hard X-ray photoelectron spectroscopy instrument	2.4 – 15 keV	DESY U Mainz U Würzburg
P10 Coherence applications		
5 m undulator (U29), low-ß		
Hutch1 Instrument for X-ray photon correlation spectroscopy and coherent diffraction imaging in SAXS geometry, rheology setup	4 – 25 keV	DESY
Hutch2 Instrument for X-ray photon correlation spectroscopy and coherent diffraction imaging at large angles X-ray waveguide setup Apparatus for lensless microscopy of biological cells Setup for XPCS with reference beams	4 – 25 keV	DESY U Göttingen
P11 Biological imaging / diffraction		
2 m undulator (U32), high-ß		
Single-axis diffractometer for macromolecular crystallography Setup for imaging of biological systems	6 – 33 keV 3 – 12 keV	HZI/DESY MPG
P12 Biological small-angle X-ray scattering		
2 m undulator (U29), high-ß		
Instrument for biological SAXS on protein solutions and time resolved experiments, biomembrane related and soft matter research, tunable sample-detector distance	4 – 20 keV	EMBL HZG U Freiburg
P13 Macro molecular crystallography I		
2 m undulator (U29), high-ß		
Instrument for highly collimated beams and variable focus size, in crystallo spectroscopies	4 – 17 keV	EMBL
P14 Macro molecular crystallography II		
2 m undulator (U29), high-ß		
Protein micro-crystallography instrument	7 – 35 keV	EMBL

Note: for each undulator, high-ß and low-ß operation can be chosen freely.

DORIS III.

Beamlines and parameters

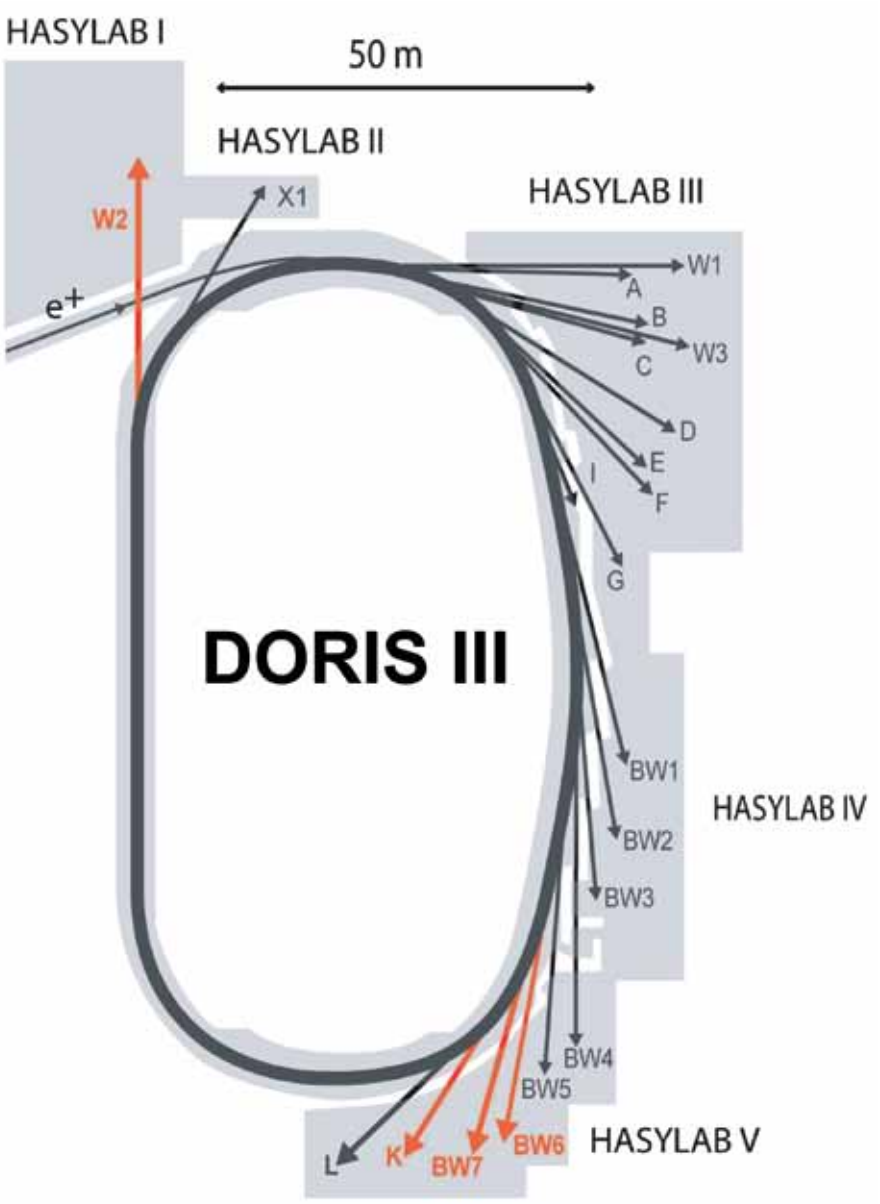

Machine parameters DORIS III

Positron energy	4.45 GeV
Circumference of the storage ring	289.2 m
Number of buckets	482
Number of bunches	1 (for tests), 2, and 5
Bunch separation (minimum)	964 ns (for tests), 480 ns, and 192 ns
Positron beam current	140 mA (5 bunches)
Horizontal positron beam emittance	410 nmrad (rms)
Coupling factor	3%
Vertical positron beam emittance	12 nmrad (rms)
Positron beam energy spread	0.11% (rms)
Curvature radius of bending magnets	12.18 m
Magnetic field of bending magnets	1.218 T
Critical photon energy from bending magnets	16.0 keV

DORIS III beamlines and instruments

A1 X-ray absorption spectroscopy		
Bending magnet (Ec = 16 keV)		
Instrument for in-situ XAFS including fast energy scanning	2.4 – 8 keV	DESY
A2 Small-angle X-ray scattering		
Bending magnet (Ec = 16 keV)		
Multi setup instrument for (simultaneous) small and wide angle scattering from soft matter samples	8 keV	DESY
B1 Anomalous small-angle X-ray scattering		
Bending magnet (Ec = 16 keV)		
Instrument for anomalous scattering (ASAXS)	5 – 35 keV	DESY
B2 X-ray powder diffraction		
Bending magnet (Ec = 16 keV)		
Heavy duty diffractometer including special setups for in-situ studies	5 – 44 keV	DESY
BW1 X-ray diffraction / scattering		
4 m X-ray undulator		
Horizontal diffractometer for liquid surface scattering	9.5 keV	DESY
UHV instrument for surface diffraction / standing waves including MBE sample preparation	2.4 – 12 keV	DESY U Bremen
Multi purpose heavy load 8-circle diffractometer	5 – 18 keV	DESY
Rheometer	9.9 keV	DESY
BW2 X-ray spectroscopy / diffraction / tomography		
4 m X-ray wiggler (Ec = 15.4 keV)		
UHV instrument for hard X-ray photoelectron spectroscopy	2.4 – 10 keV	DESY
X-ray micro-tomography setup	6 – 24 keV	HZG
Heavy load vertical diffractometer with CCD detector arm for grazing incidence diffraction	5 – 11 keV	DESY
BW3 Soft X-ray spectroscopy		
4 m XUV (double) undulator		
High-resolution SX-700 plane grating monochromator, beam port for user supplied instruments	50 – 1500 eV	DESY
BW4 Ultra small-angle X-ray scattering		
2.7 m X-ray wiggler (Ec = 15.4 keV)		
Flexible instrument for (ultra) small angle (grazing incidence) scattering experiments	6 – 14 keV	DESY
BW5 High-energy X-ray diffraction		
4 m X-ray wiggler (Ec = 26 keV)		
Triple axis diffractometer in horizontal Laue scattering geometry including high magnetic field (10 T) sample environment	60 – 250 keV	DESY

DORIS III beamlines and instruments

BW7A Macromolecular crystallography		
4 m X-ray wiggler (Ec = 15.4 keV)		
Crystallographic end-station with CCD detector, double multilayer optics, optimized for high-flux fast data collection	12.8 keV	EMBL
BW7B Macromolecular crystallography		
4 m X-ray wiggler (Ec = 15.4 keV)		
Crystallographic end-station with CCD detector, new high-precision Phi spindle, EMBL Hamburg robotic sample changer (MARVIN)	14.7 keV	EMBL
C X-ray absorption spectroscopy / diffraction		
Bending magnet (Ec = 16 keV)		
Setup for high-energy XAFS in-situ studies including fast energy scanning	5 – 44 keV	DESY
Vertical diffractometer for grazing incidence X-ray diffraction	5 – 44 keV	DESY
D1 (X33) Small-angle X-ray scattering		
Bending magnet (Ec = 16 keV)		
Instrument optimized for automated solution scattering studies of biological macromolecules	8 keV	EMBL
D3 Chemical crystallography		
Bending magnet (Ec = 16 keV)		
4-circle diffractometer	8 – 50 keV	DESY
D4 Grazing incidence X-ray scattering		
Bending magnet (Ec = 16 keV)		
2-circle diffractometer, horizontal scattering plane	5 – 20 keV	DESY
E1 (Flipper2) Soft X-ray spectroscopy		
Bending magnet (Ec = 16 keV)		
UHV instrument for soft X-ray photoelectron spectroscopy	10 – 150 eV	U Hamburg
E2 X-ray reflectometry / grazing incidence diffraction		
Bending magnet (Ec = 16 keV)		
6-circle diffractometer for reflectometry & high-resolution diffraction	4 – 35 keV	DESY / RWTH Aachen
F1 Chemical crystallography		
Bending magnet (Ec = 16 keV)		
Kappa-diffractometer for low/high-temperature / high-pressure single-crystal diffraction	5 – 41 keV white beam	U Hamburg
F2 X-ray diffraction / VUV spectroscopy		
Bending magnet (Ec = 16 keV)		
Hutch1 MAX80 Multi-Anvil-X-ray apparatus for high pressure X-ray diffraction	5 – 80 keV white beam	GFZ
Hutch2 UHV instrument for angle-resolved UV photoelectron spectroscopy	5 – 41 eV	U Hamburg
F3 Energy dispersive scattering		
Bending magnet (Ec = 16 keV)		
Horizontal diffractometer with heavy load sample stage	white beam	DESY U Kiel

F4 X-ray test beam		
Bending magnet (Ec = 16 keV)		
Used for detector characterization		DESY
G3 Diffraction X-ray imaging		
Bending magnet (Ec = 16 keV)		
4-circle diffractometer for position resolved diffraction	5.4 – 26 keV	DESY
I Superlumi) UV luminescence spectroscopy		
Bending magnet (Ec = 16 keV)		
Superlumi setup for luminescence analysis	3 – 40 eV	DESY
K1.1 (X11) Macromolecular crystallography		
Bending magnet (Ec = 16 keV)		
Crystallographic end-station with large surface area flat panel detector, cryoshutter, single horizontal axis of rotation	15.3 keV	EMBL
K1.2 (X12) Macromolecular crystallography		
Bending magnet (Ec = 16 keV)		
Crystallographic end-station with CCD and fluorescence detector, single axis of rotation, opt. for MAD and SAD	6 – 18 keV	EMBL
K1.3 (X13) Macromolecular crystallography		
Bending magnet (Ec = 16 keV)		
Crystallographic end-station with CCD detector, cryoshutter, micro-spectrophotometer, single horizontal axis of rotation, optimised for automated expert data collection	15.3 keV	EMBL
L X-ray micro probe		
Bending magnet (Ec = 16 keV)		
X-ray microprobe combining fluorescence analysis, absorption spectroscopy and diffraction	5 – 80 keV white beam	DESY
W1 X-ray spectoscopy / diffraction		
2 m X-ray wiggler (Ec = 8 keV)		
High-resolution fluorescence in vacuo spectrometer	4 – 11.5 keV	DESY
Heavy load diffractometer for grazing incidence diffraction in vertical or horizontal scattering geometry	4 – 11.5 keV	DESY
W2 (HARWI II) High-energy X-ray engineering materials science		
4 m X-ray wiggler (Ec = 26 keV)		
Hutch1 Materials Science Diffractometer (heavy load up to 600 kg) Micro-tomography setup (attenuation and phase contrast) Diffraction-tomography “DITO” instrument	60 – 250 keV 20 – 250 keV 20 – 150 keV	HZG HZG TU Dresden TU Berlin
Hutch2 MAX200x Multi-Anvil X-ray apparatus for high pressure and temperature conditions	white beam	GFZ
X1 X-ray absorption spectroscopy		
Bending magnet (Ec = 16 keV)		
Setup for high-energy fast-scanning XAFS for in-situ studies including chemistry lab	7 – 100 keV	DESY

Committees 2011.

Photon Science Committee PSC	
Colin Norris (Chair)	Diamond, CCLRC, UK
Simone Techert (Vice Chair)	Max-Planck-Institut Göttingen, D
Markus Drescher	Universität Hamburg, D
Michael Fröba	Universität Hamburg, D
Roland Horisberger	PSI Villigen, CH
Koen Janssens	University of Antwerp, B
Chi-Chang Kao	SSRL, SLAC, USA
Franz Pfeiffer	TU München, D
Harald Reichert	ESRF Grenoble, F
Jean-Pierre Samama	Synchrotron Soleil, F
Edgar Weckert	DESY, Hamburg, D
Philip J. Withers	University of Manchester, UK
Wiebke Laasch (PSC Secretary)	DESY, Hamburg, D

HASYLAB User Committee HUC	
Peter Müller-Buschbaum (Chair)	TU München, D
Thomas Möller	TU Berlin, D
Markus Perbandt	Universität Hamburg, D
Christian Schroer	TU Dresden, D
Joachim Wollschläger	Universität Osnabrück, D

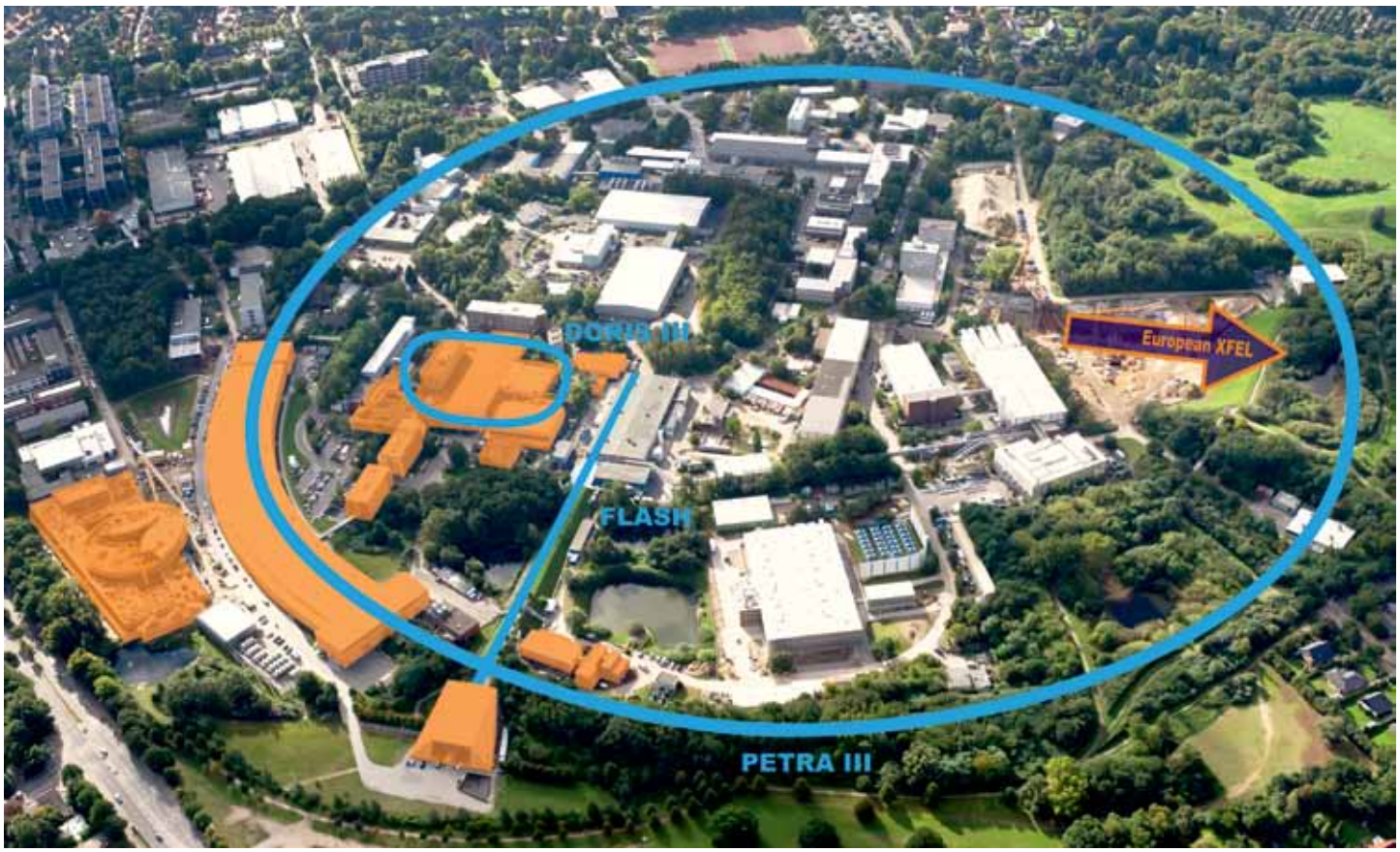

Project Review Panel PRP1: VUV- and Soft X-Ray - Spectroscopy	
Wolfgang Drube (PRP Secretary)	DESY, Hamburg, D
Lutz Kipp	University of Kiel, D
Marco Kirm	University of Tartu, EE
Andries Meijerink	Debye Institute, NL
Joseph Woicik	NIST, USA
Project Review Panel PRP2: X-Ray - Hard Condensed Matter - Spectroscopy	
Wolfgang Drube (PRP Secretary)	DESY, Hamburg, D
Johannes Hendrik Bitter	Utrecht University, NL
Melissa Denecke	KIT, Karlsruhe, D
Thorsten Ressler	TU Berlin, D
Christina Streli	TU Wien, A
Project Review Panel PRP3: X-Ray - Hard Condensed Matter / Diffraction and Imaging	
Hermann Franz (PRP Secretary)	DESY, Hamburg, D
Peter D. Hatton	University of Durham, UK
Raphael Hermann	FZ Jülich, D
Christian Kumpf	FZ Jülich, D
Bert Müller	University Basel, CH
Martin Müller	HZG Geesthacht, D
Ulrich Schwarz	MPI, Dresden, D
Denis Andrault	Université Blaise Pascal, Clermont-Ferrand, F
Michael Nickel	Friedrich-Schiller-Universität, Jena, D
Project Review Panel PRP4: Soft X-Ray - FEL Experiments (FLASH)	
Josef Feldhaus (PRP Secretary)	DESY, Hamburg, D
Massimo Altarelli	European XFEL GmbH, Hamburg, D
Robert Donovan	University of Edinburgh, UK
Roger W. Falcone	Lawrence Berkely Lab., USA
Maya Kiskinova	Sincrotrone Trieste, I
Jon Marangos	Imperial College London, UK
Jan Michael Rost	Max-Planck-Institut Dresden, D
Christian Schroer	TU Dresden, D
Bernd Sonntag	Universität Hamburg, D
Urs Staub	PSI Villigen, CH
Svante Svensson	Uppsala University, S
Edgar Weckert	DESY, Hamburg, D
Gwyn P. Williams	Jefferson Lab., USA
Project Review Panel PRP5: X-Ray - Soft Condensed Matter / Scattering	
Rainer Gehrke (PRP Secretary)	DESY, Hamburg, D
Jochen S. Gutmann	Universität Mainz, D
Beate Klösgen	Univ. of Southern Denmark, DK
Yongfeng Men	Changchun Inst. of Applied Chemistry, CN
Christine Papadakis	TU München, D
Project Review Panel PRP6: Methods and Instrumentation	
Horst Schulte-Schrepping (PRP Secretary)	DESY, Hamburg, D
Kawal Sawhney	Diamond Light Source, UK
Frank Siewert	HZB Berlin, D

Photographs and Graphics:
CFEL
DESY
EMBL
European XFEL
HZG
Max-Planck Unit for Structural Molecular Biology
Heiner Müller-Elsner/Agentur-Focus.de, Hamburg
Dominik Reipka, Hamburg
Reimo Schaaf, Hamburg
University of Hamburg

Figures of the Research Highlights were reproduced by permission from authors or journals.

Acknowledgement
We would like to thank all authors and all those who helped in the creation of this annual report.

Imprint

Publishing and Contact:
Deutsches Elektronen-Synchrotron DESY
A Research Centre of the Helmholtz Association

Hamburg location:
Notkestr. 85, 22607 Hamburg, Germany
Tel.: +49 40 8998-0, Fax: +49 40 8998-3282
desyinfo@desy.de

Zeuthen location:
Platanenallee 6, 15738 Zeuthen, Germany
Tel.: +49 33762 7-70, Fax: +49 33762 7-7413
desyinfo.zeuthen@desy.de

Photon Science at DESY
Tel.: +49 40 8998-2304, Fax: +49 40 8998-4475
photon-science@desy.de
photon-science.desy.de

www.desy.de

ISBN 978-3-935702-62-1

Online version:
photon-science.desy.de/annual_report

Realisation:
Lucia Incoccia-Hermes, Tim Laarmann, Wiebke Laasch

Editing:
Rainer Gehrke, Heinz Graafsma, Lucia Incoccia-Hermes, Wiebke Laasch, Tim Laarmann, Wolfgang Morgenroth, Ralf Röhlsberger, Rolf Treusch, Ulla Vainio, Martin von Zimmermann

Layout: Britta Liebaug, Heike Becker

Printing: Hartung Druck + Medien, Hamburg

Copy deadline: December 2011

HELMHOLTZ
ASSOCIATION

Deutsches Elektronen-Synchrotron
A Research Centre of the Helmholtz Association

The Helmholtz Association is a community of 17 scientific-technical and biological-medical research centres. These centres have been commissioned with pursuing long-term research goals on behalf of the state and society. The Association strives to gain insights and knowledge so that it can help to preserve and improve the foundations of human life. It does this by identifying and working on the grand challenges faced by society, science and industry. Helmholtz Centres perform top-class research in strategic programmes in six core fields: Energy, Earth and Environment, Health, Key Technologies, Structure of Matter, Aeronautics, Space and Transport.

www.helmholtz.de